

THERMODYNAMIC MODELING AND MOLECULAR DYNAMICS SIMULATION
OF SURFACTANT MICELLES

By

ROBERT ANTHONY FARRELL

A DISSERTATION PRESENTED TO THE GRADUATE SCHOOL
OF THE UNIVERSITY OF FLORIDA IN
PARTIAL FULFILLMENT OF THE REQUIREMENTS
FOR THE DEGREE OF DOCTOR OF PHILOSOPHY

UNIVERSITY OF FLORIDA

1988

To Peggy, for her support,
encouragement, and patience

TABLE OF CONTENTS

	<u>Page</u>
ABSTRACT	v
CHAPTERS	
1 INTRODUCTION	1
2 A MOLECULAR THERMODYNAMIC MODEL OF MICELLE FORMATION	4
2.1 Background	4
2.2 Stoichiometry and Reaction Equilibria for Multicomponent Micelles	8
2.3 Estimation of Free Energy Changes	11
2.4 The Calculational Technique	17
3 RESULTS OF THERMODYNAMIC MODELING	23
3.1 Parameter Estimation	23
3.2 Behavior of the Model for Single-Component Nonionic Systems	30
3.3 Aggregate Size Distribution and Concentration Behavior	40
3.4 Chain Length and Temperature Effects.	43
4 MOLECULAR DYNAMICS SIMULATION OF SURFACTANT MICELLES	52
4.1 Background	52
4.2 The Molecular Dynamics Method	55
4.3 The Model Surfactant Molecule	60
4.4 The Model Micelle	65
4.5 Summary of Computer Simulations	71
5 RESULTS OF MOLECULAR DYNAMICS SIMULATION	78
5.1 Mean Radial Positions of Groups	78
5.2 Probability Distributions of Group Positions.	90
5.3 Conformations of Chain Molecules	107
5.4 Shape Fluctuations	126
5.5 Pair Correlations of Groups	133
6 CONCLUSIONS	137

APPENDICES

A	MICELLE SIZE AND SHAPE	143
B	HEAD GROUP INTERACTION IN A BINARY MICELLE	150
C	PROGRAM LISTING FOR SINGLE-COMPONENT NONIONIC MICELLE CALCULATION	160
D	MOLECULAR DYNAMICS PROGRAM LISTING FOR SIMULATIONS 1 AND 2	174
E	DERIVATION OF HEAD GROUP INTRAMOLECULAR INTERACTIONS	218
F	MOLECULAR DYNAMICS PROGRAM LISTING FOR SIMULATION 3	224
REFERENCES		268
BIOGRAPHICAL SKETCH		276

Abstract of Dissertation Presented to the Graduate School
of the University of Florida in Partial Fulfillment of the
Requirements for the Degree of Doctor of Philosophy

THERMODYNAMIC MODELING AND MOLECULAR DYNAMICS SIMULATION
OF SURFACTANT MICELLES

By

ROBERT ANTHONY FARRELL

April, 1988

Chairman: John P. O'Connell
Major Department: Chemical Engineering

The association of surfactant molecules into aggregates known as micelles gives them a broad range of applications. In spite of the widespread use of this class of chemicals, there is not yet sufficient scientific understanding to predict their behavior in solution.

A molecular thermodynamic model has been developed to describe the formation of micelles in multicomponent surfactant solutions. Using a hypothetical, reversible seven-step process, the total free energy of micellization is calculated by summing the contributions due to solvophobic interaction, mixing, surface formation, conformational change, head group interactions and electrostatics. Distributions of micelle sizes and compositions can then be generated through a set of reaction equilibria. Where

possible, the free energy contributions are related to comparable processes on which experimental measurements have been made. Aggregate size distributions have been generated from the model for single-component solutions of nonionic surfactants of different chain lengths and at different temperatures and solution concentrations.

It has been found that a detailed description of micelle structure and entropy effects on chain conformation is necessary to fully describe the thermodynamics of micelle formation without empirical parameterization. To this end, computer simulations of model micelles have been conducted by the molecular dynamics method. Micelles of three different head group characteristics and a comparable hydrocarbon droplet have been simulated. A spherical shell is used to contain the aggregate, providing estimated solvophobic interactions with the molecules.

The simulation results reveal that internal structure of the aggregates is relatively insensitive to the head group characteristics with the greatest effect resulting from head group size. While the micelles all showed chain ordering and the hydrocarbon droplet did not, the bond conformations averaged approximately 71 percent trans in all cases. Results of other simulations and experimental studies are

generally similar to those of the present work for the effects of chain length, aggregate size, and simulation technique on static properties.

CHAPTER 1 INTRODUCTION

There are few classes of chemical species which have received more attention in the scientific literature, or have exhibited a more ubiquitous presence in everyday life, than the amphiphilic molecules known as surfactants. Their unique solution properties of association and adsorption at interfaces give rise to a broad range of applications. Long the essential component in detergency applications, in more recent times surfactants have assumed roles of importance in applications as diverse as enhanced oil recovery and pharmacy.

The association of surfactant molecules in solution into aggregates known as micelles is the primary attribute which has garnered interest among the scientific community. Since the discovery of micelles in solution (McBain and Salmon, 1920), many experimental and theoretical studies have been conducted, yet full understanding of these systems of molecules has not been achieved. True predictive capability is not yet a reality.

This investigation takes a two-fold approach toward the ability to make quantitative predictions of the behavior of systems of surfactants in solution. Since the behavior of

the surfactant solution is a consequence of its thermodynamics, a model set in the framework of molecular thermodynamics is developed to describe the formation of micelles in a multicomponent surfactant solution.

A thermodynamic description of a micellar system is limited by a precise knowledge of the structure of micelles. To this end, computer simulations of model micelles by the molecular dynamics method are conducted. By accurately modeling the forces present, pertinent descriptions of micelle structure are obtained.

In Chapter 2 of this work, further background on micellar systems is given and the development of a model for the free energy change upon formation of micelles in a multicomponent surfactant solution is described. A multi-step reversible process is employed to generate contributions to the total free energy change due to hydrophobic interaction, mixing effects, conformational change, head group interaction, and electrostatic interaction.

Some brief results obtained with the thermodynamic model are presented in Chapter 3. Distributions of free energy change of micellization and aggregate size are calculated for surfactants of different chain lengths and for solutions of different temperature. Due to limitations in the scope

of this portion of the investigation, calculations were carried out only for cases of single-component solutions of nonionic surfactants.

The computer simulation of surfactant micelles is described in Chapter 4. Following a concise description of the molecular dynamics method, its application to the simulation of micelles is discussed. A summary of the computer simulations of the four models--three micelles and one hydrocarbon droplet--is given.

In Chapter 5, the results of analyses of the computer simulations are presented. Elements of aggregate internal structure, chain conformations, aggregate shapes, and changes in the aggregate with time are investigated for the four model aggregates.

Chapter 6 provides a summary of the significant conclusions of this work. Recommendations are made toward the future progress of both of the projects described in the previous chapters.

CHAPTER 2 A MOLECULAR THERMODYNAMIC MODEL OF MICELLE FORMATION

2.1 Background

The forces present in liquid solutions dictate that solution of a polar solute in a polar solvent is more favored than is a polar solute in a nonpolar solvent. Similarly, the nonpolar solvent is more accommodating toward a nonpolar solute than a polar one. Therefore, molecules which contain both polar and nonpolar groups exhibit a unique behavior when present in a polar or nonpolar solvent. Such molecules, known as surfactants, will tend to minimize the unfavored contact (i.e., polar-nonpolar) while maximizing the favored contact (i.e., polar-polar). At an interface between polar and nonpolar liquids, the surfactants will penetrate the interface to achieve "like" interactions on both sides, reducing the "unlike" interactions encountered in the bulk liquid. The polar groups of a large number of surfactant molecules packed closely at an interface will repel each other, producing a spreading pressure which reduces the interfacial tension.

In the bulk liquid, surfactant molecules will aggregate into structures known as micelles which can afford much the same benefits as the interface. In the typical case, a

surfactant with a polar "head group" and a nonpolar "tail," when present in sufficient quantity in a polar solvent such as water, will form micelles having an interior consisting of tails and possibly some nonpolar solubilize and a surface comprised mostly of head groups. The head groups remain in contact with the water--a favored interaction--while the tails reduce their contact with the water--an unfavored interaction. When the solvent is nonpolar, inverted micelles can form.

The ability of surfactants to adsorb at interfaces and aggregate into micelles makes them a very useful class of compounds. The reduction of interfacial tension has many applications, ranging from oil recovery to biological processes. In addition, micelles can solubilize other solutes in their interior, as in drug delivery processes, and reactions can even take place there, as in emulsion polymerization. The earliest and best known use of surfactants, detergency, uses both aspects of their behavior. As useful as these phenomena are, they are not understood to a degree that would allow their full potential to be realized. The ability to predict behavior rather than just explain it is the goal of this undertaking. This requires a knowledge of the thermodynamics of surfactant phenomena.

The formation of surfactant aggregates in solution instills a certain ambiguity in the description of the system by a traditional thermodynamic formalism. The aggregation of surfactant monomers into micelle structures has been treated as the formation of a "phase" (Blankschtein et al., 1985; Kamrath and Franses, 1983; Matijevic and Pethica, 1958) or as a stepwise association "reaction" (Tanford, 1974; Mukerjee, 1972; Murray and Hartley, 1935). Although the former description may aid in visualizing certain aspects of micellar solutions, the thermodynamic idea of a phase cannot be used in a rigorous manner. Its requirements of continuity and homogeneity are not met by a collection of micelles in solution and a single micelle cannot be treated as a phase since its properties are size-dependent.

The treatment of micelle formation as reaction equilibrium is plagued by the lack of a single stoichiometry. Since a distribution of products is formed (Vold, 1950), one must consider each micelle to be in reaction equilibria with the dispersed monomers. The determination of the many equilibrium constants by experimental methods is impossible. Hall and Pethica (1967) proposed using a small-systems thermodynamics approach to

avoid the difficulties of these two treatments. But their approach cannot be used with ionic systems and is mainly formal, not lending itself to practical use.

The thermodynamics of micelle formation remains an interesting problem. The literature is abundant with studies. In addition to the quantities of temperature, pressure, and composition which typically define the thermodynamic state of a typical solution, the thermodynamic behavior of solutions containing surfactant species can depend on the size, shape, and structure of the aggregates which are formed. Thermodynamic properties have been measured and correlated (Burchfield and Woolley, 1984; Woolley and Burchfield, 1984, 1985). Aggregate formation has been investigated from the points of view of classical thermodynamics (Moroi et al., 1984; Muller, 1973) and statistical thermodynamics (Hoeve and Benson, 1957; Owenson and Pratt, 1984). Investigations have focused on size distributions (Ruckenstein and Nagarajan, 1975; Ben-Naim and Stillinger, 1980), the role of micelle shape (Tanford, 1974; Israelachvili et al., 1976; Ljunggren and Eriksson, 1984, 1986; Eriksson and Ljunggren, 1985; Vold, 1985), and shape transitions (Van de Sande and Persoons, 1985; Ikeda, 1984; Missel et al., 1983; Mukerjee, 1977).

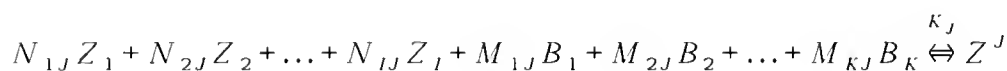
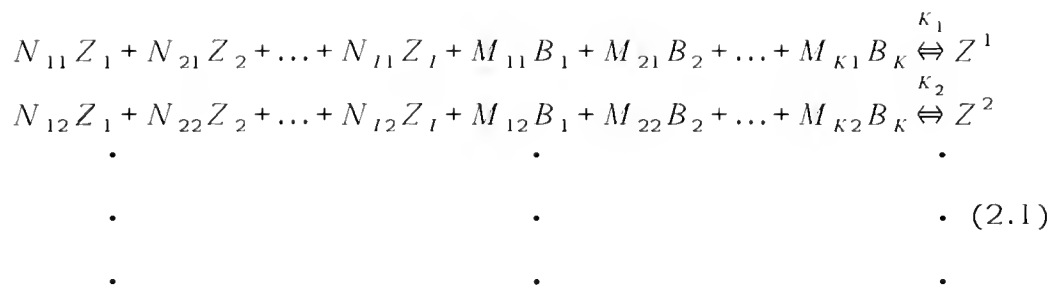
While contributing to our understanding of the complex nature of micelle formation, none of these works produced a practical model with predictive capabilities. A semi-empirical model for the thermodynamic properties of surfactant aggregate formation based on molecular thermodynamic processes was developed by Hourani (1984) and was successful at predicting thermodynamic quantities and aggregate size distributions for systems of a single surfactant species in solution. Benedek (1985) developed a different model in the framework of molecular thermodynamics. While it was demonstrated successfully, the use of empirical parameters was more extensive than in Hourani's work. The model of Hourani showed promise of being extendable to multicomponent systems and of being more closely related to other observable molecular phenomena. The beginnings of such an extension are given in this chapter.

2.2 Stoichiometry and Reaction Equilibria for Multicomponent Micelles

Since the free energy of a process is independent of the path chosen between the initial and final states, Hourani proposed a process consisting of a series of steps for which the free energy change can be modeled. In this process, the monomers were removed from the solvent and placed in a vacuum at their original density--a gaseous state. Cavities of excluded volume remained in the solvent, to be coalesced

in a subsequent step. The monomer gas, considered ideal, was compressed to micellar density, and placed into larger cavities which had been formed in the solvent. Essential to the modeling was the elimination and creation of the solvent cavities. The counterions were handled in the same fashion, with the addition of the necessary electrostatic calculations. Extending Hourani's molecular thermodynamic model to solutions containing two or more surfactant species required the addition of new steps and modification of others. The solvent cavity steps were eliminated and the monomers are removed to a liquid state rather than the gaseous. These changes facilitate the handling of multiple components. The development of the multicomponent model is detailed below.

Micelle formation in solution yields a distribution of micelle sizes. In addition, a multicomponent surfactant solution has a distribution of compositions (Warr et al., 1983; Scamehorn et al., 1982; Birdi, 1975; Moroi et al., 1974, 1975a, 1975b; Rubingh, 1979; Clint, 1975). To describe this, a set of equilibrium reactions can be written for the formation of J micelles of distinct sizes and/or compositions. For I different surfactant species, Z_i , and K counterion species, B_k , aggregating to form J micelles, Z_j^j ,



where N_{ij} is the number of monomers of species i present in the j^{th} micelle and M_{kj} is the number of k counterions bound to it. The equilibrium constant K_j for the formation of the micelle is given by

$$K_j = \frac{[Z^j]}{[Z_1]^{N_{1j}}[Z_2]^{N_{2j}} \dots [Z_i]^{N_{ij}}[B_1]^{M_{1j}}[B_2]^{M_{2j}} \dots [B_k]^{M_{kj}}} \quad (2.2)$$

These are related to the standard state free energy of micellization of the j^{th} micelle by

$$\Delta G_j^\circ = -RT \ln K_j \quad (2.3)$$

The total number of monomers in this micelle is

$$N_j = \sum_i N_{ij} \quad (2.4)$$

so that

$$N_j \Delta \underline{G}_j^\circ = -RT \ln K_j \quad (2.5)$$

where $\Delta \underline{G}_j^\circ$ is on a per monomer basis.

The mole fraction of monomers in the j^{th} micelle is found by combining equations (2.2) and (2.5). For the dilute concentration range of micellar solutions, ideality

of the monomer solution can be assumed, and

$$\frac{X_j}{N_j} = \exp \left[N_j \left(-\frac{\Delta G_j^\circ}{RT} + \sum_i x_{ij} \ln [Z_i] \right) + \sum_k M_{kj} \ln [B_k] - \ln C_o \right] \quad (2.6)$$

where C_o is the total solution concentration

$[]$ indicates concentration of species

x_j is the monomer mole fraction in j^{th} micelle

N_j is the aggregation number of the j^{th} micelle

Within the material balance constraint for each species,

$$x_i = \sum_j x_{ij} \quad (2.7)$$

equation (2.6) describes the distributions of micelle size and composition in solution when provided with the free energy change as a function of the size and composition of the micelle formed.

2.3 Estimation of Free Energy Changes

The standard state free energy of micellization is calculated via the seven-step process shown in Figure 2-1. The standard state free energy of formation for a single micelle in solution is the sum of the free energies of the seven steps. Each step is modeled as closely as possible from an observable phenomenon of a similar nature.

Certain free energy terms are dependent on the shape of the micelle. The micelle grows as a roughly spherical aggregate until the additional volume of one more monomer would cause the radius of the sphere to exceed the length of the longest all-trans chain. With the addition of the next

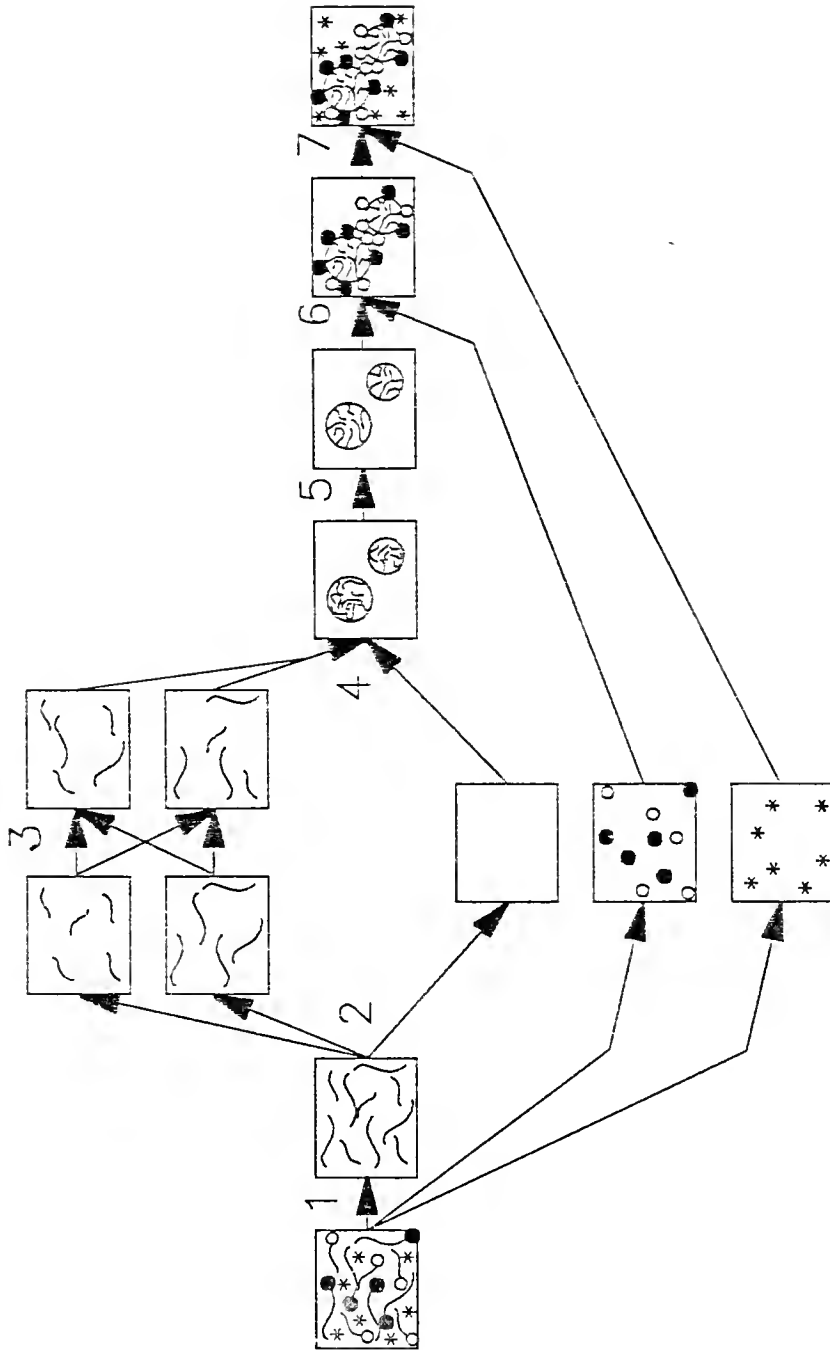


Figure 2-1. The seven-step reversible process used in the estimation of contributions to the total Free Energy of micellization in a multicomponent surfactant solution. From left to right: Head groups and counterions are removed; surfactant chains (hydrocarbons) and solvent are separated into discrete phases; the hydrocarbons are mixed into compositions of the micelles; hydrocarbon droplets are placed in the solvent; chain ends are brought to the surface; head groups are replaced; and counterions are replaced.

monomer the micelle must grow with a nonspherical geometry to avoid the formation of a material-free core. Several geometries have been proposed: spherical dumbbells, oblate ellipsoids, prolate ellipsoids, and spherocylindrical rods. While Ljunggren and Eriksson (1984, 1986; Eriksson and Ljunggren, 1985) have proposed that the shape fluctuates between spherical, rod-shaped, and even disc-shaped, Vold (1985) has found little effect of the particular geometric model on the thermodynamics of micelle formation. In this work nonspherical micelles are modeled as prolate spherocylindrical rods. The derivation of micelle dimensions and surface area based on this geometric model is given in Appendix A.

In step 1, a standard state solution of surfactants is transformed into a solution of hydrocarbon chains by reversibly removing the head groups and counterions. Since these are reversibly replaced in steps 6 and 7, the net free energy change for the mere removal and replacement of the head groups and counterions is zero. If no free energy contributions due to the replacement of head groups and counterions are contained in steps 6 and 7, then

$$\Delta G_1^\circ = 0 \quad (2.8)$$

In step 2 the hydrocarbon solution is separated into I pure hydrocarbon liquids and the pure solvent. This is the

reverse process of hydrocarbon solubility, so

$$\frac{\Delta G_2^\circ}{RT} = \sum_j \sum_i x_{ij} \ln C_i^{\text{eq}} \quad (2.9)$$

In step 3 the I pure hydrocarbons are placed into J ideal hydrocarbon mixtures of different compositions and amounts. For this ideal mixing,

$$\frac{\Delta G_3^\circ}{RT} = \sum_j \sum_i x_{ij} \ln x_{ij} \quad (2.10)$$

In step 4 the J hydrocarbon mixtures are formed into J droplets and placed into the solvent. The free energy of this step is the free energy of forming the hydrocarbon-solvent interface. There are both surface area and curvature contributions to this step. The expression for ΔG_4° , based on Buff (1955) and Stillinger (1973), is the surface area of the droplet, S, times the planar interfacial tension, γ , of the hydrocarbon mixture, corrected for curvature:

$$\frac{\Delta G_4^\circ}{RT} = \frac{S\gamma}{NkT} \left(1 - \frac{g}{R} \right) \quad (2.11a)$$

The curvature effect is dependent on the parameter, g. The surface area depends on the size and shape of the micelle. For the spherocylindrical micelle, a second curvature parameter, gc, is used for the cylindrical portion:

$$\frac{\Delta G_4^\circ}{RT} = \frac{2\pi R\gamma}{NkT} \left[2R \left(1 - \frac{g}{R} \right) + L \left(1 - \frac{gc}{R} \right) \right] \quad (2.11b)$$

This approximates the cylindrical curvature effect, whose uncertainty has been discussed by Henderson and Rowlinson (1984).

In step 5 conformational changes in the hydrocarbon chains are made so that one end of each chain is at the surface of the droplet. The contribution from this step is entirely entropic and may only be estimated. The expression used in this model is

$$\frac{\Delta G_s^\circ}{RT} = -S_c \left(\frac{l_c}{R} \right)^2 \quad (2.12)$$

where S_c is a parameter of the model. The squared ratio of chain length, l_c , to micelle radius, R , takes into account the very severe conformational restrictions present when the micelle radius is much smaller than the chain length.

As indicated in the discussion of step 1, step 6 contains no contribution due to the reattachment of head groups. The quantity ΔG_6° is the free energy change due to the interaction between the head groups in their positions at the micelle surface. The head groups are modeled as dipoles. For the ionic surfactant species, a charged head group paired with a counter ion forms a strong dipole. Nonionic head groups exhibit weak-to-moderate dipole moments. The dipole-dipole interactions of adjacent pairs are summed for the free energy contribution of this step. The separation and orientation between two dipoles are

dependent on the size and shape of the micelle, with the head groups evenly spaced over the surface of the micelle. The derivation of the head group interactions is carried out in Appendix B. The potential between a pair of adjacent head groups is

$$E_{12} = \frac{\mu_1 \mu_2}{D r^3} \left[1 + \left(\frac{r}{2R} \right)^2 \right] \quad (2.13)$$

where μ is the dipole moment

r is the pair separation

R is the micelle radius

D is the dielectric constant of the solvent

As indicated in the derivation, this form of the potential takes into account the angle between adjacent dipoles as a function of micelle radius. The total energy contribution from this step is found by summing the contributions from the different pairs in the manner described by equations (B.25) through (B.28) in Appendix B.

Step 7 contains no contribution for the replacement of the counterions back into solution. The free energy of this step is due to the difference between the original random distribution of counterions in the micelle-free solution and the final Poisson-Boltzmann distribution of counterions around the surface of the micelle with a fraction bound in a Guoy-Chapman electrical double layer. The derivation of Hourani (1984) for the numerical solution of this charge

distribution model is applicable here. The entire step is actually the process of discharging the counterions in their original distribution, compressing them into the bound layer and final distribution, and then recharging the counterions. Therefore ΔG_7° contains an entropy contribution from the compression and an enthalpy contribution from the distribution. The bound layer will be populated with dipoles formed by head group/counterion bound pairs and unbound head groups. The charge interactions in the bound layer are included in the dipole and point charge pairings of the head group term, ΔG_6° .

2.4 The Computational Technique

The free energy of formation for a single mixed micelle with nonionic head groups is obtained by summing the contributions from steps 1 through 6:

$$\frac{\Delta G_f^\circ}{RT} = \sum_i (x_{ij} \ln C_i^{\text{eq}} + x_{ij} \ln x_{ij}) + \frac{2\pi R_j \gamma_j}{NkT} \left[L \left(1 - \frac{gc}{R_j} \right) + 2R_j \left(1 - \frac{g}{R_j} \right) \right] - S_c \left(\frac{l_c}{R_j} \right)^2 + \frac{E_j}{RT} \Big|_{\text{heads}} \quad (2.14)$$

To include the presence of ionic head groups and counterions, the contributions of step 7 must be added to equation (2.14). Such calculations were not carried out here, so this section will pertain only to mixtures of nonionic surfactants. Table 1 summarizes the model's variables, parameters, and required data.

Table 1
Arguments of the Thermodynamic Model

Variables	x_{ij}	Compositions of micelles
	N_j	Aggregate sizes of micelles
	T	Temperature of system, Kelvin
	x_i	Composition of system
	n_c	Number of carbons in surfactant chain
	C_{tot}	Overall system concentration, moles/liter
Data	C_i^{eq}	Solubility concentrations of hydrocarbons, moles/liter
	γ_j	Interfacial tensions of hydrocarbon mixtures, dynes/cm
	μ_i	Dipole moments of head groups, Debyes
	D	Dielectric constant of water
	l_c	Surfactant chain length, Angstroms
Parameters	v_c	Surfactant chain volume, Angstroms ³
	g	Spherical curvature parameter, Angstroms
	gc	Cylindrical curvature parameter, Angstroms
	S_c	Entropy of conformation parameter

The values of chain length (Ang.) and chain volume (Ang.³) used in the determination of micelle size and shape are calculated from Tanford's correlations (Tanford, 1972):

$$l_c = 1.265n_c + 1.5 \quad (2.15)$$

$$v_c = 26.9n_c + 27.4 \quad (2.16)$$

To facilitate the use of computer programs in carrying out the calculations, correlations are used for the required physical data. The aqueous solubility of hydrocarbons used in the calculation of ΔG_2° is obtained from a correlation due to Leinonen et al. (1971):

$$x^{eq} = \exp \left\{ - \left[\left(1 - 2x^{eq} \right) \frac{K}{RT} - \ln(1 - x^{eq}) \right] \right\} \quad (2.17)$$

The parameter K is fit to the solubility data of McAulliffe (1966), Polak and Lu (1973), and Sutton and Calder (1974). It is found to be a linear function of the hydrocarbon chain length for the n-alkanes, but since hydrocarbon solubility in water exhibits a break at decane, two linear relationships for K are used, one for the longer chains and one for the shorter chains. Equation (2.17) is solved iteratively for the hydrocarbon solubility, x^{eq} .

For the hydrocarbon-water interfacial tension required in the calculation of ΔG_4° , a correlation based on the works of Aveyard et al. (1972), on the surface tension of hydrocarbons, and Jasper (1972), on the surface tension of

water, is used:

$$\gamma = 1.381 \frac{57.868n_c + 117.99 - .059n_c + .1768T}{n_c + 2.4} \quad (2.18)$$

where the temperature is in Kelvin and the surface tension is in dynes/cm.

The value of the dielectric constant of water used in the evaluation of ΔG_6° is given by

$$D = 252.422 - .806329T + .0007469T^2 \quad (2.19)$$

which is a polynomial fit of the data of Owen et al. (1961) at atmospheric pressure with temperature in Kelvin. The values of dipole moments used in this calculation are estimated as the dipole moments of molecules of similar structure to the head groups.

The three parameters, g , g_c , and S_c , are fit to the measurable data on the micellar system. These are the mean aggregate size of the micelles and the set of mixture critical micelle concentrations (CMCs) at the system temperature. Equation (2.6) generates an I-dimensional surface of the aggregate size distribution of the multicomponent micelles. This is accomplished by first choosing values of the temperature, T , the total concentration, C_{tot} , and the system composition, x_i . Then for each possible micelle composition, x_{ij} , equation (2.6) is evaluated at values of N_j from two to infinity (in practice, until X_j/N_j becomes negligible). This generates

the distribution of aggregate sizes with micelle composition. The parameters must be chosen such that the distribution meets the material balance constraints of equation (2.7).

To find the proper values of the parameters, the mean size is calculated as

$$\bar{N} = \frac{\sum_j \underline{X}_j}{\sum_j \underline{X}_j / N_j} \quad (2.20)$$

and the CMC is taken to be the value for which

$$\lim_{C_{tot} \rightarrow CMC} \frac{\partial(C_1 + C_M)}{\partial C_{tot}} = 0.5 \quad (2.21)$$

as put forth by Hall and Pethica (1967). Here, C_1 is the free monomer concentration and C_M is the concentration of micelles, calculated as

$$C_M = \frac{C_{tot} - C_1}{\bar{N}} \quad (2.22)$$

Once a set of parameters is determined for a system, the response of the size distribution to changes in any of the input variables can be investigated.

The program listing in Appendix C gives the FORTRAN source for the interactive fitting of parameters and calculation of aggregate size distribution on systems of a

single nonionic surfactant species in water. This is the simplest application of the model and was used to generate the results presented in the next chapter.

CHAPTER 3 RESULTS OF THERMODYNAMIC MODELING

3.1 Parameter Estimation

Three parameters of the model, g , g_c , and S_C , must be found by fitting the mean aggregate size generated by the model to the experimental value at the critical micelle concentration (CMC). The model output is considered to be at the CMC when the total surfactant concentration is equal to the experimental value of the CMC and the derivative of the monomer concentration with respect to the total concentration satisfies equation (2.21), indicating that one out of two surfactant monomers added to the solution at this concentration would join a micelle. The model convergence is quite sensitive to the values of the parameters, so in fitting them to the data, one must either use good initial guesses or approach the values conservatively. Failure to do either of these can result in an aggregate size distribution which has infinite values of C_{tot} and \bar{N} , providing no useful information.

Each of the parameters has a physical significance which can aid in the choice of the initial guesses. The parameters g and g_c are used in the curvature corrections to the planar interfacial tension for the spherical and

cylindrical geometries, respectively. Physically, g is the thickness of the spherical interface in Angstroms (Buff, 1955). Although experimental values are not available, it is expected to be positive and small relative to the micelle radius. The parameter g_c does not have the same physical connection to the interface (Henderson and Rowlinson, 1984), but by comparison it is expected to be positive and less than g . The parameter S_C is the (dimensionless) conformational entropy change for a monomer joining a large micelle. Conformational contributions of the aggregated monomers were studied via a statistical thermodynamic theory by Ben-Shaul and coworkers (Ben-Shaul, Szleifer and Gelbart, 1985; Szleifer, Ben-Shaul and Gelbart, 1985) and values of the conformational entropy were found to be in the range of -8 to -7 for a chain with seven bonds. While these values are based strictly on theoretical considerations with no experimental corroboration, the parameter S_C is expected to be of the same sign and magnitude.

In approaching the parameter fitting conservatively, the initial values of the parameters are chosen such that the aggregate size distribution will definitely converge. That is, the condition

$$\lim_{N \rightarrow \infty} \frac{\partial \left(\frac{x_i}{N} \right)}{\partial N} < 0 \quad (3.1)$$

must be satisfied. Equation (2.6) defines the aggregate size distribution. In this equation, ΔG_j° is the only term influenced by the parameters. In order for the distribution to converge as N becomes large, this free energy change must be greater than the logarithm of the monomer concentration. Overestimating the parameters toward a less negative free energy change will assure that the size distribution converges. The parameters can then be adjusted toward a more negative free energy change as they are fit to the data.

The effect of adjusting the parameters can be foreseen by analyzing the corresponding terms. The parameters g and g_c affect the behavior of the surface free energy, ΔG_4° . For $g < R$ and $g_c < l_c$, the usual cases, increasing the parameter decreases the free energy, consistent with equation (2.11). In equation (2.12) it can be seen that increasing the parameter S_c decreases the conformational free energy, ΔG_5° .

The aggregate size distribution can be divided into two regions. By designating the value of N for which $R = l_c$ as N_{trans} , the transition of the micelle geometry from spherical to spherocylindrical defines the two regions of the size distribution. For $N \leq N_{trans}$, the micelle is spherical with radius R . For $N > N_{trans}$, the micelle is spherocylindrical with radius l_c and length L . For sizes

above N_{trans} , the conformational free energy is constant with a value of $-S_C$. At N_{trans} the surface free energy makes the transition from being equal to the spherical contribution to becoming dominated by the cylindrical contribution for large N . Figures 3-1 and 3-2 show the effect of aggregate size and parameter values on the surface and conformational free energies.

A typical aggregate size distribution generated for a nonionic surfactant is shown in Figure 3-3. A peak occurs at N_{trans} , beyond which the fraction of aggregate decreases with increasing N . The total surfactant concentration is proportional to the area under the distribution and is thus influenced by both the height of the peak and the slope of the distribution above N_{trans} . Because the distribution below N_{trans} rises so rapidly, the mean aggregate size, \bar{N} , is dependent only on the slope of the distribution above N_{trans} .

The parameter S_C , since it contributes over the entire range of N , affects both C_{tot} and \bar{N} . The parameter g_C , contributing only above N_{trans} , has a significant effect on \bar{N} but only a slight effect on C_{tot} , while g influences only C_{tot} and not \bar{N} . This causes such interplay between the parameters that a range of parameter sets can produce identical values of C_{tot} and \bar{N} . The derivative constraint,

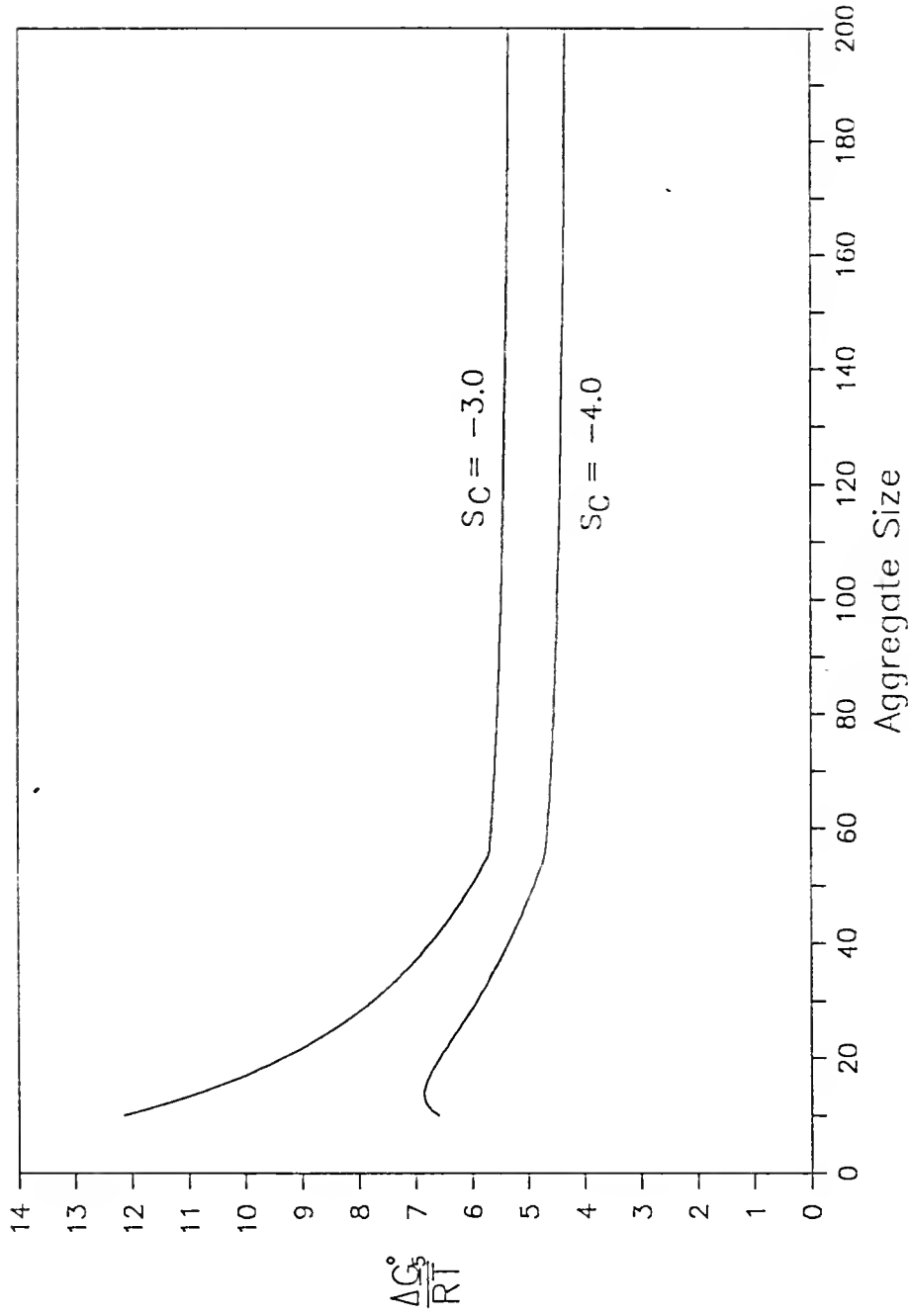


Figure 3-1. The surface contribution to the free energy of micelle formation for the C12 nonionic micelle at the CMC and a temperature of 298.15 Kelvin. The lower curve was generated with $S_C = -4.0$, $g = 6.9586$, $g_c = 3.6272$. The upper curve was generated with $S_C = -3.0$, $g = 4.8879$, $g_c = 0.51846$. The lower curve demonstrates the effect of g exceeding the micelle radius at low values of N .

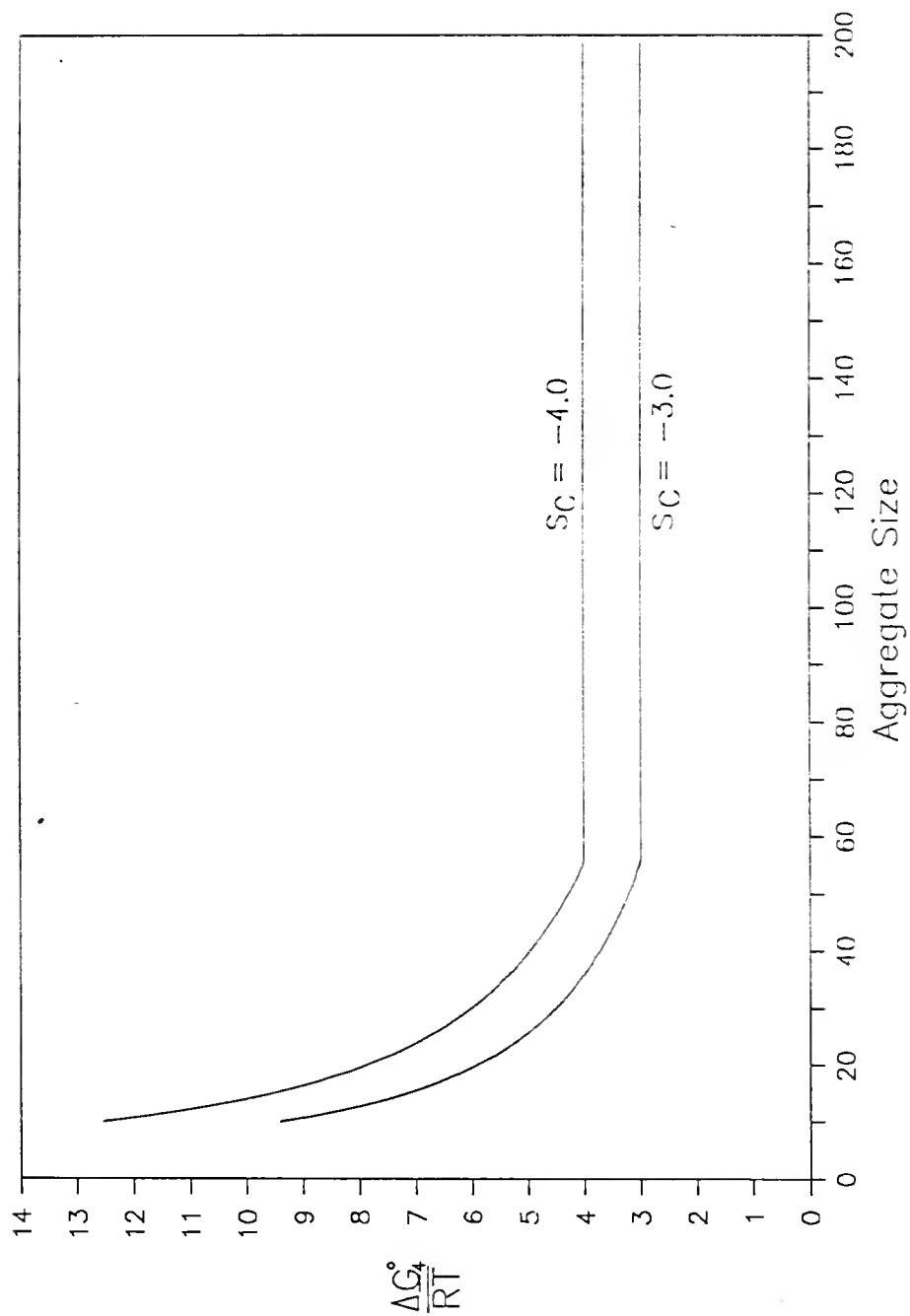


Figure 3-2. The conformational contribution to the free energy of micelle formation for the C12 nonionic micelle at the CMC and a temperature of 298.15 Kelvin. The parameters are as in Figure 3-1, showing the effect of S_C .

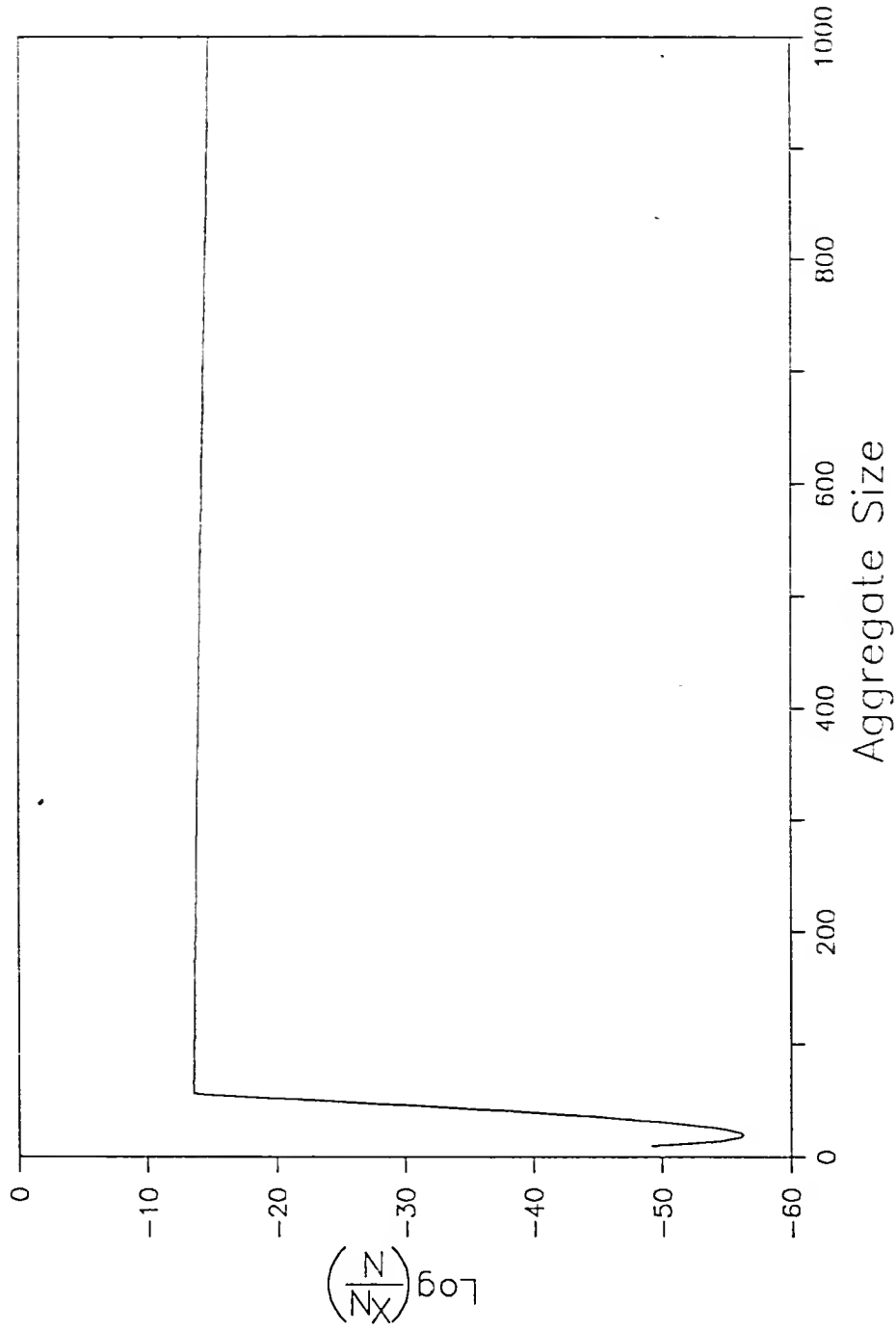


Figure 3-3. Aggregate size distribution for the C12 nonionic micelle at the CMC and a temperature of 298.15 Kelvin. Typical behavior of the size distributions of nonionic surfactants is exhibited.

(2.21), can also be satisfied by these parameter sets if they are fit at a value of the free monomer concentration, C_1 , just below the critical micelle concentration.

The method used to fit parameters consisted of first choosing low values of the parameters, resulting in a C_{tot} essentially equal to C_1 and an \bar{N} insignificantly larger than N_{trans} . The parameter gc was increased until \bar{N} reached the desired value, and then g was adjusted to result in the proper C_{tot} . This is repeated for different values of S_C to generate the range of parameter sets fitting the data. The experimental data used to generate the parameters is given in Table 2.

3.2 Behavior of the Model for Single-Component Nonionic Systems

Parameter fitting was carried out on systems of different surfactant chain lengths and at different temperatures. For each system, linear relationships were found to exist between each pairing of the three parameters. Corresponding to the manner in which the fitting was accomplished, the curvature parameters g and gc can each be expressed as a straight line plotted against the S_C abscissa. Such a plot is given in Figure 3-4. These expressions are of the form

$$g = mS_C + b \quad (3.2)$$

$$gc = nS_C + d \quad (3.3)$$

Table 2
Data Used in Fitting Model Parameters for Aqueous Solutions
of Nonionic Surfactants

<u>Surfactant</u>	<u>T (Kelvin)</u>	<u>CMC (M)</u>		<u>Mean Size</u>	
$C_{10}H_{21}(OC_2H_4)_6OH$	298.15	9.0E-04	a	73	a
	308.15	6.6E-04		260	
	318.15	6.4E-04		640	
$C_{12}H_{25}(OC_2H_4)_6OH$	298.15	8.7E-05	b	400	c
$C_{14}H_{29}(OC_2H_4)_6OH$	298.15	1.1E-05	a	3100	a

a: Balmbra et al. (1964)

b: Corkill et al. (1961)

c: Balmbra et al. (1962)

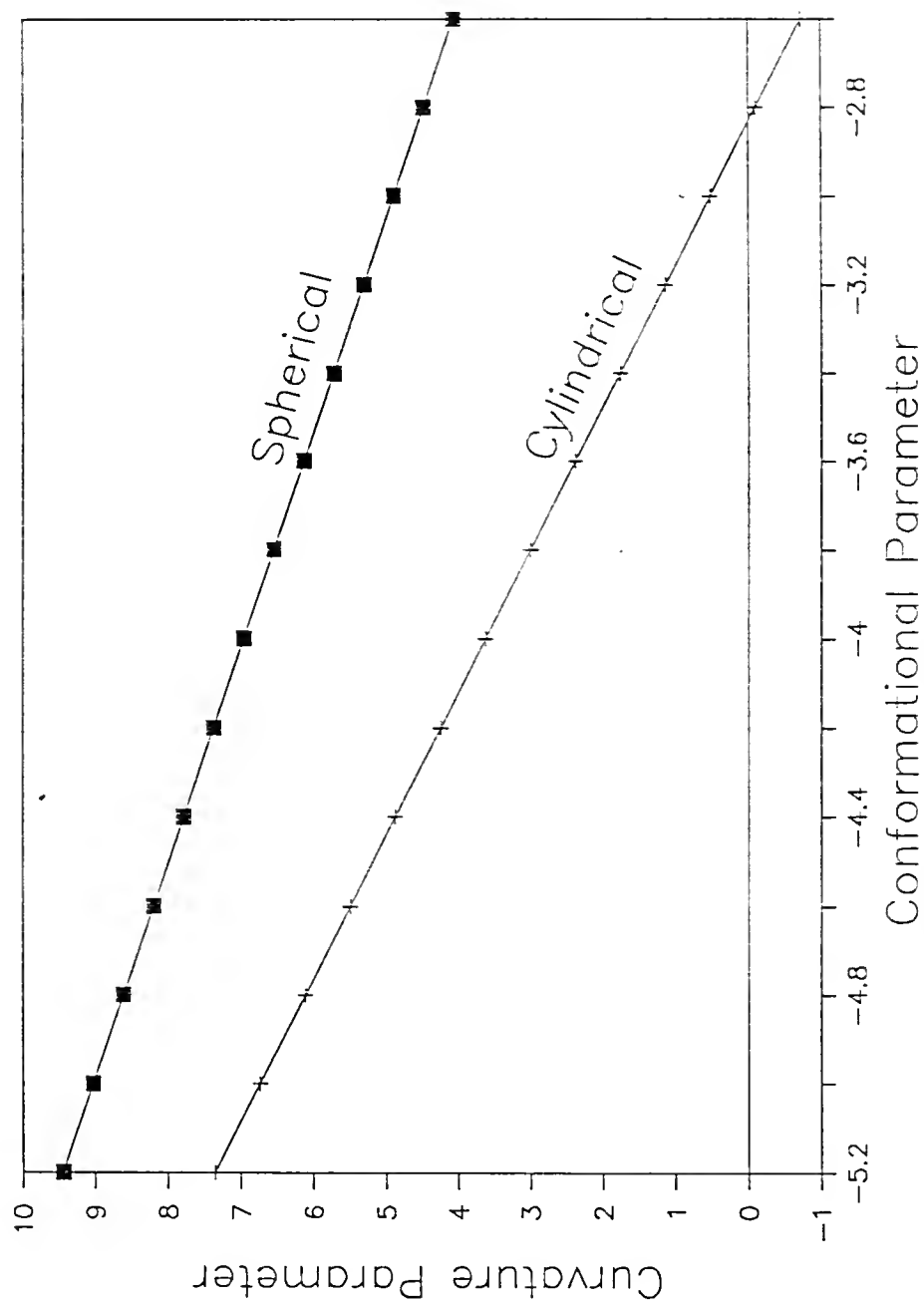


Figure 3-4. Interdependence of the model parameters for the C12 nonionic micelle at 298.15 Kelvin. The symbols represent the values of the spherical (g) and cylindrical (gc) curvature parameters. The lines give the regression results $g = -1.3235 - 2.0705S_C$ and $gc = -8.808 - 3.1087S_C$.

The values of the slopes and intercepts found for the systems modeled are given in Table 3.

Many aspects of surfactant behavior have been found to be linearly dependent on chain length and/or temperature (Rosen, 1978). The information in Table 3 indicates that such relationships are also possible for the interaction of the parameters of this model. Though the three chain lengths and three temperatures investigated cannot conclusively indicate linear behavior, they can indicate whether this behavior is likely. Linear regression of the slopes and intercepts of Table 3 versus chain length and temperature resulted in the following equations and correlation coefficients:

$$m = -.0089T + .8817 \quad R = .9998 \quad (3.4)$$

$$b = .0549T - 20.20 \quad R = .9778 \quad (3.5)$$

$$n = -.0137T + 1.421 \quad R = .9999 \quad (3.6)$$

$$d = .1125T - 45.09 \quad R = .9810 \quad (3.7)$$

for the 10 carbon nonionic, and

$$m = -.1464n_c - .3170 \quad R = .9999 \quad (3.8)$$

$$b = 1.418n_c - 18.10 \quad R = .9988 \quad (3.9)$$

$$n = -.2201n_c - .4676 \quad R = 1.000 \quad (3.10)$$

$$d = 1.553n_c - 27.29 \quad R = .9991 \quad (3.11)$$

at a temperature of 298.15 Kelvin.

Table 3
Slopes and Intercepts of Curvature Parameter Dependence
on Conformational Parameter

<u>n_C</u>	<u>T (Kelvin)</u>	<u>g slope</u>	<u>g int.</u>	<u>gc slope</u>	<u>gc int.</u>
10	318.15	-1.96163	-2.80775	-2.94330	-9.43866
10	308.15	-1.86885	-3.15286	-2.80330	-10.1776
10	298.15	-1.78296	-3.90518	-2.66898	-11.6881
12	298.15	-2.07048	-1.32359	-3.10874	-8.80775
14	298.15	-2.36862	1.74162	-3.54946	-5.47762

Substituting (3.4) through (3.11) into (3.2) and (3.3), the temperature relations for C10 nonionic are

$$g = (.0549 - .0089S_c)T - 20.20 + .8817S_c \quad (3.12)$$

$$gc = (.1125 - .01372S_c)T - 45.09 + 1.4214S_c \quad (3.13)$$

and the chain length relations at 298.15 Kelvin are

$$g = (1.418 - .1464S_c)n_c - 18.10 - .3170S_c \quad (3.14)$$

$$gc = (1.553 - .2201S_c)n_c - 27.29 - .4676S_c \quad (3.15)$$

These relations are only valid for values of S_c which, for each chain length, produce values of the curvature parameters which are neither negative nor larger than the micelle radius. In this sense, S_c is dependent on chain length, but there remains a lack of uniqueness in the parameter fitting for the single component case. This results from the finding that the CMC and the concentration derivative (2.21) are not independent of each other.

The free energy of micellization and its various contributions, as given by the model, are shown in Figures 3-5 through 3-8. These plots were made for two chain lengths at the same temperature, two temperatures with the same chain length, and two parameter sets at the same chain length and temperature. Figures 3-5 and 3-8 show the effect of two different parameter sets for the same system. While the surface and conformational contributions are different due to the different parameters, the total free energy of micellization is the same in the two figures. This follows

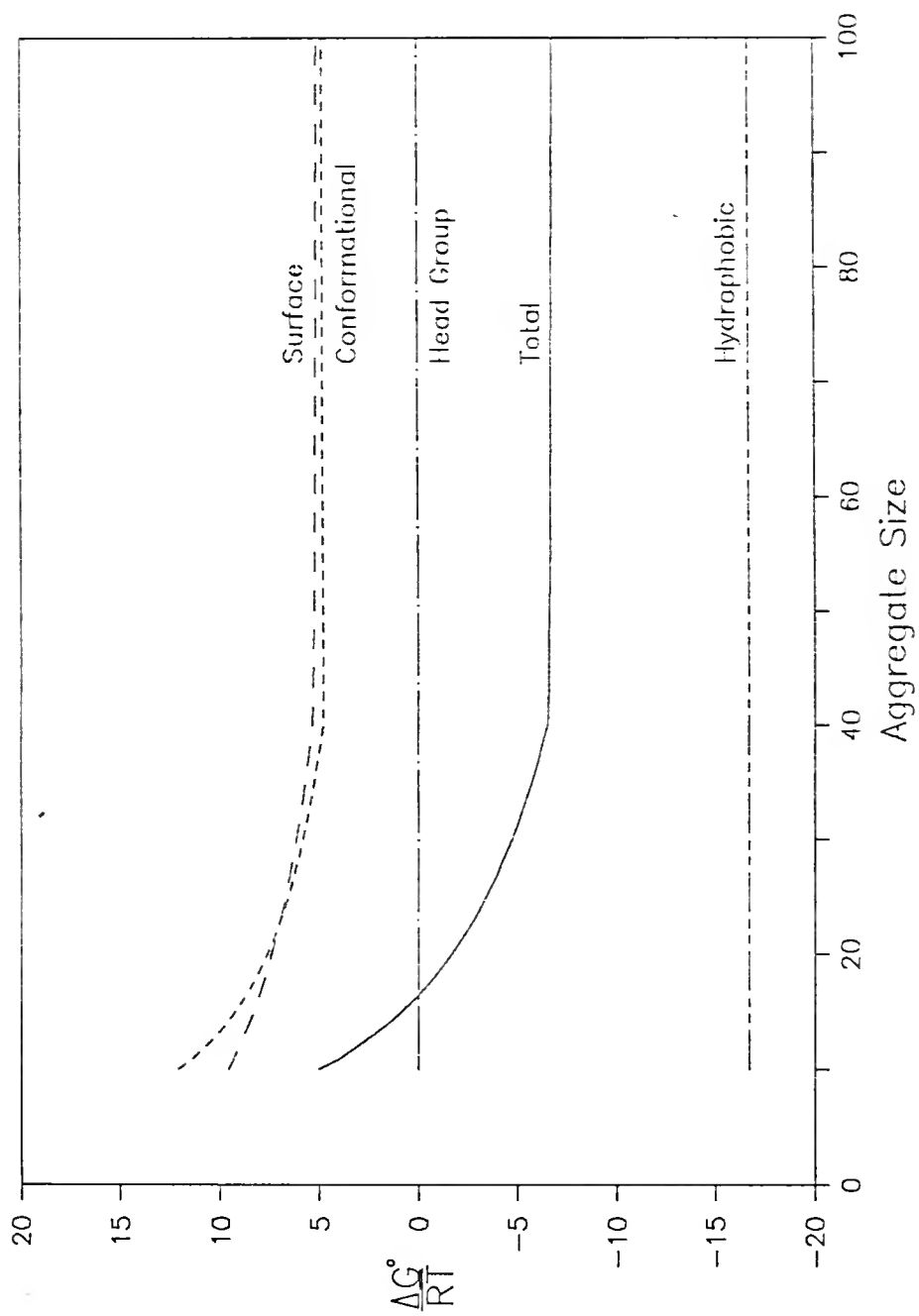


Figure 3-5. Free energy contributions for the C10 nonionic micelle at the CMC and a temperature of 298.15 Kelvin. A value of -4.8 is used for the conformational parameter, s_G , with the curvature parameters fit to the data.

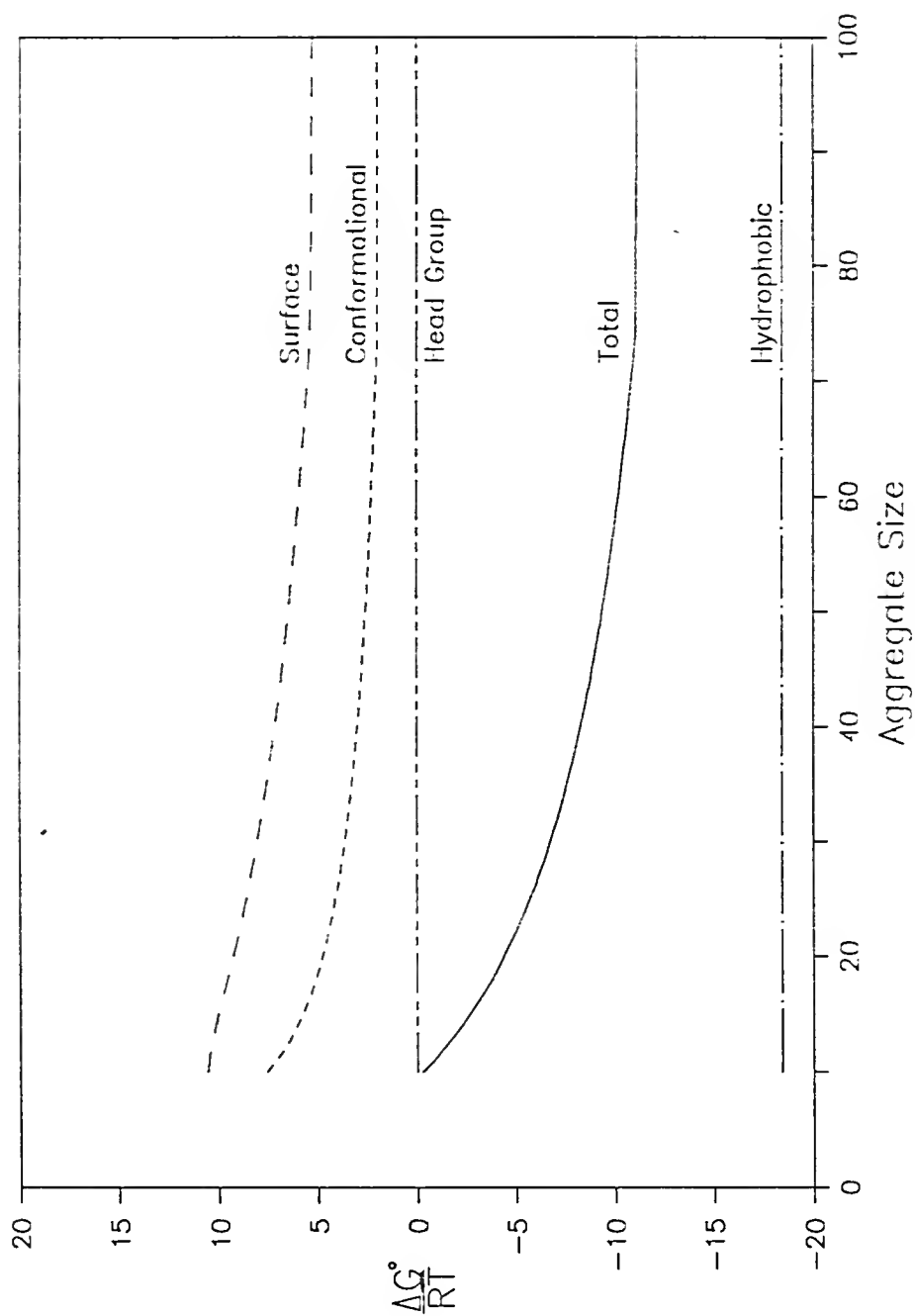


Figure 3-6. Free energy contributions for the C14 nonionic micelle at the CMC and a temperature of 298.15 Kelvin. A value of -2.0 is used for the conformational parameter, S_C .

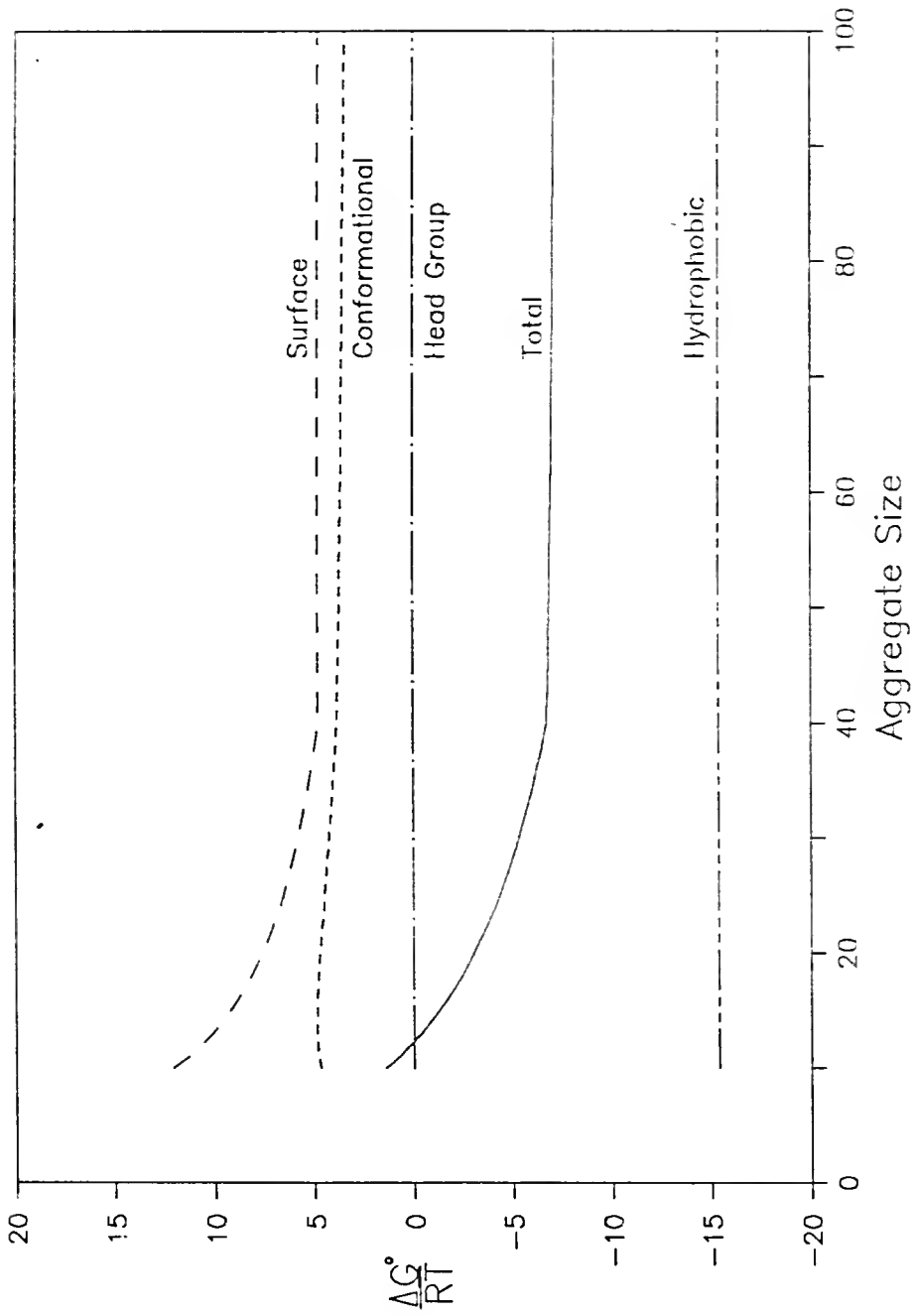


Figure 3-7. Free energy contributions for the C10 nonionic micelle at the CMC and a temperature of 318.15 Kelvin. A value of -4.8 is used for the conformational parameter, s_C .

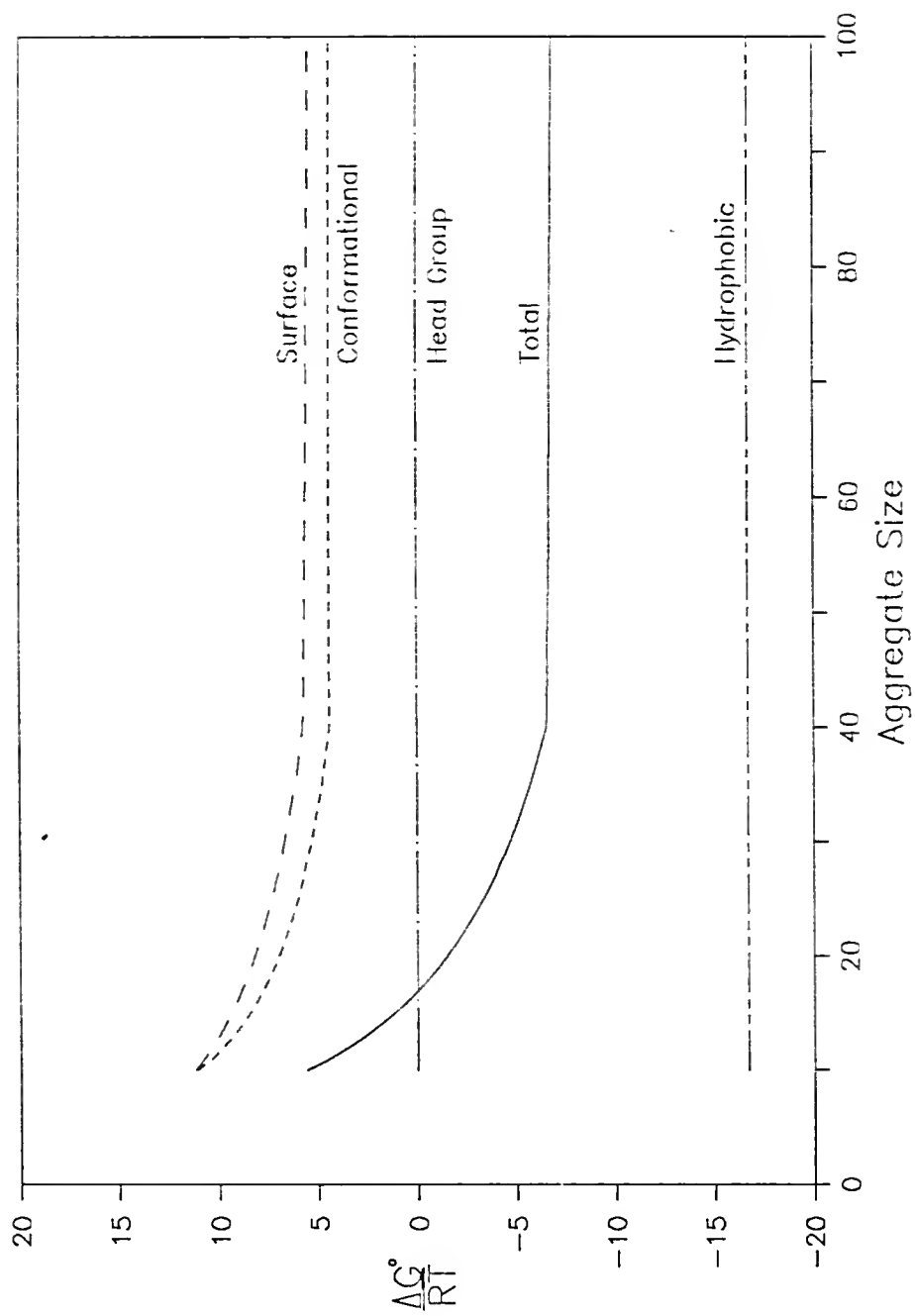


Figure 3-8. Free energy contributions for the C10 nonionic micelle at the CMC and a temperature of 298.15 Kelvin. A value of -4.0 is used for the conformational parameter, S_C .

from the fact that the parameter sets were fit to the same concentration and mean size data and generate identical size distributions.

3.3 Aggregate Size Distribution and Concentration Behavior

With the parameter sets determined by the methods described above, the aggregate size distributions and the effects of surfactant concentration were investigated for the nonionic alkyl surfactants. The size distributions for this class of surfactants exhibit a rapid increase in the spherical region of N , peaking at N_{trans} . In the nonspherical region, the distribution decreases very slowly through large values of N , producing the large mean aggregate sizes which have been measured for the nonionic surfactants.

The size derivative of the distribution in the nonspherical region is negative. With increasing free surfactant monomer concentration, it becomes less negative, resulting in a higher mean aggregate size and total surfactant concentration. The effect of surfactant concentration on the modeled size distribution and mean aggregate size of the C12 nonionic surfactant is shown in Figures 3-9 and 3-10. Below the CMC, the model calculates a mean aggregate size approximately equal to N_{trans} , present as the initial plateau in figure 3-10. This value is meaningless, however, since the concentration of micelles in this range

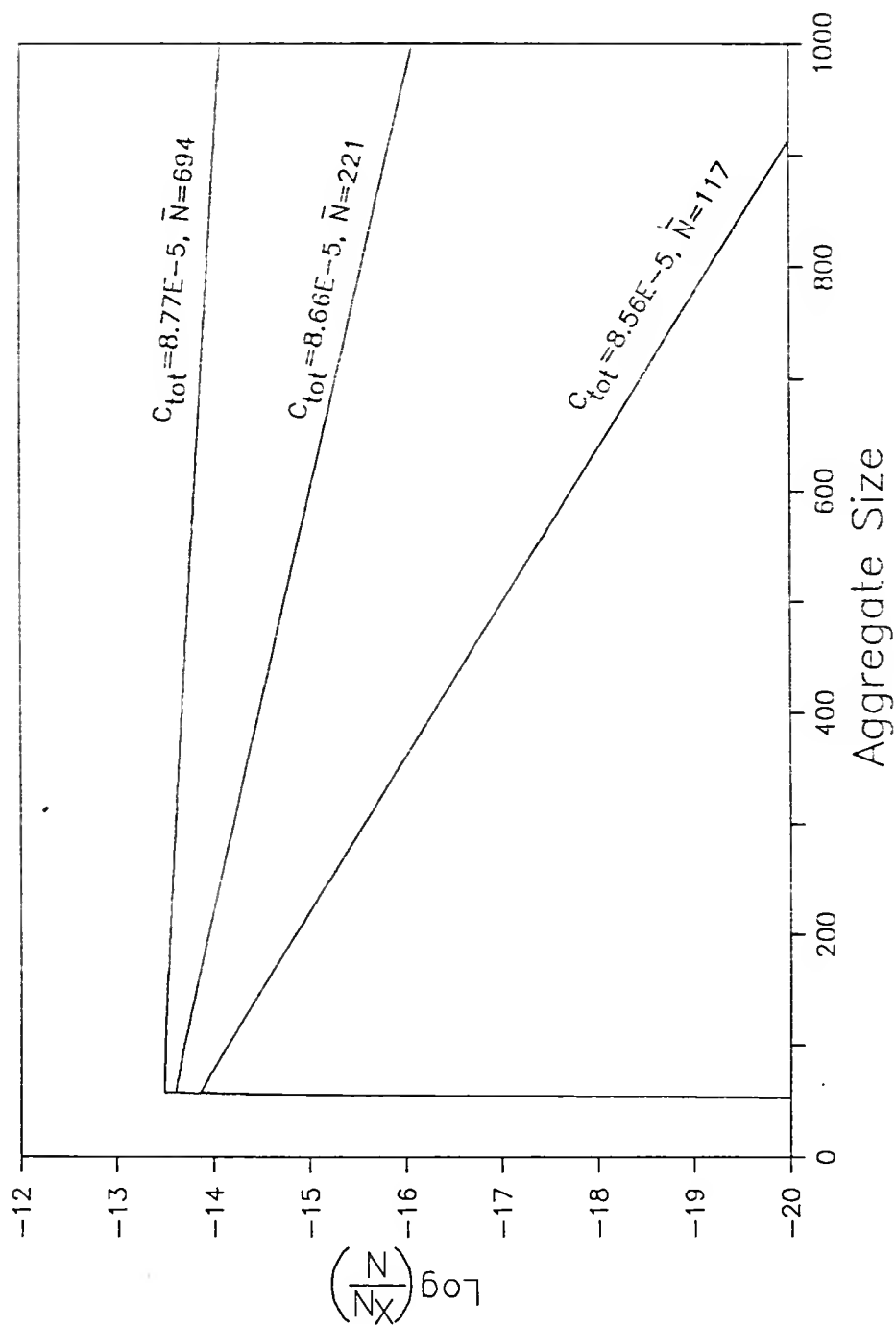


Figure 3-9. Effect of total surfactant concentration on the aggregate size distribution of the C12 nonionic micelle at 298.15 Kelvin.

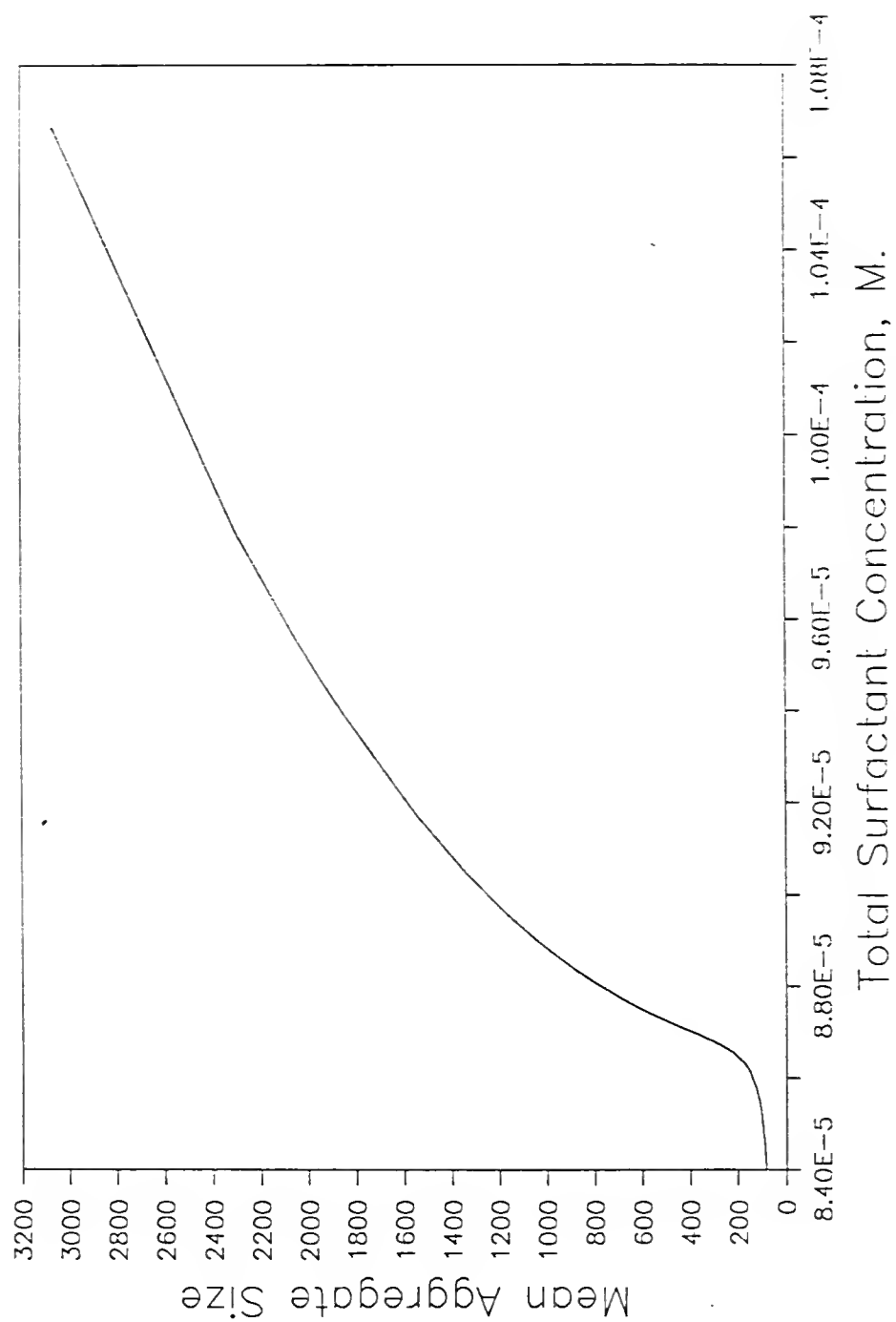


Figure 3-10. Effect of total surfactant concentration on the mean aggregate size of the C12 nonionic micelle at 298.15 Kelvin.

of surfactant concentration is insignificant. The result is merely the ratio of two extremely small numbers, since the model always produces a finite value for the concentration of micelles (equation (2.6)).

Measurement of properties such as surface tension, which depend on the free monomer concentration, show that beyond the CMC the free monomer concentration is virtually unaffected by an increase in the total surfactant concentration. The relationship between the free and total surfactant concentrations, as predicted by the model, is exhibited in Figure 3-11. At total concentrations lower than the CMC, the majority of any surfactant added to the solution exists as free monomers, while at concentrations higher than the CMC the bulk of any additional surfactant micellizes. The definition of the CMC used in this work, as expressed in equation (2.21), quantifies the break between these two behaviors of the solution. Figure 3-12 shows the concentration derivative of equation (2.21) for the data of Figure 3-11 with the CMC identified.

3.4 Chain Length and Temperature Effects

It is known that the hydrophobic nature of the alkyl chain increases with its chain length, as evidenced by the decreasing solubility in water of the increasingly long

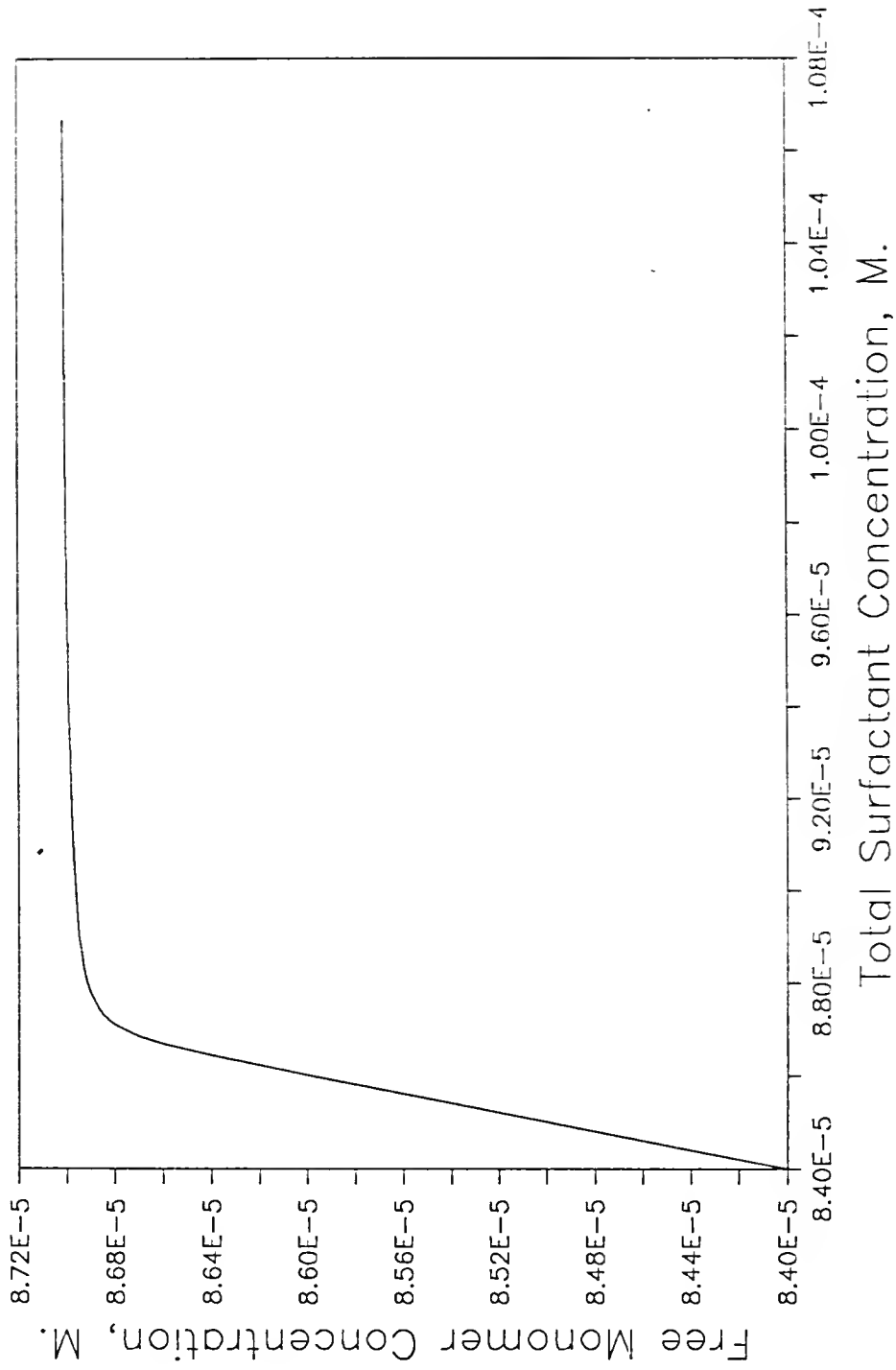


Figure 3-11. Effect of total surfactant concentration on the free monomer concentration of the C12 nonionic at 298.15 Kelvin. The CMC of this system is $8.70\text{E}-5$ M.

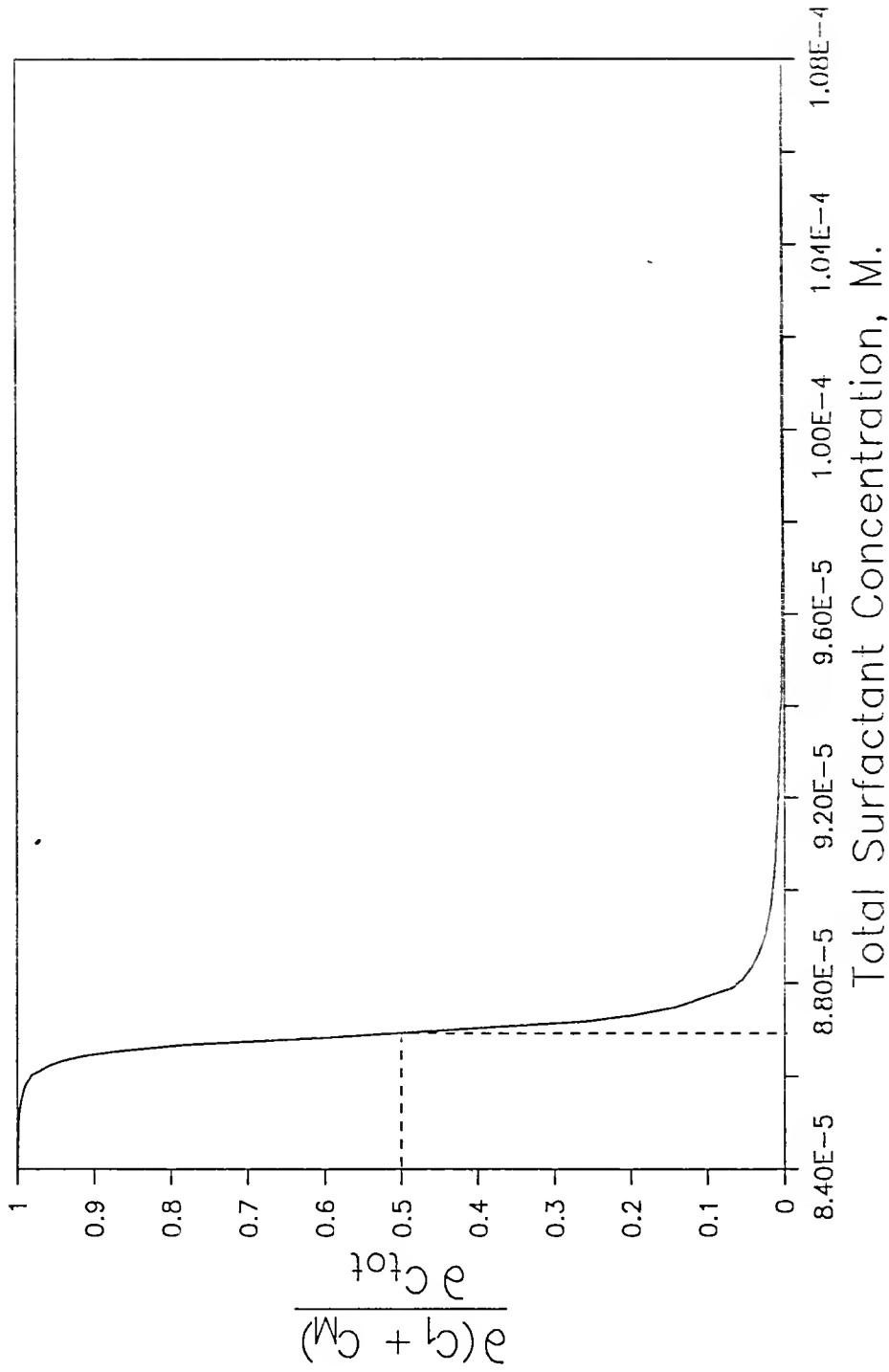


Figure 3-12. Effect of total surfactant concentration on the concentration derivative of equation (21) for the C12 nonionic at 298.15 Kelvin. The dashed line shows that the value of this derivative is 0.5 at the CMC of $8.7\text{E-}5$ M.

chains (McAulliffe, 1966). With alkyl surfactants, this increasing hydrophobicity promotes micellization. While no significant aggregate formation is observed for chains of six carbons or less, increasing chain length brings about the formation of larger micelles at lower critical micelle concentrations (Table 2).

The elements of the model which depend on chain length are the hydrophobic free energy, taken directly from the aqueous solubility, the curvature parameters, accounting for the difference in micelle radius, and the conformational free energy. Equations (3.14) and (3.15) show the relationship of the parameters to the chain length. The aqueous solubility of the alkane, which is chain-length dependent, is used by the model in the fitting of the parameters. The dependence of the aggregate size distribution and free energy change on the surfactant chain length is shown in Figures 3-13 and 3-14. The size distribution broadens with increasing chain length, yielding a much larger mean aggregate size with a less significant increase in the CMC. The free energy of micellization becomes more negative with increasing chain length, showing that micelle formation by surfactants with more hydrophobic area is more thermodynamically favored.

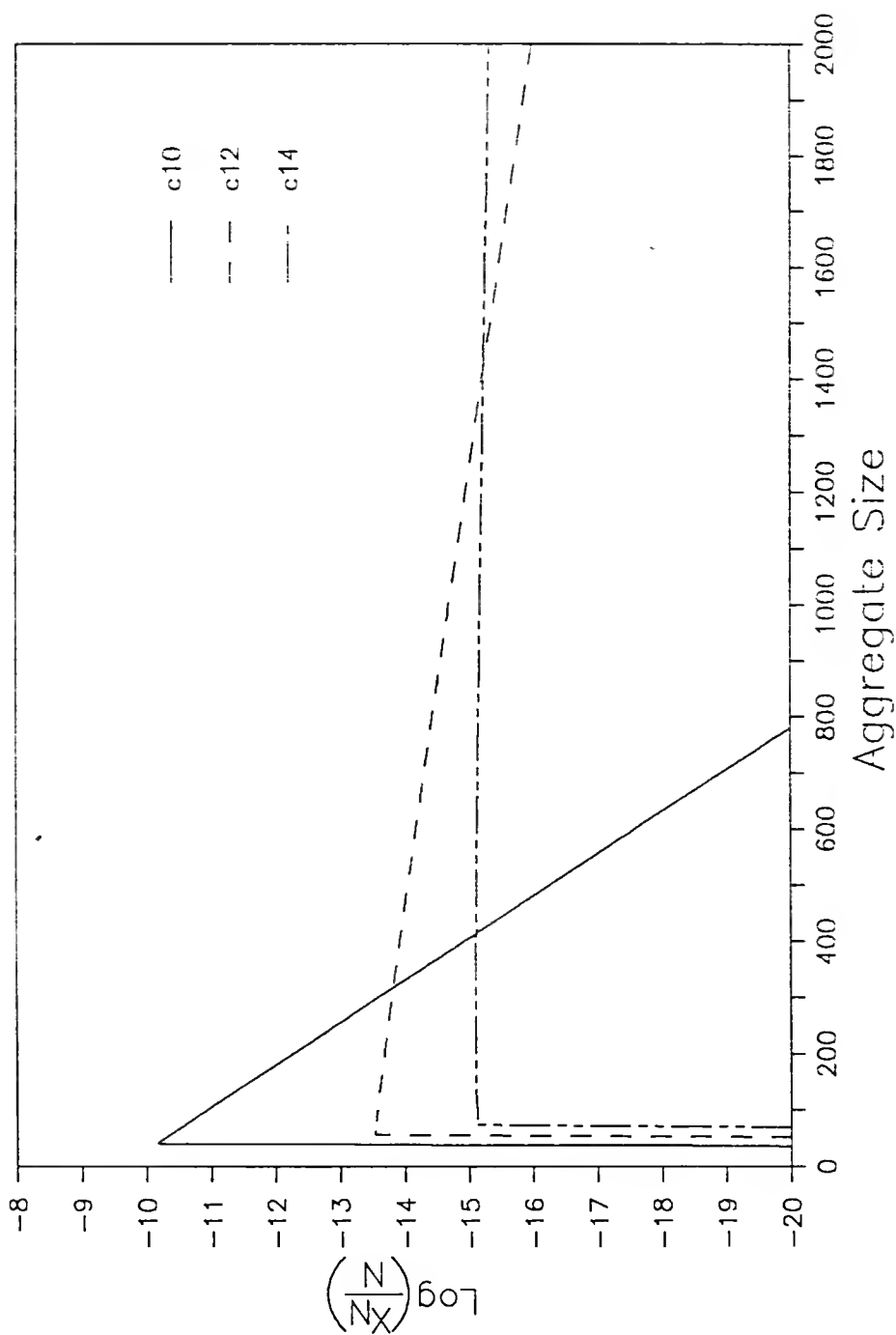


Figure 3-13. The effect of chain length on the aggregate size distribution. Results are shown for the nonionic surfactants at 298.15 Kelvin and their respective CMCs (Table 2).

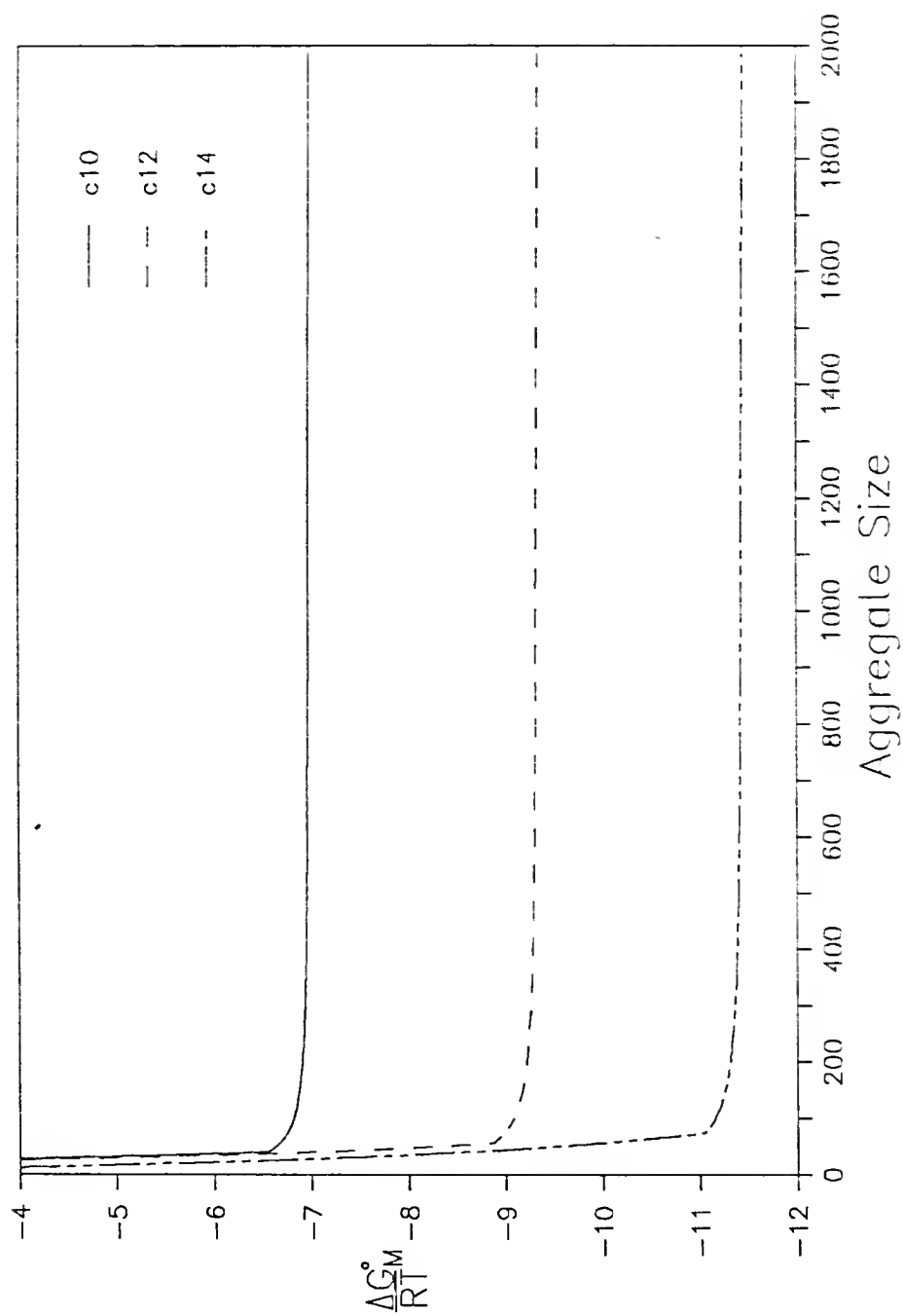


Figure 3-14. The effect of chain length on the free energy of micellization. Results are shown for the nonionic surfactants at 298.15 Kelvin and their respective CMCs.

Just as the aqueous solubility of an alkane decreases with increasing temperature, the CMC of the corresponding surfactant decreases and the mean aggregate size increases. Again, by incorporating the solubility data into the model, the proper temperature dependence is given to the parameters. The temperature dependence of the parameters is in the form of equations (3.12) and (3.13). The dependence of the aggregate size distribution and free energy change on temperature is shown in Figures 3-15 and 3-16. The effect of increased temperature is similar to that of increasing the surfactant chain length: a broadened size distribution and a more negative free energy of micellization. But while the first increase of ten degrees Kelvin has a much more pronounced effect on the free energy change (and hence the size distribution) than the next increase of ten degrees, the mean aggregate size is more affected by the latter.

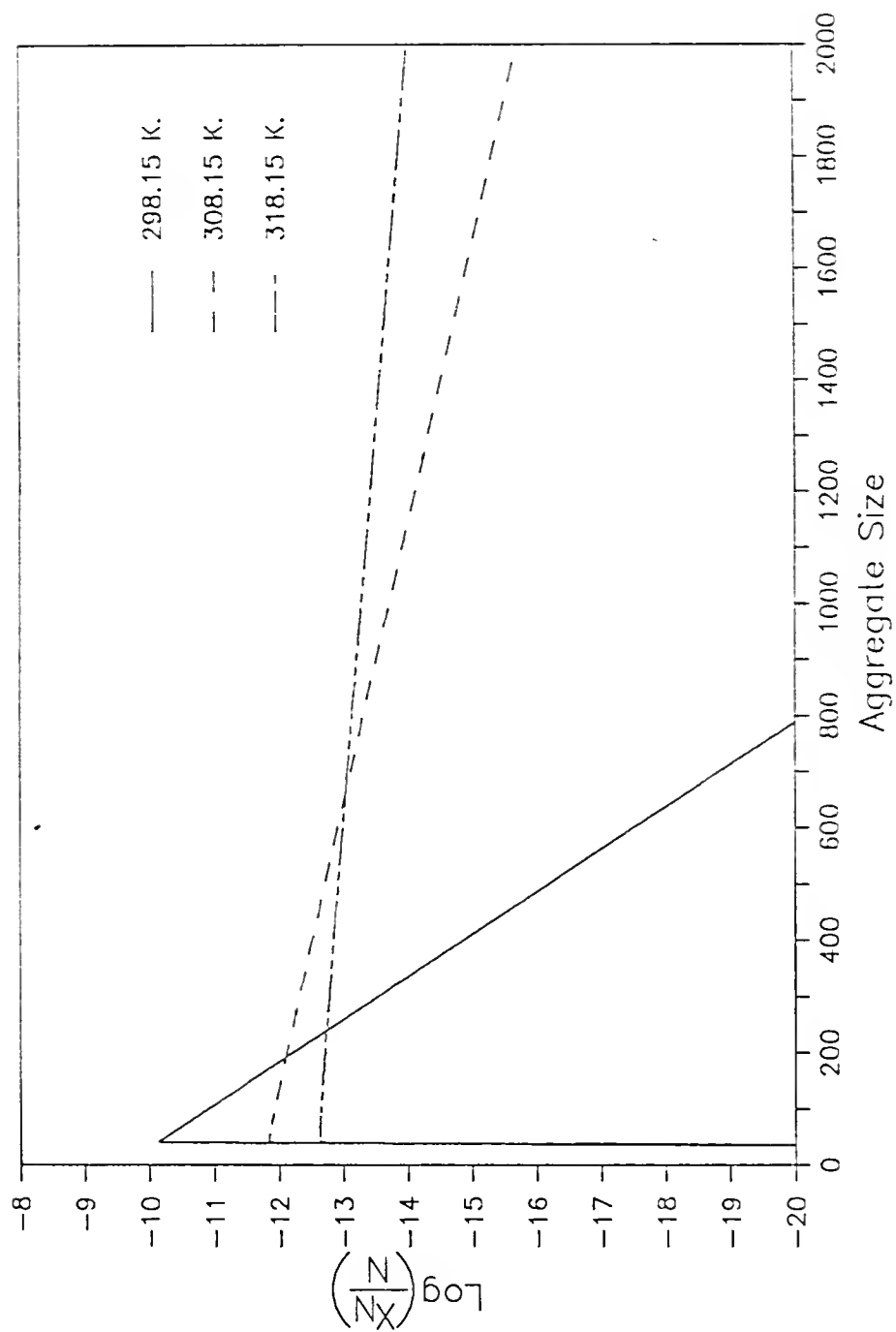


Figure 3-15. The effect of temperature on the aggregate size distribution. Results are shown for the C10 nonionic surfactant at its CMC.

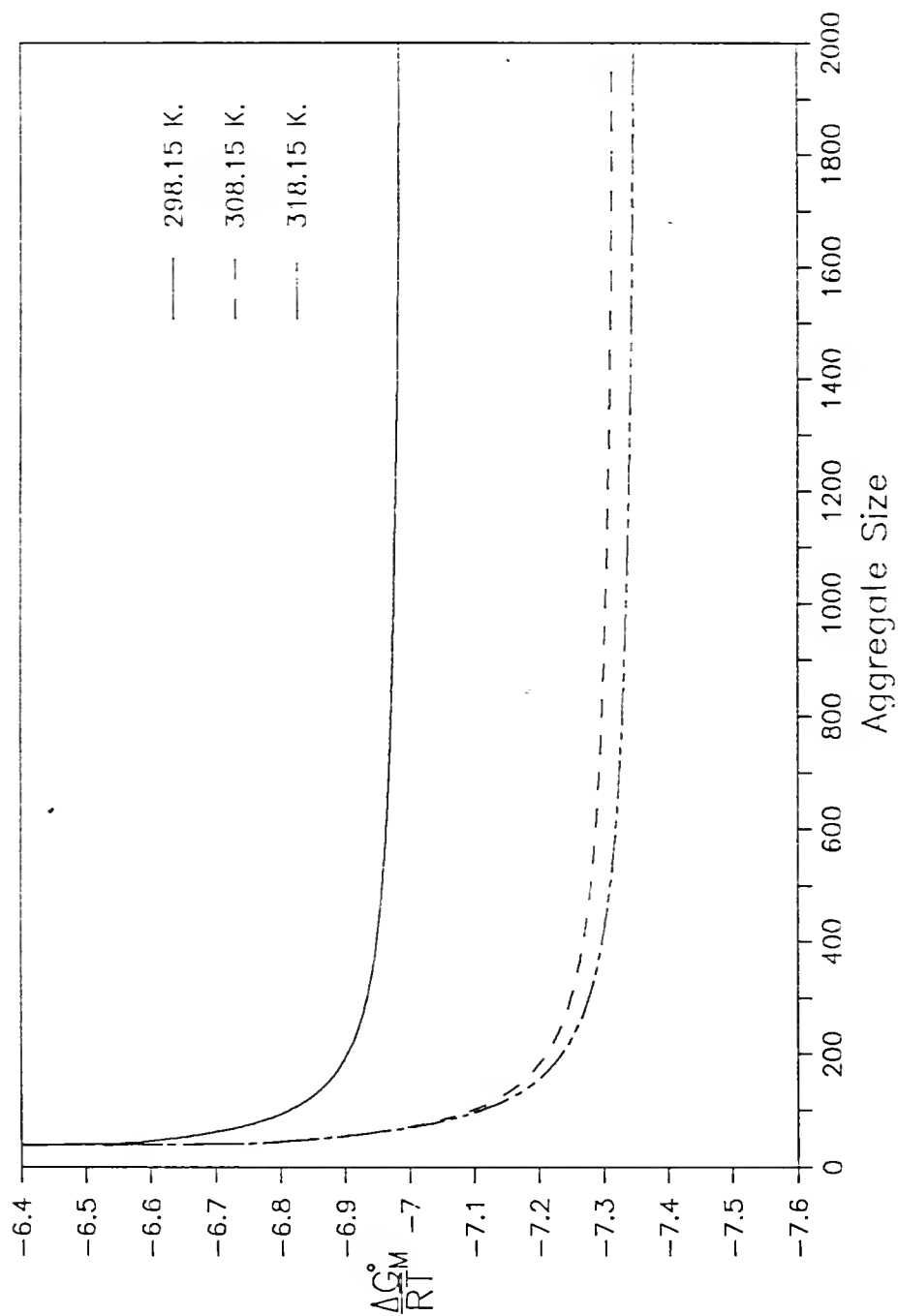


Figure 3-16. The effect of temperature on the free energy of micellization. Results are shown for the C10 nonionic surfactant at its CMC.

CHAPTER 4 MOLECULAR DYNAMICS SIMULATION OF SURFACTANT MICELLES

4.1 Background

The development of a predictive model of micelle behavior, such as that of Chapter 2, requires a knowledge of the structure of the aggregate in order to describe its thermodynamic properties. The calculation of a surface free energy contribution necessitates certain assumptions about micelle size, shape, and surface roughness. The solvent interface must be modeled and solvent penetration must be estimated. Calculation of the conformational contribution to the free energy calls for details of the molecular conformations in the free and aggregated states. The head group contribution depends on the average positions of the head groups.

While experimental results are the most desirable basis for thermodynamic models, measurements of the structure of micelles are limited in the information they can provide. Therefore, current models of micelle behavior, including that derived in Chapter 2, are based primarily on theoretical considerations.

The most informative techniques for studying micelles in solution are spectroscopic. Light scattering, NMR, and

small-angle neutron scattering (SANS) have been used extensively to study micelles. However, results of these experiments often conflict, as in the question of whether there is solvent penetration into the micelle core, and their description of the micelle surface and internal structure is incomplete (Tabony, 1984).

Quasi-elastic light scattering has been used effectively to determine micelle size and shape (Corti and Degiorgio, 1981a, 1981b) and Raman light scattering has been used to investigate chain conformations (Kalyanasundaram and Thomas, 1976). The absence of solvent from the micelle core was determined with NMR techniques (Mitra et al., 1984), though the opposite had been reported earlier (Menger, 1979). The most promising experimental means available of studying micelle structure is SANS. It has been used to study the micelle surface (Hayter and Zemb, 1982), solvent penetration (Tabony, 1984; Cabane et al., 1985), and chain conformations in the micelle interior (Bendedouch et al., 1983a, 1983b).

The spectra generated by the above methods must be carefully interpreted to yield correct information about the micelle surface and interior. It is in this interpretation of the results, particularly in accounting for intermicellar effects, that inconsistencies arise (Cabane et al., 1985). Computer simulation is an alternative means to answer questions raised by the experimental measurements. For a

given model of surfactant and micelle behavior, simulation can provide exact quantitative descriptions of micelle structure.

Simulations of micelles have been conducted by both Monte Carlo (Haan and Pratt, 1981a, 1981b; Owenson and Pratt, 1984) and molecular dynamics (Haile and O'Connell, 1984; Woods et al., 1986; Jonsson et al., 1986) methods. Thus far, results of the simulation studies have been promising. Their contribution to a better understanding of micelle structure has been limited only by the uncertainties about the model micelle.

Monte Carlo calculations are carried out on a lattice of sites. Movement of a molecular segment from one site to another is allowed or disallowed based on the energy change associated with the move. The restriction of segment positions to the lattice sites limits the possible conformations available to the molecules. To allow more possible conformations, the number of lattice points, and hence the computing effort, must be increased. This restricts how far such a simulation can go in accurately representing reality; in addition, the Monte Carlo method precludes the opportunity to study the dynamics of a system by simulation.

The molecular dynamics method provides a continuum of sites for molecular positions and is limited only by the accuracy of the forces built into the model. In the present work, molecular dynamics models were developed based on the work of Haile and coworkers (Haile and O'Connell, 1984; Woods et al., 1986) to investigate the effects of surfactant chain length, head group mass, and head group size.

4.2 The Molecular Dynamics Method

The molecular dynamics approach to computer simulation consists of summing the forces on each particle in the system and solving Newton's equations of motion for the resultant positions and momenta (Haile, 1980). The problem of constructing a realistic model system then becomes one of supplying appropriate models for the intermolecular and intramolecular potentials. It is assumed that a given particle's interactions with its neighbors are pairwise additive. Thus, the potential between two particles at time t is of the form

$$U(r_{ij}(t)) = U(\vec{r}_i(t), \vec{r}_j(t)) \quad (4.1)$$

The force between the two particles is given by

$$\vec{F}(r_{ij}(t)) = -\vec{\nabla} U(r_{ij}(t)) \quad (4.2)$$

and the total force on the particle of interest is the sum of the forces resulting from interactions with all other particles:

$$\vec{F}_i(t) = \sum_j \vec{F}(r_{ij}(t)) \quad (4.3)$$

The resulting acceleration and velocity of the particle are obtained from Newton's Second Law of Motion, relating force, mass, and acceleration:

$$\vec{F}_i(t) = m_i \frac{\partial^2 \vec{r}_i(t)}{\partial t^2} \quad (4.4)$$

The set of second-order differential equations for all of the particles in the system is solved at each time step of the simulation. The means employed in this work for determining the new positions of all of the particles from the forces at the previous time step is a fifth-order predictor-corrector algorithm (Gear, 1971). This algorithm consists of three procedures which are repeated at each time step. The position and its first five time derivatives at time $(t+\Delta t)$ are predicted for all of the particles by Taylor's series expansion of their values at time t :

$$\begin{aligned} r_i(t + \Delta t) = & r_i(t) + \frac{dr_i(t)}{dt} \Delta t + \frac{d^2 r_i(t)(\Delta t)^2}{dt^2 2!} + \frac{d^3 r_i(t)(\Delta t)^3}{dt^3 3!} \\ & + \frac{d^4 r_i(t)(\Delta t)^4}{dt^4 4!} + \frac{d^5 r_i(t)(\Delta t)^5}{dt^5 5!} \end{aligned} \quad (4.5)$$

$$\begin{aligned} \frac{d}{dt} r_i(t + \Delta t) = & \frac{dr_i(t)}{dt} + \frac{d^2 r_i(t)}{dt^2} (\Delta t) + \frac{d^3 r_i(t)(\Delta t)^2}{dt^3 2!} \\ & + \frac{d^4 r_i(t)(\Delta t)^3}{dt^4 3!} + \frac{d^5 r_i(t)(\Delta t)^4}{dt^5 4!} \end{aligned} \quad (4.6)$$

$$\frac{d^2}{dt^2} r_i(t + \Delta t) = \frac{d^2 r_i(t)}{dt^2} + \frac{d^3 r_i(t)}{dt^3} (\Delta t) + \frac{d^4 r_i(t)(\Delta t)^2}{dt^4 2!} + \frac{d^5 r_i(t)(\Delta t)^3}{dt^5 3!} \quad (4.7)$$

$$\frac{d^3}{dt^3}r_i(t + \Delta t) = \frac{d^3r_i(t)}{dt^3} + \frac{d^4r_i(t)}{dt^4}(\Delta t) + \frac{d^5r_i(t)}{dt^5}\frac{(\Delta t)^2}{2!} \quad (4.8)$$

$$\frac{d^4}{dt^4}r_i(t + \Delta t) = \frac{d^4r_i(t)}{dt^4} + \frac{d^5r_i(t)}{dt^5}(\Delta t) \quad (4.9)$$

$$\frac{d^5}{dt^5}r_i(t + \Delta t) = \frac{d^5r_i(t)}{dt^5} \quad (4.10)$$

The forces $F_i(t+\Delta t)$ are then evaluated at the predicted positions. Finally, the predicted values of the position and its derivatives are corrected according to the error between the acceleration predicted by the series expansion and the acceleration calculated from $F_i(t+\Delta t)$. These calculations are carried out by the subroutines PREDCT, EVAL, and CORR in Appendix D.

The simulations described in this work were carried out at constant temperature. The temperature of the system is related to the velocities of the particles by

$$T = \frac{1}{3Nk} \sum_i m_i v_i^2 \quad (4.11)$$

The velocities of all particles are scaled at each time step so that the temperature is maintained at a constant value. Subroutine EQBRAT in Appendix D accomplishes this task.

To start a simulation, values of the positions are required to evaluate the initial forces. Initial values of the five derivatives of position are required by the fifth order predictor-corrector algorithm. In these simulations, initial positions were assigned according to a lattice of

sites and random velocities were assigned the particles (subroutines INTPOS and INTVEL). The momenta were scaled so that there was no net linear momentum of the system. The initial accelerations are calculated by equation (4.4) and the third and higher derivatives of position are assigned initial values of zero, since there is no way of evaluating them. The algorithm recovers rapidly from this initial condition, arriving at proper values of all derivatives within 10-20 time steps.

Since intermolecular potentials are significant over a pair separation which is usually small relative to the dimensions of the molecular system, computing effort can be reduced by employing truncated potentials (Haile, 1980) and maintaining a neighbor list (Verlet, 1967). In a simulation where the majority of possible pair separations are so large that the corresponding pair potentials will be very small, it is more efficient not to calculate the potential for pair separations which are beyond a certain value and do not contribute significantly to the system properties. Instead, these contributions are neglected during the simulation and a correction is made to the system properties. A cutoff distance, r_c , is set such that the potential can be neglected for $r_{ij} > r_c$. The intermolecular forces are truncated at r_c and shifted vertically, going to zero smoothly at r_c (Nicolas et al., 1979). The truncated

potential is obtained from this shifted force by equation (4.2). This eliminates a step change in the potential and force at $r_{ij} = r_c$, which could have a disruptive effect on the energy conservation of the simulated system. The general equations of a shifted force, $F_s(r)$, and its potential, $U_s(r)$, are given below:

$$F_s(r) = -\frac{dU_s(r)}{dr} + r \left[\frac{d_s U(r)}{dr} \right]_{r=r_c}, \quad r < r_c \quad (4.12)$$

$$U_s(r) = U(r) - U(r_c) - (r - r_c) \left[\frac{dU(r)}{dr} \right]_{r=r_c}, \quad r < r_c \quad (4.13)$$

By checking the value of r_{ij} and bypassing the calculation of $F(r_{ij})$ for $r_{ij} > r_c$, a significant savings in computing effort can be realized.

Further savings can be made by not checking pairs which have a low probability of $r_{ij} < r_c$. This is accomplished through the use of a neighbor list. A particle (i) in the system is surrounded by a sphere of radius r_c . Other particles (j) inside this sphere will interact with it, since $r_{ij} < r_c$. From one time step to the next, particles will enter and exit this sphere. Over some short period of time, all of the particles which have interacted with the central particle will lie inside a larger sphere whose radius is r_{list} . If, over this brief period of time, only those particles inside the larger sphere were checked, all of the particles interacting with the central particle would

be found without checking all of the other particles in the system. Through a neighbor list a record is maintained of all the "neighbors" within a distance r_{list} of each particle in the system. Only these neighbors are checked for $r_{ij} < r_c$. The neighbor list is updated periodically based on the value of r_{list} and the dynamics of the system.

The molecular dynamics method represents a massive computing effort for any system large enough to be of interest. However, using the techniques described above to improve efficiency, and with the development of supercomputers and parallel processors, it has become a practical tool for quantitatively studying molecular behavior.

4.3 The Model Surfactant Molecule

The surfactant molecule studied in this work has a linear alkyl chain of eight carbon groups. All of the groups are considered to be methylenes. A polar head group is attached to one chain end; head groups of different sizes and masses were used in the simulations. The bond lengths and angles along the chain are those of a normal alkane. These are given in Figure 4-1.

Three types of intramolecular interaction take place in the model surfactant molecule:

1. Bond vibration
2. Bond bending
3. Bond rotation

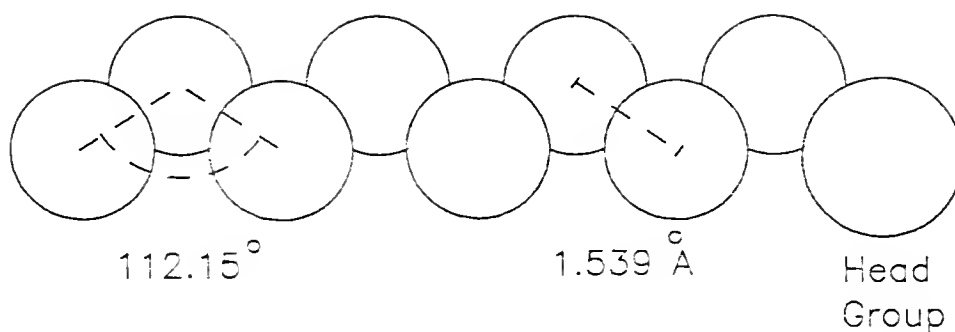


Figure 4-1. The model surfactant molecule, consisting of an eight-member alkane chain attached to a polar head group, shown in the all-trans conformation. Bond angles and lengths of the alkane chain are indicated. The bond to the head group is head group dependent in the different simulations conducted.

The bond vibration potential used is that of Weber (1978), taken from a simulation of n-butane. It is a harmonic potential about the equilibrium bond length. The potential and the forces on the two groups are given by

$$U_{\text{vib}}(b_i) = \frac{1}{2} \gamma_i (b_i - b_0)^2 \quad (4.14)$$

$$\bar{F}_i^{\text{vib}}(b_i) = -\gamma_i (b_i - b_0) \frac{\bar{b}_i}{b_i} \quad (4.15)$$

$$\bar{F}_{i-1}^{\text{vib}}(b_i) = \gamma_i (b_i - b_0) \frac{\bar{b}_i}{b_i} \quad (4.16)$$

where b_i is the bond length between groups i and $i-1$, b_0 is the equilibrium bond length, and γ_i is the force constant.

The bond bending potential is also taken from the simulation of Weber (1978). It is a harmonic potential about the cosine of the equilibrium bond angle with forces on the three groups forming the bond angle. For the angle θ formed by groups i , $i-1$, and $i-2$,

$$U_{\text{bend}}(\theta_i) = \frac{1}{2} \gamma_{\theta} (\cos \theta_i - \cos \theta_0)^2 \quad (4.17)$$

$$\bar{F}_i^{\text{bend}}(\theta_i) = -\gamma_{\theta} (\cos \theta_i - \cos \theta_0) \frac{1}{b_i} \left(\frac{\bar{b}_i - 1}{b_i - 1} - \frac{\bar{b}_i}{b_i} \cos \theta_i \right) \quad (4.18)$$

$$\begin{aligned} \bar{F}_{i-1}^{\text{bend}}(\theta_i) = & \gamma_{\theta} (\cos \theta_i - \cos \theta_0) \left[\frac{1}{b_i} \left(\frac{\bar{b}_i - 1}{b_i - 1} - \frac{\bar{b}_i}{b_i} \cos \theta_i \right) \right. \\ & \left. - \frac{1}{b_i - 1} \left(\frac{\bar{b}_i}{b_i} - \frac{\bar{b}_i - 1}{b_i - 1} \cos \theta_i \right) \right] \quad (4.19) \end{aligned}$$

$$\vec{F}_{i+2}^b(\theta_i) = \gamma_b(\cos\theta_o - \cos\theta_i) \frac{1}{b_i+1} \left(\frac{\vec{b}_i}{b_i} + \frac{\vec{b}_{i+1}}{b_{i+1}} \cos\theta_i \right) \quad (4.20)$$

The model surfactant molecule is comprised of eight bonds connecting its nine groups. Rotation about any of the inner six bonds results in a change in the conformation of the molecule and a change in its potential energy. A set of four groups in sequence along the chain molecule contains a dihedral angle formed by the three bonds connecting the groups. This angle is a measure of rotation about the middle bond, and the potential energy is a function of the dihedral angle. The bond rotation potential chosen for these simulations is that of Ryckaert and Bellemans (1975):

$$U(\phi) = \gamma_r(1.116 - 1.462\cos\phi - 1.578\cos^2\phi + 0.368\cos^3\phi + 3.156\cos^4\phi + 3.788\cos^5\phi) \quad (4.21)$$

where ϕ is the dihedral angle in radians. The bond rotation potential is illustrated in Figure 4-2. The force on each of the four groups resulting from this potential and equation (4.2) has been derived by Woods (1985) and the resulting calculations are carried out by subroutine RYFOR in Appendix D.

The intramolecular potentials account for all of the interactions among adjacent groups on a molecule as they are taken two (vibration), three (bending), or four (rotation) at a time. Two groups on the same molecule which are separated by more than three intervening groups do not

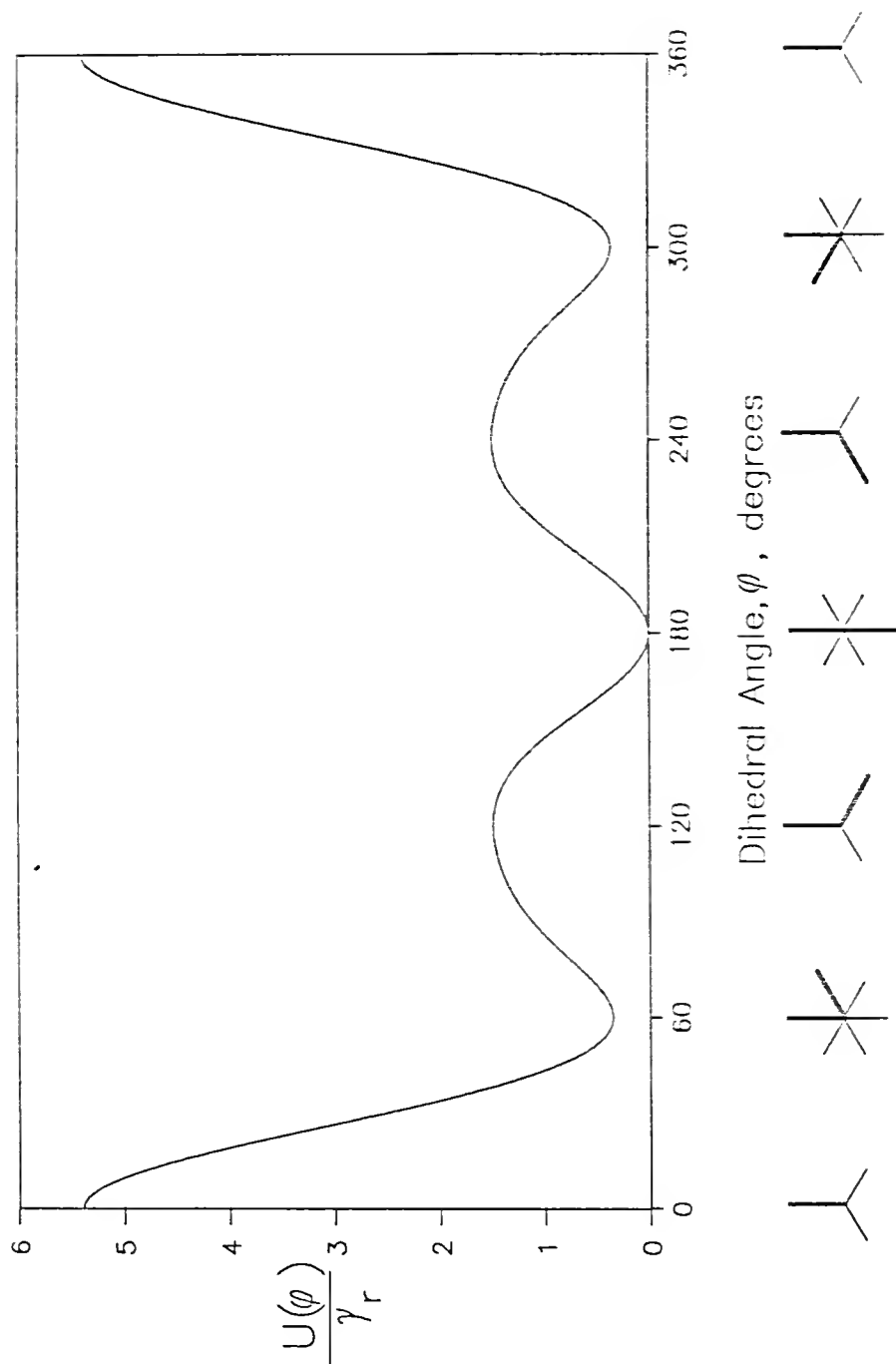


Figure 4-2. The bond rotation potential as a function of the dihedral angle formed by four consecutive groups along the surfactant chain. The diagrams below the plot depict the relative orientations of the second and third groups and their attached hydrogens (thin lines) and methylenes (heavy lines).

interact through any of these three potentials, but may experience the intermolecular potential if they become sufficiently close to one another.

4.4 The Model Micelle

The micelle used in the simulations contains 24 surfactant molecules. The individual groups of the molecules interact through intermolecular potentials, and the micelle is surrounded by a spherical shell which models the solvophilic effect on the head groups and the solvophobic effect on the chains. The intermolecular interactions which take place in the micelle are

1. Head group-shell
2. Alkane group-shell
3. Head group-head group
4. Alkane group-alkane group
5. Head group-alkane group

The shell does not attempt to explicitly model the solvent molecules. To do so greatly increases the computing requirements of the simulation and a previous attempt at such explicit modeling (Jonsson et al., 1986) did not show it to be a clear improvement over the present potential-field model. Rather, the solvophilic and solvophobic natures of the head group and alkane group are modeled in a simple manner intended to keep the head groups close to the surface of the micelle and prevent the chains from extending

out from the micelle. This simulates the minimum chain-solvent contact of accepted experimental results (Tabony, 1984).

The head group interaction with the shell is through a harmonic potential about an equilibrium radial position:

$$U(r_i) = \gamma_h (r_i - r_o)^2 \quad (4.22)$$

$$\vec{F}(r_i) = -2\gamma_h (r_i - r_o) \frac{\vec{r}_i}{r_i} \quad (4.23)$$

where r_i is the position of the head group and r_o is the equilibrium position. The force constant is γ_h .

The alkane group interaction with the shell is through a repulsive potential:

$$U(r_{iw}) = \epsilon \left(\frac{r_m}{r_{iw}} \right)^{12} \quad (4.24)$$

$$\vec{F}(r_{iw}) = 12\epsilon \frac{(r_m)^{12}}{(r_{iw})^{13}} \frac{\vec{r}_{iw}}{r_{iw}} \quad (4.25)$$

where r_{iw} is the quantity $r_w - r_i$, r_w being the radial position of the spherical repulsive shell, and r_m and ϵ are the radius and energy of minimum potential for the alkane-alkane intermolecular potential.

The interaction between two head groups is described by a potential comprised of both dipole (r^{-3}) and soft-sphere (r^{-12}) repulsions:

$$U(r_{ij}) = \epsilon \left[\left(\frac{r_{hh}}{r_{ij}} \right)^3 + \left(\frac{r_{hh}}{r_{ij}} \right)^{12} \right] \quad (4.26)$$

This potential is designed to spread the head groups apart on the exterior of the micelle. The force between a pair of head groups is obtained by applying equation (4.2) to equation (4.26).

$$\vec{F}(r_{ij}) = \epsilon \left[\frac{3r_{hh}^3}{r_{ij}^4} + \frac{12r_{hh}^{12}}{r_{ij}^{13}} \right] \frac{\vec{r}_{ij}}{r_{ij}} \quad (4.27)$$

Applying equations (4.12) and (4.13) to use the shifted-force potential for $r_{ij} < r_c$,

$$U_s(r_{ij}) = \epsilon \left\{ \left(\frac{r_{hh}}{r_{ij}} \right)^3 + \left(\frac{r_{hh}}{r_{ij}} \right)^{12} - 4 \left(\frac{r_{hh}}{r_c} \right)^3 - 13 \left(\frac{r_{hh}}{r_c} \right)^{12} + \frac{r_{ij}}{r_{hh}} \left[3 \left(\frac{r_{hh}}{r_c} \right)^4 + 12 \left(\frac{r_{hh}}{r_c} \right)^{13} \right] \right\} \quad (4.28)$$

$$\vec{F}_s(r_{ij}) = \epsilon \left\{ \frac{3r_{hh}^3}{r_{ij}^4} + \frac{12r_{hh}^{12}}{r_{ij}^{13}} + \frac{r_{ij}}{r_c} \left[3 \left(\frac{r_{hh}}{r_c} \right)^3 + 12 \left(\frac{r_{hh}}{r_c} \right)^{12} \right] \right\} \frac{\vec{r}_{ij}}{r_{ij}} \quad (4.29)$$

The intermolecular potential between two alkane groups is a (6,9) form of the Mie (m,n) potential (Reed and Gubbins, 1973):

$$U(r_{ij}) = \epsilon \left[2 \left(\frac{r_m}{r_{ij}} \right)^9 - 3 \left(\frac{r_m}{r_{ij}} \right)^6 \right] \quad (4.30)$$

$$\vec{F}(r_{ij}) = 18\epsilon \left[\frac{r_m^9}{r_{ij}^{10}} + \frac{r_m^6}{r_{ij}^7} \right] \frac{\vec{r}_{ij}}{r_{ij}} \quad (4.31)$$

$$U_s(r_{ij}) = \epsilon \left\{ 2 \left(\frac{r_m}{r_{ij}} \right)^9 - 3 \left(\frac{r_m}{r_{ij}} \right)^6 - 20 \left(\frac{r_m}{r_c} \right)^9 + 21 \left(\frac{r_m}{r_c} \right)^6 - 18 \frac{r_{ij}}{r_m} \left[\left(\frac{r_m}{r_c} \right)^7 - \left(\frac{r_m}{r_c} \right)^{10} \right] \right\} \quad (4.32)$$

$$\vec{F}_s(r_{ij}) = 18\epsilon \left\{ \frac{r_m^9}{r_{ij}^{10}} + \frac{r_m^6}{r_{ij}^7} - \frac{r_{ij}}{r_c} \left[\left(\frac{r_m}{r_c} \right)^7 - \left(\frac{r_m}{r_c} \right)^{10} \right] \right\} \frac{\vec{r}_{ij}}{r_{ij}} \quad (4.33)$$

This potential is also used for the interaction between a head group and an alkane group, except that the radius of minimum potential, r_m , is adjusted to account for the difference between the diameter of the head group and that of the alkane group:

$$r_m^{\text{head-alkane}} = \frac{1}{2}(r_m + r_{hh}) \quad (4.34)$$

Figure 4-3 illustrates the intermolecular potentials used in the model micelle, and Table 4 gives the values of the parameters used in the intramolecular and intermolecular potentials.

The model micelle is assembled by initially placing the 24 molecules with their head groups evenly spaced over the surface of a sphere of twice the expected micelle radius. Each chain is directed radially inward, in the all-trans conformation. With the bond rotation force constant reduced to one-tenth of its normal value to facilitate chain packing during startup, the simulation is begun. The radius of the confining sphere is reduced every ten time steps until the appropriate radius is achieved. This is the value that would give the density of the analogous liquid alkane, adjusted to a pressure which fluctuates about zero with an amplitude of less than ten atmospheres. After this, the

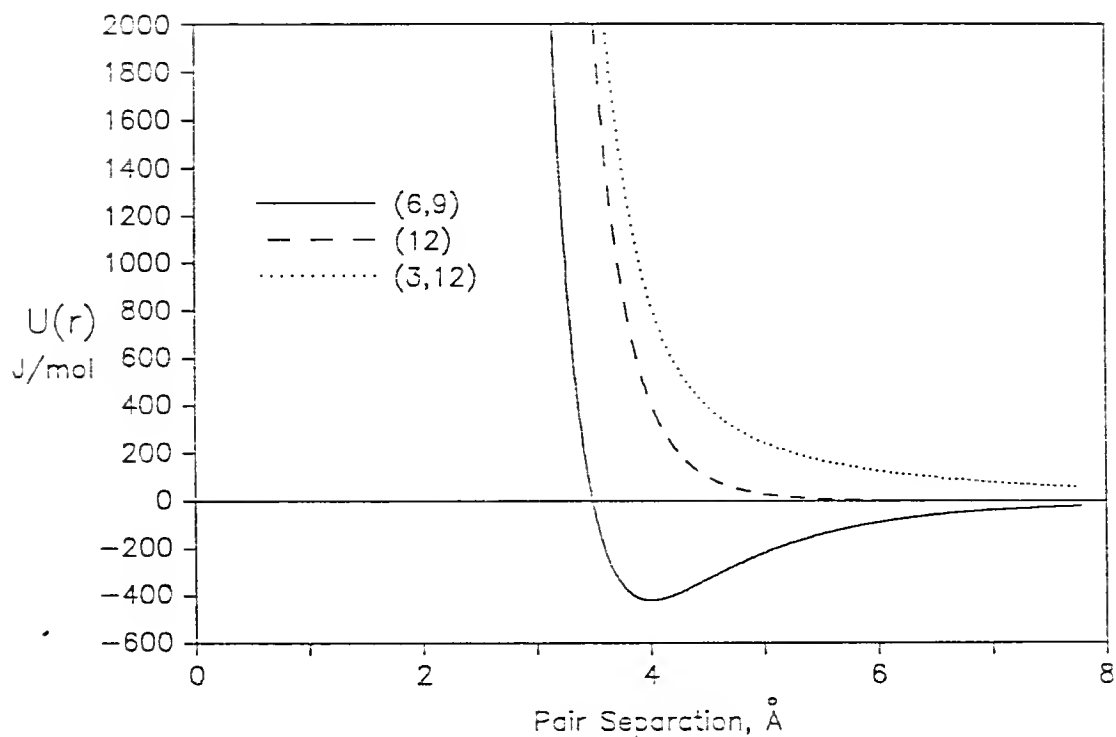


Figure 4-3. The intermolecular potentials for segment-segment (6,9), segment-shell (12), and head-head (3,12). A value of 419 Joule/mole was used for ϵ ; both r_m and r_{hh} were assigned values of 4 Angstroms.

Table 4
Parameter Values for Potentials Used in Simulations

<u>Potential</u>	<u>Parameter</u>	<u>Value</u>	<u>Units</u>
------------------	------------------	--------------	--------------

Bond vibration +	γ_v	9.25×10^5 a	Joule/A ² /mole
	b_o	1.539 a	Angstrom
Bond bending +	γ_b	1.3×10^5 a	Joule/mole
	θ_o	112.15 a	degree
Bond rotation +	γ_r	8313 b	Joule/mole
Head-shell	γ_h	785 c	Joule/A ² /mole
	r_o	4 c	Angstrom
Segment-shell	ϵ	419	Joule/mole
	r_m	4	Angstrom
Head-head	ϵ	419	Joule/mole
	r_{hh}	*	Angstrom
Segment-segment	ϵ	419 a	Joule/mole
	r_m	4 a	Angstrom
Head-segment	ϵ	419	Joule/mole
	r_m^{h-a}	$\frac{1}{2}(r_m + r_{hh})$	Angstrom

a Weber (1978)

b Ryckaert and Bellemans (1975)

c Woods (1985)

* Parameter varies with head group size.

+ See also Table 6.

rotational force constant is restored to its desired value and the system is allowed to equilibrate. When there is no net drift in the energy of the system or in the fraction of trans bonds, equilibrium is considered to have been reached. The simulation is continued, periodically saving the positions and velocities of all of the groups for subsequent analysis.

The time step used in simulation must be small enough to track the motions of the molecules and maintain stability, yet large enough to avoid unnecessary computing effort. The ideal time step can only be found by trial, which was conducted on a simulated liquid alkane system by Weber (1978). That result, $\Delta t = .002$ psec., is the basis for the time steps used in the present work.

4.5 Summary of Computer Simulations

The following simulations were carried out on the model micelle:

1. Head group mass and size same as chain segment.
2. Head group mass greater than segment, size the same.
3. Head group mass and size greater than segment.

In addition, a fourth simulation was carried out on a hydrocarbon droplet of 24 nine-segment molecules by setting the head group to the size and mass of a methylene and replacing head-head and head-shell interactions with segment interactions. From these simulations the independent

effects of head group size, mass, and solvophilic nature can be observed, and by comparison with comparable simulations of dodecyl surfactant micelles (Woods et al., 1986) the effect of chain length can be evaluated. A brief summary of the simulations is given in Table 5.

To carry out the first two simulations, 24 model surfactant molecules were placed with their head groups on a sphere of radius 24 Angstroms and their chains directed radially inward in the all-trans configuration. The groups were given initial velocities, the rotational force constant was reduced to one-tenth of its normal value, and the simulation was begun. Every ten time steps, the radius of the confining sphere was decreased by .01 Angstrom. This scaling down of the model micelle was continued until the radius of the spherical shell reached a value of 12.00 Angstroms, slightly higher than the radius of an analogous hydrocarbon droplet. Ten-thousand time steps were run at this radius to allow the micelle to recover from the scaling down procedure and observe the pressure at the shell. The pressure fluctuated about zero with an amplitude of approximately two atmospheres and analysis of the positions of the groups revealed no effect of the initial conditions. This model micelle was chosen as the starting point for simulation 1.

Table 5
Summary of Simulation Computations

Simulation	Head Group Diameter	Head Group Mass	Micelle Radius, Å.	Equilibrium Run, psec.	Time Step, psec.	CPU Usage, sec.
1	1	1	12.000	79	1.98×10^{-3}	6719
2	1	7	12.000	99	1.98×10^{-3}	8602
3	2.45	7	12.800	28	1.40×10^{-3}	8699
4	1 a	1 a	11.928	119	1.98×10^{-3}	8342

73

a Hydrocarbon droplet, head group interactions same as chain segments.

Note: Head group diameter and mass are relative to chain segment (methylene.)

Simulation 2 was started from this same model micelle, after increasing the mass of all head groups by a factor of seven and allowing 10,000 time steps for equilibration. This mass was chosen to represent a common ionic head group, the sulfate ion. Only the mass of the head group was changed; all of the intermolecular and intramolecular interactions remained the same as in the previous simulation. The expected result of this would be simply a change in the dynamics of the head group. The program used to compute simulations 1 and 2 is listed in Appendix D.

In simulation 3, the change in the head group was more extensive. An attempt was made to represent the sulfate head group in all of its intermolecular and intramolecular interactions. The mass of the group remained at seven times that of a methylene, while the diameter was increased to 2.45 times that of a methylene. The equilibrium bond length and bond angle for the head group were changed, as were the force constants for bond vibration, bond-angle bending, and bond rotation involving the head group. These values are given in Table 6 and compared with the methylene values. The derivation of the head group intramolecular interaction parameters based on the work of Muller and coworkers (Muller and Nagarajan, 1967; Muller et al., 1968), Cahill et al. (1968), and Blukis et al. (1963) is given in Appendix E.

Table 6
Bond Parameters of "Sulfate" and "Methylene" Groups

<u>Parameter</u>	<u>"Methylene" Value</u>	<u>"Sulfate" Value</u>	<u>Units</u>
γ_v	9.25×10^5	2.7×10^4	Joule/A ² /mole
b_o	1.539	2.6	Angstrom
γ_b	1.3×10^5	9.1×10^5	Joule/mole
θ_o	112.15	140	degree
γ_r	8313	20000	Joule/mole

Due to the increase in the size of the head group, the range of head group interactions was significant in comparison to the size of the micelle and truncation of the potentials could no longer be justified. Therefore, neighbor-listing and truncation of intermolecular potentials were not employed in this simulation. It was also found to be necessary to decrease the time step to maintain stability in the energetics of the system. It is for these two reasons that the computing efficiency (simulation time per CPU time) of simulation 3 is dramatically lower than the other simulations (Table 5). The program used to compute simulation 3 is listed in Appendix F.

Simulation 4, the hydrocarbon droplet, was conducted in the same manner as simulation 1, except that the head group was replaced by a chain segment (all segments have the same properties to simplify computation) in its interactions with the shell and other groups. The radius was scaled down to 11.928 Angstroms to achieve the liquid hydrocarbon density of .7176 g/cc. Since there was no sorting out of the head groups for separate interactions, the efficiency of this simulation was 18 percent greater than that of the first two simulations.

The simulation computations were conducted on a Control Data Corporation (CDC) Cyber 205 computer at the

Supercomputer Research Institute (SCRI) in Tallahassee, Florida. Access to the SCRI facilities was provided through a grant from the United States Department of Energy.

All of the simulation programs were modified for the CDC FORTRAN 200 Vector-optimizing compiler. By employing parallel processing techniques when possible, this compiler provides very efficient operation from code which is highly compatible with ANSI standard FORTRAN. One important difference lies in the default word length of the Cyber 205. Real numbers on this computer are eight bytes in length, compared to four bytes on most other computers. To achieve eight-byte precision in standard FORTRAN, the REAL*8 variable type is used. The programs in Appendices D and F achieve this level of precision on the Cyber 205 with default variable-type coding.

Further detail about the simulations, along with the results of their analysis, is given in the next chapter.

CHAPTER 5 RESULTS OF MOLECULAR DYNAMICS SIMULATION

In this chapter the results of structural and dynamic analyses performed on the output of the simulations are reported. Certain of these results are reported as time-averaged properties; others are given as the change in a property with time. The former are averaged over the entire length of the equilibrium run (Table 5); the latter appear in the figures over a common time period for ease of comparison. The simulations are referenced by number, Run 1 being the case with head groups of the size and mass of a chain segment (methylene); Run 2 the case with head groups of the same size as a chain segment, but a mass seven times greater; Run 3 the case with head groups of 2.45 times the size and seven times the mass of a chain segment, and a revised head group intramolecular potential; and in Run 4 the head groups replaced by chain segments to model a hydrocarbon droplet.

5.1 Mean Radial Positions of Groups

The measurement of mean radial positions of the groups on the surfactant chains is one of the simplest, yet most

telling, evaluations of micelle structure that can be made on simulation output. While this measurement cannot be obtained reliably for all groups by experiment, the position of groups is a fundamental attribute of structural models of micelles (Gruen, 1981). The mean radial position for group i ($i=1$ for head, $i=9$ for tail) is given by

$$\bar{R}_i = \frac{1}{N} \int_0^{\infty} \langle N_i(r) \rangle r dr \quad (5.1)$$

The quantity $N_i(r)$ is the number of occurrences of the center of a group i at a radial position (relative to the center of mass of the micelle) r at time t and the angle brackets denote the average over the time period of the simulation. The unsubscripted N is the number of molecules in the system, equal to the sum of $N_i(r)$ over all values of r and i . The standard deviation corresponding to this mean is given by

$$\sigma_i = \left[\frac{1}{N} \int_0^{\infty} \langle N_i(r) \rangle (r - \bar{R}_i)^2 dr \right]^{\frac{1}{2}} \quad (5.2)$$

The mean radial positions of the centers of the nine groups bracketed by one standard deviation in each radial direction are plotted for the four simulations in Figures 5-1 through 5-4. Assuming a normal distribution of a group's position over time, the range shown for each group in the figures includes 68 percent of its positions, while twice this range includes 95 percent.

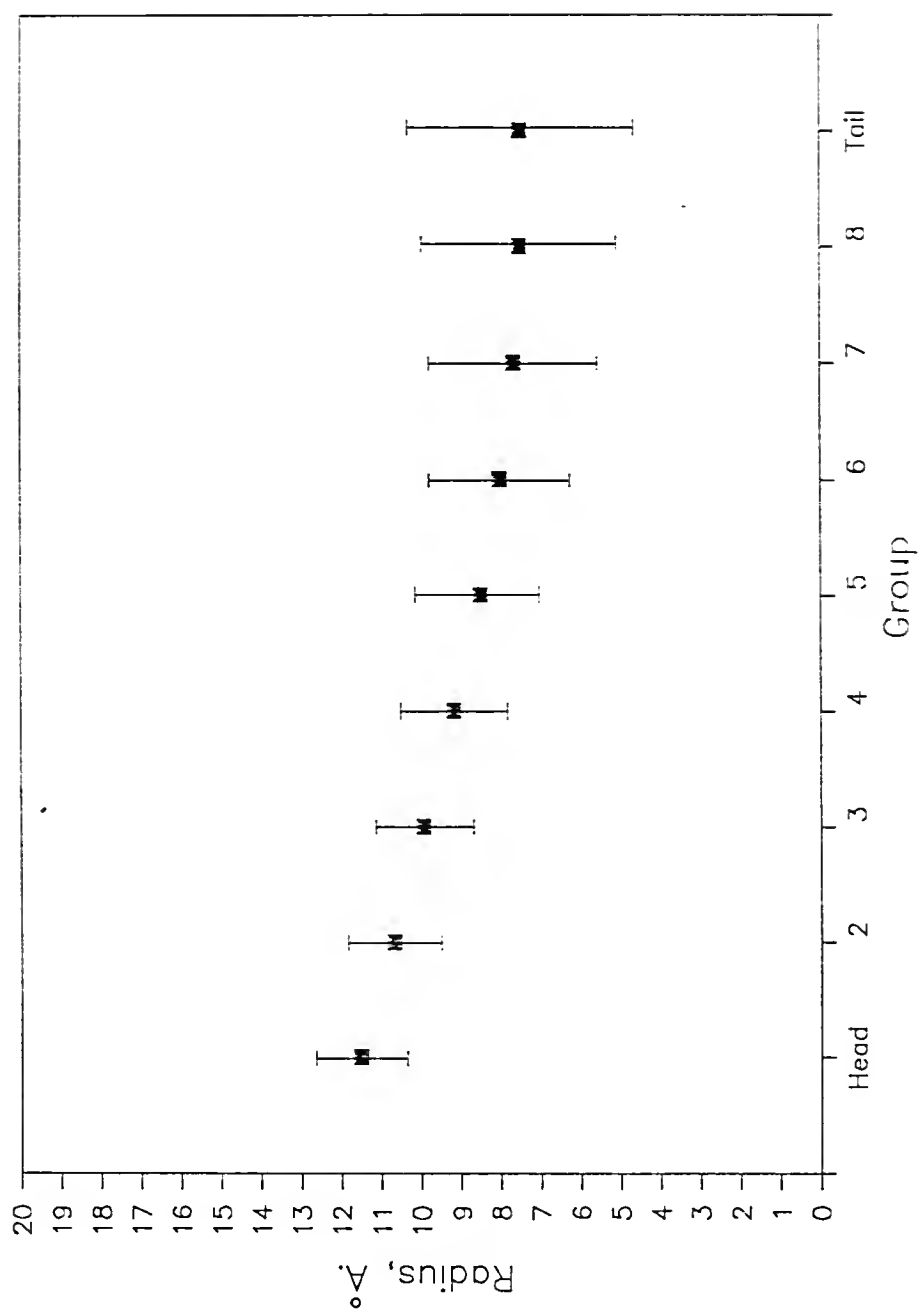


Figure 5-1. Mean radial positions of the nine groups of the surfactant molecules of Run 1. The vertical bars show one standard deviation on either side of the mean.

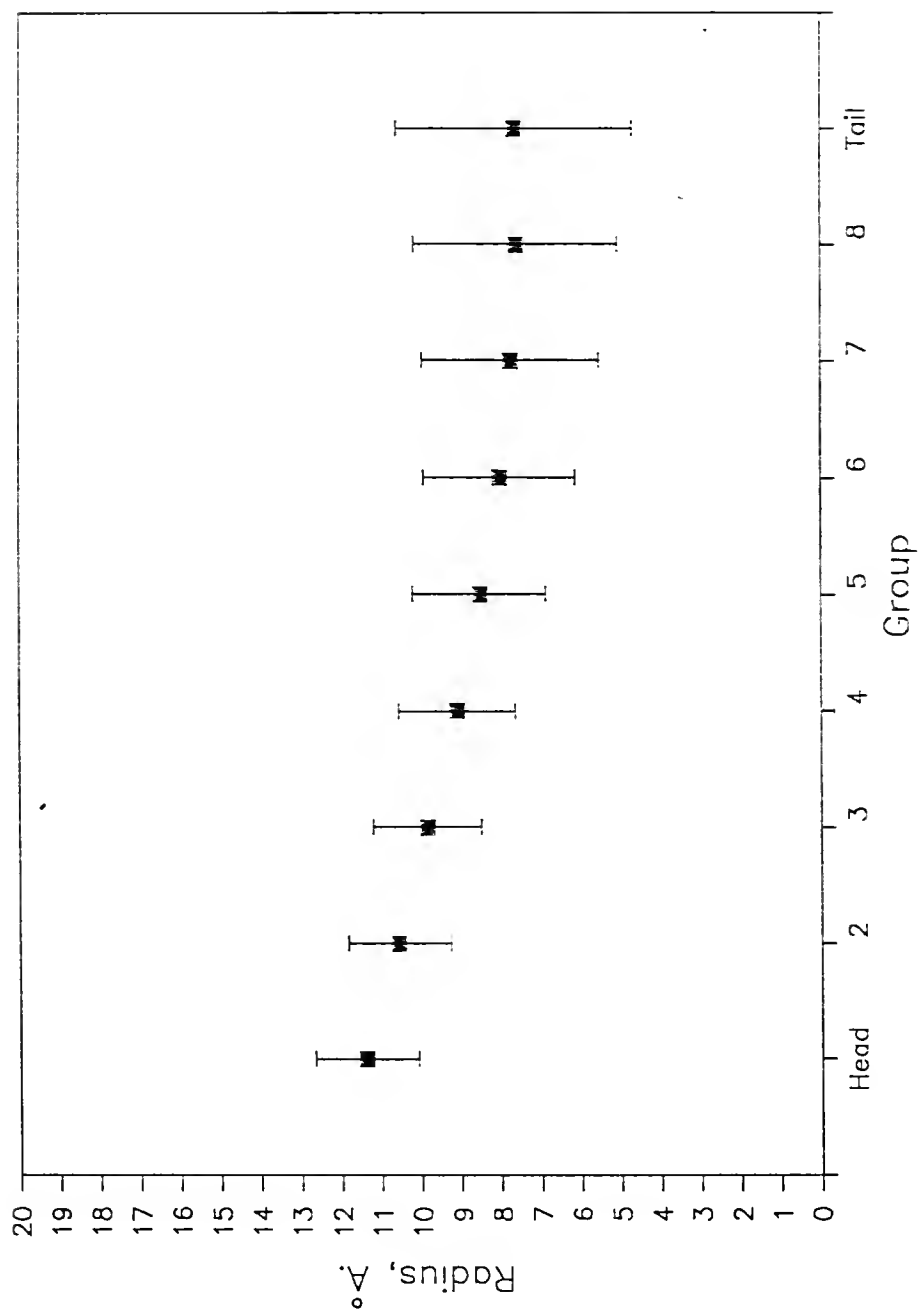


Figure 5-2. Mean radial positions of the nine groups of the surfactant molecules of Run 2. The vertical bars show one standard deviation on either side of the mean.

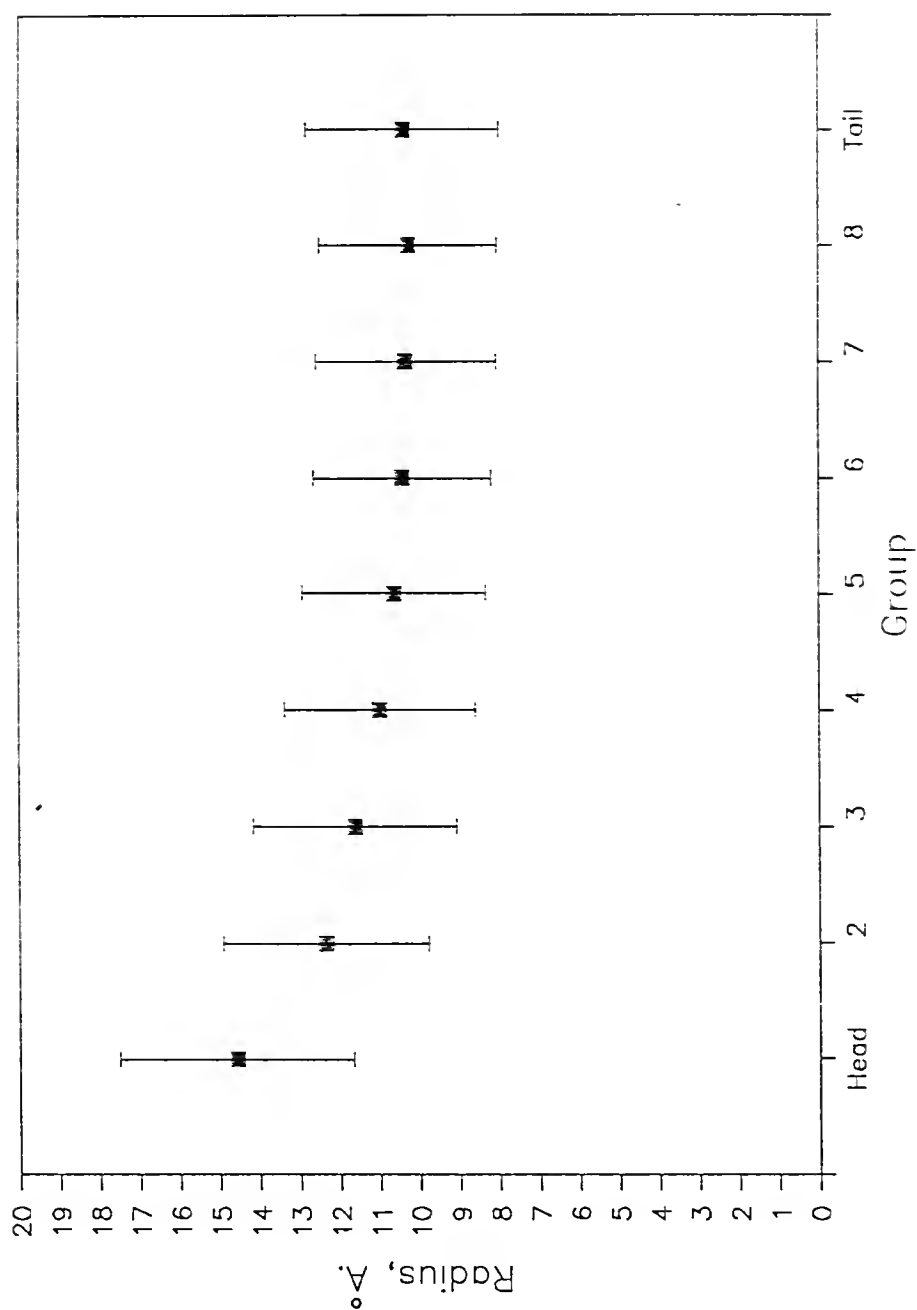


Figure 5-3. Mean radial positions of the nine groups of the surfactant molecules of Run 3. The vertical bars show one standard deviation on either side of the mean.

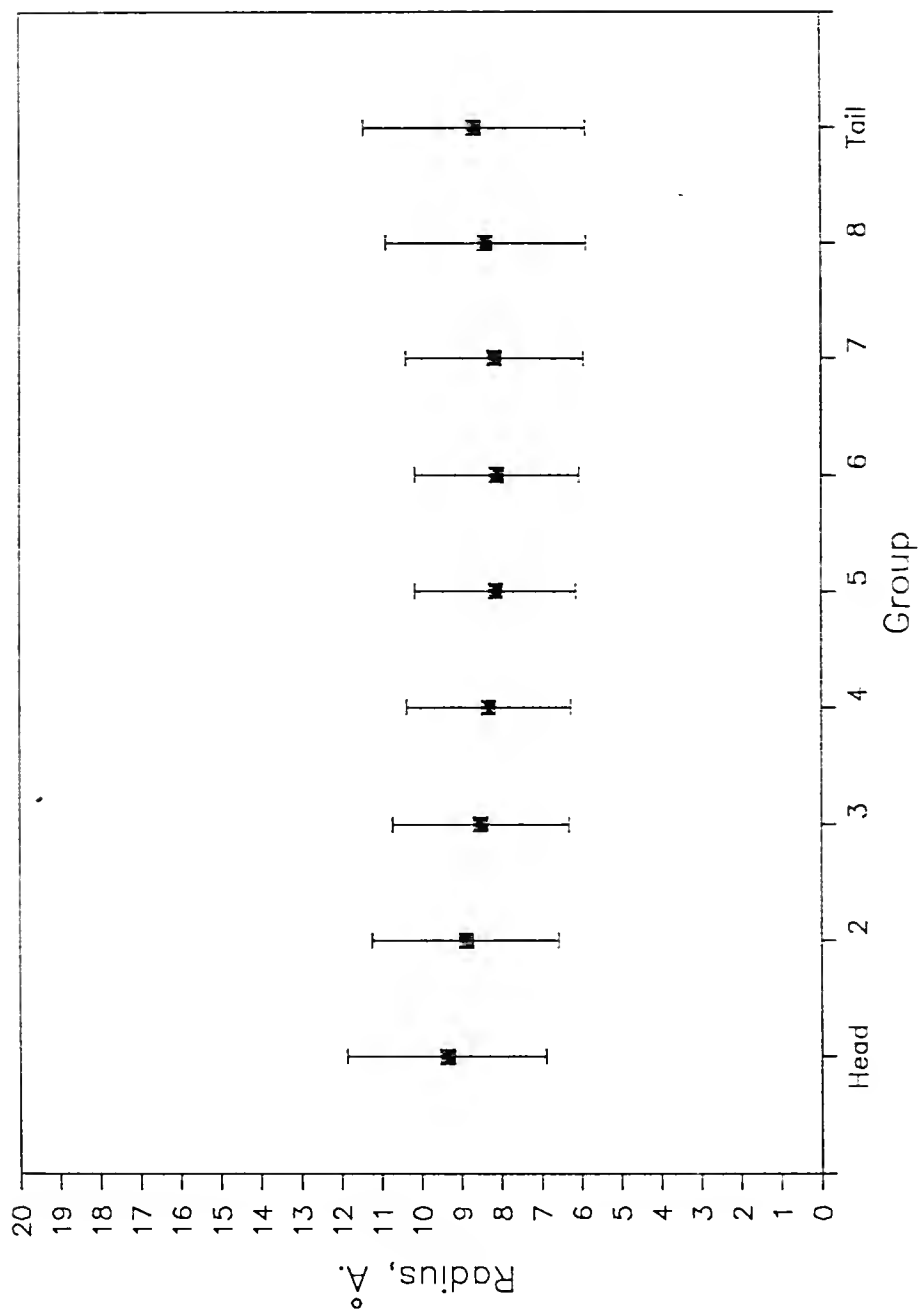


Figure 5-4. Mean radial positions of the nine groups of the hydrocarbon molecules of Run 4. The vertical bars show one standard deviation on either side of the mean.

Although no group has its mean position in the center of the micelle, this does not indicate a void within the micelle. Rather, it is an artifact of the coordinate system chosen. Each chain segment has a diameter of 3.56 Angstroms, and subsequently excludes a spherical volume of this diameter to any other group. Since the spherical coordinate system provides an available volume which decreases with r , the excluded volume effect results in low values of $N_i(r)$ near the center of the micelle. Thus, no group has its average position near the center, but the center is always within the excluded volume of one of several different groups. A range of three standard deviations about the mean includes approximately all of a group's positions, and, in Figures 5-1 through 5-4, approaches within a segment diameter of the center for several chain segments in each simulation.

The mean position results for Runs 1 and 2 are virtually identical. This is to be expected, since the two models differ only in the mass of the head group, a difference that should manifest itself in the dynamic behavior of the system, but not in a time-averaged result. In these two simulations, the head groups are found at the surface of the micelle with a relatively small deviation from the mean. Progressing along the chain toward the tail, the mean radial positions decrease and the deviations remain roughly

constant through group five. The mean positions of the last four groups are at approximately the same radius, but toward the tail the deviations increase, a consequence of the excluded volume effect near the center of the micelle.

The results for Run 3 are markedly different. Figure 5-3 shows larger values of mean positions for the chain segments and greater deviations for the head group and its adjacent three groups. This simulation differs from Run 2 in the size of the head group and the nature of the head-chain bond. With a diameter of 8.72 Angstroms, the larger head group creates a steric effect which brings about greater disorder in the micelle. The head groups are spread over a greater range of radial positions, altering the positions of the chain segments from those observed in Runs 1 and 2.

Figure 5-4 shows the results for Run 4, the hydrocarbon droplet. The mean positions and deviations are symmetric about group 5, the center of the molecule. This is the proper result, since the two ends of a chain are indistinguishable from one another. The chain ends have a slightly larger mean position and deviation, a result of the greater mobility of the chain end relative to the interior groups of the chain. Overall, the means and deviations are quite uniform, indicating a random arrangement of the

molecules within the droplet. Again, the excluded volume effect places the mean positions of all groups over two segment diameters away from the center of the droplet.

In a simulation of a micelle of forty dodecyl surfactant chains, the same shell model was used to surround the micelle and the head groups were identical to Run 1 in size, mass, and potentials (Woods et al., 1986). Comparison with this simulation reveals the effect of chain length on the micelle model. In Figure 5-5, the average radial positions of Woods' simulation are shown next to those of Run 1, pairing the groups of Run 1 with the nine groups furthest from the head group of the longer chain's thirteen. The dodecyl micelle being larger than those of the present work, its average radial positions are greater. Qualitatively, however, the trend observed in the radial positions of the groups and their standard deviations is quite similar in the two simulations.

In Figure 5-6, the average radial positions of Run 1 are compared to those resulting from a statistical model of 30 twelve-member chains with one end of each fixed at the surface (Gruen, 1981). In this model, all possible configurations of the surfactant chains were sampled. Though Gruen's micelle is again larger than that of Run 1, the results of the two models show notably similar radial position behavior on a qualitative basis.

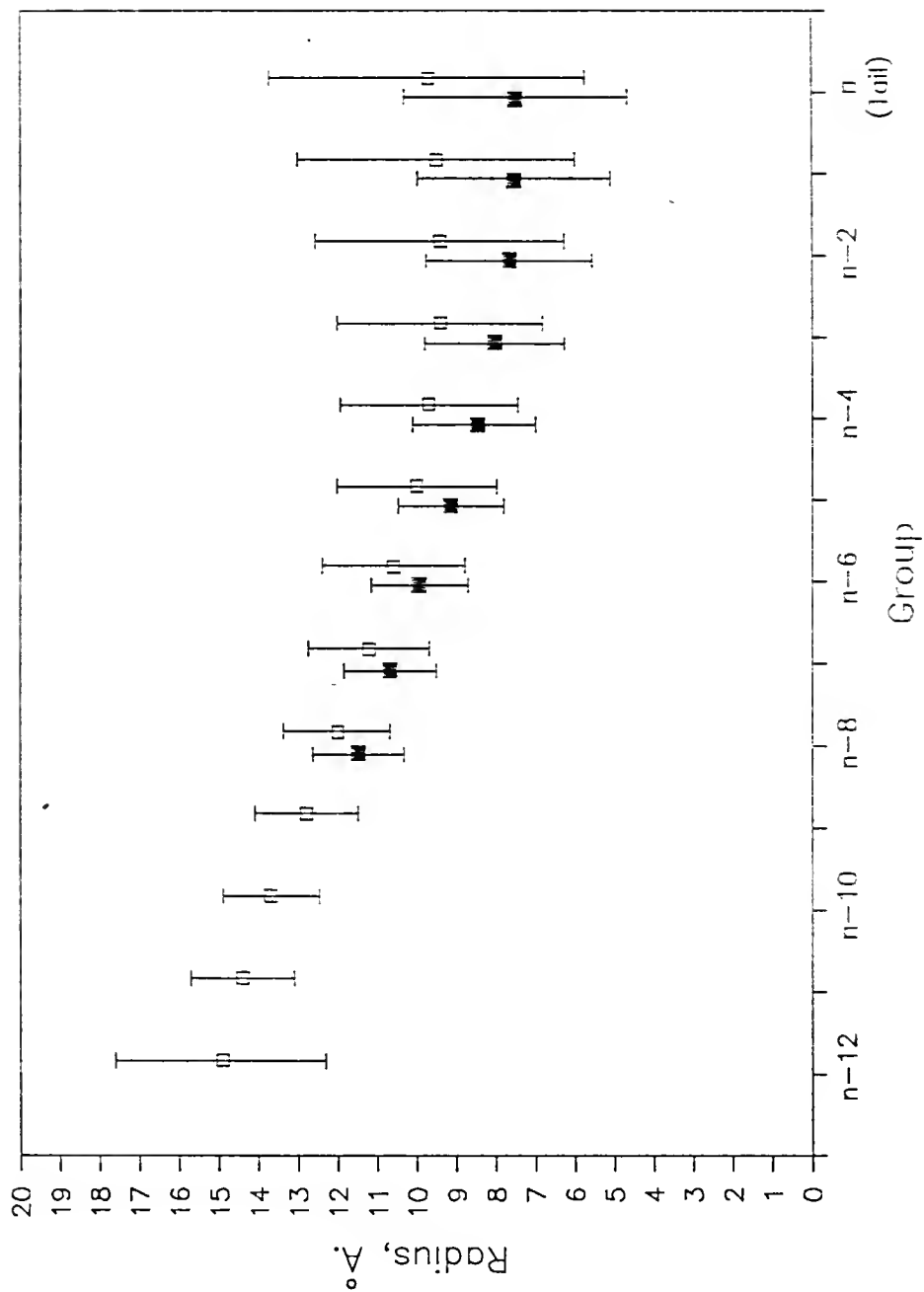


Figure 5-5. A comparison of the mean radial positions of groups in Run 1 and those obtained in a simulation of 40 dodecyl surfactant molecules by Woods et al. (1986).

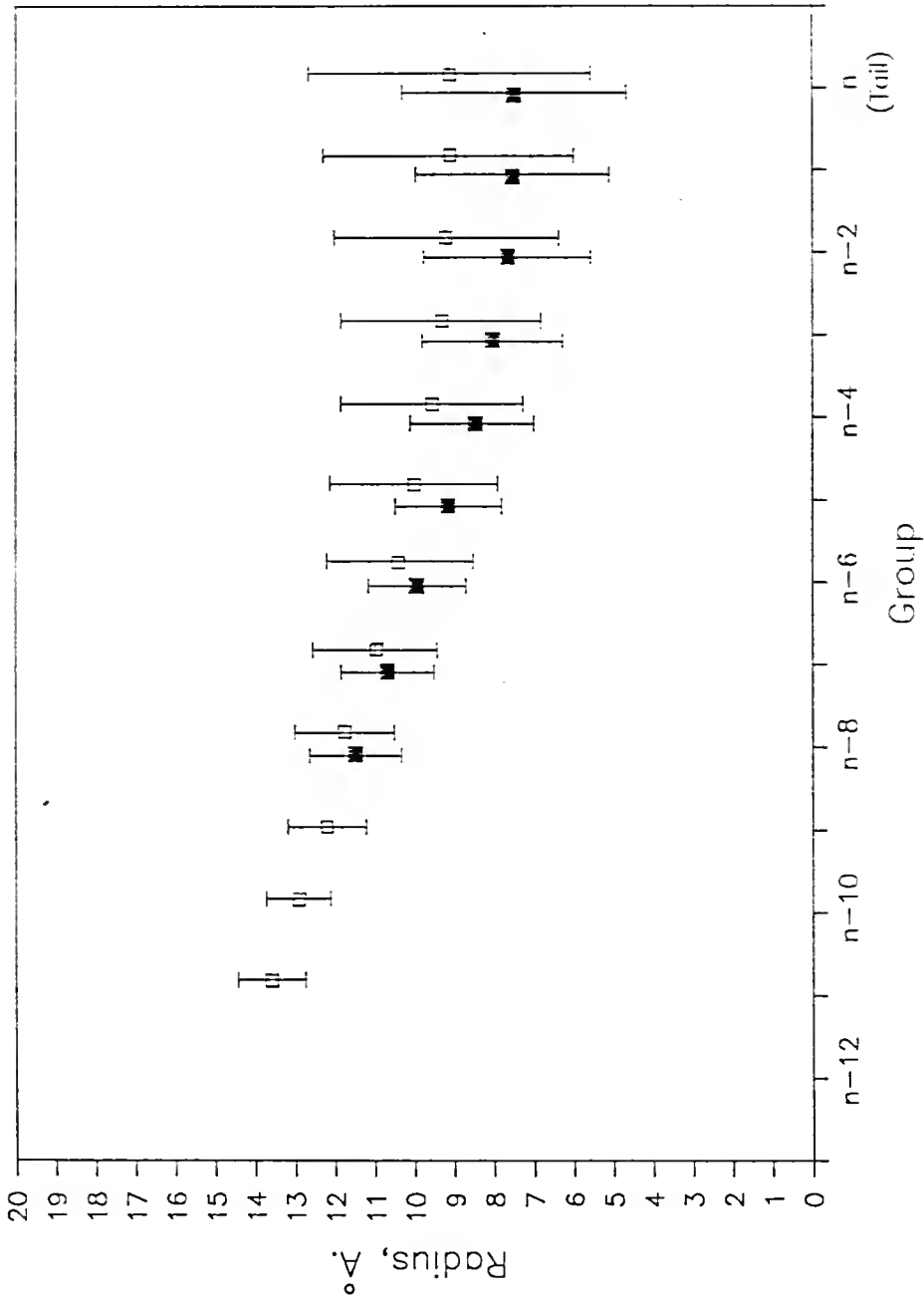


Figure 5-6. A comparison of the mean radial positions of groups in Run 1 and those obtained in a statistical model of 30 twelve-segment chains proposed by Gruen (1981).

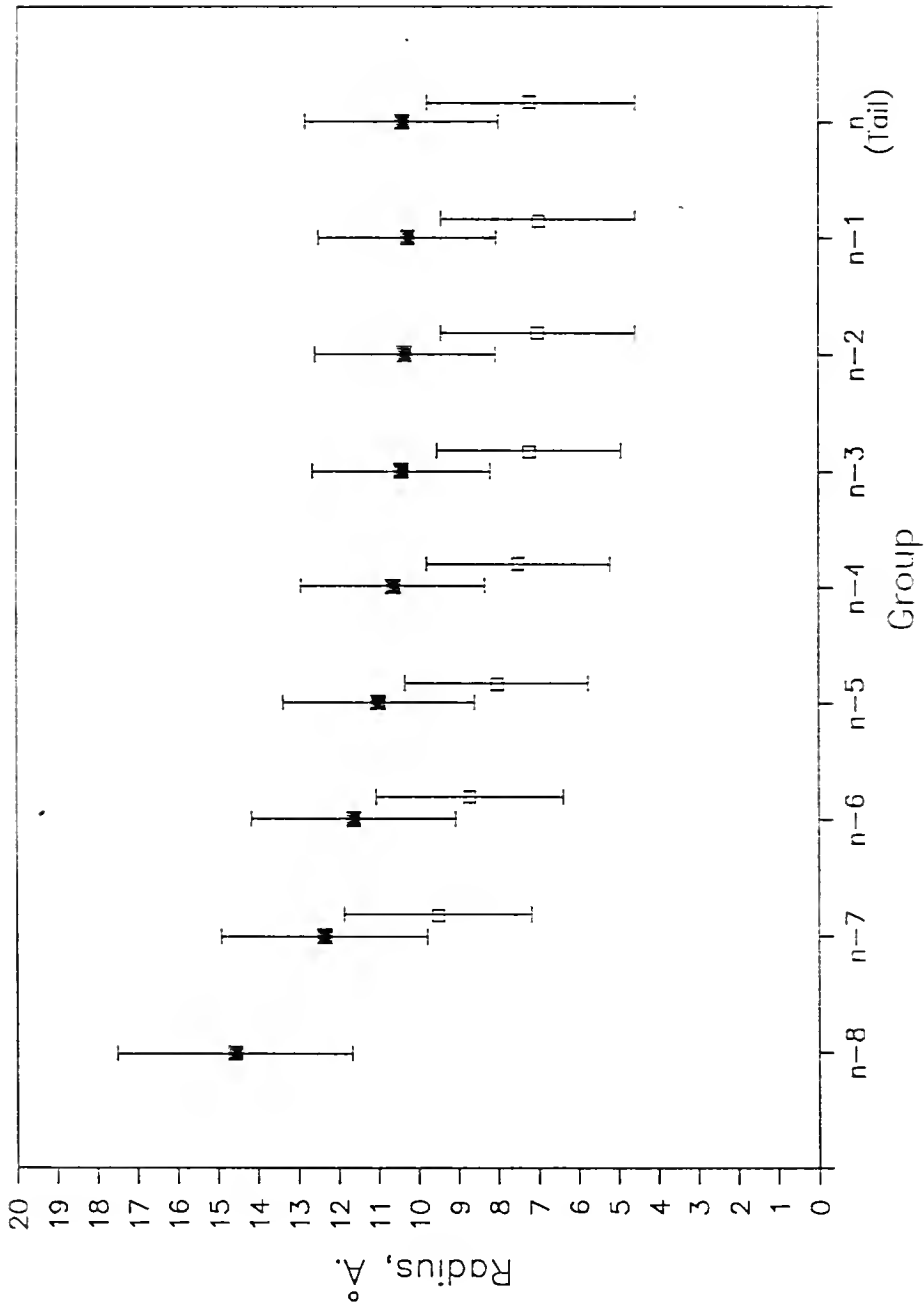


Figure 5-7. A comparison of the mean radial positions of groups in Run 1 and those obtained in a simulation of 15 sodium octanoate molecules by Jonsson et al. (1986).

A model micelle of 15 sodium octanoate molecules, along with surrounding molecular water, was the subject of another molecular dynamics simulation (Jonsson et al., 1986). The sodium carboxylate head group was explicitly modeled and surrounding water molecules were included in the simulation. Jonsson found it necessary to reduce the charge on the head groups to produce acceptable results. Run 3, with the model sulfate head group, is compared to Jonsson's reduced charge simulation in Figure 5-7. Accounting for the difference in the size of the two micelles, the radial positions of the chain segments compare favorably.

5.2 Probability Distributions of Group Positions

The positions of groups within the micelle can be studied in more detail by evaluating, at each radial position, the probability of finding a given group at any given time. The probability density function used in this analysis is the time-averaged number of occurrences of the center of a group i within a spherical volume element centered at r :

$$\rho_i(r) = \frac{\langle N_i(r) \rangle}{4\pi r^2 \Delta r} \quad (5.3)$$

Evaluating this function over all values of r generates a probability density distribution for each molecular group. The results of this analysis for each of the four simulations are given in Figures 5-8 through 5-11. The

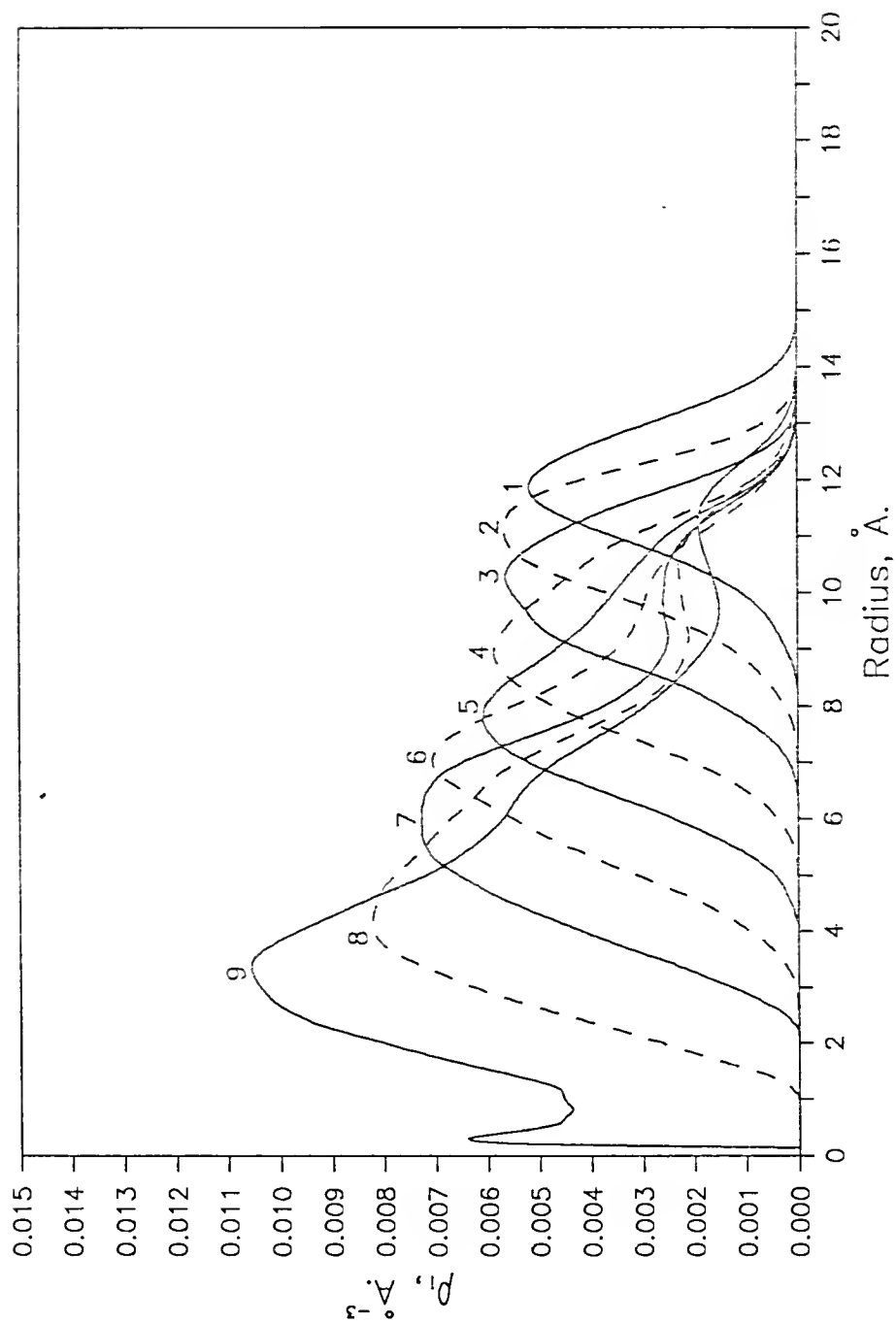


Figure 5-8. Probability density distributions of the nine groups of the surfactant molecules of Run 1. Group 1 is the head group and group 9 is the tail group.

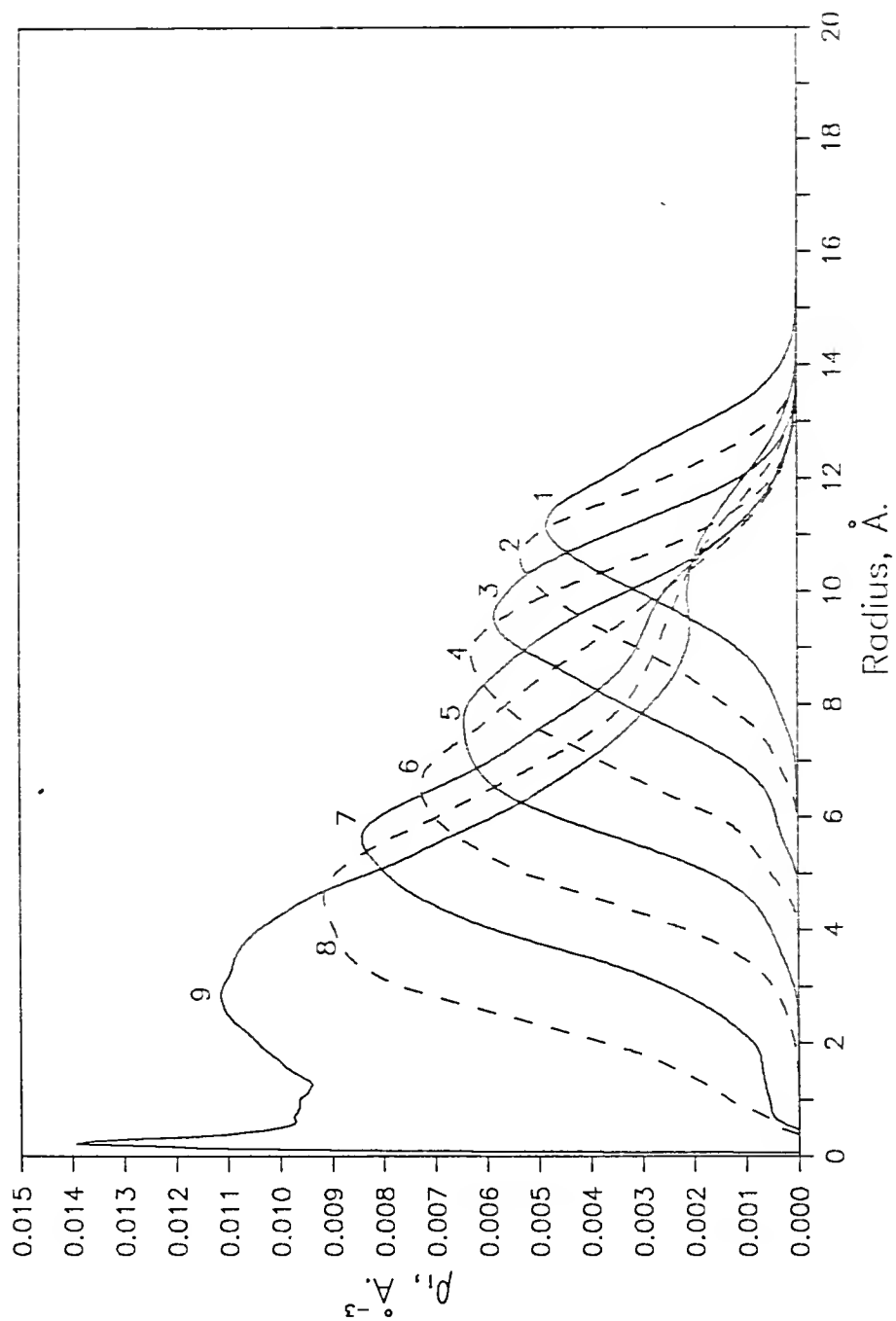


Figure 5-9. Probability density distributions of the nine groups of the surfactant molecules of Run 2. Group 1 is the head group and group 9 is the tail group.

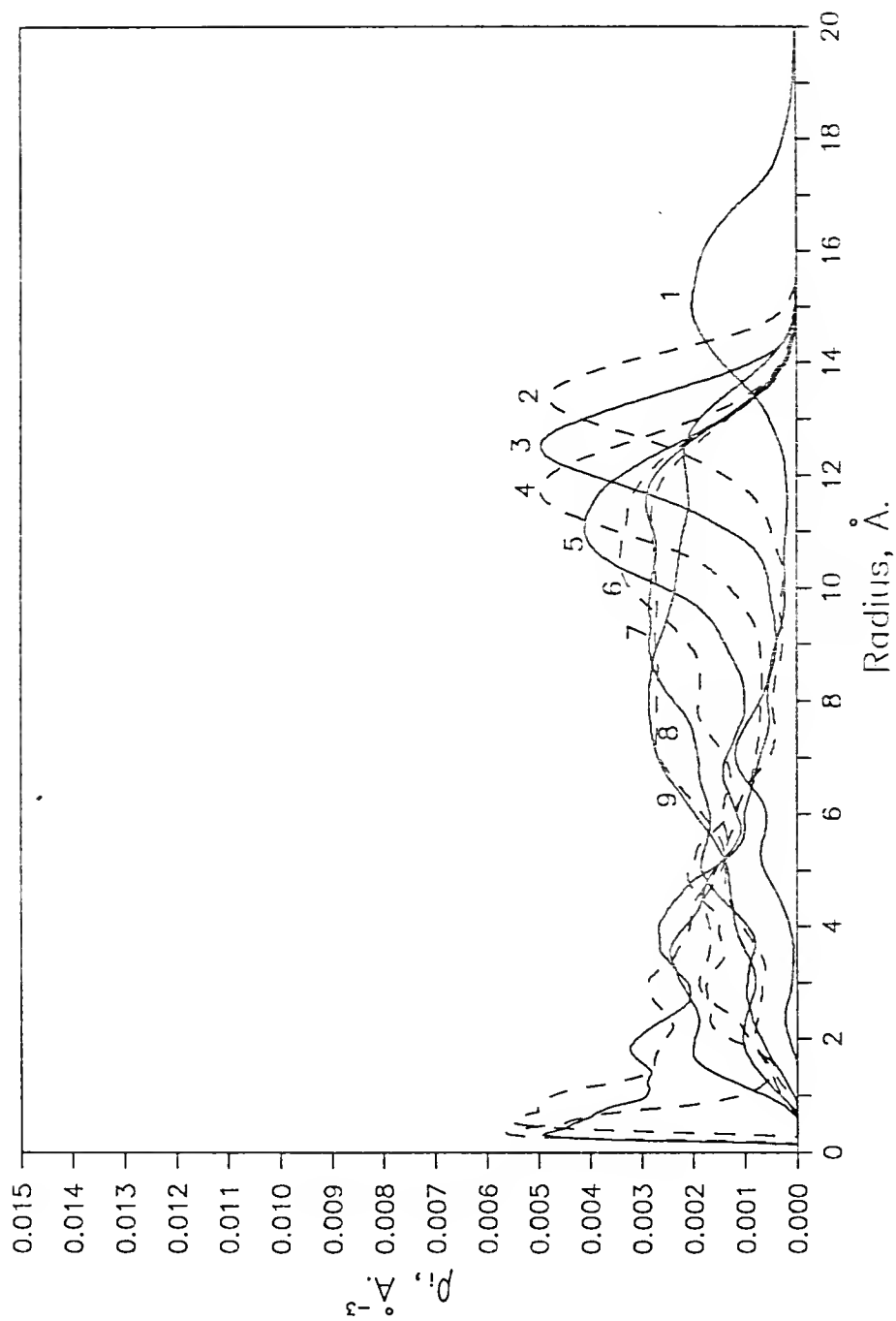


Figure 5-10. Probability density distributions of the nine groups of the surfactant molecules of Run 3. Group 1 is the head group and group 9 is the tail group.

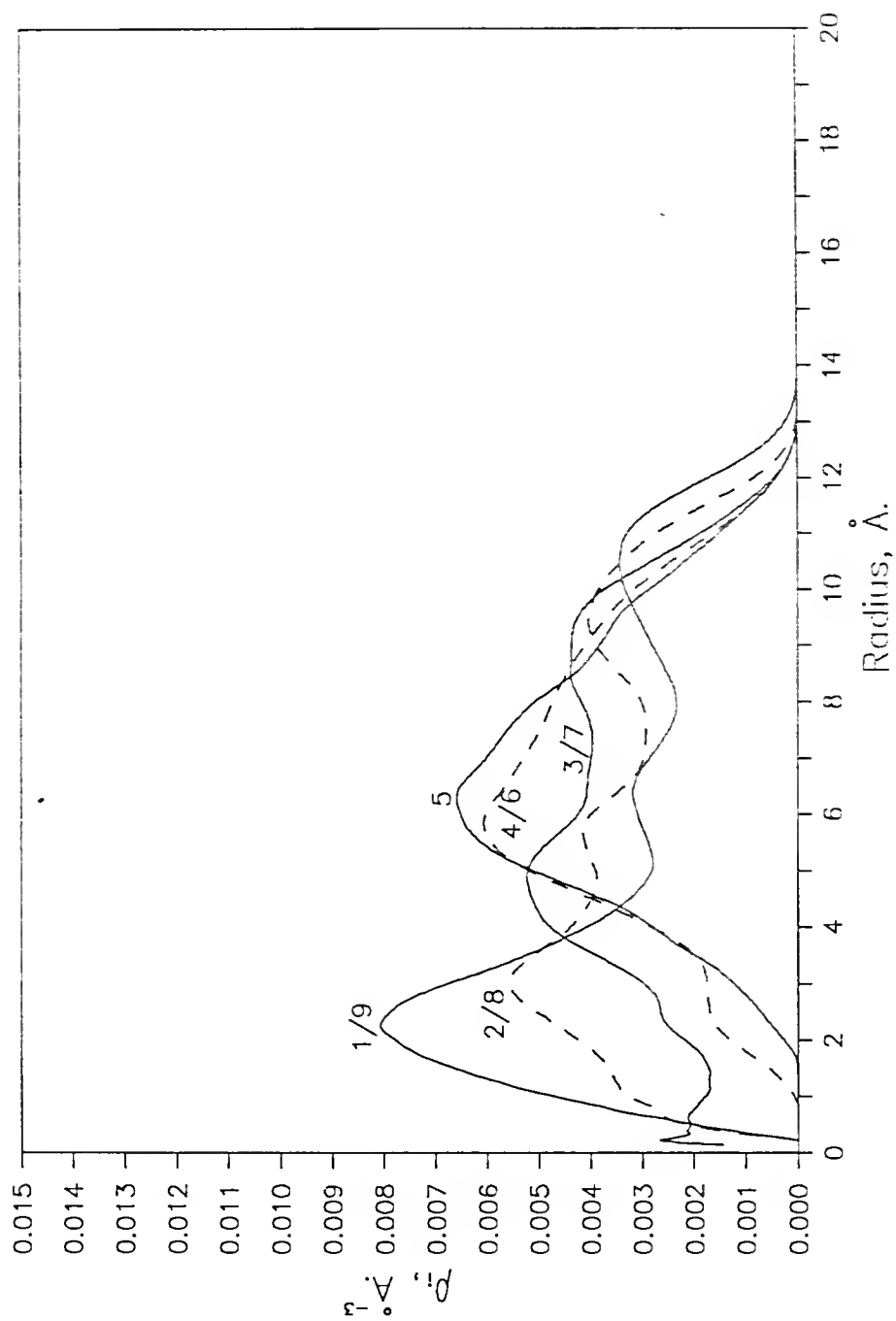


Figure 5-11. Probability density distributions of the five indistinguishable groups of the hydrocarbon molecules of Run 4. The label 1/9 denotes the terminal groups of the linear molecule and group 9 is the tail group.

probability density function is indefinite at the center of the micelle, but by choosing a finite value of Δr the indefinite result is avoided. Some scatter is introduced in the distributions at small r , however. Division by the volume element eliminates the excluded volume effect that produced no mean radial positions near the center of the micelle, as described in Section 5.1. Rather, the probability density distributions have peaks throughout the micelle for the various groups.

As in the case of the mean positions, the results for Runs 1 and 2 are quite similar and show the same degree of order. The head groups in these two simulations remain near the surface of the micelle. Moving along the chain toward the tail, the peak for each group occurs closer to the center and the distribution broadens. There is some probability of finding each of the groups at the surface, but there is no probability of finding the head group and the adjacent three groups within a segment diameter of the center. Two molecular configurations can lead to this result. First, with the head group at the surface, the chain is directed inward from the surface and then is bent around such that its tail is at the surface. Second, a molecule can lie along the surface. The output shows that both of these configurations do occur in Runs 1 and 2.

The results of two analogous simulations of micelles of 40 and 52 dodecyl surfactants (Woods et al., 1986) give distributions which are, except for micelle radius and surfactant chain length, remarkably similar to the results of Runs 1 and 2. These simulations also exhibited comparable average radial position behavior in the previous section. For the micelle model used in these four simulations, the difference in surfactant chain length, other than increasing the size of the micelle, has a negligible effect on the arrangement of chain segments in the micelle interior.

Figure 5-10 better displays the disorder present in Run 3 which was evidenced by the mean positions in Figure 5-3. The distribution of head group probabilities has two major peaks: one at the surface, and one approximately one head group diameter from the surface. Groups two through four have roughly the same peak arrangement, but the distributions become more random toward the end of the chain. With the larger head group size, the excluded volume effect at the surface forces one or more head groups into the micelle interior and disrupts the orderly arrangement of chain segments found in Runs 1 and 2.

Figure 5-11 shows the distributions for Run 4, the hydrocarbon droplet. Since the symmetry of the chains was demonstrated in the previous section, the combined

probabilities for the indistinguishable pairs of groups are plotted. All groups have a finite probability of being found anywhere between the center and the surface of the droplet, and, within statistical uncertainties, the distributions indicate a random arrangement of the molecules.

While the probability density function serves well to remove the effect of excluded volume at the center of the micelle in evaluating group positions, the r^2 dependence causes some difficulties in interpreting the results. The distribution curves do not enclose equal areas, and they do not correspond to the mean radial positions of Section 5.1. In that section it was assumed that the distribution of $N_i(r)$ was normal in assigning a percentage of the distribution to the standard deviation. By multiplying the probability density function by r^2 , a distribution is generated which will enclose equal areas for each group, and will serve to evaluate the assumption of symmetry made in the previous section. It is apparent from the probability densities that the three groups adjacent to the head group follow the head group while the three or four groups adjacent to the tail follow the tail. By plotting the quantity $\rho_i r^2$ for only the heads and tails in Figures 5-12 through 5-15, clarity is improved without excessive loss of information.

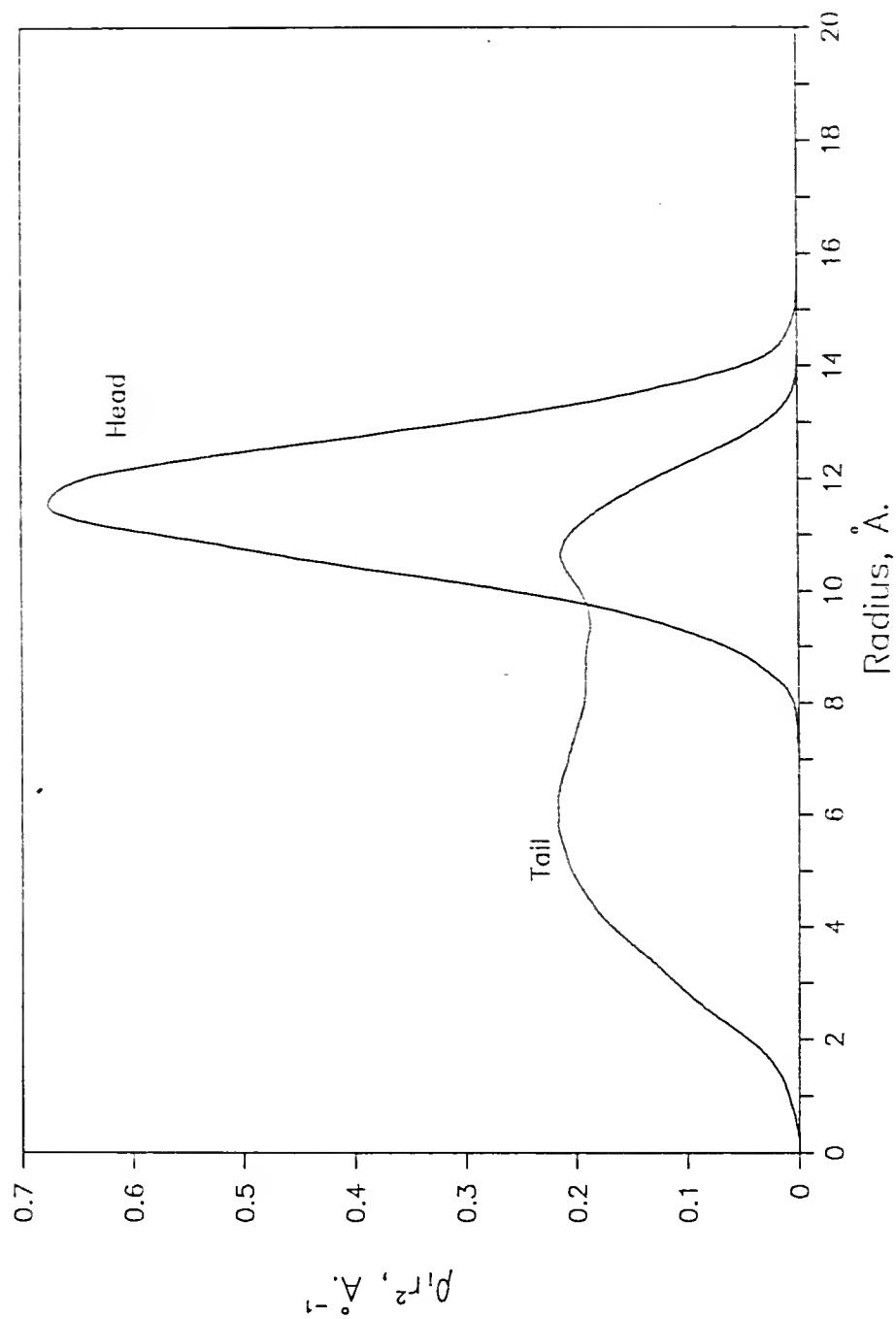


Figure 5-12. The distributions of probability density multiplied by the square of the radial position for the heads and tails of the surfactant molecules of Run 1. The plotted curves enclose equal areas and correspond to the mean radial positions of Figure 5-1.

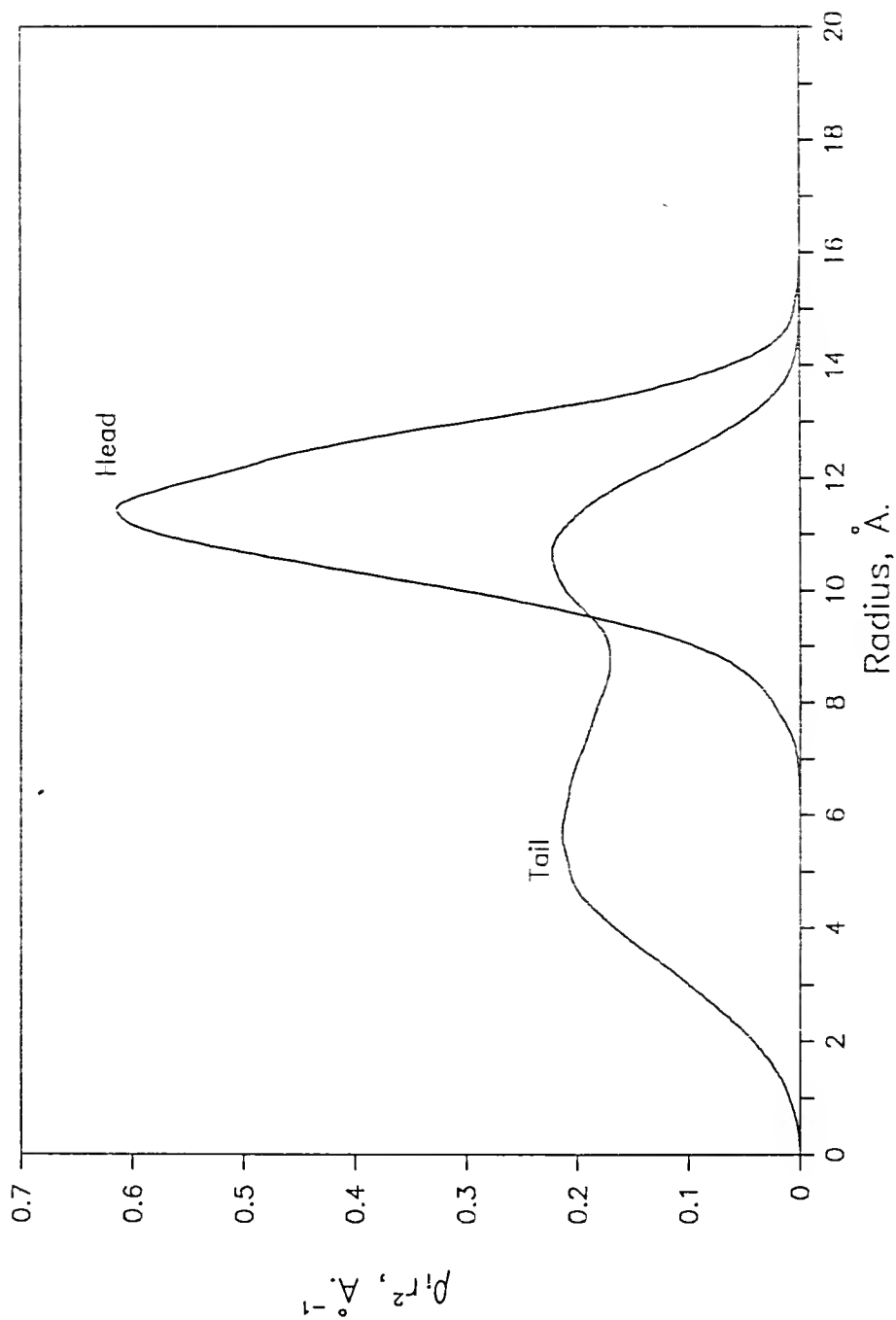


Figure 5-13. The distributions of probability density multiplied by the square of the radial position for the heads and tails of the surfactant molecules of Run 2. The plotted curves enclose equal areas and correspond to the mean radial positions of Figure 5-2.

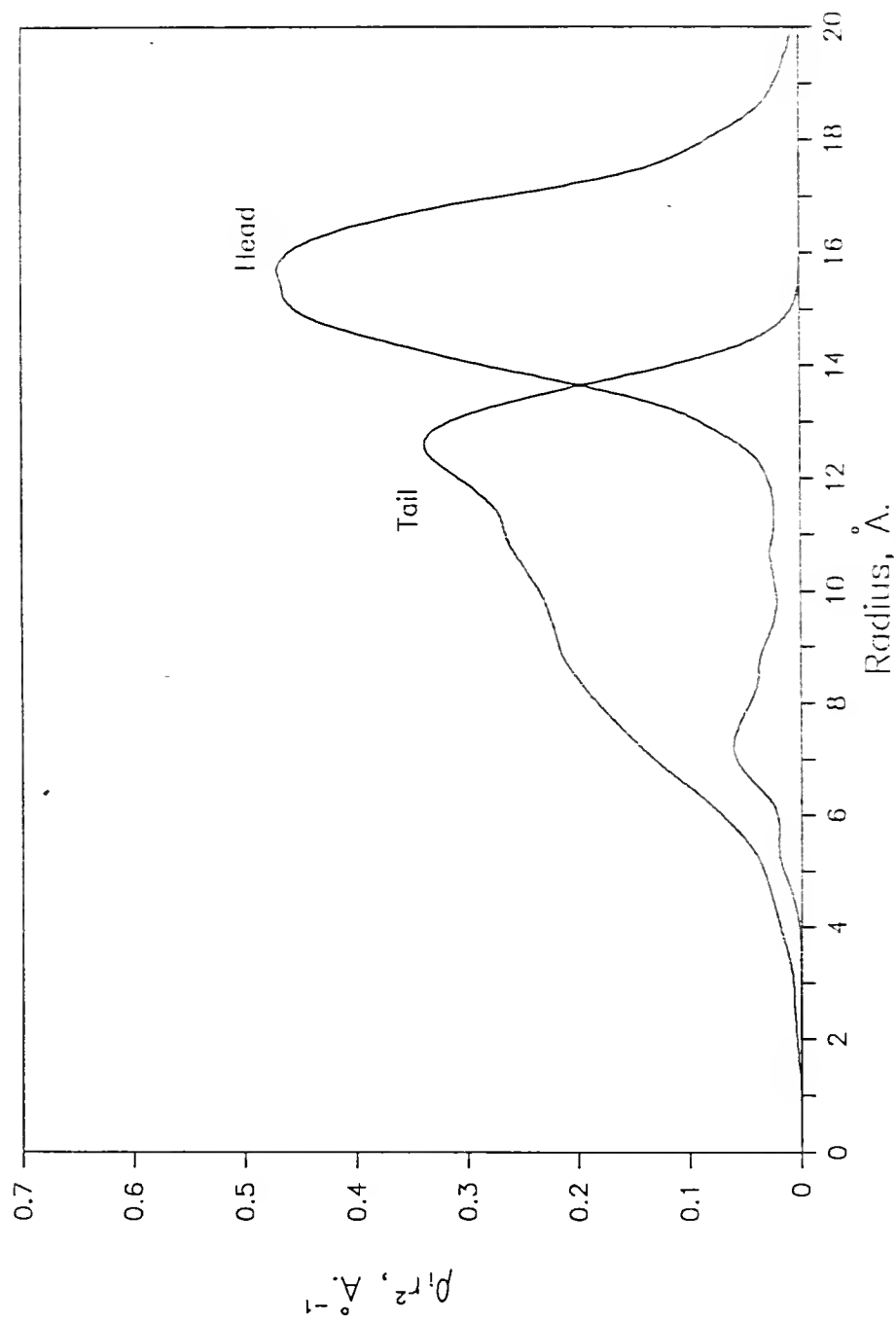


Figure 5-14. The distributions of probability density multiplied by the square of the radial position for the heads and tails of the surfactant molecules of Run 3. The plotted curves enclose equal areas and correspond to the mean radial positions of Figure 5-3.

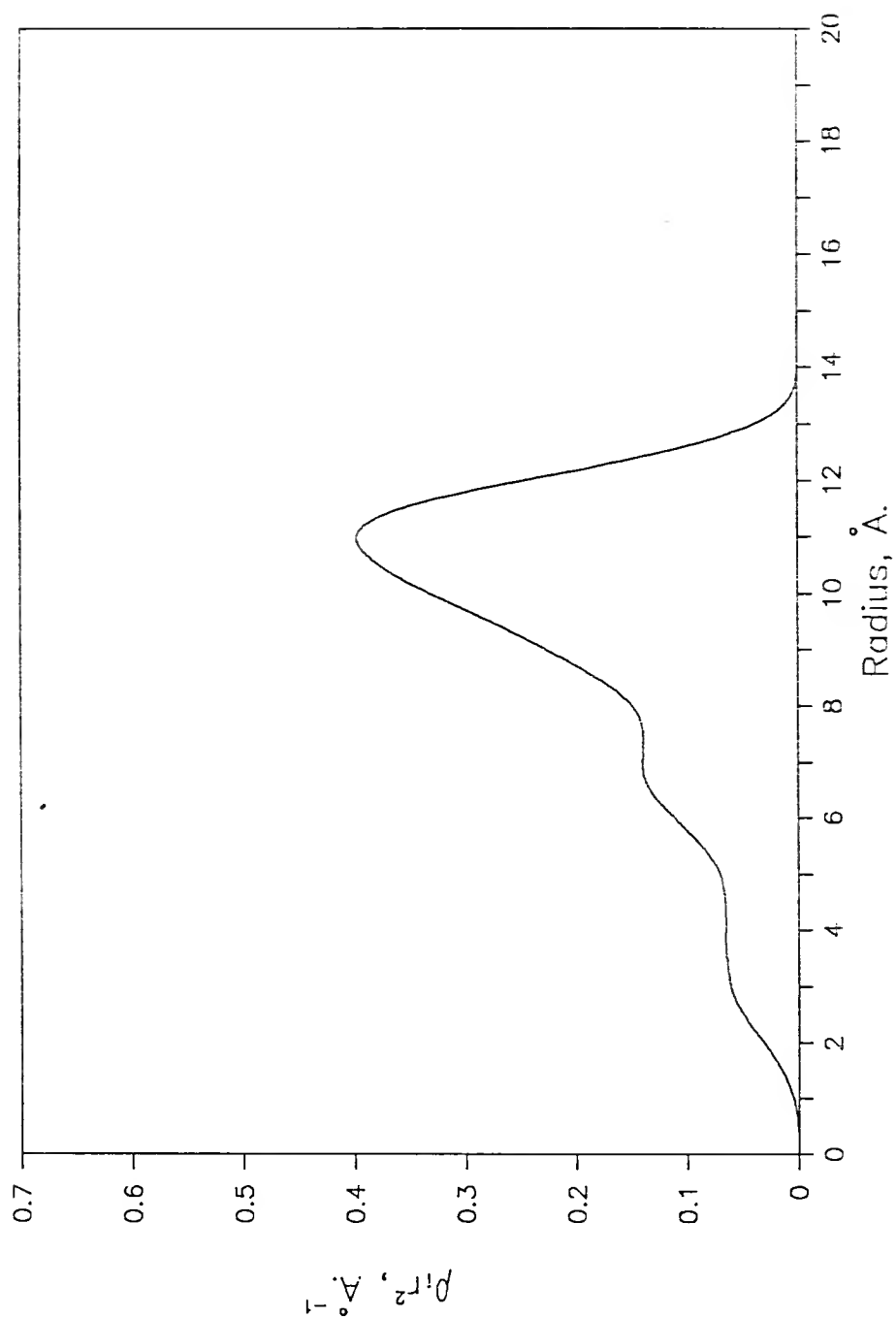


Figure 5-15. The distributions of probability density multiplied by the square of the radial position for the terminal groups of the hydrocarbon molecules of Run 4. The curve corresponds to the mean radial positions groups 1 and 9 in Figure 5-4.

These plots for Runs 1 (Figure 5-12) and 2 (Figure 5-13) show the head groups to have a very nearly normal distribution, centered at the mean radial position, with a range of less than three standard deviations in each direction along the abscissa. The tails have broader distributions, not quite as symmetric, but with a range within three standard deviations in each direction. The tails have a finite probability of radial positions well within a segment diameter of the center, confirming the statistical assumptions of the previous section.

The ρ, r^2 plot for Run 3 (Figure 5-14) reveals a symmetric peak for the head group, centered just above the mean position. It is broader than those of Runs 1 and 2, with a smaller peak in the interior of the micelle, as discussed above. A comparison of the areas of the two peaks indicates that, on the average, two head groups can be found in the interior of the micelle. The tail distribution is skewed toward the outer portion of the micelle since fewer groups can be accommodated in the center than in the outer portion. The tail distribution does, however, show finite probability of radial positions within a segment diameter of the center. The result for the chain ends of Run 4 is similar to that of the tail in Run 3. There is probability

of end groups occurring throughout the hydrocarbon droplet, with the curve skewed toward the outer portion of the droplet.

Simulations of a micelle of 15 sodium octanoate molecules in water have been carried out by groups led by Jonsson (Jonsson et al., 1986) and Watanabe (Watanabe et al., 1988). Jonsson reduced the charge on the head groups, while Watanabe used the Ewald method to handle the long range electrostatic effects. The chain length of the surfactant monomer of these simulations differs from that of the present work by only one chain segment. By scaling the probability density function with respect to the aggregate size, the result from these previous simulations can be compared to that of this work. Such a comparison for the tail groups is made in Figure 5-16. The larger micelle of Run 3 exhibits a distribution with a higher mean value of the radial position. It is not symmetric, but skewed toward the surface of the micelle. The tails of Run 3 are distributed over a range equal to that of the other two simulations.

The experimental technique of small angle neutron scattering (SANS) can be used to obtain information which may be indicative of micelle structure. Scattering

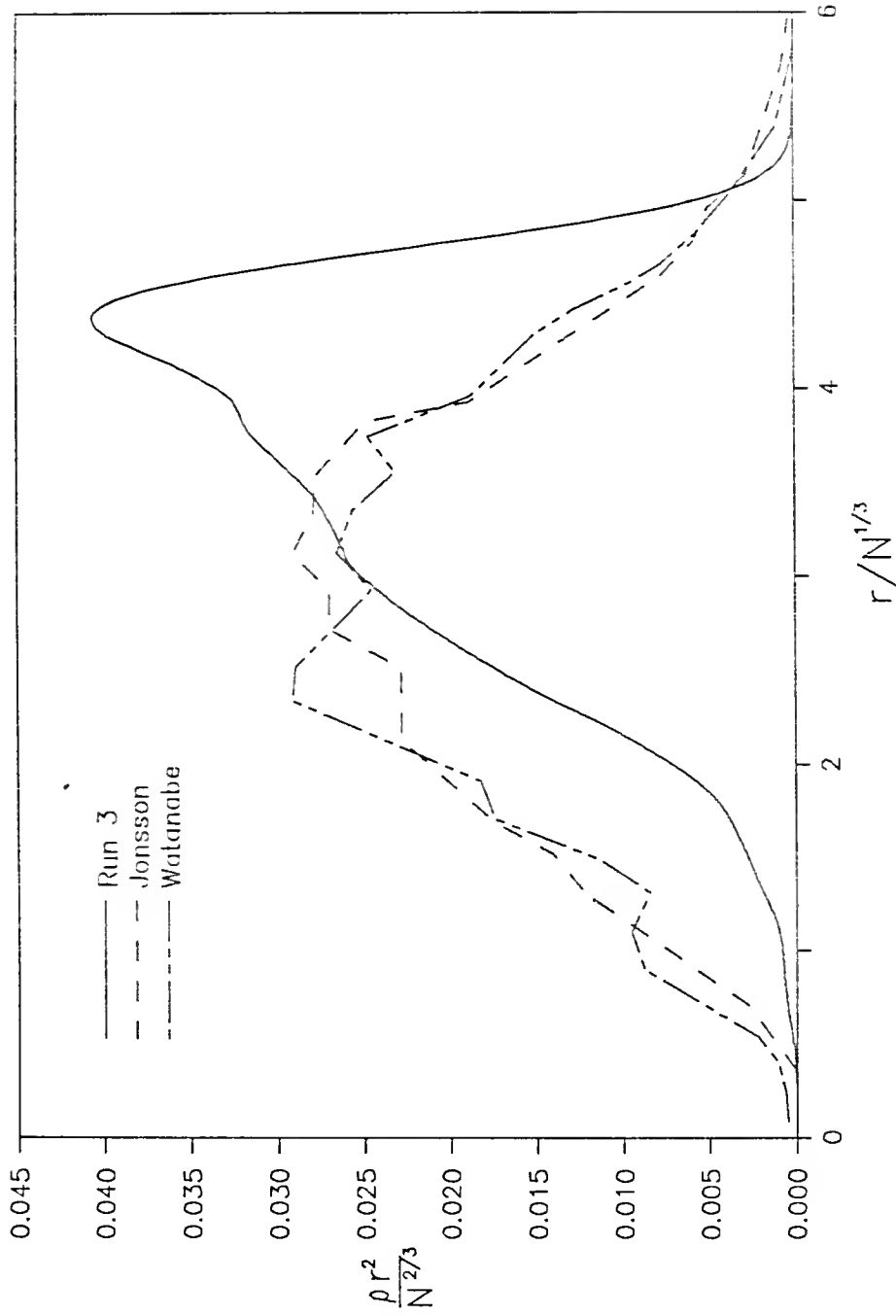


Figure 5-16. Probability distributions of the tail group position in three micelle simulations. Results are scaled to remove the impact on the distribution of the aggregate number, N . The solid line is the result obtained for Run 3, the dashed line for Jonsson et al. (1986) and the dash-dot line for Watanabe et al. (1987).

measurements were made on aqueous solutions of lithium dodecyl sulfate above the critical micelle concentration (Bendedouch et al., 1983a). The results of this study showed the alkyl core to have more order than the liquid state, yet less than the all-trans model, and to be free of water. One result of the SANS study is the Fourier transform of the scattering amplitude due to the distribution of methyl tails. This can be written as

$$\frac{A(Q)}{A(0)} = \frac{4\pi}{N} \int_0^\infty r \rho_{Me}(r) \frac{\sin(Qr)}{Q} dr \quad (5.4)$$

where $A(Q)$ is the Fourier transform of the scattering amplitude

$\rho_{Me}(r)$ is the probability density of the tail group position

Q is the scattering vector

Plots of $A(Q)/A(0)$ for the SANS result and Runs 1 through 4 are given in Figure 5-17. Again the results for Runs 1 and 2 confirm nearly identical structure. A plot of $A(Q)/A(0)$ for a uniform distribution of tails through the micelle nearly coincides with the result for Run 4, the hydrocarbon droplet. As the size of the aggregate increases, the $A(Q)/A(0)$ curve is shifted to lower values of Q . The order present in the aggregate affects the shape of the curve, as seen in the curves for the highly-ordered Run 1 and the uniform result without order. The SANS result,

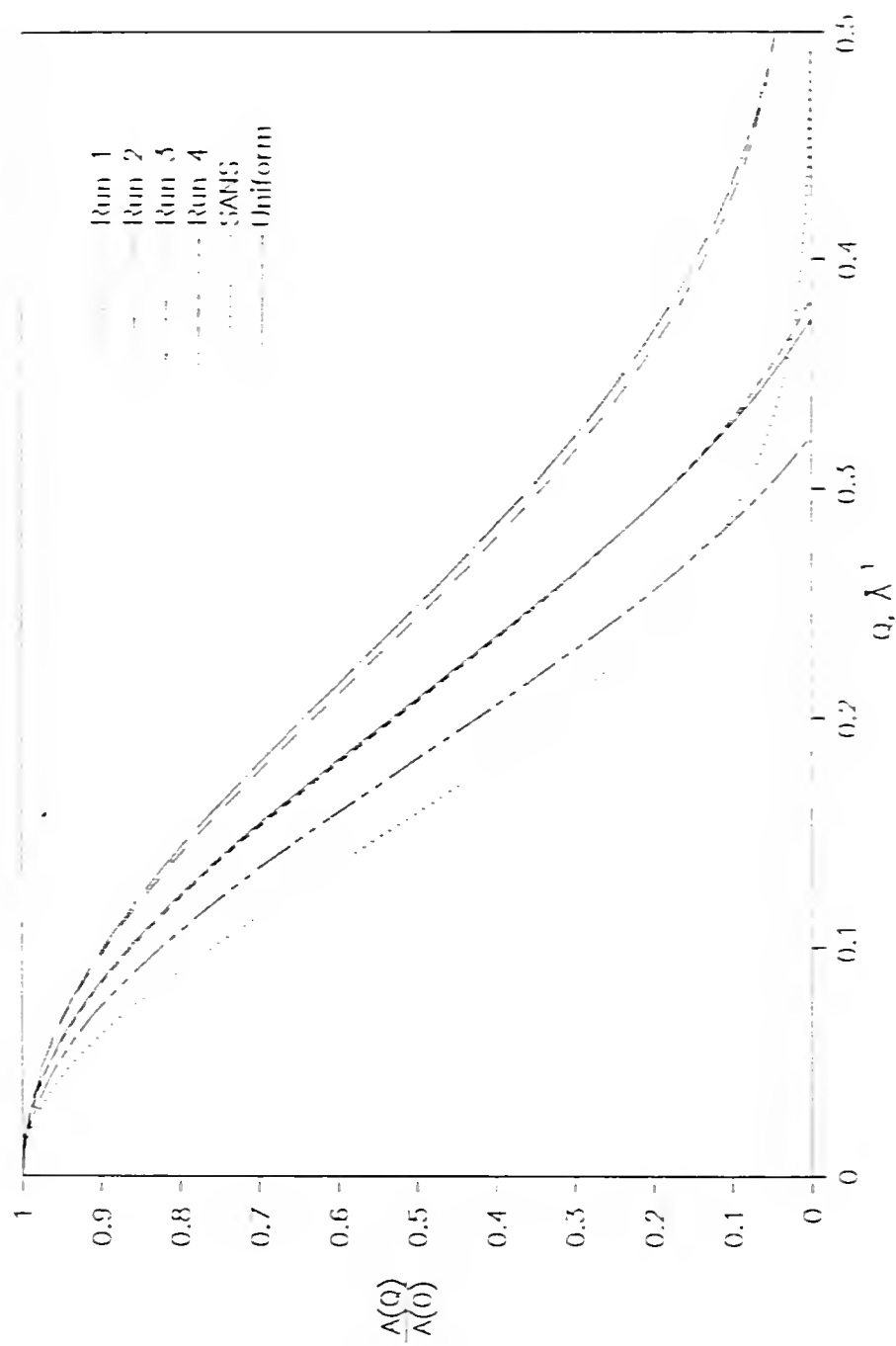


Figure 5-17. Fourier transform of tail group density for Run 1-4, the SANS data of Bendelouch et al. (1983a), and the result for a uniform distribution of tails throughout the aggregate.

for an aggregate of approximately 78 dodecyl chains, falls off much more rapidly than the result for the much smaller micelles of Runs 1 and 2. Its shape, however, is quite similar to the curves for Runs 1 and 2, suggesting that the structure of Runs 1 and 2 may be more like the experimental result than that of Run 3.

The $A(Q)/A(0)$ curve for Run 3 falls off more rapidly than those of the other three simulations, due to the larger size of the Run 3 micelle. Its shape is very much like the Run 4 result. The disorder in structure of the Run 3 micelle may be greater than is indicated for this experimental result, though it is difficult to make any real conclusion regarding this since the two micelles are of such drastically different size. Such a size difference could affect internal structure, and, in fact, the experimentally determined aggregate number of 78 for dodecyl chains yields a nonspherical micelle.

5.3 Conformations of Chain Molecules

From the analysis of the positions of the groups along the surfactant chain within the micelle, it is apparent that the majority of the molecules are not in the all-trans conformation of the simulation's initial condition. In order to achieve the distributions of positions observed, chain bending involving the transition of bonds from the trans to the gauche conformation must occur. The

conformations of the chains, in terms of numbers of gauche and trans bonds, gives further information about the internal structure of the micelle.

In this analysis, a bond is considered to be in the trans conformation if the cosine of its dihedral angle is less than -0.5 (Weber, 1978; Woods et al., 1986):

$$\cos\phi < -0.5 \quad (5.5)$$

Thus, a trans bond in this analysis has a rotational potential between zero and the surrounding relative maxima (see Figure 4-2).

The instantaneous percentage of trans bonds versus time for each of the four simulations is given in Figures 5-18 through 5-21. With six dihedral angles per molecule, the transition of one bond is represented by a change of 0.69 percent in these figures. Changes of this magnitude occur almost continuously (within two femtoseconds), while changes on the order of five percent take place over a range of five to ten picoseconds. The fluctuations in trans percentage have a mean value which is dependent on the simulation model. The mean value for Run 1 is 68 ± 2 , for Run 2, 70 ± 3 , for Run 3, 74 ± 2 , and for Run 4, 73 ± 3 . In their simulation of 15 sodium octanoate molecules, Watanabe et al. (1988) reported a value of 78 ± 2 percent. Jonsson et al. (1986), in a simulation of the same system, reported a value of 50 ± 3 percent for their reduced charge model. In the

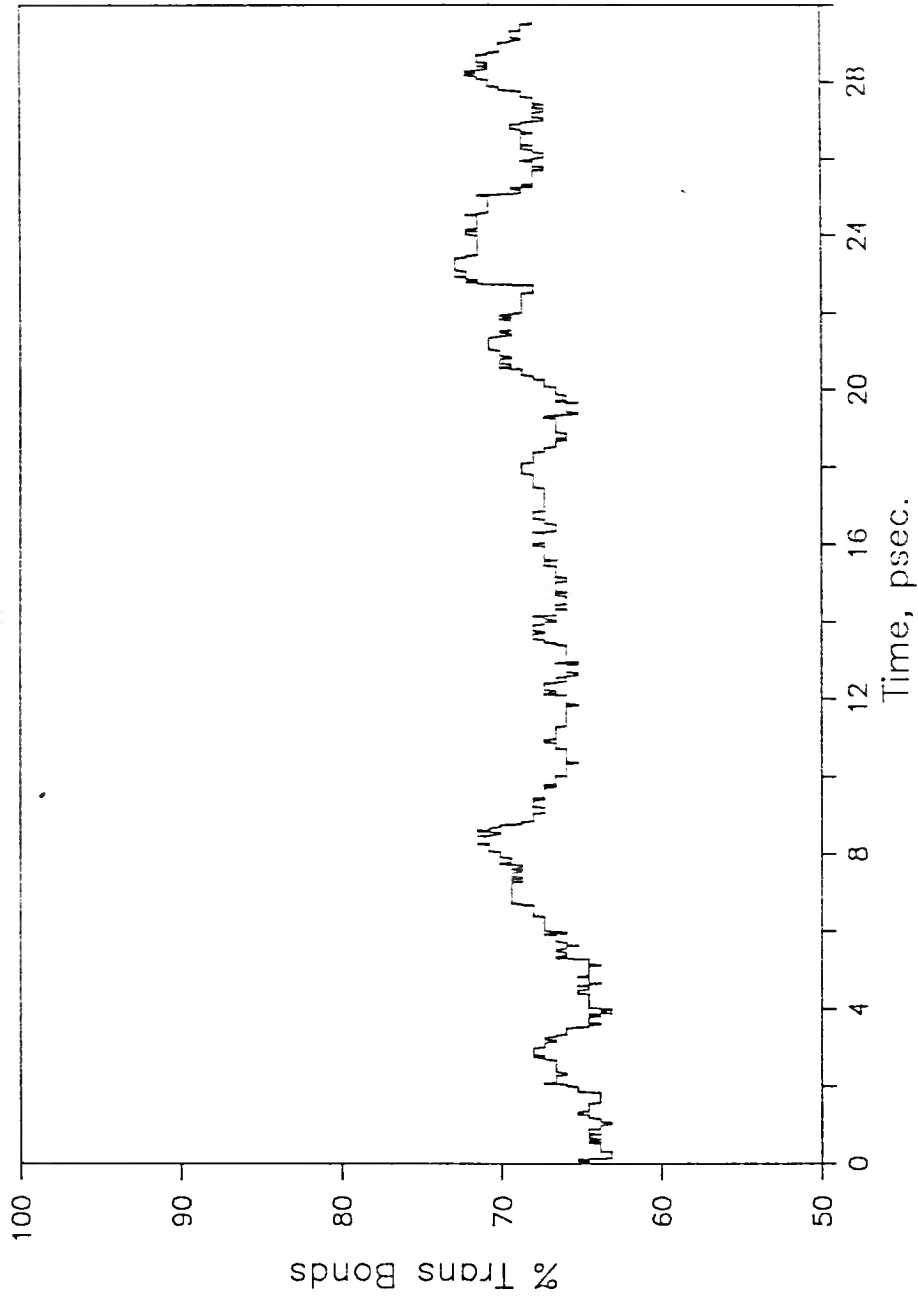


Figure 5-18. The percentage of surfactant molecule bonds of Run 1 which are in the trans conformation. The percentage is reported at intervals of .0198 picosecond. The mean value is 67.7 percent with a standard deviation of 2.2 percent.

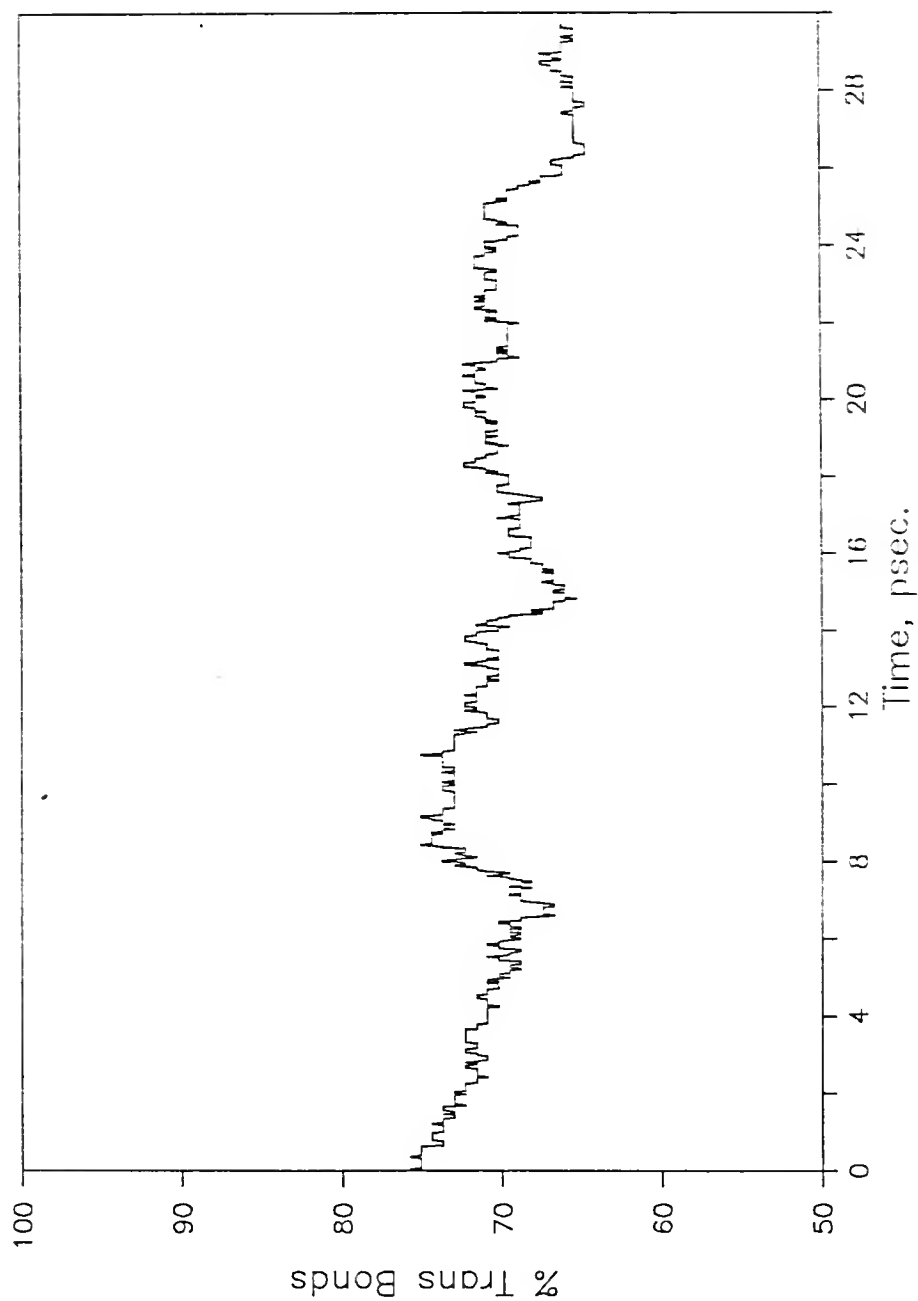


Figure 5-19. The percentage of surfactant molecule bonds of Run 2 which are in the trans conformation. The percentage is reported at intervals of .0198 picosecond. The mean value is 70.1 percent with a standard deviation of 2.6 percent.

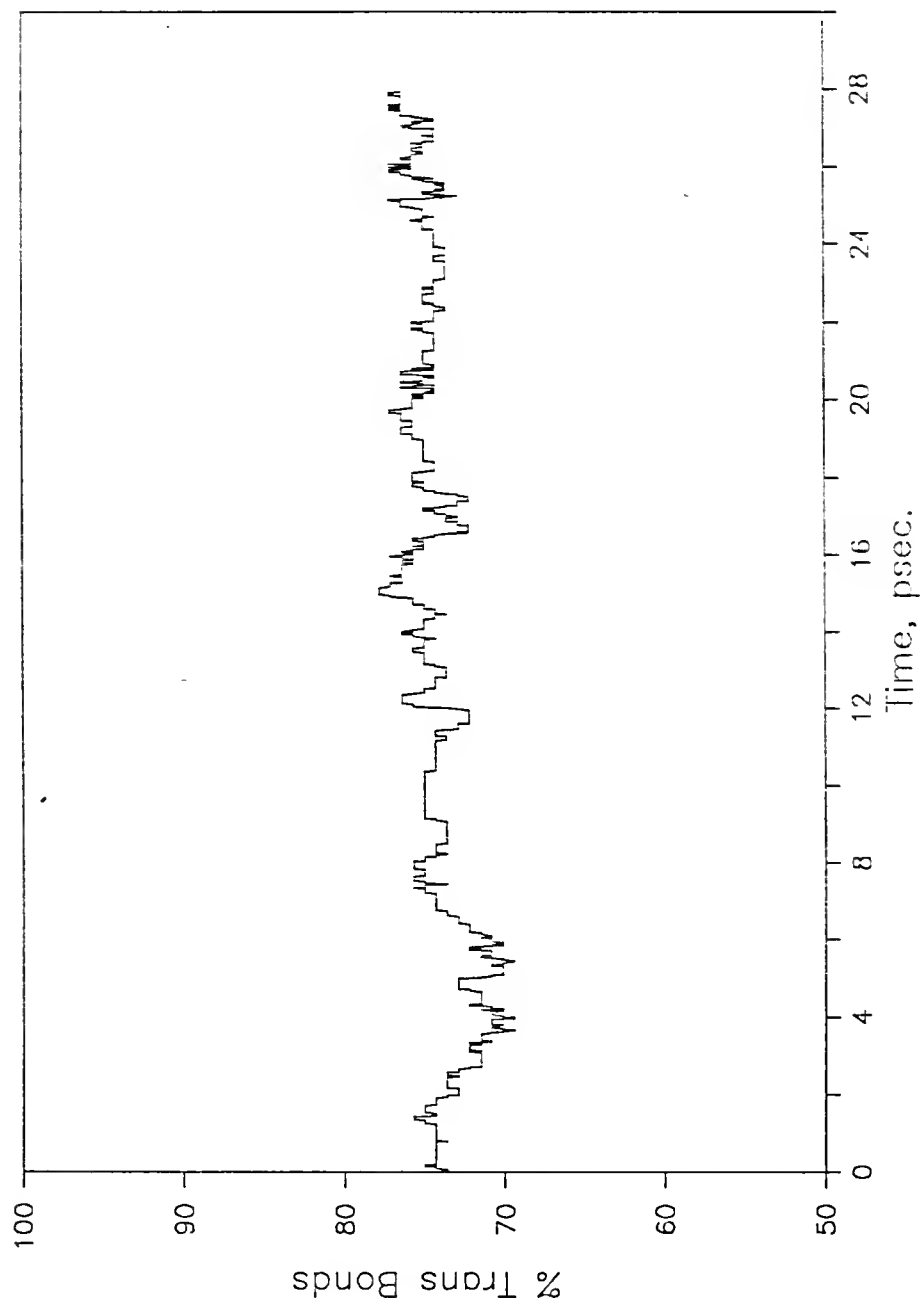


Figure 5-20. The percentage of surfactant molecule bonds of Run 3 which are in the trans conformation. The percentage is reported at intervals of .0140 picosecond. The mean value is 74.3 percent with a standard deviation of 1.6 percent.

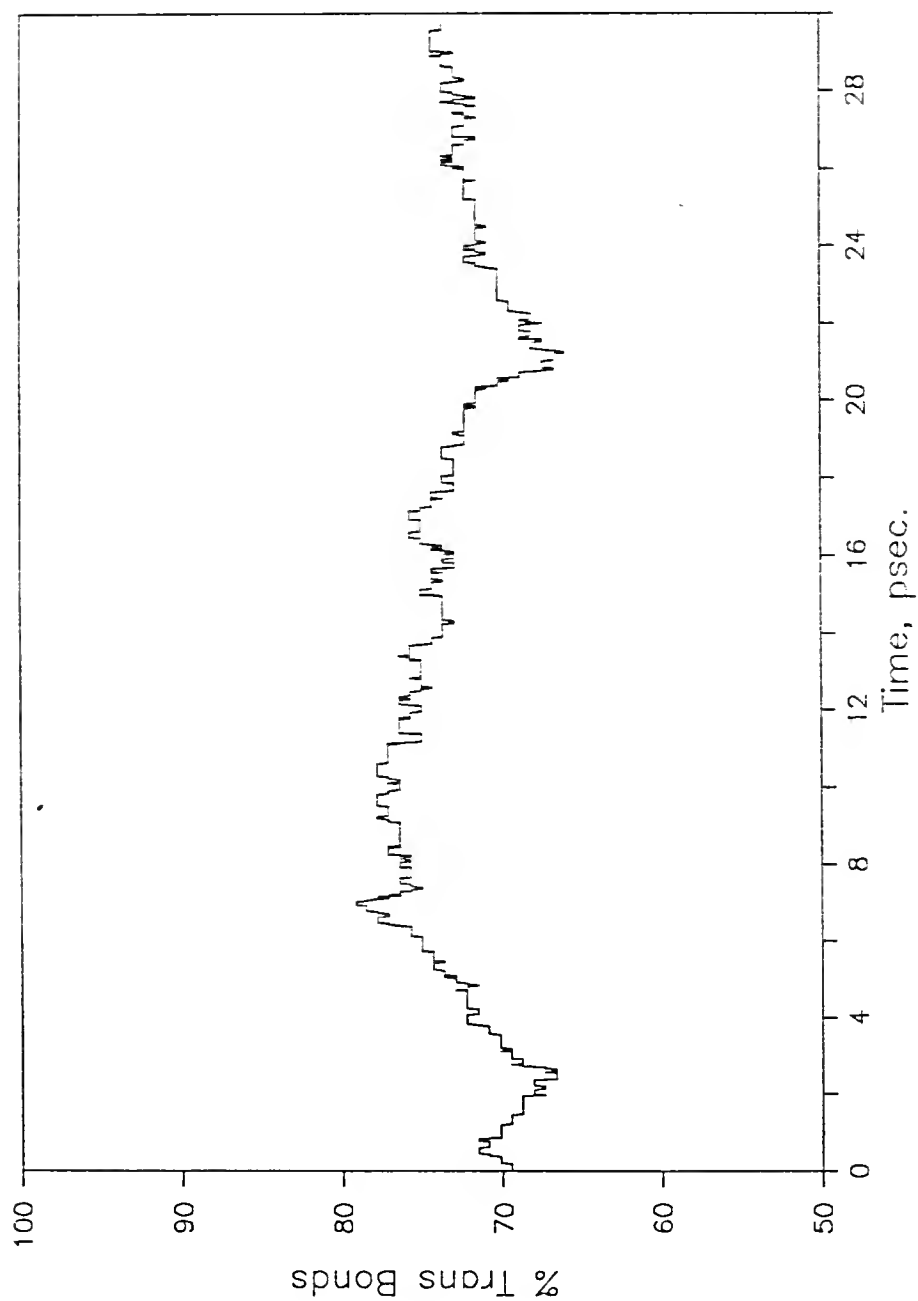


Figure 5-21. The percentage of hydrocarbon molecule bonds of Run 4 which are in the trans conformation. The percentage is reported at intervals of .0198 picosecond. The mean value is 73.0 percent with a standard deviation of 2.8 percent.

simulations of dodecyl surfactants (Woods et al., 1986), a mean value of 72 ± 3 percent for aggregates of both 40 and 52 surfactant molecules.

With the exception of the group led by Jonsson, all of the above-mentioned simulations found a percentage of bonds in the trans conformation roughly within one standard deviation of one another. It is interesting to note that the hydrocarbon droplet, even at liquid density, produced a mean trans percentage in the range corresponding to the micelles, indicating that no significant straightening occurs when the head group is constrained near the surface. Whether chain straightening occurs due to the spherical geometry of the aggregate is not known, since no simulations of hydrocarbon molecules of this length in the bulk liquid or aqueous solution phases have been reported.

Figures 5-22 through 5-25 break the trans fraction down by bond number, each plot showing the fraction of the twenty-four bonds of that number which is in the trans conformation. The bond numbering scheme sets Bond 1 as the bond between the head group (or segment 1) and chain segment 2. Bond 2 is the bond between segments 2 and 3, and its dihedral angle is formed by groups 1 through 4. The data for these figures was sampled at one-tenth the frequency used in the previous four figures, causing the plots to

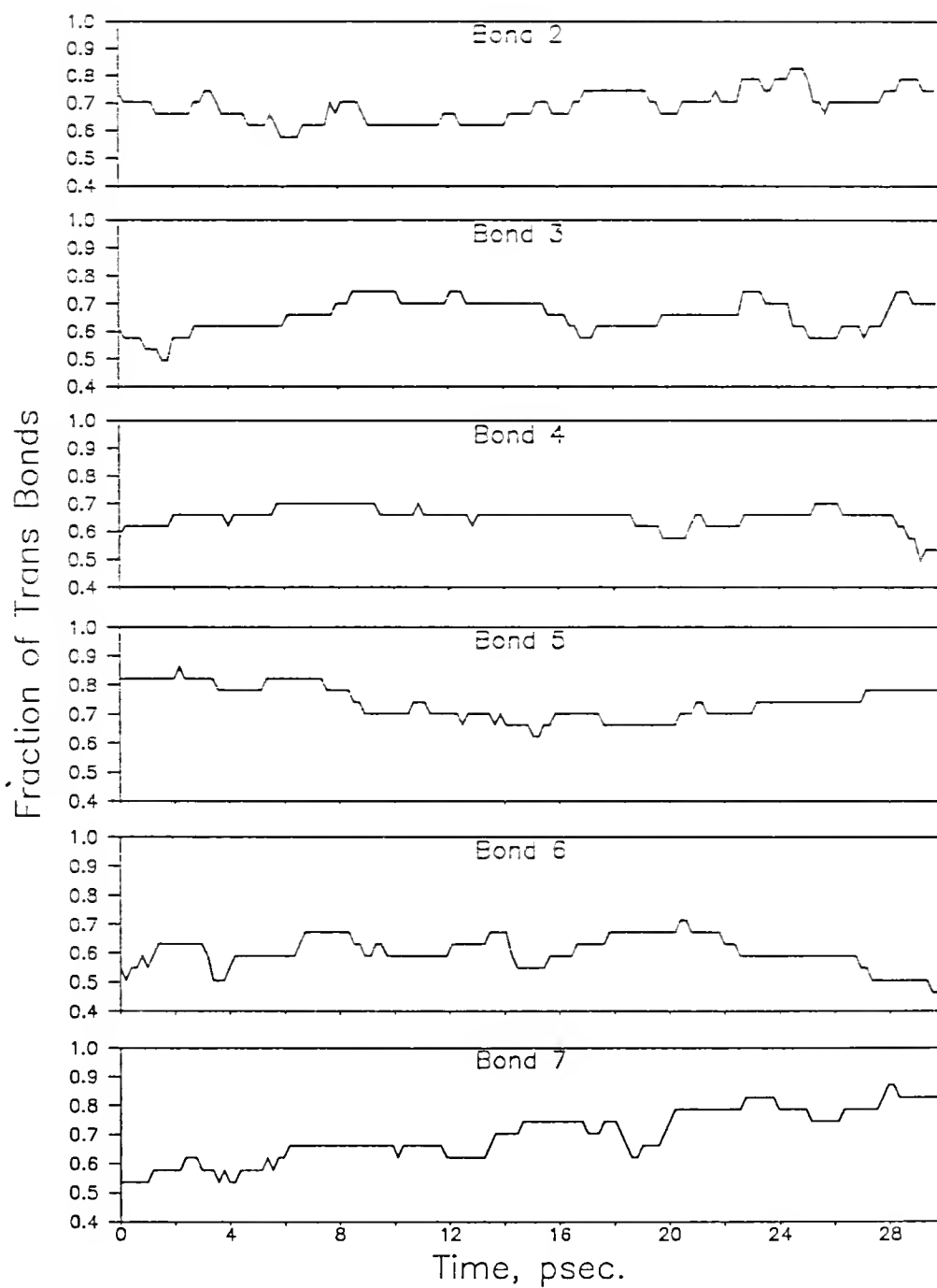


Figure 5-22. Fraction of trans conformations for each of the rotational bonds of Run 1. Result is shown for every hundredth time step.

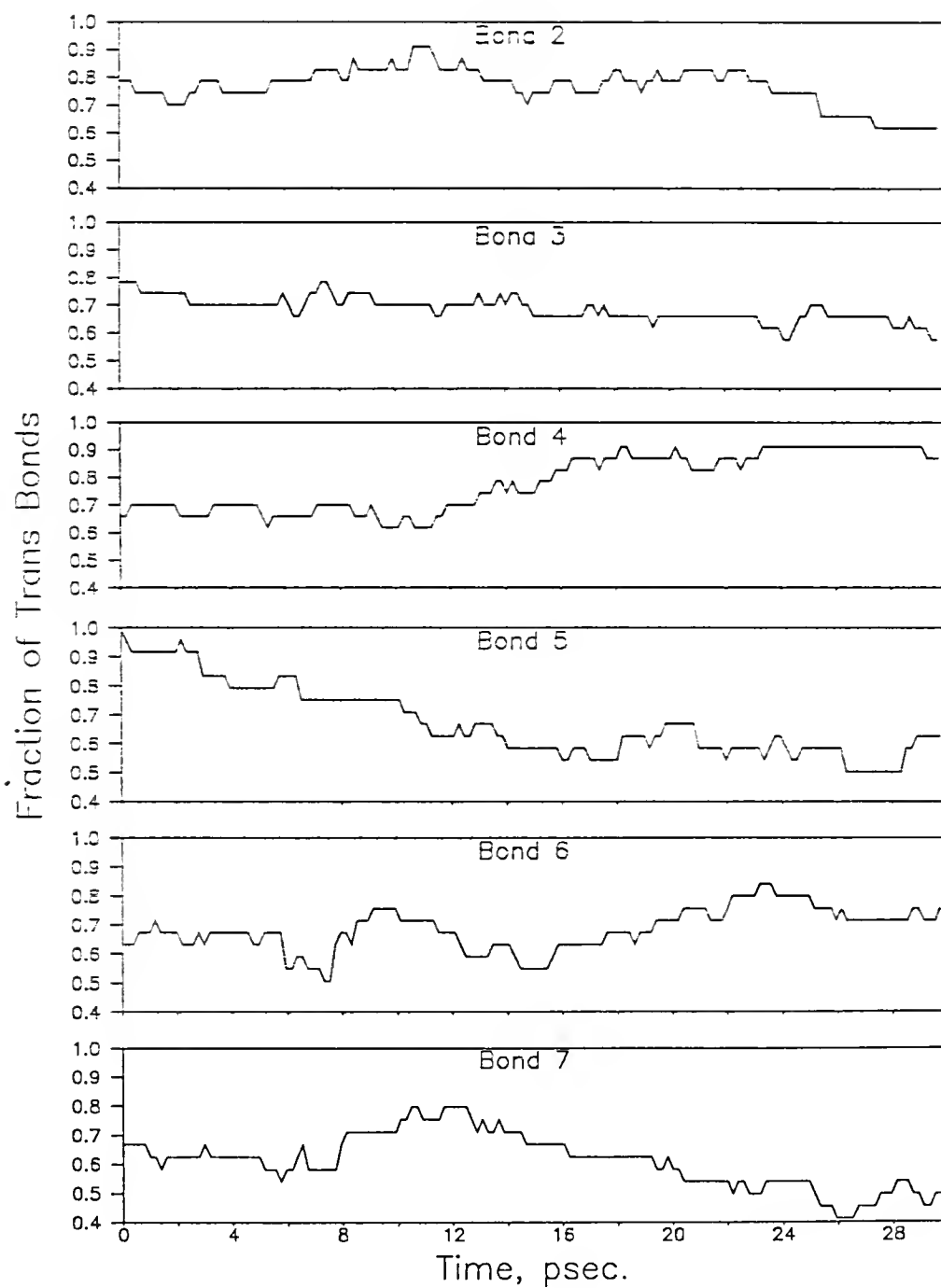


Figure 5-23. Fraction of trans conformations for each of the rotational bonds of Run 2. Result is shown for every hundredth time step.

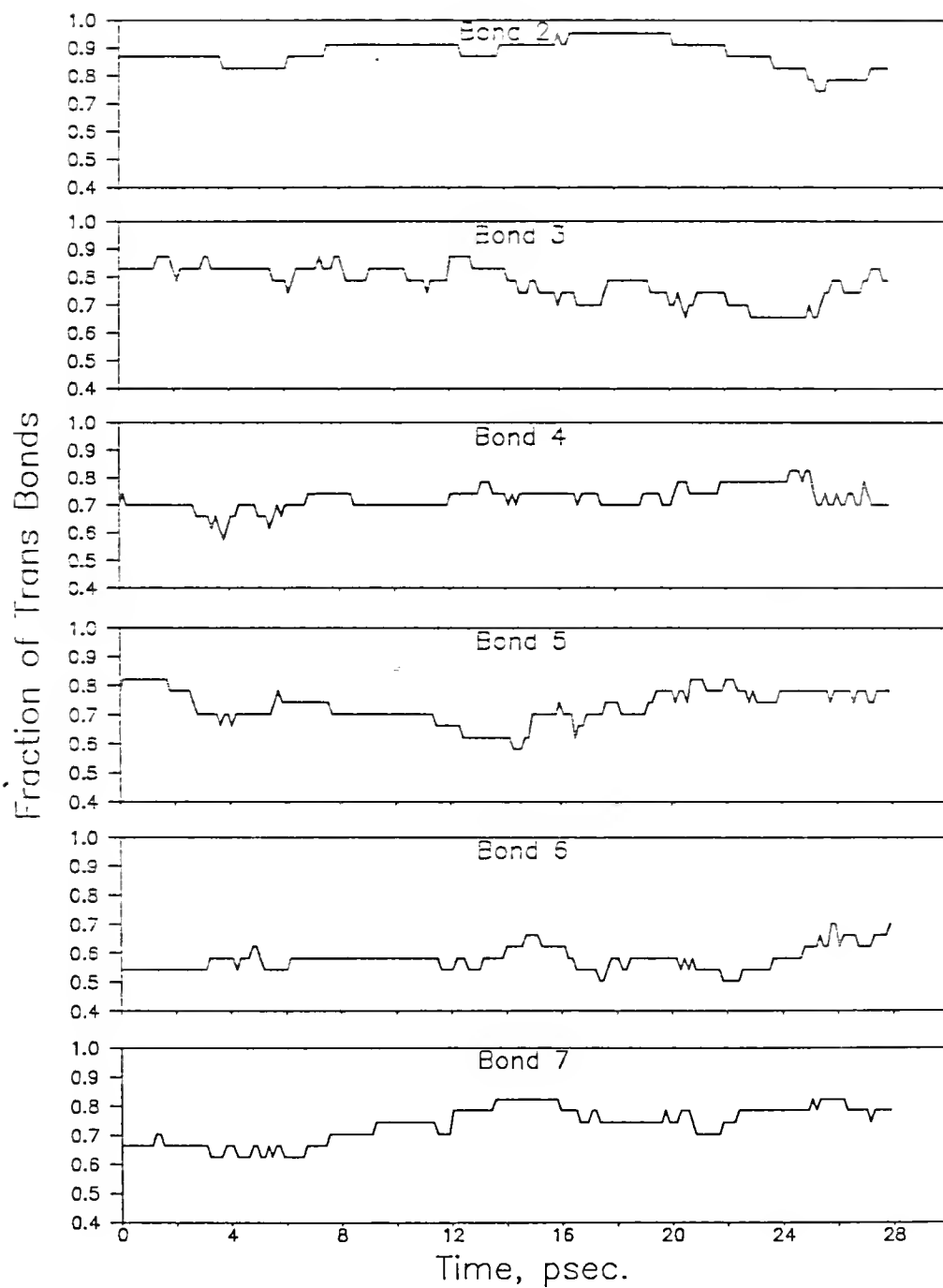


Figure 5-24. Fraction of trans conformations for each of the rotational bonds of Run 3. Result is shown for every hundredth time step.

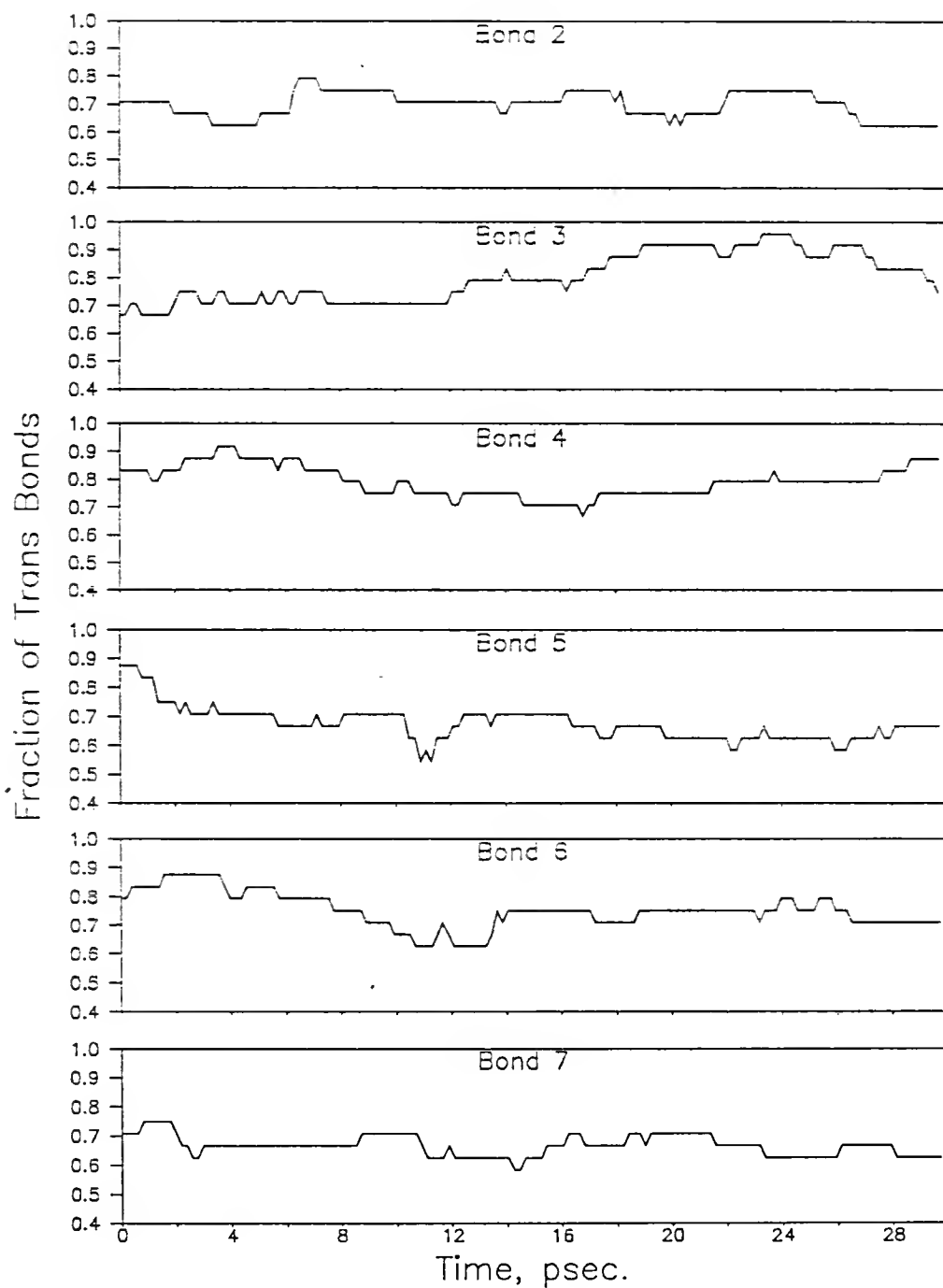


Figure 5-25. Fraction of trans conformations for each of the rotational bonds of Run 4. Result is shown for every hundredth time step.

appear smoother. One significant result apparent in these figures is the very high fraction of trans bonds near the head group in Run 3. In this simulation the head group size and bond rotational force constant were greater than in Runs 1 and 2.

Another indicator of micelle structure is the bond order parameter, $S(r)$, defined by

$$S(r) = \left\langle \frac{1}{2} (3 \cos^2 \theta - 1) \right\rangle \quad (5.6)$$

where θ is the angle formed by the bond vector between adjacent groups on a chain and the radial vector from the aggregate center of mass to the center of the bond. The parameter is averaged over all bonds whose centers are found at a distance r and over time. An average over completely random bond orientations would result in an order parameter of zero.

Plots of $S(r)$ are given for the four simulations in Figures 5-26 through 5-29. In all cases little ordering of bond orientations exists in the intermediate portion of the aggregate between the center and the surface. In Runs 1, 2, and 3, the micelle simulations, $S(r)$ approaches unity at the surface, indicating that the bonds near the surface tend to parallel the radial vector. This also occurs at the center of the micelle, where a group whose center is coincident

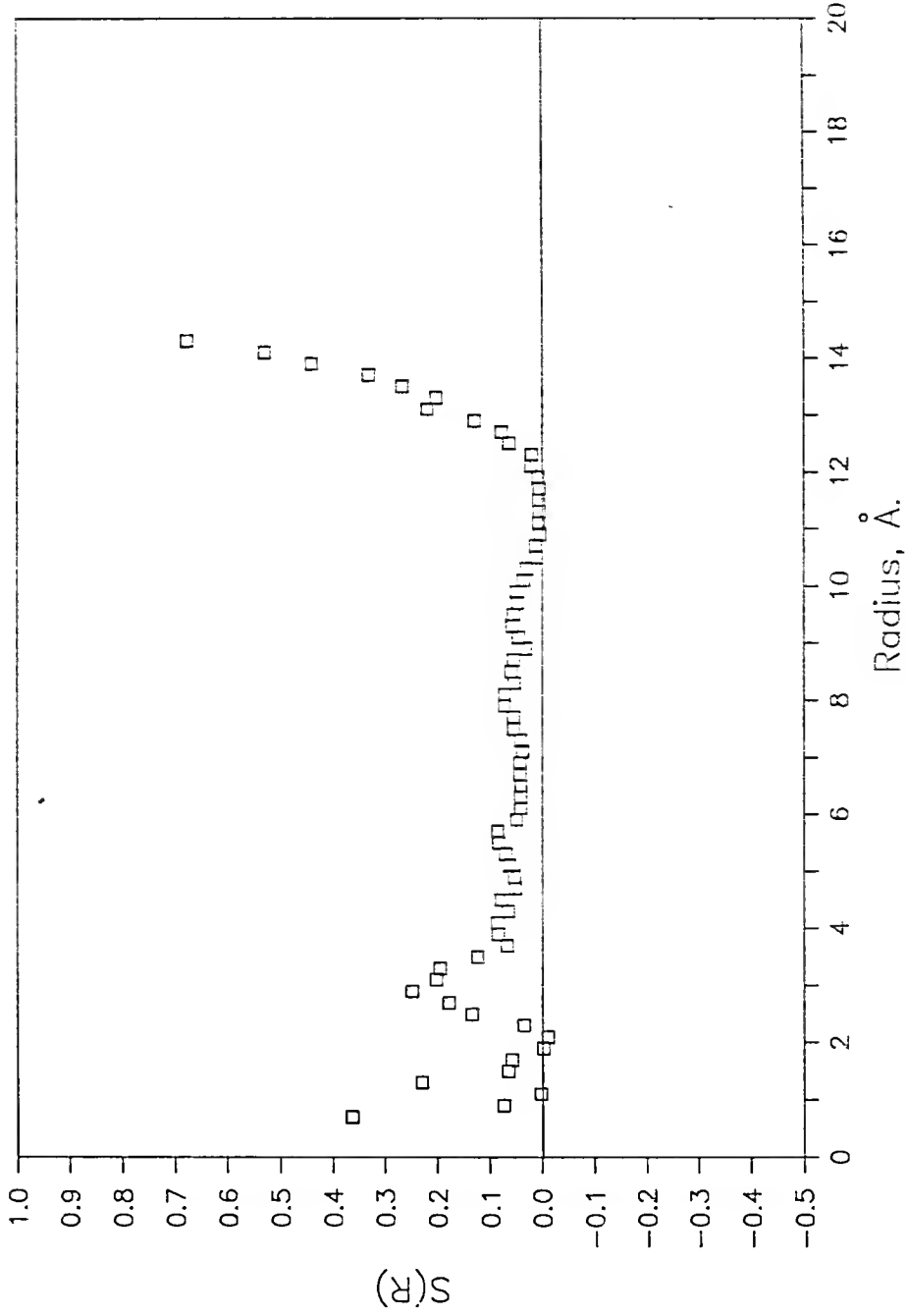


Figure 5-26. The distribution of the bond order parameter, $S(R)$, through the interior of the micelle of Run 1. A value of 1.0 indicates bonds aligned in the radial direction, while a value of 0.0 results from no preferential order in the bonds.

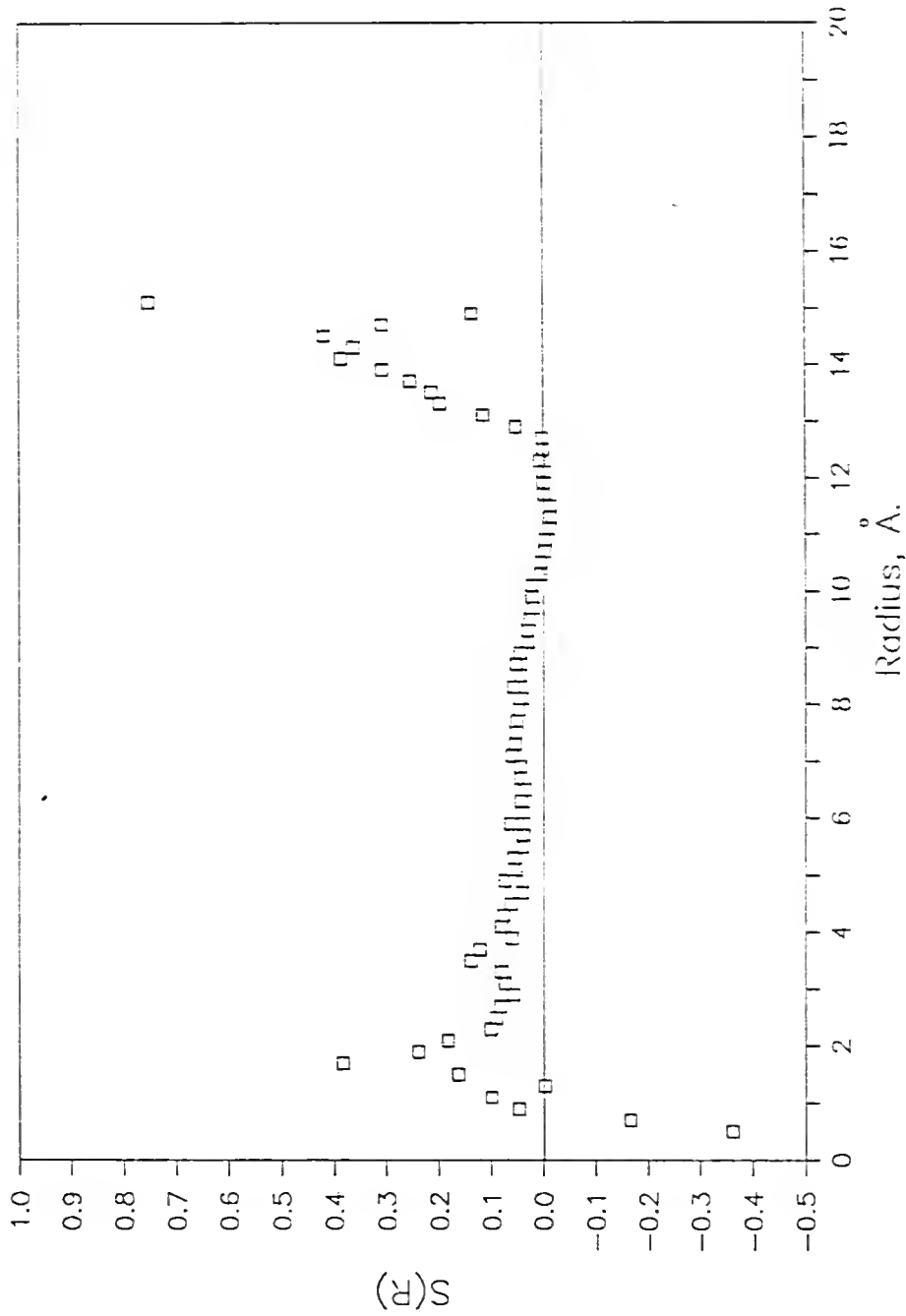


Figure 5-27. The distribution of the bond order parameter, $S(R)$, through the interior of the micelle of Run 2. A value of 1.0 indicates bonds aligned in the radial direction, while a value of 0.0 results from no preferential order in the bonds.

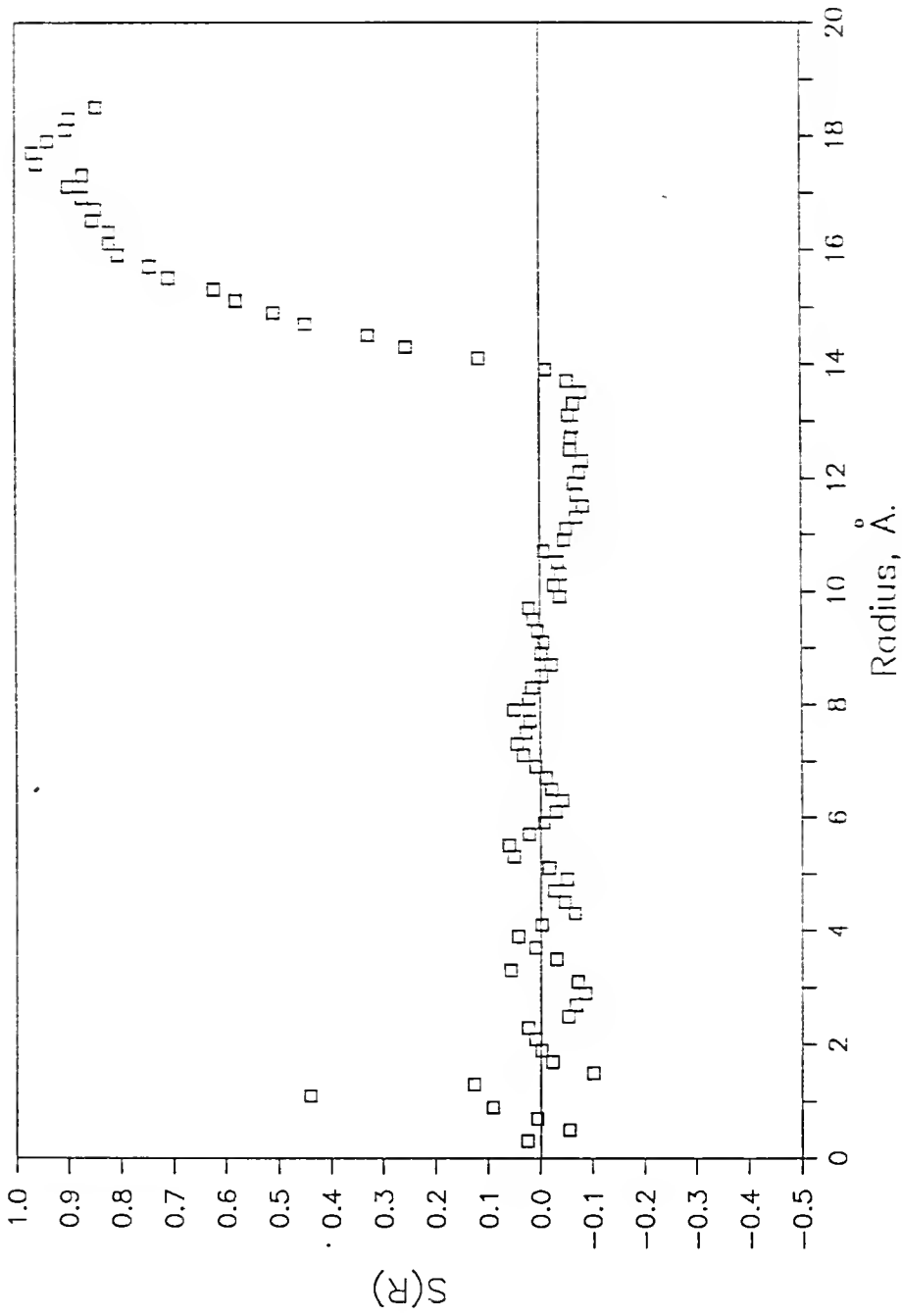


Figure 5-28. The distribution of the bond order parameter, $S(R)$, through the interior of the micelle of Run 3. A value of 1.0 indicates bonds aligned in the radial direction, while a value of 0.0 results from no preferential order in the bonds.

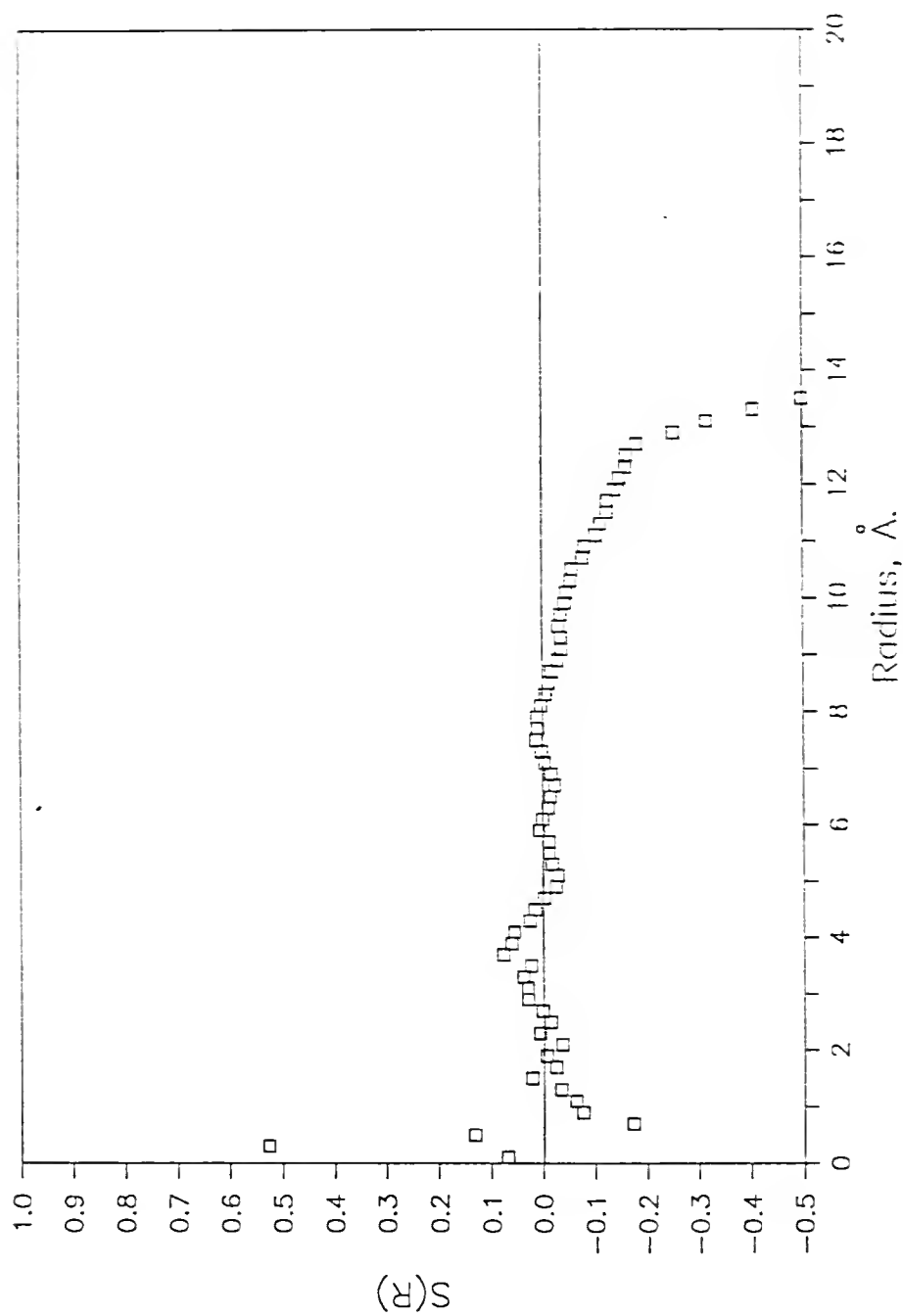


Figure 5-29. The distribution of the bond order parameter, $S(R)$, through the interior of the droplet of Run 4. A value of 1.0 indicates bonds aligned in the radial direction, a value of 0.0 results from no preferential order in the bonds, and a value of -0.5 indicates bonds perpendicular to the radial direction.

with the center of the micelle would require that $S(r)=1$ for a bond attaching it to another segment. The same behavior of $S(r)$ was found by Woods et al. (1986).

In Run 4, the hydrocarbon droplet simulation, $S(r)$ goes to -0.5 at the surface, indicating that most bonds at the surface are perpendicular to the radial vector. Similar behavior to the other simulations is observed in the interior of the aggregate. The difference in the bond orientations at the surface of the micelle and the hydrocarbon droplet lies in the head group interaction with the shell. In the micelle, forces act to maintain the head groups at the surface while the chain segments are repelled from the shell. This tends to orient the bond between the head group and its adjacent segment perpendicularly to the shell. In the droplet all of the chain segments experience the same repulsive force at the shell, resulting in bonds which lie parallel to the shell.

Gruen (1981) has obtained the bond order parameter as a function of the carbon number from his statistical model. Chevalier and Chachaty (1985) also express a result of their NMR study of sodium mono-n-octyl hydrogen phosphate micelles in this way. The bond order parameter as a function of group number, S_i , can be approximated from $S(r)$ by

$$S_i = \frac{\int N_i(r) S(r) dr}{\int N_i(r) dr} \quad (5.7)$$

The approximation is due to the N_i values being taken at group centers while the S values are taken at bond centers. Since the difference between the two can be no longer than one-half the bond length, accuracy does not suffer greatly. Comparisons between these two studies and Run 3 are made in Figure 5-30. The NMR result was given as S_i values relative to that of the head group bond without a value for the head group bond; in the figure the same head group value as Run 3 was used. The simulation result shows considerable radial orientation of the head group bond, with groups removed from the head group showing no preferential orientation. This corresponds to the high trans fraction observed near the head group in Figure 5-24. The NMR result shows a decrease in radial orientation going from head to tail, but more gradually than the simulation. The statistical model does not show this trend in bond orientation along the chain.

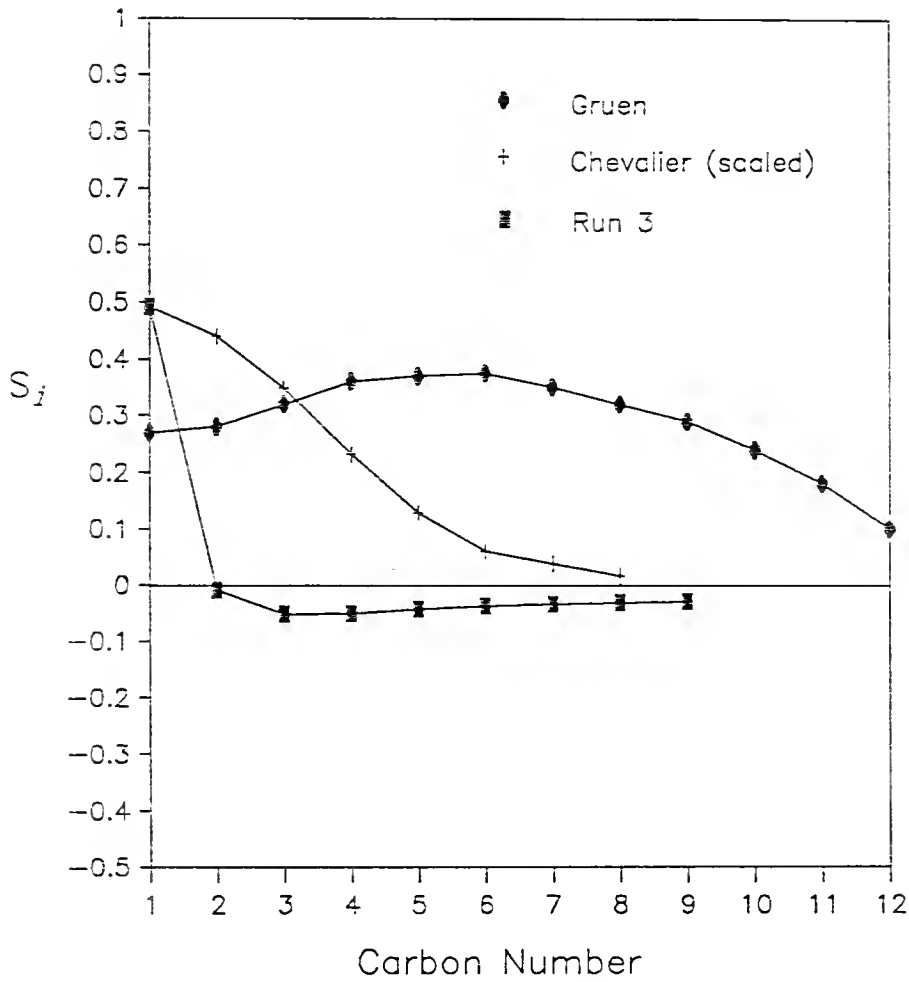


Figure 5-30. Bond order parameter by chain segment. Results are shown for the statistical model of Gruen (1981), the NMR study of Chevalier and Chachaty (1985), and Run 3 of the present work.

5.4 Shape Fluctuations

The shape of the model micelles and droplet can be investigated through the moment of inertia tensor, \underline{I} :

$$\underline{I} = \begin{bmatrix} I_{xx} & I_{xy} & I_{xz} \\ I_{yx} & I_{yy} & I_{yz} \\ I_{zx} & I_{zy} & I_{zz} \end{bmatrix} \quad (5.8)$$

whose diagonal and off-diagonal elements are calculated from the mass and position of each of the 216 particles in the system as follows:

$$I_{xx} = \sum_v m_v (y_v^2 + z_v^2) \quad , \quad v = 1, 2, \dots, 216 \quad (5.9)$$

$$I_{xy} = - \sum_v m_v x_v y_v \quad , \quad v = 1, 2, \dots, 216 \quad (5.10)$$

The eigenvalues of this tensor are the principal moments of inertia, I_1 , I_2 , and I_3 . In the case of all particles being of equal mass, such as in Runs 1 and 4, a spherical micelle or droplet would result in $I_1=I_2=I_3$. In Runs 2 and 3, where the mass of the head group is different than that of a chain segment, a spherical micelle with the head groups equally spaced over the surface would yield equality of the principal moments.

Figures 5-31 through 5-34 show the change over time of the ratio of the maximum principal moment to the minimum principal moment. Any deviation from the conditions given above for equality of the principal moments will result in this ratio being greater than unity. In all four of the simulations, the ratio I_{\max}/I_{\min} never attained a value of

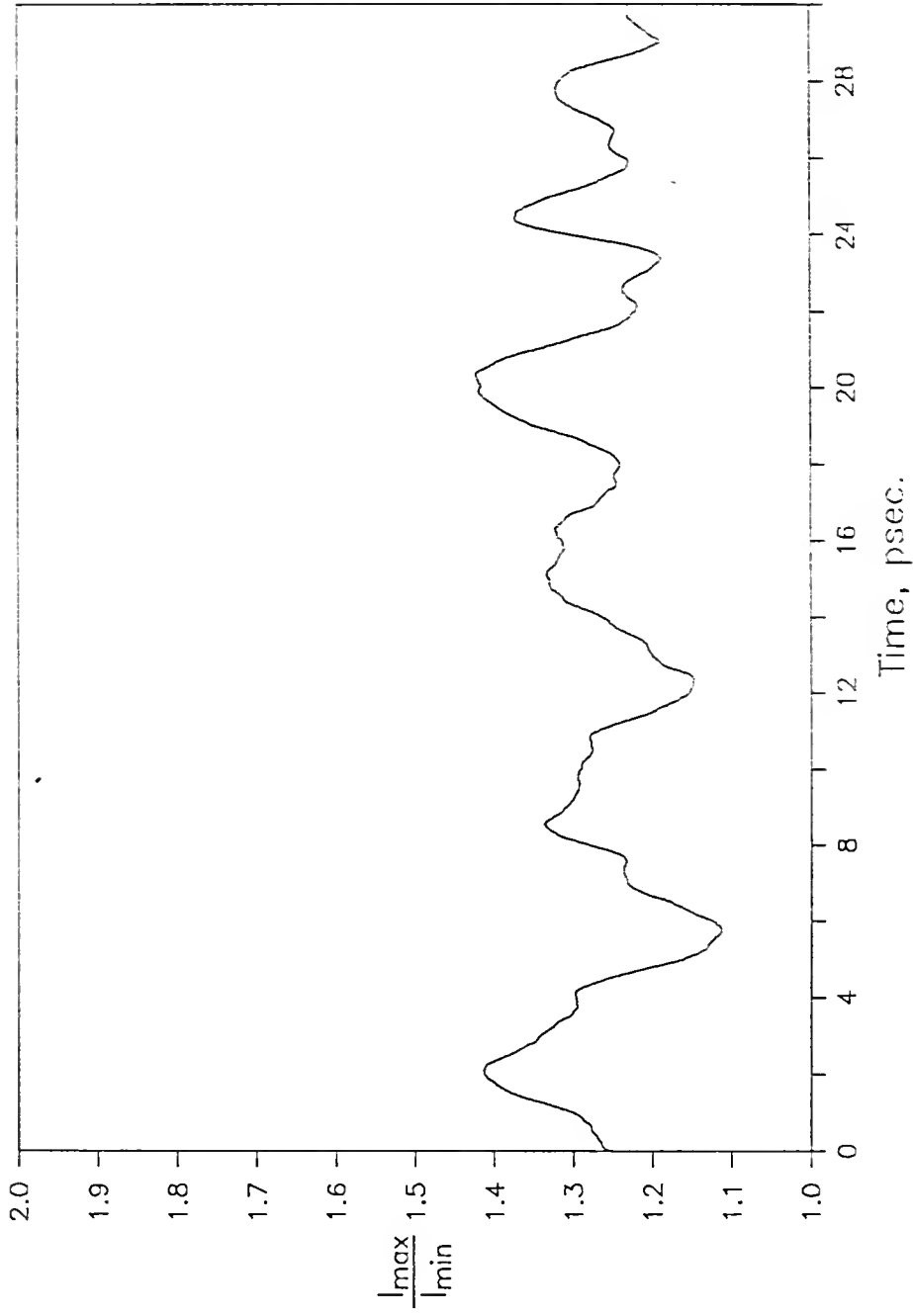


Figure 5-31. The ratio of the largest principal moment of inertia to the smallest for Run 1. A value of unity would be necessary for a spherical aggregate. The mean value of I_{\max}/I_{\min} is 1.28 with a standard deviation of 0.07.

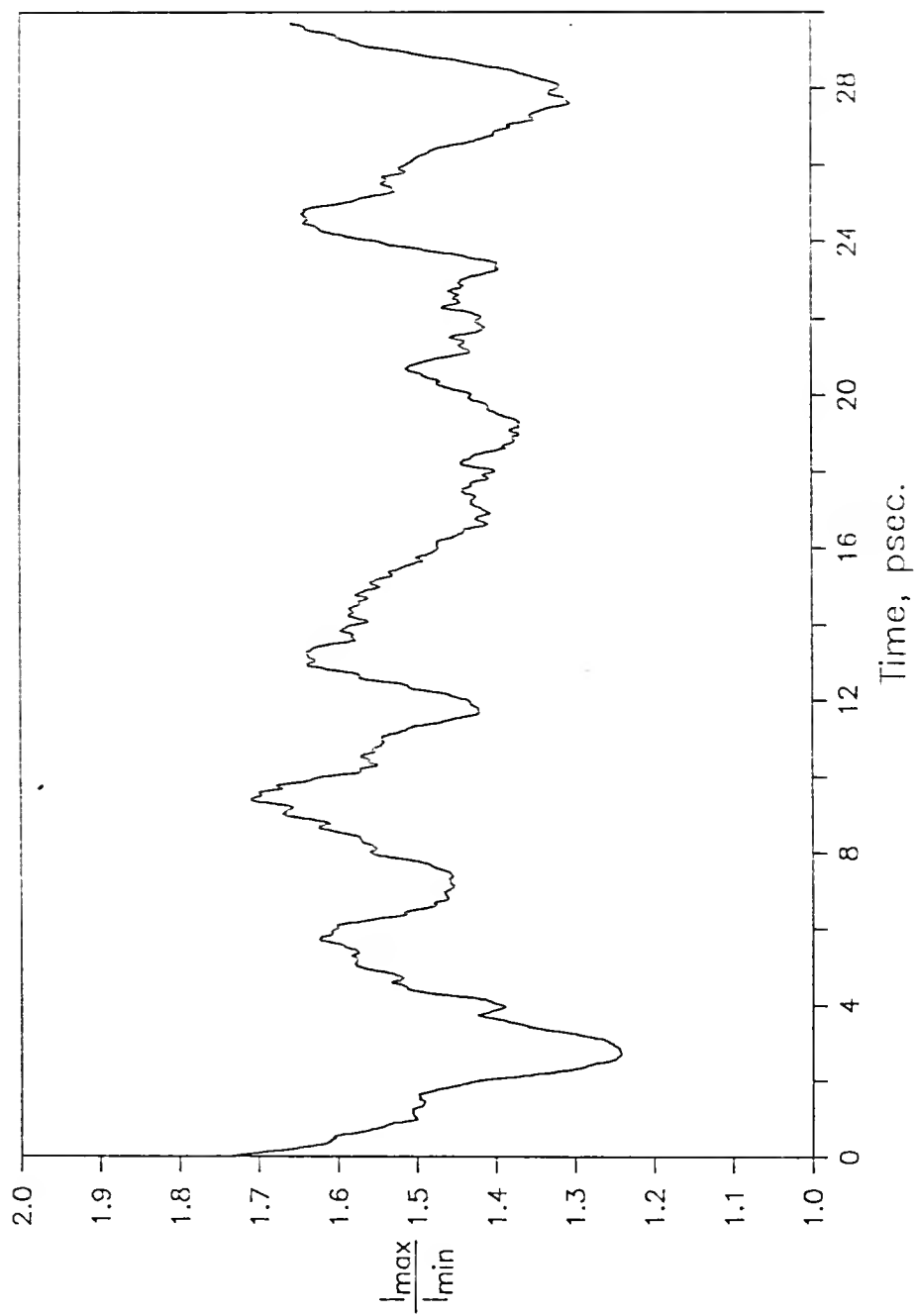


Figure 5-32. The ratio of the largest principal moment of inertia to the smallest for Run 2. A value of unity would be necessary for a spherical aggregate. The mean value of I_{\max}/I_{\min} is 1.49 with a standard deviation of 0.10.

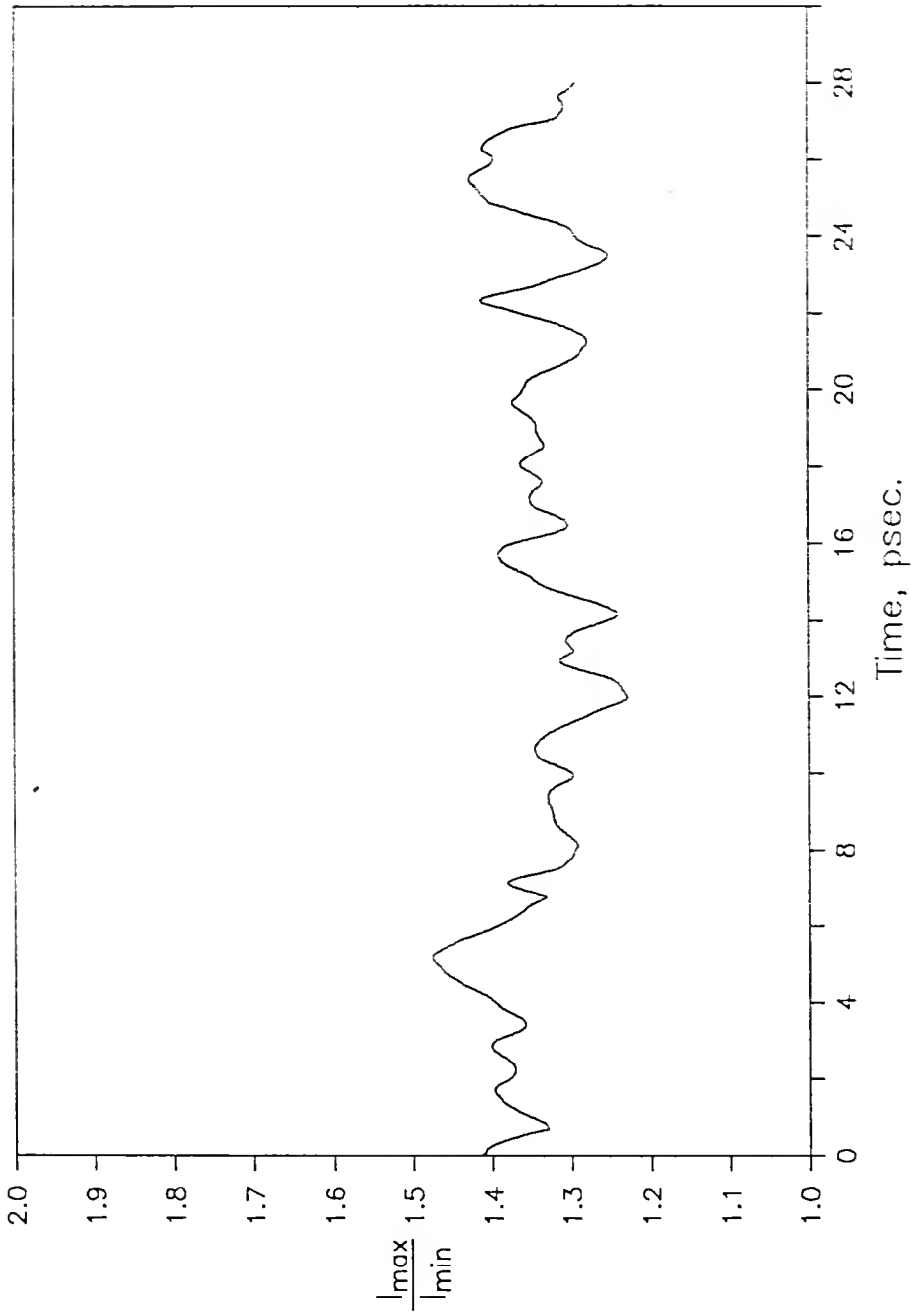


Figure 5-33. The ratio of the largest principal moment of inertia to the smallest for Run 3. A value of unity would be necessary for a spherical aggregate. The mean value of I_{\max}/I_{\min} is 1.35 with a standard deviation of 0.05.

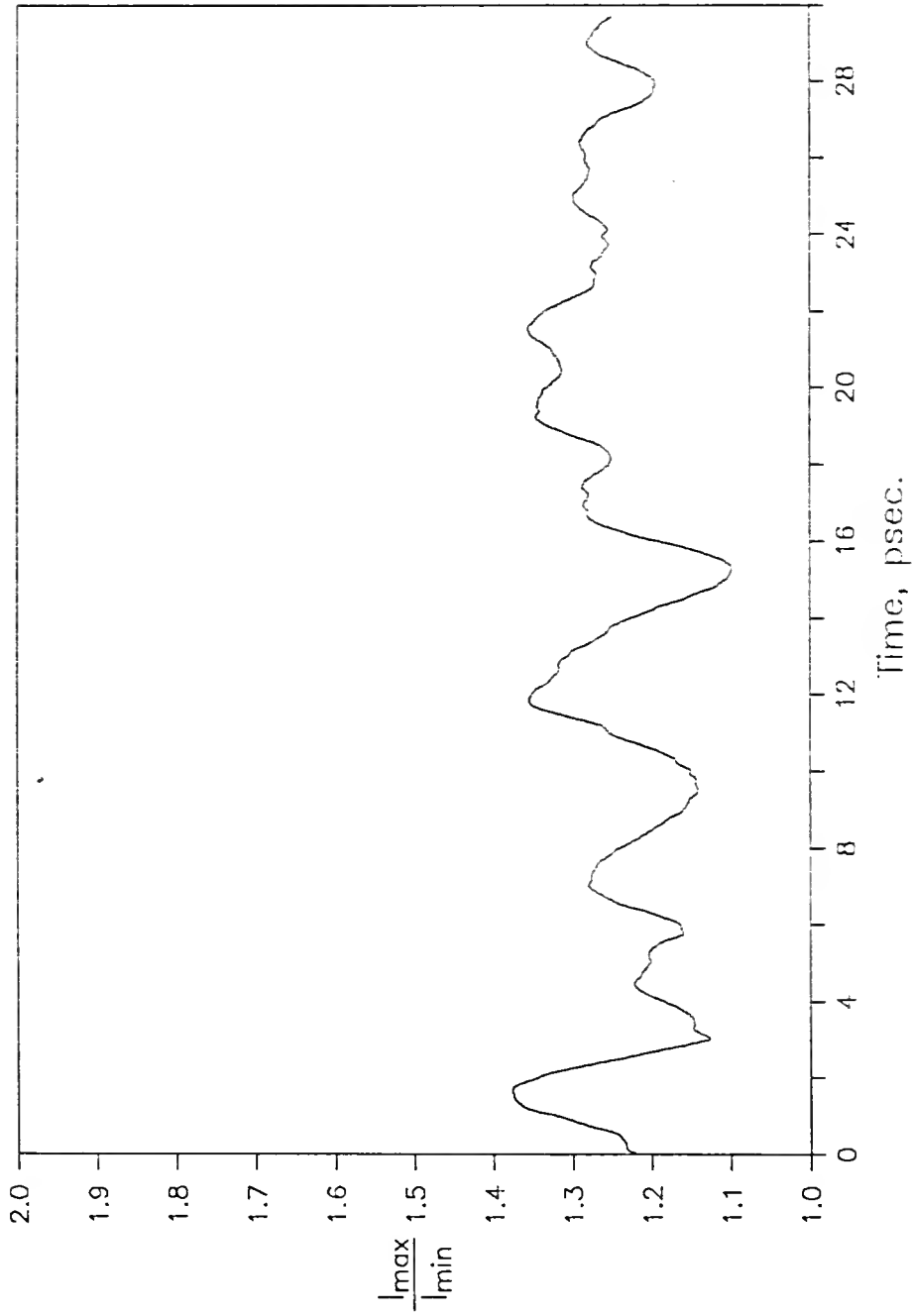


Figure 5-34. The ratio of the largest principal moment of inertia to the smallest for Run 4, the hydrocarbon droplet. A value of unity would be necessary for a spherical aggregate. The mean value of I_{\max}/I_{\min} is 1.25 with a standard deviation of 0.06.

unity, despite the aggregate being confined in a spherical shell. Rather, it fluctuates about a mean value slightly greater than 1.0.

The result for Run 1 shows a mean value of I_{\max}/I_{\min} of 1.28, with an approximate range of values from 1.1 to 1.4. The large fluctuations are fairly regular, with a period of about five picoseconds. Smaller fluctuations are minimal, on the order of 0.05 on the I_{\max}/I_{\min} scale. The result for Run 4 is quite similar to that of Run 1, with a mean of 1.25 and range from approximately 1.1 to 1.4. There is not a regular frequency with which fluctuations occur, however.

Run 2 experienced fluctuations in the approximate range of 1.2 to 1.7 with a mean value of I_{\max}/I_{\min} of 1.5. Large fluctuations occurred with a period of about four picoseconds. Smaller fluctuations were distinct and regular, occurring with a period of less than one picosecond and an amplitude of approximately 0.01 I_{\max}/I_{\min} . The result for Run 3 produced a mean value of I_{\max}/I_{\min} of 1.35 and a range within 1.1 and 1.5. Fluctuations of varying amplitude occurred with a period ranging from one to four picoseconds.

Woods et al. (1986) obtained mean values of I_{\max}/I_{\min} of 1.25 and 1.18, respectively, for their 40 and 52 member

dodecyl micelles. Jonsson et al. (1986) obtained a value of 1.49 in their octanoate simulation using the reduced charge model.

The micelle simulations, Runs 1 through 3, exhibited greater regularity in the fluctuations of I_{\max}/I_{\min} than did Run 4, the hydrocarbon droplet. The head group interaction with the confining shell must be considered largely responsible for this difference. Runs 2 and 3, with the head groups of higher mass, had higher values of I_{\max}/I_{\min} than Runs 1 and 4, in which all groups were of equal mass. The higher mass head groups contribute to greater inequality among the principal moments of inertia if they are asymmetrically arranged about the center of mass of the micelle. This was much more prevalent in Run 2 than in Run 3. The smaller diameter of the head groups in Run 2 allows a higher local concentration of the mass on the micelle surface than does the larger diameter of the head groups of Run 3.

Neutron scattering experiments conducted by Cabane et al. (1985) on sodium decyl sulfate micelles concluded that the average shape of the micelles must be spherical, with nonspherical shapes possible as fluctuations. This result is consistent with the results of the simulations. A theoretical study of shape fluctuations in spherical micelles (Ljunggren and Eriksson, 1984) estimated shape

fluctuations due to capillary wave effects on a time scale of 100 picoseconds. The simulations of this work were not of sufficient length to comment on fluctuations of this long a period, but, as demonstrated, shape fluctuations of significant proportion did occur on a time scale of one order of magnitude less.

5.5 Pair Correlations of Groups

An experimental measurement that can be used to test the validity of structural models of micelles is the pair correlation distribution function. This is a measure of the probability of a pair of groups being separated by a given distance. Cabane et al. (1985) have measured the pair correlations for certain groups in sodium dodecyl sulfate micelles of mean size 74. Using deuterium labeling and small angle neutron scattering (SANS), they obtained results for tail-tail and γCH_2 - γCH_2 correlations.

Comparing their SANS result with the theoretical predictions of several structural models, they found that the models consistently predict the tails to be closer to each other and the γCH_2 groups to be further from each other than the experimental result. The models predicted a tendency for tails to be concentrated near the center of the micelle and γCH_2 groups to remain in a spherical shell near the micelle surface.

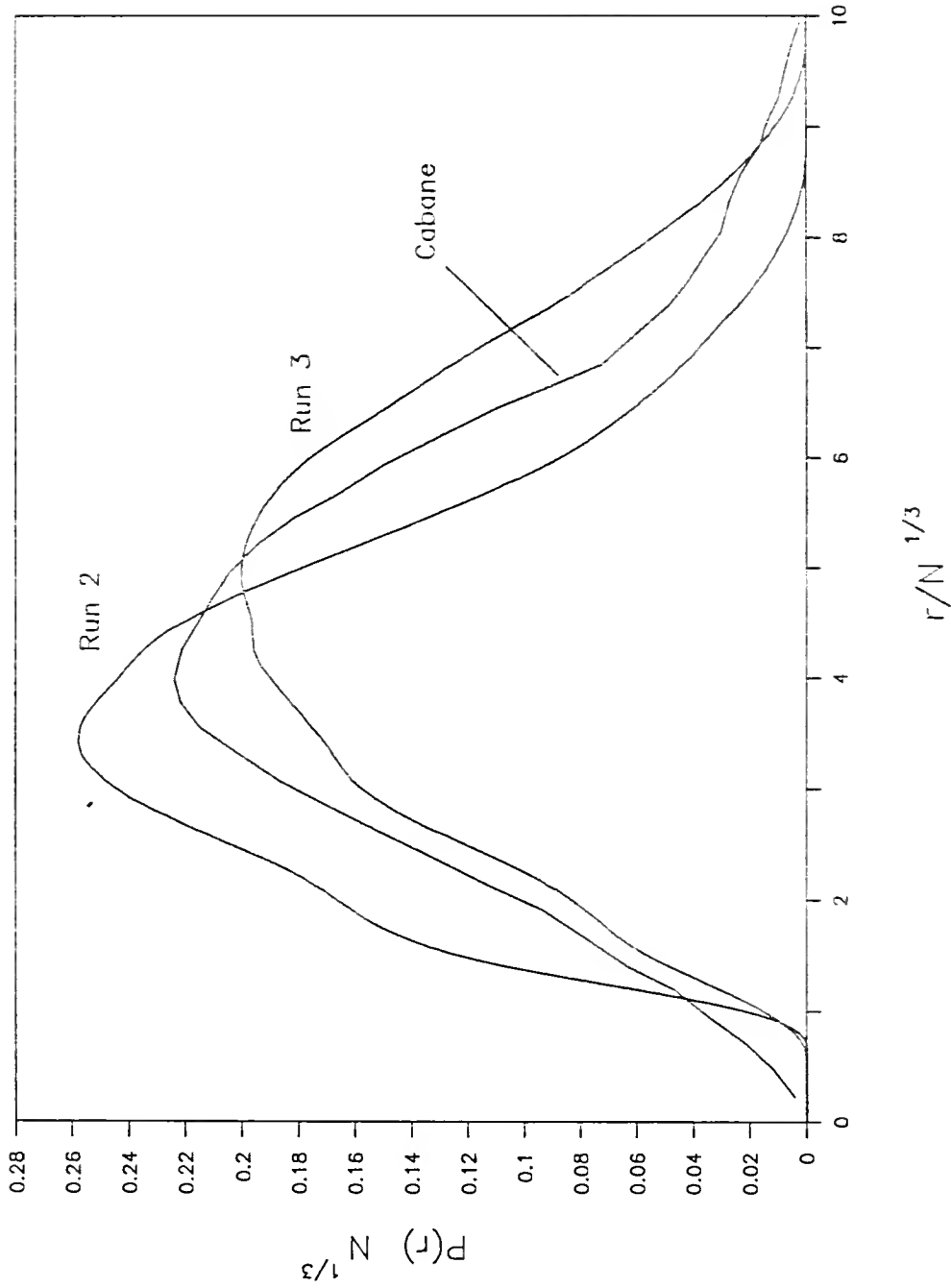


Figure 5-35. Tail-tail pair correlation function distributions resulting from Run 2, Run 3, and the SANS study of Cabane et al. (1985). Scaling of axes places all results on an equivalent basis in aggregate size.

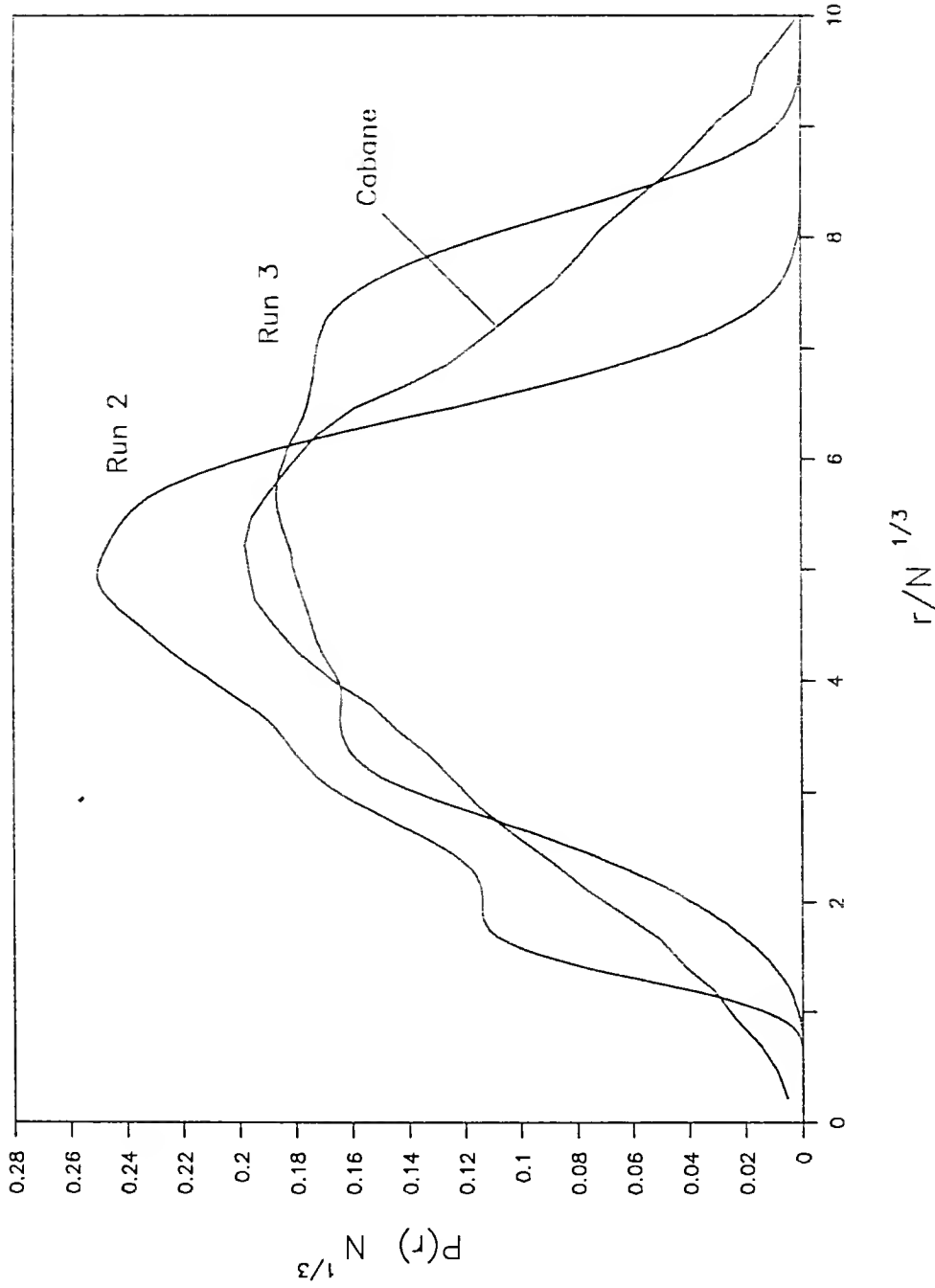


Figure 5-36. Correlation function distributions for $\text{CH}_2\text{-CH}_2$ (gamma position) pairs resulting from Run 2, Run 3, and the SANS study of Cabane et al. (1985). Scaling of axes places all results on an equivalent basis in aggregate size.

In Figures 5-35 and 5-36, the tail-tail and γCH_2 - γCH_2 pair correlation results from Runs 2 and 3 are plotted along with the SANS result of Cabane et al. The axes are scaled to put the results on an equivalent basis in aggregate size. Run 3, with its larger head groups, is of a greater radius (Table 5) and a lower number density than Run 2. The experimental results lie between those of Run 2 and Run 3, with Run 2 giving slightly lower pair separations and Run 3 slightly higher. There is good agreement between Run 3 and the experimental result for the tail-tail correlation. The agreement between Run 3 and the experimental result for the γCH_2 - γCH_2 correlation is better than that of Run 2.

The SANS results show that tails are not concentrated in the center of the micelle, but rather are distributed throughout. It is also indicated by experiment that the γCH_2 groups are not strictly in the surface region, but are distributed throughout the micelle. The simulation results, particularly Run 3, exhibit this same behavior.

CHAPTER 6

SUMMARY AND CONCLUSIONS

A molecular thermodynamic model has been developed to describe the formation of micelles in a solution of multiple surfactant components. Each micelle of distinct size and composition is treated as the product of a reaction whose equilibrium constant is the result of the total free energy of micellization for the micelle. A seven-step, reversible process is employed to calculate the change in free energy for the surfactant molecules changing their state from free monomers in solution to aggregated molecules in micelles of distributed sizes and compositions. Contributions to the total free energy are obtained due to solvophobic interaction, mixing, surface formation, conformational change, head group interactions and electrostatics. With the model for the free energy as a function of temperature and composition, distributions of micelle sizes and compositions can be generated through a set of reaction equilibria relationships.

Where possible, the free energy contributions are related to comparable processes on which experimental measurements have been made. The solvophobic term is obtained from hydrocarbon solubility; the surface term

is related to the interfacial tension between hydrocarbon and solvent phases. In addition, reasonable assumptions of ideal mixing of hydrocarbon chains and ideal solution behavior of the dilute surfactant solution are made. Aggregate size distributions have been generated from the model for single-component solutions of nonionic surfactants of different chain lengths and at different temperatures and solution concentrations.

Three parameters are required by the model: one to estimate the entropy change due to conformational changes in the surfactant molecules upon micellization and two to estimate the curvature effects on the surface free energy of spherical and cylindrical interfaces. The parameters can be fitted to the mean aggregate size at the critical micelle concentration--only two independent results. The consequent interrelation among the parameters gives curvature parameters which are linearly dependent on the conformational parameter. Within the physically plausible range of values, the conformational parameter has a range which gives identical size distributions when corresponding values of the curvature parameters are used.

This variation of the parameters reveals a need for more fundamental information to establish a truly predictive model for the thermodynamics of micelle formation. While structure and geometry of the micelle are fundamental to the

calculation of free energy contributions, experimental evidence is insufficient to completely define the thermodynamics of micelle formation.

In order to acquire some of the detailed molecular-level information necessary for the modeling, the structure of the micelle has been investigated through the molecular dynamics computer simulation of model micelles. Simulations of three micelles with different head group attributes and one hydrocarbon droplet were conducted. In each case, the aggregate consisted of 24 nine-member, linear chain molecules. The solvent was not explicitly modeled. Instead, the aggregate was surrounded by a spherical shell. Interactions of the molecules with the shell were designed to mimic the appropriate interaction of a chain segment or head group with solvent.

The results of the simulations have been analyzed for the distributions of molecular groups within the aggregate, bond conformations and orientations, and shape fluctuations. Comparisons have been made among the runs to study the effects of head group size and mass, with other simulations to study the effects of chain length, aggregate size, and simulation technique, and with experimental results to reveal the differences and similarities between the simulations and experiment.

An increase in head group mass by a factor of seven had no effect on the structure of the micelle. The results for Runs 1 and 2 are virtually identical for the mean radial positions of groups, probability distributions of group positions, percentage of bonds in the trans conformation, bond order parameter, and Fourier transform of tail distribution. There was an effect of head group mass on the dynamic quantities. More rapid gauche/trans transitions were observed in the first dihedral angle of Run 2 than in Run 1. Larger and more rapid fluctuations were observed in the principal moments of inertia of Run 2 than in Run 1.

The model sulfate head group of Run 3, with its higher mass, larger diameter, and different intramolecular potentials, had a great effect on the structure. With the larger head group size, the excluded volume effect at the surface forced an average of two head groups into the interior of the micelle, disrupting the order displayed by the chains in Runs 1 and 2. While this result is entirely possible, the shell around the micelle did not allow other possible outcomes of the excluded volume effect at the surface, such as head groups moving into the solvent. Though the distributions are similar to other simulations, the internal structure of Run 3 may not be accurate.

The hydrocarbon droplet simulation resulted in a nearly uniform distribution of groups within the droplet, and a percentage of trans bonds equivalent to that of the three micelle simulations. This is in contrast to statements based on other micelle simulations which suggest there is a higher percentage of trans bonds than that found experimentally in bulk liquid alkanes as proof of order in the micelle. The present results may mean that chain straightening is more a product of the spherical geometry than head group interactions, or it may just be an artifact of simulation. Simulations of aggregates cannot be compared with experimental bulk liquid results until the same surfactant molecules are simulated under "bulk" conditions.

Comparisons of the simulation results of this work with other simulations were generally consistent. In spite of different surfactant molecules, aggregate sizes and simulation techniques, the results are qualitatively quite similar.

Comparisons with experimental results also show similarities, but there is not complete agreement. Since the experimental quantities are normally interpretations of the measurements which often conflict from one study to another, the disagreements may not reflect adversely on the simulation results.

The key to the success of the thermodynamic modeling is better information about the entropy change in transforming the hydrocarbon droplet into the head-group-free micelle. The results of the present simulations are inadequate to determine chain conformations of monomers in micelles, droplets, and bulk solvents. This can serve as the basis for future efforts on both of these projects. Chain conformations and their energy and entropy effects must be better understood. Simulations of these molecules as bulk liquids, in vacuum, and at infinite dilution in water would be quite beneficial in understanding this phenomena.

Future micelle simulations should incorporate an improved solvent model, with less restrictions on head group movement and shape fluctuations. Since changes in head group size had such dramatic effects, the size of the terminal methyl tail group should also be reconsidered.

APPENDIX A MICELLE SIZE AND SHAPE

As the aggregate size of a micelle increases, a shape transition must occur so that the volume of the additional monomers can be accommodated while maintaining a uniform density throughout. In the case of a single surfactant species, a micelle can remain spherical only until the radius of the sphere reaches the length of an extended, all-trans, surfactant chain. In the multicomponent case, the composition of the micelle also plays a role in determining its shape. The geometric model for a binary micelle will be derived to demonstrate this effect.

The two surfactant components will be designated 1 and 2, each with an aggregate number, N , an extended chain length, l , and a chain volume, v . Component 2 will have the longer chain length and the larger chain volume. As in the single component case, the maximum possible radius of a spherical micelle is the length of the longest chain present in the micelle, so

$$N_1 v_1 + N_2 v_2 = \frac{4\pi}{3} R^3 \quad . \quad R \leq l_2 \quad (\text{A.1})$$

When the radius of the sphere is greater than the shorter chain length, there is a spherical "core" in the center of the micelle which must be devoid of component 1. In order to form a sphere of such a radius, a sufficient amount of component 2 must be present to completely fill the core. This is illustrated in Figure A-1. The radius of the core, r , is given by

$$r = R - l_1 \quad , \quad R > l_1 \quad (\text{A.2})$$

A fraction, f , of the total volume of component 2 in the micelle will make up the core.

$$f N_2 v_2 = \frac{4\pi}{3} (R - l_1)^3 \quad (\text{A.3})$$

Since a chain of component 2 extending into the core must pass through the outer portion of the micelle, there is an upper limit on the fraction of component 2's volume that can make up the core.

$$f \leq 1 - \frac{l_1}{l_2} \quad (\text{A.4})$$

If both (A.1) and (A.4) are satisfied, a spherical micelle will form. Combining (A.1) and (A.3) yields the expression for f :

$$f = \frac{\frac{4\pi}{3} \left\{ \left[\frac{3}{4\pi} (N_1 v_1 + N_2 v_2) \right]^{\frac{1}{3}} - l_1 \right\}^3}{N_2 v_2} \quad (\text{A.5})$$

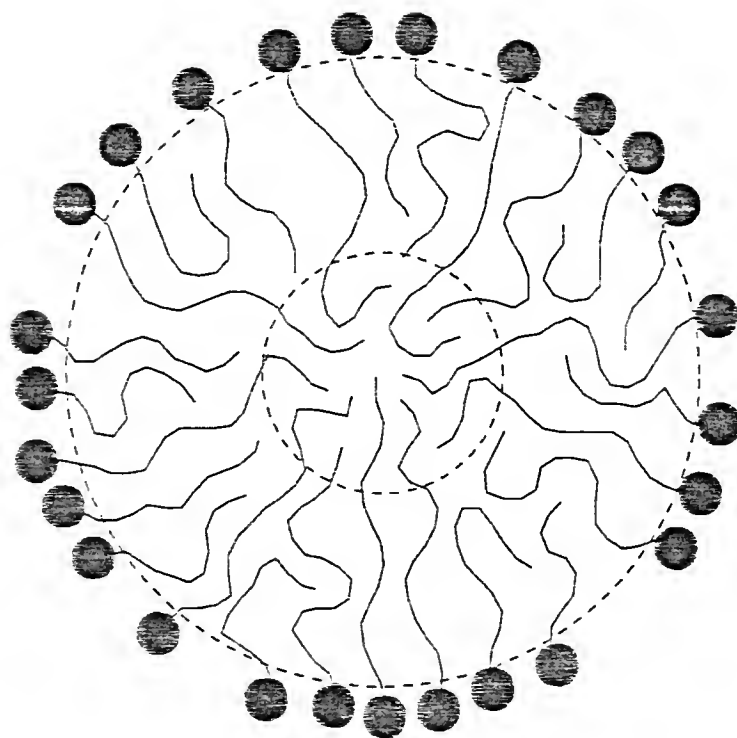


Figure A-1. Schematic of a binary micelle with monomers of different chain lengths. Inner dashed circle depicts the micelle core devoid of the shorter chains.

A "core fraction constraint" on spherical micelle formation is obtained by substituting (A.4) for f and solving for N_1 :

$$N_1 \leq \frac{\frac{4\pi}{3} \left\{ \left[\frac{3}{4\pi} N_2 v_2 \left(1 - \frac{l_1}{l_2} \right) \right]^{\frac{1}{3}} + l_1 \right\}^3 - N_2 v_2}{v_1} \quad (\text{A.6})$$

From A-1 a "radius constraint" is written:

$$N_1 \leq \frac{\frac{4\pi}{3} l_2^3 - N_2 v_2}{v_1} \quad (\text{A.7})$$

The possible combinations of N_1 and N_2 which will form a spherical micelle are bounded by these two constraints, as shown in Figure A-2. There are four regions defined by the two constraints:

- I) Both constraints met -- spherical micelle.
- II) Only radius constraint met -- nonspherical.
- III) Only core fraction constraint met -- nonspherical.
- IV) Neither constraint met -- nonspherical.

Nonspherical micelles are modeled as prolate spherocylinders. The spherical caps and their cores have radii of R and r , as in the spherical case. The cylindrical portion has these same radii and length L . These dimensions are shown in Figure A-3.

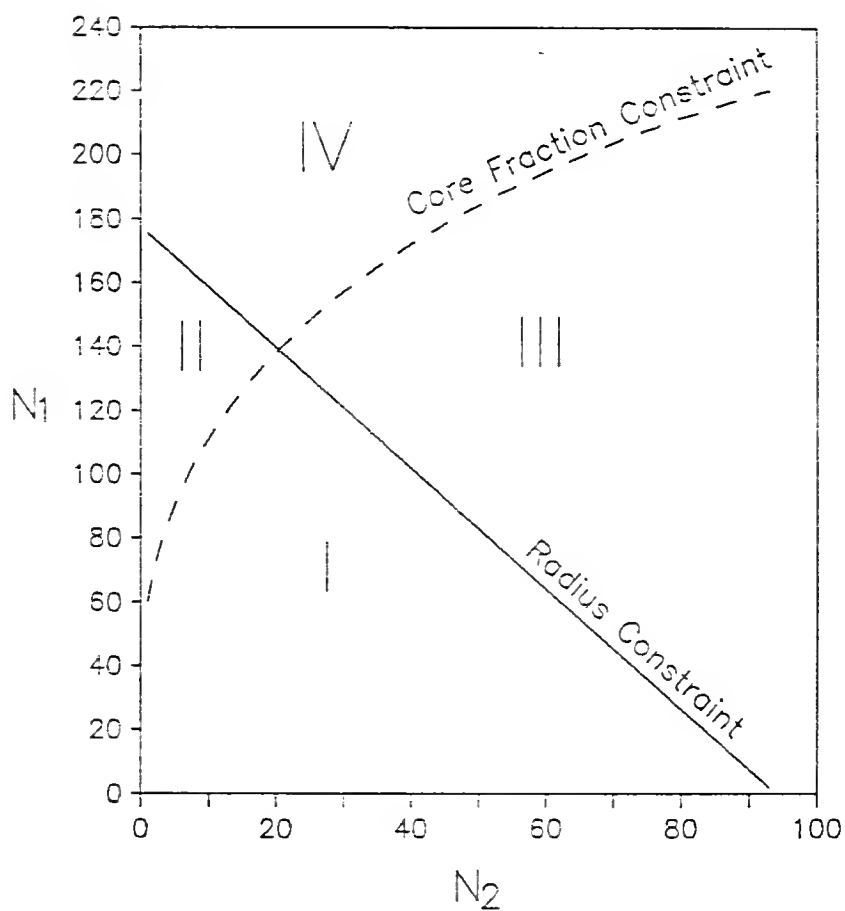


Figure A-2. Possible combinations of shorter chains (1) and longer chains (2) in a binary micelle. Four regions are defined by the two composition constraints on micelle geometry.

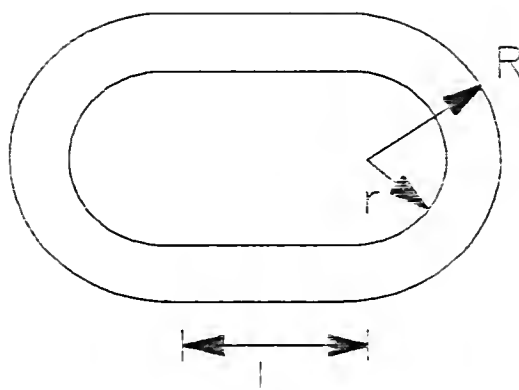


Figure A-3. Side view of the prolate spherocylinder model of a binary micelle. The micelle is of radius R and length L , while the core is of radius r and length L .

As in the spherical case, equations can be written for the total volume

$$N_1 v_1 + N_2 v_2 = \frac{4\pi}{3} R^3 + \pi L R^2 \quad (\text{A.8})$$

and the core volume

$$f N_2 v_2 = \frac{4\pi}{3} (R - l_1)^3 + \pi L (R - l_1)^2 \quad (\text{A.9})$$

The two volume equations can be combined to eliminate L, resulting in a polynomial in R:

$$\begin{aligned} \frac{4\pi}{3} l_1 R^4 - \frac{8\pi}{3} l_1 R^3 + \left[\frac{4\pi}{3} l_1^3 - (1-f) N_2 v_2 - N_1 v_1 \right] R^2 \\ + 2 l_1 (N_1 v_1 + N_2 v_2) R - l_1 (N_1 v_1 + N_2 v_2) = 0 \end{aligned} \quad (\text{A.10})$$

For the spherical micelle of region I, L is zero and (A.1) gives the value of R. In region III, the R is set equal to l_2 and L is given by (A.9). In regions II and IV, f is set equal to $1 - l_2/l_1$ and (A.10) is solved for its root between l_1 and l_2 .

APPENDIX B

HEAD GROUP INTERACTION IN A BINARY MICELLE

The potential energy due to the interaction of polar head groups at the surface of the micelle can be calculated as the sum of the potentials of all possible interacting pairs. Considering ionic head groups to be point charges and nonionic head groups to be dipoles, the types of pairs possible are dipole/dipole, charge/dipole, and charge/charge. The potentials for all three are functions of the inter-group distance, and for the first two are also functions of the orientations of the dipole(s).

Assuming that the mean distance between adjacent head groups is the inter-group distance for every adjacent pair, head groups can be arranged hexagonally on the surface (Figure B-1.) In this arrangement, each head group has six adjacent groups, each at a distance " r ". If each group is taken as the center of a hexagon and the adjacent pairs formed with it are summed, each pair will be counted twice in the total of all adjacent pairs formed by all groups.

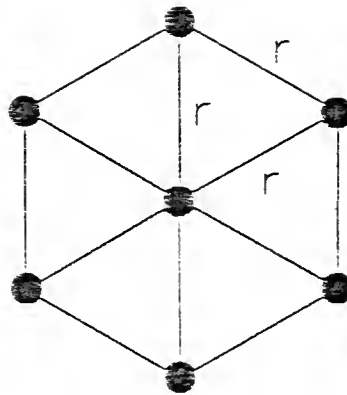


Figure B-1. Hexagonal arrangement of head groups on the micelle surface, with equal separation, r , between adjacent groups.

For a micelle of N head groups,

$$E_{\text{tot}} = \frac{1}{2} \sum_m^N \sum_n^6 E_{mn} \quad m = 1, 2, \dots, N \quad (B.1)$$

$$n = 1, 2, \dots, 6$$

The distance r will first be determined for head groups on a spherical surface, as in a spherical micelle or the spherical portions of a spherocylindrical micelle. Taking a great circle of the sphere such that adjacent head groups lie on the circle (Figure B-2), R is the radius of the sphere and $\delta(N)$ is the angle formed by two radii meeting the surface at the adjacent groups, as a function of N . From planar trigonometry,

$$\delta = 2 \sin^{-1} \left(\frac{r}{2R} \right) \quad (B.2)$$

Each triad of mutually adjacent groups defines an equilateral spherical triangle with sides of arclength $R\delta$. Each group is a vertex of six triangles. If six triangles are assigned to each group and all groups are summed each triangle is counted three times, so the number of spherical triangles is $2N$.

From spherical trigonometry, the area of each triangle is:

$$A = (3\alpha - \pi)R^2 \quad (B.3)$$

where α is the angle at each vertex of the equilateral

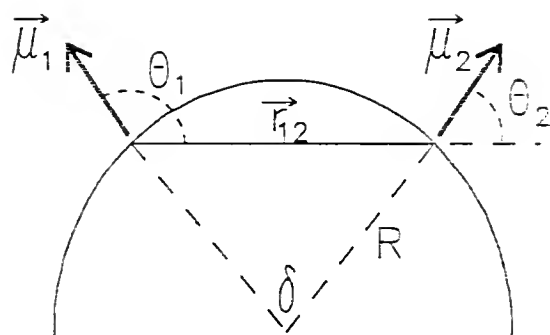


Figure B-2. Vectors and angles used in the calculation of dipole - dipole interaction potential. The magnitude of the separation vector, r_{12} , is the separation given in Figure B-1.

spherical triangle. From the Law of Cosines for sides of spherical triangles,

$$\cos \alpha = \frac{\cos \delta - \cos^2 \delta}{\sin^2 \delta} \quad (\text{B.4})$$

$$= \cos \left[\frac{2 \sin^{-1} \left(\frac{r}{2R} \right)}{1 + \cos \left(2 \sin^{-1} \left(\frac{r}{2R} \right) \right)} \right] \quad (\text{B.5})$$

and from the double-angle relation,

$$2 \sin^{-1} \left(\frac{r}{2R} \right) = 1 - \frac{1}{2} \left(\frac{r}{R} \right) \quad (\text{B.6})$$

Combining (B.3), (B.5), and (B.6) yields an expression for the area of a triangle in terms of r and R :

$$A = \left\{ 3 \cos^{-1} \left[\frac{1 - \frac{1}{2} \left(\frac{r}{R} \right)^2}{2 - \frac{1}{2} \left(\frac{r}{R} \right)^2} \right] - \pi \right\} R^2 \quad (\text{B.7})$$

The area of a triangle is also equal to the total area divided by the number of triangles:

$$A = \frac{4\pi R^2}{2N} \quad (\text{B.8})$$

Eliminating the area in these two equations and solving for r gives the distance between groups for the spherical surface:

$$r = R \sqrt{\frac{4 \cos \left(\frac{\pi}{3} + \frac{2\pi}{3N} \right) - 2}{\cos \left(\frac{\pi}{3} + \frac{2\pi}{3N} \right) - 1}} \quad (\text{B.9})$$

The surface of the spherocylinder can be separated into those of a sphere of radius R and cylinder of radius R and length L . The number of groups on the surface of the

micelle is the sum of the numbers of groups on the two surfaces:

$$N = N_{sph} + N_{cyl} \quad (B.10)$$

From (B.7) and (B.8) the number of groups on the spherical portion is given by

$$N_{sph} = \frac{2\pi}{3 \cos^{-1} \left[\frac{2 - \left(\frac{r}{R}\right)^2}{4 - \left(\frac{r}{R}\right)^2} \right] - \pi} \quad (B.11)$$

On the cylindrical portion, the hexagonal pattern will have the groups lying on circles evenly spaced along the length of the cylinder. In this arrangement,

$$\# \text{ of circles} = \frac{2L}{\sqrt{3}r}$$

$$\# \text{ of groups per circle} = \frac{\pi}{\sin^{-1} \left(\frac{r}{2R} \right)}$$

so that

$$N_{cyl} = \frac{2\pi L}{\sqrt{3}r \sin^{-1} \left(\frac{r}{2R} \right)} \quad (B.12)$$

Equation (B.10) can then be written as the following nonlinear equation in r ,

$$0 = \frac{2\pi}{3 \cos^{-1} \left[\frac{2 - \left(\frac{r}{R}\right)^2}{4 - \left(\frac{r}{R}\right)^2} \right] - \pi} + \frac{2\pi L}{\sqrt{3}r \sin^{-1} \left(\frac{r}{2R} \right)} - N \quad (B.13)$$

which can be solved for r by iterative techniques. The values of R and L are calculated by the method given in Appendix A.

For the calculation of pair potentials, Weston and Schwarz (1972) give:

$$E_{\text{charge/charge}} = \frac{z_1 z_2 e^2}{D r_{12}} \quad (\text{B.14})$$

$$E_{\text{charge/dipole}} = \frac{-z_1 e \mu_2 \cos \theta_2}{D r_{12}^2} \quad (\text{B.15})$$

where θ_2 is the angle between the directions r_{12} and μ_2 .

Murrell et al. (1978) give:

$$E_{\text{dipole/dipole}} = \frac{\vec{\mu}_1 \cdot \vec{\mu}_2}{D r_{12}^3} - \frac{3(\vec{\mu}_1 \cdot \vec{r}_{12})(\vec{\mu}_2 \cdot \vec{r}_{12})}{D r_{12}^5} \quad (\text{B.16})$$

Assuming all dipoles to be radially oriented, all of the dot products are two-dimensional, so

$$E_{\text{dipole/dipole}} = \frac{\mu_1 \mu_2}{D r_{12}^3} (\cos \delta - 3 \cos \theta_1 \cos \theta_2) \quad (\text{B.17})$$

where the angles are those shown in Figure B-2. Only adjacent pairs are being considered in this model, and all pair separations are equal to r , so the subscripts on r will not be used. Since δ is known (B.2), the angle terms in (B.15) and (B.17) can be eliminated:

$$E_{\text{charge/dipole}} = \frac{-z_1 e \mu_2}{2 D R r} \quad (\text{B.18})$$

$$E_{\text{dipole/dipole}} = \frac{\mu_1 \mu_2}{D r^3} \left[1 + \left(\frac{r}{2R} \right)^2 \right] \quad (\text{B.19})$$

The total number of adjacent pairs formed among N head groups is 3N. For a binary micelle,

$$N = N_1 + N_2$$

$$x_1 = \frac{N_1}{N}$$

$$x_2 = \frac{N_2}{N}$$

Assuming only adjacent pairs contribute to the total interaction potential, the single component limit is

$$E_{\text{tot}} = 3N E_{ii} \quad , \quad x_i = 1 \quad (\text{B.20})$$

At $x_2=0$, replacing a "1" with a "2" replaces six "1-1" pairs by six "1-2" pairs. With replacements distributed evenly over the surface, this continues until $x_2= 1/4$. The next replacement of "1" by "2" replaces four "1-1" pairs by two "1-2" pairs and two "2-2" pairs. This continues until $x_2= 1/2$. Beyond this, two "1-1" and two "1-2" pairs are replaced by four "2-2" pairs until $x_2= 3/4$. Finally, six "1-2" pairs are replaced by six "2-2" pairs until $x_2= 1$.

$$\frac{dE_{\text{tot}}}{dX_1} = 6N(E_{12} - E_{11}) \quad 0 \leq x_2 \leq \frac{1}{4} \quad (\text{B.21})$$

$$= N(2E_{22} + 2E_{12} - 4E_{11}) \quad \frac{1}{4} \leq x_2 \leq \frac{1}{2} \quad (\text{B.22})$$

$$= N(4E_{22} - 2E_{12} - 2E_{11}) \quad \frac{1}{2} \leq x_2 \leq \frac{3}{4} \quad (\text{B.23})$$

$$= 6N(E_{22} - E_{12}) \quad \frac{3}{4} \leq x_2 \leq 1 \quad (\text{B.24})$$

Integrating the above and writing on a per monomer basis:

$$\underline{E} = E_{11}(3 - 6x_1) + E_{12}(6x_1) \quad 0 \leq x_2 \leq \frac{1}{4} \quad (\text{B.25})$$

$$= E_{11}\left(\frac{5}{2} - 4x_1\right) + E_{12}(1 + 2x_1) + E_{22}\left(2x_1 - \frac{1}{2}\right) \quad \frac{1}{4} \leq x_2 \leq \frac{1}{2} \quad (\text{B.26})$$

$$= E_{11}\left(\frac{3}{2} - 2x_1\right) + E_{12}(3 - 2x_1) + E_{22}\left(4x_1 - \frac{3}{2}\right) \quad \frac{1}{2} \leq x_2 \leq \frac{3}{4} \quad (\text{B.27})$$

$$= E_{12}(6 - 6x_1) + E_{22}(6x_1 - 3) \quad \frac{3}{4} \leq x_2 \leq 1 \quad (\text{B.28})$$

By substituting in the appropriate pair potentials from (B.14) through (B.16) the total energy of interaction of adjacent pairs of a micelle of binary composition is be calculated with one of equations (B.25) through (B.28.)

APPENDIX C
PROGRAM LISTING FOR SINGLE-COMPONENT
NONIONIC MICELLE CALCULATION

```

REAL*8 XSUM,XN,ARG,X

CHARACTER CONT,P,DISP,WHAT,SHOW,SAV,NAME*8

REAL N,NAVG,SAMP(3,5),NSAM(5)

COMMON N,DGM/I/G,GC,SCONF/J/C1,C0

COMMON /K/U,T,ZZ/L/GVAL(6)

WRITE(*,*) 'NUMBER OF CARBONS '

READ(*,*) CN

OPEN(9,FILE='INVALS',FORM='FORMATTED',ACCESS=
&'SEQUENTIAL',STATUS='OLD')

READ(9,*) T,U,C0,C1,G,GC,SCONF

READ(9,*) IMIN,IMAX,(NSAM(J),J=1,5)
5 WRITE(*,100) C1,C0,U,T,G,GC,SCONF,IMIN,IMAX

READ(*,'(A)')WHAT

IF(WHAT.EQ.'D') THEN

    WRITE(*,*) 'Enter C1, C0, U, T:'

    READ(*,*) C1,C0,U,T

ELSEIF(WHAT.EQ.'P') THEN

    WRITE(*,*) 'Enter G, GC, SCONF:'

    READ(*,*) G,GC,SCONF

ELSEIF(WHAT.EQ.'R') THEN

    WRITE(*,*) 'Enter min and max values of N:'

    READ(*,*) IMIN,IMAX

ELSEIF(WHAT.EQ.'G') THEN

    GO TO 6

ENDIF

```

```

GO TO 5

6 WRITE(*,*) 'PRINT GVALUES TO FILE? (Y/N) '
  READ(*, '(A) ') P
  IF(P.EQ.'Y') THEN
    WRITE(*,*) 'ENTER NAME OF FILE (1-8 CHAR.): '
    READ(*, '(A) ') NAME
    OPEN(UNIT=8, FILE=NAME, FORM='FORMATTED', ACCESS=
&'SEQUENTIAL', STATUS='NEW')
    WRITE(8,81) ' ', 'N', 'G2', 'SC', 'G4', 'G6', 'GM',
&'LOG(X/N) ', 'X/N'
  ENDIF
  WRITE(*,*) 'CALCULATING DISTRIBUTION. . .'
  C0LG=ALOG(C0)
  C1LG=ALOG(C1)
  CALL HCSOL(XEQ,CN)
  DG2=ALOG(XEQ*C0)
  X1=C1/C0
  XSUM=0.
  L0=1
  SUM1=0.0
  SUM2=0.0
  IF(P.EQ.'Y') THEN
    KOUNT=0
    KOUNT2=1
    KUP=0

```



```

DO 8 I=IMIN,IMAX

N=I

IF(KOUNT2.EQ.80) THEN

    WRITE(8,81) ' ', 'N', 'G2', 'SC', 'G4', 'G6', 'GM',
&'LOG(X/N)', 'X/N'

    KOUNT2=1

ENDIF

CALL DELTAG(DG2,CN)

ARG=N*(-DGM+C1LG)-COLG

IF(DABS(ARG).GT.174.673) THEN

    IF(ARG.GT.0.0) THEN

        WRITE(*,85) N,DGM

        GO TO 11

    ELSE

        XN=0.0

    ENDIF

ELSE

    XN=DEXP(ARG)

ENDIF

IF(L0.GT.5) GO TO 7

IF(N.EQ.NSAM(L0)) THEN

    SAMP(1,L0)=N

    SAMP(2,L0)=GVAL(6)

    SAMP(3,L0)=XN

    L0=L0+1

```

```

ENDIF
7  X=XN*N
   XSUM=XSUM+X
   KOUNT=KOUNT+1
   IF(N.EQ.100.) THEN
       KOUNT=11
       KUP=1
   ENDIF
   IF(N.EQ.1000.) THEN
       KOUNT=101
       KUP=2
   ENDIF
   IF(KUP.EQ.0) THEN
       WRITE(8,82) ' ', (GVAL(M),M=1,6), ARG/2.303, XN
       KOUNT2=KOUNT2+1
   ELSEIF(KUP.EQ.1.AND.KOUNT.EQ.11) THEN
       WRITE(8,82) ' ', (GVAL(M),M=1,6), ARG/2.303, XN
       KOUNT2=KOUNT2+1
       KOUNT=1
   ELSEIF(KUP.EQ.2.AND.KOUNT.EQ.101) THEN
       WRITE(8,82) ' ', (GVAL(M),M=1,6), ARG/2.303, XN
       KOUNT2=KOUNT2+1
       KOUNT=1
   ENDIF
   SUM1=SUM1+XN

```

```

SUM2=SUM2+X
IF(XN.LT.1.0D-24.AND.I.GT.10000) GOTO 10009
8  CONTINUE
10009 NAVG=SUM2/SUM1
CMON=XSUM*C0 + C1
WRITE(6,84) C1,C0,U,T
WRITE(6,101) G,GC,SCONF,NAVG,CMON
WRITE(*,*) 'DISPLAY SAMPLE GVALUES? (Y/N) '
READ(*, '(A) ') DISP
IF(DISP.EQ. 'Y') WRITE(6,83) ((SAMP(J,K),J=1,3),K=1,5)
11  WRITE(*,*) 'CONTINUE? (Y/N) '
READ(*, '(A) ') CONT
WRITE(8,84) C1,C0,U,T
WRITE(8,101) G,GC,SCONF,NAVG,CMON
C  ENDFILE(UNIT=8)
CLOSE(UNIT=8)
ELSE
DO 10 I=IMIN,IMAX
N=I
CALL DELTAG(DG2,CN)
ARG=N*(-DGM+C1LG)-COLG
IF(DABS(ARG).GT.174.673) THEN
IF(ARG.GT.0.0) THEN
WRITE(*,85) N,DGM
GO TO 12

```

```

        ELSE
            XN=0.0
        ENDIF
    ELSE
        XN=DEXP(ARG)
    ENDIF
    IF(L0.GT.5) GO TO 9
    IF(N.EQ.NSAM(L0)) THEN
        SAMP(1,L0)=N
        SAMP(2,L0)=GVAL(6)
        SAMP(3,L0)=XN
        L0=L0+1
    ENDIF
9      X=XN*N
      XSUM=XSUM+X
      SUM1=SUM1+XN
      SUM2=SUM2+X
      IF(XN.LT.1.0D-24.AND.I.GT.1000) GOTO 10000
10     CONTINUE
10000  NAVG=SUM2/SUM1
      CMON=XSUM*C0 + C1
      WRITE(6,84) C1,C0,U,T
      WRITE(6,101) G,GC,SCONF,NAVG,CMON
      WRITE(*,*) 'DISPLAY SAMPLE GVALUES? (Y/N) '
      READ(*,'(A)') DISP

```

```

      IF (DISP.EQ.'Y') WRITE(6,83) ((SAMP(J,K),J=1,3),K=1,5)
12  WRITE(*,*) 'CONTINUE? (Y/N) '
      READ(*,'(A)') CONT
ENDIF
IF (CONT.EQ.'Y') GO TO 5
WRITE(*,*) 'SAVE DATA AND PARAMETER VALUES?'
READ(*,'(A)') SAV
IF (SAV.EQ.'Y') THEN
      REWIND(9)
      WRITE(9,*) T,U,C0,C1,G,GC,SCONF
      WRITE(9,*) IMIN,IMAX,(NSAM(J),J=1,5)
ENDIF
CLOSE(9)
STOP
81  FORMAT(A,2X,A,6X,A,6X,A,6X,A,6X,A,8X,A,5X,A,4X,A,
      &5X,A,E10.4,A,F4.1,A,F6.2)
82  FORMAT(A,F6.0,1X,F6.2,2X,F6.3,2X,F6.3,2X,F6.5,3X,
      &F8.4,2X,F6.1,2X,E9.2)
83  FORMAT(5X,'N=',F6.0,5X,'DGM=',F7.3,5X,'XN/N=',E9.2)
84  FORMAT(1X,'C1=',E12.5,4X,'C0=',F5.1,4X,'U=',F4.1,4X,
      &'T=',F7.2)
85  FORMAT(1X,'FOR N=',F6.0,'DG)M=',E10.3/1X,
      &'OVERFLOW ON ', 'XN/XN CALCULATION')
86  FORMAT(1X,'FOR N=',F6.0,'DG)M=',E10.3/1X,
      &'X/N SET TO 0 ', 'TO AVOID UNDERFLOW')

```

```

100 FORMAT(1X,'Current values of Data and Parameters are:'
&/6X,'DATA: C1=',E12.5,2X,'C0=',F5.1,2X,'U=',F4.1,2X,
&'T=',F7.2/6X,'PARAMETERS: G=',F7.4,3X,'GC=',F7.5,3X,
&'SCONF=',F8.4/6X,'RANGE of N is from ',I3,' to ',I6//
& 1X,'Change values of D)ata, P)arameters, R)ange,
& or G)o?'/)

```

```

101 FORMAT(1X,'G=',F7.4,3X,'GC=',F7.5/1X,'SCONF=',F8.4
& /1X,'MEAN AGGREGATE SIZE IS',F9.2,5X,
& 'SURFACTANT CONCENTRATION IS',E13.6)

END

```

C *****

```

SUBROUTINE DELTAG(DG2,CN)

REAL NTRANS

COMMON EN,DGM/H/R,XLM/I/G,GC,SCONF/J/C1,C0/K/U,T,DG6
COMMON /L/GVAL(6)

CALL SHAPE1(XLC(CN),VC(CN))

NTRANS=4.1888*XLC(CN)**3/VC(CN)

IF(EN.LE.NTRANS) THEN

    SURF=12.5664*R*R*(NTRANS/EN)**(1./3.)

    DG4=SURF*GAM(CN)*(1.-G/R)/(1.381*EN*T)

ELSE

    DG4=6.2832*R*GAM(CN)*(XLM*(1-GC/R)+2*R*(1-G/R))/

& (1.381*EN*T)

ENDIF

CALL DHHEDS(D)

```

```
SC=-SCONF*(XLC(CN)/R)**2
```

```
DGM=DG2+DG4+SC+DG6
```

```
GVAL(1)=EN
```

```
GVAL(2)=DG2
```

```
GVAL(3)=SC
```

```
GVAL(4)=DG4
```

```
GVAL(5)=DG6
```

```
GVAL(6)=DGM
```

```
RETURN
```

```
END
```

```
C *****
```

```
FUNCTION XLC(CN)
```

```
XLC=1.265*CN + 1.5
```

```
RETURN
```

```
END
```

```
C *****
```

```
FUNCTION VC(CN)
```

```
VC=26.9*CN + 27.4
```

```
RETURN
```

```
END
```

```
C *****
```

```
FUNCTION GAM(CN)
```

```
COMMON /K/Z,T,ZZ
```

```
GAM=1.381*(57.868*CN + 117.99 - (.059*CN + .1768)*T)/
```

```
& (CN + 2.4)
```

RETURN

END

C *****

SUBROUTINE HCSOL(XEQ,CN)

REAL K

REAL*8 X1(10),EXPK

DIMENSION A(2),B(2)

COMMON /K/Z0,T,Z1

DATA A/997.098,258.015/B/1603.72,9686.96/R/1.987/

IF(CN.LT.10.) THEN

I=1

ELSE

I=2

ENDIF

K=A(I)*CN + B(I)

EXPK=EXP(-K/(R*T))

X1(1)=EXPK/(1.+EXPK)

DO 60 J=2,10

X1(J)=DEXP(-(1.-2.*X1(J-1))*K/(R*T)+DLOG(1.-X1(J-1)))

TEST=DABS(X1(J)-X1(J-1))/X1(J)

IF(TEST.LT.1.0E-8) GO TO 61

60 CONTINUE

61 XEQ=X1(J)

RETURN

END

C *****

```

SUBROUTINE SHAPE1(XLC,VC)
COMMON AG,Z/H/R,XL
DATA B/4.18879/
XL=0.0
R=(AG*VC/B)**(1./3.)
IF(R.GT.XLC) THEN
    R=XLC
    XL=(AG*VC-B*XLC**3)/(3.14159*XLC**2)
ENDIF
RETURN
END

```

C *****

```

SUBROUTINE HEDSEP(D)
CHARACTER*1 FLAG
COMMON AG,Z/H/R,XL
EXTERNAL F,DF
IF(XL.GT.0.) THEN
    CALL NEWTON(F,DF,D,.01,D0,50,FLAG)
    IF(FLAG.EQ.'N') GO TO 49
    D=D0
RETURN
49 WRITE(6,400) AG
RETURN
ENDIF

```

```

T=COS(1.04720*(1.+2./AG))
D=SQRT((4.*T-2.)/(T-1.))*R
RETURN

```

```

400 FORMAT(1X,'NO HEAD SEP. FOUND, N=',F7.0)

```

```

END

```

```

C *****

```

```

FUNCTION F(D)
COMMON AG,XZ/H/R,XL
DATA E/6.28319/
Z=(D/R)**2
F=E/(3*ACOS((2.-Z)/(4.-Z))-3.14159)+E*XL/(1.732*D
& *ASIN(D/(2.*R))) - AG
RETURN
END

```

```

C *****

```

```

FUNCTION DF(D)
COMMON/H/R,XL
Z=D/(2.*R)
Z2=(D/R)**2
DF=-3.6276*XL*(1./(D*D*ASIN(Z)) +1./(2.*R*D*(ASIN(Z)
& **2*SQRT(1.-Z*Z)))-75.398*D/(R*R*(4.-Z2)**2*(3.*ACOS(
& (2.-Z2)/(4.-Z2))-3.14159)**2*SQRT(1.-((2.-Z2)/(4.-Z2
& ))**2))
RETURN
END

```

```

C *****
SUBROUTINE DHHEDS(D)
COMMON /H/R,XL/K/U,T,DG6
DI(T)=(.0007469*T-.8063294)*T+252.422
CALL HEDSEP(D)
DG6=3*U*U*(1.+(D/(2.*R))**2)/(DI(T)*D**3*T*1.381E-23)
& *9.9907E-20
RETURN
END

C *****
SUBROUTINE NEWTON(F,DFDX,A1,EPS,X0,J,FLAG)
CHARACTER*1 FLAG
FLAG='Y'
X=A1
DO 11 I=1,J
FX=F(X)
IF(ABS(FX).LT.EPS) THEN
X0=X
RETURN
ENDIF
X=X-FX/DFDX(X)
11 CONTINUE
FLAG='N'
RETURN
END

```

C MOLECULAR DYNAMICS SOURCE PROGRAM FOR A SIMPLE
C MODEL OF A MICELLE ENCLOSED IN A SHELL. A
C FIFTH-ORDER PREDICTOR-CORRECTOR ALGORITHM IS
C USED TO SOLVE THE EQUATIONS OF MOTION. A
C SKELETAL MODEL DUE TO WEBER IS USED FOR EACH
C ALKANE MOLECULE.

C
C
C INTENDED FOR LONGER-RANGE POTENTIALS. NO
C TRUNCATION OF POTENTIALS OR NEIGHBOR-LISTING
C IS EMPLOYED.

C
C ALL HEAD GROUP ATTRIBUTES CAN BE SET.

C
C PARAMETER(MHEAD=7,HDSGMA=2.45,BLHEAD=.65,GLHEAD=
& 1.03103E3,BAHEAD=-.82904,GAHEAD=2.17184E3,GTHEAD=
& 47.733)
C COMMON/POS/X0(216),Y0(216),Z0(216)
C COMMON/VEL/X1(216),Y1(216),Z1(216)
C COMMON/DER/X2(216),Y2(216),Z2(216),X3(216),Y3(216),
& Z3(216),X4(216),Y4(216),Z4(216),X5(216),Y5(216),
& Z5(216)
C COMMON/FOR/FX(216),FY(216),FZ(216)
C COMMON/DISP/DAX(216),DAY(216),DAZ(216),X0L(216),
& Y0L(216),Z0L(216)

```

&  FORCON
COMMON/ENERGY/TOTE,TOTLJ,ETOR,EBON,EBEN,EINTR,TRFRAC
&  ,EXTPRS,FTOTWL
COMMON/NUM/NM,NAM,NP,NP1,NP2,NP22,KSORT,KB,NABTOT
COMMON/SCAL/RSPHER,RWALL,DELRS,ISCALE
COMMON/MASS/MASS(216)

C
C  FLAG, IF IFLAG.NE.1 USES INTPOS AND RANDOM VELOCITIES
C  IF IFLAG.EQ.1 X0,Y0,Z0,AND ALL DERIVATIVES ARE READ
C  FROM PREVIOUS RUN.
C
      IFLAG=1

C
C === SET NUMBER OF PARTICLES IN PRIMARY CELL
      NAM=9
      NM=24
      NP=NM*NAM
      PART=NP
      PART=NP
      NP1=NP-1
      NP2=NP-2
      NP22=.5*PART+.01

C
C === SET RELATIVE MASS OF PARTICLES
      DO 20 I=1,NP,NAM

```

MASS(I)=MHEAD

20 CONTINUE

C

C === SET RADIUS OF SPHERE ON WHICH HEAD GROUPS ARE ATTACHED

RSPHER= 6.000

DELRS=0.00025

ISCALE=0

RWALL =RSPHER+1.0

REQUIL=1.

FORCON=30.

C

C === SET VALUES OF PHYSICAL CONSTANTS

XNAM=FLOAT(NAM)

WTMOL=XNAM*14.+2.

WTPART=WTMOL/XNAM

RSTAR=0.4

EPS=419.

GABB=9.25E7

GAB=GABB/EPS*RSTAR*RSTAR

THA=112.15*3.14159/180.

CT0=COS(THA)

GTHAA=1.3E5

GTHA=GTHAA/EPS

C ROTATIONAL PARAMETER DIVIDED BY 10 FOR SCALE-DOWN

GTHEE= 8.314E3

```
IF ( ISCALE.EQ.1) GTHEE=GTHEE/10.
```

```
GTHE=GTHEE/EPS
```

```
BB=0.1539
```

```
B0=BB/RSTAR
```

```
B2I=1./B0/B0
```

```
AVO=6.0225E+23
```

```
BOLZ=1.38054D-23
```

```
EPSI=EPS/BOLZ/AVO
```

```
THIRD=1./3.
```

```
PI=3.1415926535
```

```
C
```

```
C === SET DESIRED FLUID STATE CONDITION
```

```
TR=5.913
```

```
T=TR*EPSI
```

```
VOL=1.333333*PI*RSPHER**3
```

```
DR=FLOAT(NM)/VOL
```

```
C
```

```
C === SET RUN FLAGS AND PARAMETERS
```

```
IFLG=-1
```

```
KB=0
```

```
KSAVE=10
```

```
KSORT=10
```

```
KWRITE=10
```

```
MAXKB=90000
```

```
XDIST=0.1
```

C

C === SET TIME-STEP AND ITS MULTIPLES

DELTA=0.000850

DELSQ=DELTA*DELTA

DELTSQ=.5*DELSQ

TSTEP=SQRT(WTPART*RSTAR**2/EPS/1.E21)*1.D+12

TT1=TSTEP*DELTA*1.D-12

C

C === SET PARAMETERS IN PREDICTOR-CORRECTOR METHOD

F02=3./16.

F12=251./360.

F32=11./18.

F42=1./6.

F52=1./60.

C

C === SET DISTANCES FOR POTENTIAL CUT-OFF, VERLET LIST, ETC.

CUBE=2.*RSPHER

CUBE2=.5*CUBE

RC=2.5

RCHH=2.5

RLIST=(RC+.25)**2

RDMAX=CUBE2*CUBE2

IF(RLIST.GT.RDMAX) RLIST=RDMAX

IF(RC.GT.CUBE2) RC=CUBE2

C

C === SCALE FACTOR FOR VELOCITIES DURING EQUILIBRATION

AHEAT=DELSQ*PART*3.*TR

C

C === WRITE TAPE HEADING

OPEN(20,FILE='C811RUN1',ACCESS='SEQUENTIAL',
& FORM='UNFORMATTED')

WRITE(20) NP,NAM,NM,DR,TR,EPS,RSTAR

WRITE(20) CUBE,VOL,RC,RLIST,RDMAX,DELTA,TSTEP

C

C === SHIFTED-FORCE CONSTANTS

RRMAX=1./RC

RRMAX6=RRMAX**6

RRMAX9=RRMAX**9

ESHFT=21.*RRMAX6-20.*RRMAX9

ESHFTA=18.*RRMAX*(RRMAX9-RRMAX6)

FSHFT=ESHFTA

C SHIFTED FORCE POTENTIALS FOR HEAD-HEAD REPULSIVE

C INTERACTIONS

C

RCI=1./RCHH

RCI2=RCI*RCI

RCI3=RCI2*RCI

RCI4=RCI3*RCI

RCI9=RCI3*RCI3*RCI3

RCI13=RCI4*RCI*RCI4*RCI4

```
HSHT=RCI3*(13.*RCI9+4.)
```

```
HSHTA=3.*RCI4*(4.*RCI9+1.)
```

```
HFSHT=HSHTA
```

```
C
```

```
C === CORRECTIONS FOR LONG-RANGE INTERACTIONS
```

```
RC3=RC**3
```

```
RC6=RC3*RC3
```

```
CORE=4.*PI*DR*(1./6./RC6-0.5/RC3)
```

```
DE=CORE
```

```
C
```

```
C === INITIALIZE SUM ACCUMULATORS
```

```
XSUM=0.
```

```
SUM=0.
```

```
C
```

```
C === PRINT PARAMETERS
```

```
WRITE(*,900)
```

```
900  FORMAT(1H1///)
```

```
WRITE(*,902)
```

```
902  FORMAT(7X,49('*'))
```

```
WRITE(*,904)
```

```
904  FORMAT(7X,'*',T56,'*')
```

```
WRITE(*,906) NM
```

```
906  FORMAT(7X,'*',2X,'MOLECULAR DYNAMICS FOR',I3,  
& ' N-ALKANE MOLECULES',T56,'*')
```

```
WRITE(*,904)
```

```

WRITE(*,917) NAM
917  FORMAT(7X,'*',5X,'WITH',I3,' PARTICLES PER
      &MOLECULE',T56,'*')
      WRITE(*,904)
      WRITE(*,902)
      WRITE(*,904)
      WRITE(*,908) EPSI,RSTAR
908  FORMAT(7X,'*',2X,'EPSI/K = ',F7.3,T36,'RSTAR = ',
      &F7.3,T56,'*')
      WRITE(*,910) TR,T
910  FORMAT(7X,'*',2X,'TR      = ',F7.3,T36,'      T = ',
      &F7.3,T56,'*')
      WRITE(*,912) DR,VOL
912  FORMAT(7X,'*',2X,'DR      = ',F7.3,T36,'VOL    = ',
      &F8.3,T56,'*')
      WRITE(*,914) CUBE
914  FORMAT(7X,'*',2X,'CUBE    = ',F7.3,T56,'*')
      WRITE(*,916) RC
916  FORMAT(7X,'*',2X,'RC      = ',F7.3,T56,'*')
      WRITE(*,918) RLIST,RDMAX
918  FORMAT(7X,'*',2X,'RLIST   = ',F7.3,T36,'RDMAX = ',
      &F7.3,T56,'*')
      WRITE(*,920) DELTA
920  FORMAT(7X,'*',2X,'DELTA   = ',F9.5,T56,'*')
      WRITE(*,904)

```

```

      WRITE(*,922) TSTEP
922   FORMAT(7X,'*',2X,'TIME UNIT = ',F6.3,'E-12 SEC',
      &T56,'*')

      WRITE(*,924) TT1
924   FORMAT(7X,'*',2X,'TIME STEP = ',1PE10.3,' SEC',
      &T56,'*')

      WRITE(*,904)

      WRITE(*,926) DE
926   FORMAT(7X,'*',2X,'ENERGY    CORRECTION = ',F7.3,T56,
      &'*')

      WRITE(*,904)

      WRITE(*,902)

      WRITE(*,932) RSPHER
932   FORMAT(////10X,'RADIUS OF SPHERE = ',F6.2)

      WRITE(*,934) GTHE
934   FORMAT(/10X,'ROTATIONAL POTENTIAL PARAMETER = ',
      *F7.3/)

```

C

C

C -----

C

```

      OPEN(30,FILE='LASTDAT',ACCESS='SEQUENTIAL',FORM=
      &'UNFORMATTED')

```

```

      IF(IFLAG.EQ.1) GOTO 199

```

C

C === LOAD INITIAL POSITIONS OF ATOMS

CALL INTPOS(RSPHER)

CALL POSPRI(KB,NM,NAM)

C

C === PRINT RUN-TABLE HEADING

WRITE(*,930)

930 FORMAT(1H1////4X,'KB',5X,'RSPH',4X,'ENRG',5X,'E1',
& 4X,'DIST',6X,'TEMP',3X,'TRFRC',3X,'NAB',3X,
&'TOT ENR',3X,'FTOTWL',3X,'PRESSURE'/)

C

C === LOAD INITIAL VELOCITIES OF ATOMS

CALL INTVEL(AHEAT,PART)

C

C === ASSIGN INITIAL ACCELERATIONS BASED ON INITIAL

C POSITIONS

CALL EVAL(RWALL)

C

C === SCALE ACCELERATIONS AND STORE STARTING POSITIONS

DO 530 I=1,NP

X2(I)=FX(I)*DELTSQ/MASS(I)

Y2(I)=FY(I)*DELTSQ/MASS(I)

Z2(I)=FZ(I)*DELTSQ/MASS(I)

530 CONTINUE

GOTO 188

C

```

C ----- READ POSITIONS AND DERIVATIVES INSTEAD OF USING
C ----- FCC, INVEL, ACCELERATION -----
C
199      WRITE(*,930)
        READ(30) KB,IFLG,NM,NAM,RSPHER,XSUM,SUME
        RWALL=RSPHER+1.0
        DO 200 K=1,NP
            READ(30) X0(K),Y0(K),Z0(K)
            READ(30) X1(K),Y1(K),Z1(K)
            READ(30) X2(K),Y2(K),Z2(K)
            READ(30) X3(K),Y3(K),Z3(K)
            READ(30) X4(K),Y4(K),Z4(K)
            READ(30) X5(K),Y5(K),Z5(K)
            READ(30) DAX(K),DAY(K),DAZ(K)
200      CONTINUE
188      DO 377 I=1,NP
            X0L(I)=X0(I)
            Y0L(I)=Y0(I)
            Z0L(I)=Z0(I)
377      CONTINUE
C
C -----
C
C === ENTER MAIN LOOP OF SIMULATION
        IF(IFLAG.NE.1) GOTO 777

```

```

      CALL PREDCT(NP)
      CALL EVAL(RWALL)
      CALL CORR(DELTSQ)
      IF(ISCALE.EQ.1) RSPHER=RSPHER+DELRS
      RWALL=RSPHER+1.0
777      NS=KB+1
      DO 599 NTIMES=NS,MAXKB
          KB=KB+1
          CALL PREDCT(NP)
          CALL EVAL(RWALL)
          CALL CORR(DELTSQ)
C
C === CALCULATE MEAN SQUARE DISPLACEMENT & KINETIC ENERGY
      SUMVEL=0.
      TDIST=0.
      DO 540 I=1,NP
          TDIST=TDIST+DAX(I)**2+DAY(I)**2+DAZ(I)**2
          SUMVEL=SUMVEL+(X1(I)**2+Y1(I)**2+Z1(I)**2)
          &*MASS(I)
540      CONTINUE
      TDIST=TDIST/PART
      EK=SUMVEL/(2.*PART*DELSQ)
C
C === ACCUMMULATE SUMS FOR PROPERTY AVERAGES
      XSUM=XSUM+SUMVEL

```

SUME=SUME+TOTE

C

C === PROPERTY CALCULATION & PRINT-OUT AT INTERVALS

IF(MOD(KB,KWRITE).NE.0) GOTO 550

FKB=FLOAT(KB)*PART

TMP=XSUM/(3.*DELSQ*FKB)

ENR=(SUME/FKB+CORE)

E1=TOTE/PART+CORE

ETOT=E1+EK

RLTIM=DELTA*FLOAT(KB)*TSTEP

WRITE(*,940) KB,RSPHER,ENR,E1,TDIST,TMP,TRFRAC,
& NABTOT,ETOT,FTOTWL,EXTPRS

C

IF(MOD(KB,1000).NE.0) GOTO 550

CALL POSPRI(KB,NM,NAM)

WRITE(*,930)

940 FORMAT(1H ,I6,4F8.3,F10.3,1X,F6.3,I6,2X,F8.4,
 & 2(3X,F9.3))

C

C === DURING FIRST OF RUN, SCALE VELOCITIES FOR TEMPERATURE

550 IF(IFLG.LT.1) CALL EQBRAT(SUMVEL,AHEAT,TDIST,XDIST
 &,NP,IFLG,KB,NAM)

C

C ---- WRITE DATA ONTO TAPE FOR LATER USE ----

IF(KB.EQ.0) GOTO 777


```

      IF(IFLG.EQ.0) GOTO 588
      IF(MOD(KB,10).NE.0) GOTO 588
      WRITE(20) KB,TMP,ETOT,E1,EK,TOTE,EINTR,TOTLJ,ETOR,
&EBON,EBEN
      WRITE(20) X0,Y0,Z0
      WRITE(20) X1,Y1,Z1
      WRITE(20) X2,Y2,Z2
C      WRITE(20) X3,Y3,Z3
C      WRITE(20) X4,Y4,Z4
C      WRITE(20) X5,Y5,Z5
588      IF(MOD(NTIMES,100).NE.0) GOTO 599
      REWIND 30
      WRITE(30) KB,IFLG,NM,NAM,RSPHER,XSUM,SUME
      DO 598 K=1,NP
          WRITE(30) X0(K),Y0(K),Z0(K)
          WRITE(30) X1(K),Y1(K),Z1(K)
          WRITE(30) X2(K),Y2(K),Z2(K)
          WRITE(30) X3(K),Y3(K),Z3(K)
          WRITE(30) X4(K),Y4(K),Z4(K)
          WRITE(30) X5(K),Y5(K),Z5(K)
          WRITE(30) DAX(K),DAY(K),DAZ(K)
598      CONTINUE
599      CONTINUE
C      CLOSE(20)
      CLOSE(30)

```

STOP

END

SUBROUTINE POSPRI (KB,NM,NAM)

COMMON/POS/X0(216),Y0(216),Z0(216)

C

II=0

WRITE(*,942) KB

942 FORMAT(1H1///7X,'POSITIONS OF GROUPS AT TIME-STEP:
&',I6//)

DO 404 JJ=1,NM

WRITE(*,935)

935 FORMAT(/2X,'MOLECULE',7X,'X',11X,'Y',12X,'Z',
&12X,'R',
& 9X,'BOND LEN'//)

DO 404 KK=1,NAM

II=II+1

RR=SQRT(X0(II)**2+Y0(II)**2+Z0(II)**2)

XXX=X0(II)-X0(II-1)

YYY=Y0(II)-Y0(II-1)

ZZZ=Z0(II)-Z0(II-1)

BB=SQRT(XXX*XXX+YYY*YYY+ZZZ*ZZZ)

IF(KK.EQ.1) WRITE(*,909) JJ,X0(II),Y0(II),
&Z0(II),RR

IF(KK.GT.1) WRITE(*,911) X0(II),Y0(II),Z0(II),
&RR,BB

```
404      CONTINUE
909      FORMAT(5X,I2,4(5X,F8.4))
911      FORMAT(7X,5(5X,F8.4))
      RETURN
      END
```

SUBROUTINE INTPOS(RSPHER)

```
C
C  SET-UP INITIAL POSITIONS OF PARTICLES. HEAD GROUPS ARE
C  ASSIGNED TO FIXED POSITIONS ON THE SURFACE OF A SPHERE
C  OF RADIUS "RSPHER".
```

C

```
      COMMON/POS/X0(216),Y0(216),Z0(216)
      COMMON/NUM/NM,NAM,NP,NP1,NP2,NP22,KSORT,KB,NABTOT
      COMMON/CONT/GAB,CT0,GTHA,GTHE,B0,B2I,A1,A0,EPS
      DIMENSION THETA(50),PHI(50)
```

C

```
      PI=3.1415926535
      PI180=PI/180.
```

C

```
C  TWENTY-FOUR MOLECULES
```

```
      THETA(1)=0.
```

```
      PHI(1)=0.
```

```
      THETA(24)=PI
```

```

    PHI(24)=0.
    PH24=0.
    DO 70 I=2,5
        PHI(I)=PH24
        PH24=PH24+PI/2.
70  THETA(I)=36.*PI/180
    DELPHI=2.*PI/7
    PH24=DELPHI/2.
    DO 71 I=6,12
        PHI(I)=PH24
        PH24=PH24+DELPHI
71  THETA(I)=72.*PI/180
    PH24=0.
    DO 72 I=13,19
        PHI(I)=PH24
        PH24=PH24+DELPHI
72  THETA(I)=108.*PI/180
    PH24=PI/4.
    DO 73 I=20,23
        PHI(I)=PH24
        PH24=PH24+PI/2.
73  THETA(I)=144.*PI/180

```

C

```

    60  WRITE(*,909)
909    FORMAT(1H1////7X,'INITIAL POSITIONS OF HEAD GROUPS'

```

```

&    //7X, 'MOLECULE', 5X, 'THETA', 8X, 'PHI' /)

DO 101 I=1, NM

    TTT=THETA(I)/PI180

    PPP=PHI(I)/PI180

    WRITE(*, 900) I, TTT, PPP

900    FORMAT(10X, I3, 2(6X, F7.3))

101    CONTINUE

C

C

C    STANDARD DISTANCES ALONG TRANS CHAIN

    XLEN=0.5*B0*SQRT(2.*(1.-CT0))

    ZLEN=SQRT(B0*B0-XLEN*XLEN)

    ZLENSQ=ZLEN*ZLEN

C

C ===  ADD ATOMS TO FORM MOL IN TRANS POS  =====

DO 120 I=1, NM

    IADD=(I-1)*NAM

    THR=THETA(I)

    PHIR=PHI(I)

    SR=SIN(THR)

    CR=COS(THR)

    SPR=SIN(PHIR)

    CPR=COS(PHIR)

C

C    ODD NUMBERED GROUPS ON A MOLECULE

```

```
DO 92 J=1,NAM,2
```

```
K=IADD+J
```

```
RK=RSPHER-FLOAT(J-1)*XLEN
```

```
X0(K)=RK*SR*CPR
```

```
Y0(K)=RK*SR*SPR
```

```
Z0(K)=RK*CR
```

```
92      CONTINUE
```

```
C
```

```
C  EVEN NUMBERED GROUPS ON A MOLECULE
```

```
DO 95 J=2,NAM,2
```

```
K=IADD+J
```

```
RDIS=RSPHER-FLOAT(J-1)*XLEN
```

```
RK=SQRT(RDIS*RDIS+ZLENSQ)
```

```
BETA=ASIN(ZLEN/RK)
```

```
THE=THR-BETA
```

```
ST=SIN(THE)
```

```
X0(K)=RK*ST*CPR
```

```
Y0(K)=RK*ST*SPR
```

```
Z0(K)=RK*COS(THE)
```

```
95      CONTINUE
```

```
120     CONTINUE
```

```
RETURN
```

```
END
```

```
SUBROUTINE INTVEL(AHEAT,PART)
```

```
C
```

C === ASSIGN INITIAL VELOCITIES TO ATOMS

C

COMMON/NUM/NM,NAM,NP,NP1,NP2,NP22,KSORT,KB,NABTOT

COMMON/VEL/X1(216),Y1(216),Z1(216)

COMMON/MASS/MASS(216)

SUMX=0.

SUMY=0.

SUMZ=0.

DO 200 I=1,NM

XX=RANF(DUM)

YY=RANF(DUM)

ZZ=RANF(DUM)

NX=(I-1)*NAM

DO 200 J=1,NAM

X1(J+NX)=XX

Y1(J+NX)=YY

Z1(J+NX)=ZZ

SUMX=SUMX+X1(J+NX)*MASS(J+NX)

SUMY=SUMY+Y1(J+NX)*MASS(J+NX)

SUMZ=SUMZ+Z1(J+NX)*MASS(J+NX)

200 CONTINUE

C

C === SCALE VELOCITIES SO THAT TOTAL MOMENTUM=ZERO

X=0.

DO 210 I=1,NP

```
X1(I)=X1(I)-SUMX/PART/MASS(I)
```

```
Y1(I)=Y1(I)-SUMY/PART/MASS(I)
```

```
Z1(I)=Z1(I)-SUMZ/PART/MASS(I)
```

```
X=X+(X1(I)**2+Y1(I)**2+Z1(I)**2)*MASS(I)
```

```
210  CONTINUE
```

```
C
```

```
C === SCALE VELOCITIES TO DESIRED TEMPERATURE
```

```
HEAT=SQRT(AHEAT/X)
```

```
DO 220 I=1,NP
```

```
  X1(I)=X1(I)*HEAT
```

```
  Y1(I)=Y1(I)*HEAT
```

```
  Z1(I)=Z1(I)*HEAT
```

```
220  CONTINUE
```

```
RETURN
```

```
END
```

```
SUBROUTINE PREDCT(NP)
```

```
C
```

```
C === USE TAYLOR SERIES TO PREDICT POSITIONS & THEIR
```

```
C   DERIVATIVES AT NEXT TIME-STEP
```

```
C
```

```
COMMON/POS/X0(216),Y0(216),Z0(216)
```

```
COMMON/VEL/X1(216),Y1(216),Z1(216)
```

```
COMMON/DER/X2(216),Y2(216),Z2(216),X3(216),Y3(216),
```



```
& Z3(216),X4(216),Y4(216),Z4(216),X5(216),Y5(216),
&Z5(216)
```

```
COMMON/FOR/FX(216),FY(216),FZ(216)
```

```
DO 300 I=1,NP
```

```
  X0(I)=X0(I)+X1(I)+X2(I)+X3(I)+X4(I)+X5(I)
```

```
  Y0(I)=Y0(I)+Y1(I)+Y2(I)+Y3(I)+Y4(I)+Y5(I)
```

```
  Z0(I)=Z0(I)+Z1(I)+Z2(I)+Z3(I)+Z4(I)+Z5(I)
```

```
  X1(I)=X1(I)+2.*X2(I)+3.*X3(I)+4.*X4(I)+5.*X5(I)
```

```
  Y1(I)=Y1(I)+2.*Y2(I)+3.*Y3(I)+4.*Y4(I)+5.*Y5(I)
```

```
  Z1(I)=Z1(I)+2.*Z2(I)+3.*Z3(I)+4.*Z4(I)+5.*Z5(I)
```

```
  X2(I)=X2(I)+3.*X3(I)+6.*X4(I)+10.*X5(I)
```

```
  Y2(I)=Y2(I)+3.*Y3(I)+6.*Y4(I)+10.*Y5(I)
```

```
  Z2(I)=Z2(I)+3.*Z3(I)+6.*Z4(I)+10.*Z5(I)
```

```
  X3(I)=X3(I)+4.*X4(I)+10.*X5(I)
```

```
  Y3(I)=Y3(I)+4.*Y4(I)+10.*Y5(I)
```

```
  Z3(I)=Z3(I)+4.*Z4(I)+10.*Z5(I)
```

```
  X4(I)=X4(I)+5.*X5(I)
```

```
  Y4(I)=Y4(I)+5.*Y5(I)
```

```
  Z4(I)=Z4(I)+5.*Z5(I)
```

```
  FX(I)=0.
```

```
  FY(I)=0.
```

```
  FZ(I)=0.
```

```
300  CONTINUE
```

```
  RETURN
```

```
  END
```

SUBROUTINE CORR(DELTSQ)

C

C === CORRECT PREDICTED POSITIONS AND THEIR DERIVATIVES

C

COMMON/POS/X0(216),Y0(216),Z0(216)

COMMON/VEL/X1(216),Y1(216),Z1(216)

COMMON/DER/X2(216),Y2(216),Z2(216),X3(216),Y3(216),
 & Z3(216),X4(216),Y4(216),Z4(216),X5(216),Y5(216),
 & Z5(216)

COMMON/FOR/FX(216),FY(216),FZ(216)

COMMON/DISP/DAX(216),DAY(216),DAZ(216),X0L(216),
 & Y0L(216),Z0L(216)

COMMON/PARM/F02,F12,F32,F42,F52

COMMON/NUM/NM,NAM,NP,NP1,NP2,NP22,KSORT,KB,NABTOT

COMMON/PROP/SUME,XSUM

COMMON/SCAL/RSPHER,RWALL,DELRS,ISCALE

COMMON/MASS/MASS(216)

C

IF(MOD(KB,10).NE.0.OR.ISCALE.NE.1) GOTO 610

C

IF(RSPHER.LE.2.800) GO TO 610

RSPHER=RSPHER-DELRS

RWALL =RWALL -DELRS

C

```
610   DO 690 I=1,NP
      XERR=X2(I)-DELTSQ*FX(I)/MASS(I)
      YERR=Y2(I)-DELTSQ*FY(I)/MASS(I)
      ZERR=Z2(I)-DELTSQ*FZ(I)/MASS(I)
      X0(I)=X0(I)-XERR*F02
      X1(I)=X1(I)-XERR*F12
      X2(I)=X2(I)-XERR
      X3(I)=X3(I)-XERR*F32
      X4(I)=X4(I)-XERR*F42
      X5(I)=X5(I)-XERR*F52
      Y0(I)=Y0(I)-YERR*F02
      Y1(I)=Y1(I)-YERR*F12
      Y2(I)=Y2(I)-YERR
      Y3(I)=Y3(I)-YERR*F32
      Y4(I)=Y4(I)-YERR*F42
      Y5(I)=Y5(I)-YERR*F52
      Z0(I)=Z0(I)-ZERR*F02
      Z1(I)=Z1(I)-ZERR*F12
      Z2(I)=Z2(I)-ZERR
      Z3(I)=Z3(I)-ZERR*F32
      Z4(I)=Z4(I)-ZERR*F42
      Z5(I)=Z5(I)-ZERR*F52
690   CONTINUE
      IF(MOD(KB,KSORT).NE.0.OR.ISCALE.NE.1) GOTO 680
      DO 691 I=1,NP
```

```
RSQ=X0(I)*X0(I)+Y0(I)*Y0(I)+Z0(I)*Z0(I)
```

```
R=SQRT(RSQ)
```

```
RFACT = 1.0-DELR/R
```

```
X0(I) = X0(I)*RFACT
```

```
Y0(I) = Y0(I)*RFACT
```

```
Z0(I) = Z0(I)*RFACT
```

```
691  CONTINUE
```

```
C
```

```
C === DISPLACEMENTS
```

```
680  DO 692 I=1,NP
```

```
      DAX(I)=DAX(I)-X0(I)+X0L(I)
```

```
      DAY(I)=DAY(I)-Y0(I)+Y0L(I)
```

```
      DAZ(I)=DAZ(I)-Z0(I)+Z0L(I)
```

```
C
```

```
C === STORE NEW POSITIONS
```

```
      X0L(I)=X0(I)
```

```
      Y0L(I)=Y0(I)
```

```
      Z0L(I)=Z0(I)
```

```
692  CONTINUE
```

```
      RETURN
```

```
      END
```

```

SUBROUTINE EQBRAT(SUMVEL,AHEAT,TDIST,XDIST,NP,
&  IFLG,KB,NAM)
```

C

C === SCALE VELOCITIES DURING INITIAL TIME-STEPS

C

COMMON/VEL/X1(216),Y1(216),Z1(216)

COMMON/PROP/SUME,XSUM

COMMON/SCAL/RSPHER,RWALL,DELRS,ISCALE

C

IF(IFLG.EQ.-1) GOTO 720

IF(TDIST.GT.XDIST.OR.IFLG.EQ.-2) GOTO 750

720 HEAT=SQRT(AHEAT/SUMVEL)

DO 730 I=1,NP

X1(I)=X1(I)*HEAT

Y1(I)=Y1(I)*HEAT

Z1(I)=Z1(I)*HEAT

730 CONTINUE

RETURN

C

C === AT END OF EQUILIBRATION STAGE, SET PROPERTY SUMS

C TO ZERO

750 IFLG= 1

KB=0

SUME=0.

XSUM=0.

RETURN

END

```
SUBROUTINE EVAL(RWALL)
```

```
C
```

```
COMMON/POS/X0(216),Y0(216),Z0(216)
```

```
COMMON/FOR/FX(216),FY(216),FZ(216)
```

```
COMMON/NABLST/LIST(12000),NABORS(216)
```

```
COMMON/CONT/GAB,CT0,GTHA,GTHE,B0,B2I,A1,A0,EPS
```

```
COMMON/PROP/SUME,XSUM
```

```
COMMON/PROPA/RC,RLIST,FSHFT,ESHFT,ESHFTA,CUBE,CUBE2,
& RDMAX,RCHH,HSHT,HSHTA,HFSHT,REQUIL,FORCON
COMMON/ENERGY/TOTE,TOTLJ,ETOR,EBON,EBEN,EINTR,TRFRAC,
& EXTPRS,FTOTWL
```

```
COMMON/NUM/NM,NAM,NP,NP1,NP2,NP22,KSORT,KB,NABTOT
```

```
DIMENSION B(216),BX(216),BY(216),BZ(216)
```

```
C
```

```
C INITIALIZE ACCUMULATORS
```

```
NABTOT=0
```

```
ICOUNT=0
```

```
K=0
```

```
ITRAN =0
```

```
TOTE=0.0
```

```
TOTLJ=0.0
```

```
FTOTWL=0.0
```

```
ETOR=0.0
```

```
EBON=0.0
EBEN=0.0
EINTR=0.0
DO 150 I=1,NP
    FX(I)=0.0
    FY(I)=0.0
    FZ(I)=0.0
150  CONTINUE
C
C  CALCULATE LJ FORCES
    LCHK=2
    IF(MOD(KB,KSORT).EQ.0) LCHK=1
C
C  OUTER LOOP OVER PARTICLES
    DO 300 I=1,NP1
        ICHK=I-1+NAM
        XI=X0(I)
        YI=Y0(I)
        ZI=Z0(I)
        IF(I.GE.NP2) GOTO 788
        IF(LCHK.EQ.1) GOTO 410
        JBEGIN=NABORS(I)
        JEND=NABORS(I+1)-1
        GOTO 415
410    NABORS(I) =K+1
```

```
        JBEGIN=I+1
        JEND=NP
415      CONTINUE
C
C  DECIDE WHICH MOLECULE ATOM I IS ON
        IM=(I-1)/NAM+1.0001
C
C  INNER LOOP
        DO 290 JX=JBEGIN,JEND
        J=JX
        IF(LCHK.EQ.2) J=LIST(JX)
C
C  IF I & J ARE HEAD GROUPS, CALCULATE HEAD-HEAD REPULSIONS
        JCHK=J+NAM-1
        IF(MOD(ICHK,NAM).NE.0.OR.MOD(JCHK,NAM).NE.0)GOTO 614
        X=XI-X0(J)
        Y=YI-Y0(J)
        Z=ZI-Z0(J)
        RSQ=X*X+Y*Y+Z*Z
        RIJ=SQRT(RSQ)
        RI=1.0/RIJ
        R3=RI*RI*RI
        R4=R3*RI
        R8=R4*R4
C
```


ELJ=R3*(R8*RI+1.0)+(RIJ*HSHFTA)-HSHFT

FLJS=3.0*R4*(4.0*R8*RI+1.0)-HFSHFT

FXD=FLJS*X*RI

FYD=FLJS*Y*RI

FZD=FLJS*Z*RI

FX(I)=FX(I)+FXD

FX(J)=FX(J)-FXD

FY(I)=FY(I)+FYD

FY(J)=FY(J)-FYD

FZ(I)=FZ(I)+FZD

FZ(J)=FZ(J)-FZD

GO TO 290

C

C DECIDE WHICH MOLECULE ATOM J IS ON

614 JM=(J-1)/NAM+1.0001

C

C CHECK WHETHER I AND J ARE ON SAME MOL

IF(IM.NE.JM) GOTO 289

C

C CHECK IF I AND J ARE FOURTH NEIGHBORS OR GREATER

KIJ=J-I

IF(KIJ.LE.3) GOTO 290

C

289 X=XI-X0(J)

Y=YI-Y0(J)

Z=ZI-Z0(J)

C

RSQ=X*X+Y*Y+Z*Z

RIJ=SQRT(RSQ)

IF(LCHK.NE.1) GOTO 419

IF(IM.EQ.JM) GOTO 701

IF(RSQ.GT.RDMAX) GOTO 290

IF(RSQ.GT.RLIST) GOTO 290

701 K=K+1

LIST(K)=J

419 IF(RIJ.GT.RC) GOTO 290

RI=1./RIJ

R3=RI**3

R6=R3*R3

ELJ=2.0*R6*(R3-1.50)+ESHFT+RIJ*ESHFTA

TOTLJ=TOTLJ+ELJ

FLJS=18.*RI*R6*(R3-1.0)-FSHFT

FXD=FLJS*X*RI

FYD=FLJS*Y*RI

FZD=FLJS*Z*RI

FX(I)=FX(I)+FXD

FX(J)=FX(J)-FXD

FY(I)=FY(I)+FYD

FY(J)=FY(J)-FYD

FZ(I)=FZ(I)+FZD

```
      FZ(J)=FZ(J)-FZD
290  CONTINUE
C
C  CALCULATE BOND LENGTHS
C  CHECK IF LAST ATOM ON MOLECULE
788  IF(MOD(I,NAM).EQ.0) GOTO 300
      BX(I)=XI-X0(I+1)
      BY(I)=YI-Y0(I+1)
      BZ(I)=ZI-Z0(I+1)
      BSQ=BX(I)**2+BY(I)**2+BZ(I)**2
      B(I)=SQRT(BSQ)
300  CONTINUE
C
      IF(LCHK.NE.1) GOTO 499
      NABORS(NP2)=K+1
      NABTOT=K
C
C  LOOP CALCULATES INTRAMOLECULAR FORCES
499  DO 600 I=1,NP1
C
C  CHECK IF LAST ATOM ON MOLECULE
      IF(MOD(I,NAM).EQ.0) GOTO 600
C
C  CALCULATE BOND FORCES
      BDIFF=B(I)-B0
```

```
EBON=EBON+0.5*GAB*BDIFF*BDIFF
```

```
FBON=GAB*BDIFF
```

```
BI=1./B(I)
```

```
BXI=BX(I)*BI
```

```
BYI=BY(I)*BI
```

```
BZI=BZ(I)*BI
```

```
FXB=FBON*BXI
```

```
FYB=FBON*BYI
```

```
FZB=FBON*BZI
```

```
FX(I) =FX(I)-FXB
```

```
FX(I+1)=FX(I+1)+FXB
```

```
FY(I) =FY(I)-FYB
```

```
FY(I+1)=FY(I+1)+FYB
```

```
FZ(I) =FZ(I)-FZB
```

```
FZ(I+1)=FZ(I+1)+FZB
```

```
C
```

```
C  CALCULATION BENDING FORCE
```

```
C  CHECK IF NEXT-TO-LAST ATOM ON MOLECULE
```

```
IF(MOD(I+1,NAM).EQ.0) GOTO 600
```

```
BII=1./B(I+1)
```

```
BXJ=BX(I+1)*BII
```

```
BYJ=BY(I+1)*BII
```

```
BZJ=BZ(I+1)*BII
```

```
CTI=-(BXJ*BXI+BYJ*BYI+BZJ*BZI)
```

```
CDIFF=CT0-CTI
```

```
EBEN=EBEN+0.5*GTHA*CDIFF*CDIFF
```

```
FT=GTHA*CDIFF
```

```
FT1=FT*BI
```

```
FT2=FT*BII
```

```
FX1=FT1*(BXJ+CTI*BXI)
```

```
FY1=FT1*(BYJ+CTI*BYI)
```

```
FZ1=FT1*(BZJ+CTI*BZI)
```

```
FX2=FT2*(BXI+CTI*BXJ)
```

```
FY2=FT2*(BYI+CTI*BYJ)
```

```
FZ2=FT2*(BZI+CTI*BZJ)
```

```
FX(I)  =FX(I)  -FX1
```

```
FX(I+1)=FX(I+1)+FX1-FX2
```

```
FX(I+2)=FX(I+2)+FX2
```

```
FY(I)  =FY(I)  -FY1
```

```
FY(I+1)=FY(I+1)+FY1-FY2
```

```
FY(I+2)=FY(I+2)+FY2
```

```
FZ(I)  =FZ(I)  -FZ1
```

```
FZ(I+1)=FZ(I+1)+FZ1-FZ2
```

```
FZ(I+2)=FZ(I+2)+FZ2
```

```
C
```

```
C  CALCULATION OF TORSION FORCES
```

```
C  CHECK WHETHER FIRST ATOM OF MOLECULE
```

```
IF(MOD(I+NAM-1,NAM).EQ.0) GOTO 600
```

```
CALL RYFOR(BX(I-1),BY(I-1),BZ(I-1),BX(I),BY(I),BZ(I),
```

```
&      BX(I+1),BY(I+1),BZ(I+1),FX1,FY1,FZ1,FX2,FY2,FZ2,
```

```
&      FX3,FY3,FZ3,FX4,FY4,FZ4,ETQ,CODI,GTHE)
```

```
C
```

```
ICOUNT=ICOUNT+1
```

```
IF(CODI.LT.-0.50) ITRAN=ITRAN+1
```

```
FX(I-1)=FX(I-1)+FX1
```

```
FY(I-1)=FY(I-1)+FY1
```

```
FZ(I-1)=FZ(I-1)+FZ1
```

```
FX(I)   =FX(I)   +FX2
```

```
FY(I)   =FY(I)   +FY2
```

```
FZ(I)   =FZ(I)   +FZ2
```

```
FX(I+1)=FX(I+1)+FX3
```

```
FY(I+1)=FY(I+1)+FY3
```

```
FZ(I+1)=FZ(I+1)+FZ3
```

```
FX(I+2)=FX(I+2)+FX4
```

```
FY(I+2)=FY(I+2)+FY4
```

```
FZ(I+2)=FZ(I+2)+FZ4
```

```
ETOR=ETOR+ETQ
```

```
600    CONTINUE
```

```
C
```

```
C  CALCULATE GROUP-SHELL INTERACTION
```

```
EWALL=0.0
```

```
RCHKSQ=(RWALL-2.0)**2
```

```
DO 650 I=1,NP
```

```
    ICHK=I-1+NAM
```

```
C
```

```

      XI=X0(I)
      YI=Y0(I)
      ZI=Z0(I)

C
C  DISTANCE FROM CENTER TO GROUP
      RSQ=XI*XI+YI*YI+ZI*ZI

C  IF HEAD GROUP, CALCULATE INTERACTIONS WITH WALL USING A
C  POTENTIAL OF THE FORM -- GAMMA*(R-R0)**2
      IF(MOD(ICK,NAM).NE.0) GO TO 384
      RR=SQRT(RSQ)
      RI=1.0/RR
      RD=RWall-RR

C
      EWall=EWall+FORCON*(RD-REQUIL)*(RD-REQUIL)
      FWall=-2.0*FORCON*(RD-REQUIL)
      FTOTWL=FTOTWL+FWall

C
      FX(I)=FX(I)-FWall*XI*RI
      FY(I)=FY(I)-FWall*YI*RI
      FZ(I)=FZ(I)-FWall*ZI*RI
      GO TO 650

C  IF NOT A HEAD GROUP, CALCULATE REPULSIVE INTERACTION WITH
C  THE WALL
384      IF(RSQ.LT.RCHKSQ) GOTO 650

C

```

C DISTANCE FROM GROUP TO SHELL

RR=SQRT(RSQ)

RI=1.0/RR

RD=RWALL-RR

RDR=1.0/RD

R3 =RDR*RDR*RDR

R6 =R3*R3

R12=R6*R6

C

C FORCE AND ENERGY FOR R-12 WALL

EWALL=EWALL+R12

FWALL=12.0*R12*RDR

FTOTWL=FTOTWL+FWALL

FX(I)=FX(I)-FWALL*XI*RI

FY(I)=FY(I)-FWALL*YI*RI

FZ(I)=FZ(I)-FWALL*ZI*RI

650 CONTINUE

C

C CALCULATE WALL PRESSURE IN ATMOSPHERES

EXTPRS=0.0085382*FTOTWL/RWALL**2

C

C CALCULATE INTRAMOLECULAR AND TOTAL ENERGY

EINTR=ETOR + EBON + EBEN

TOTE = TOTLJ + EINTR + EWALL

TRFRAC=FLOAT(ITRAN)/FLOAT(ICOUNT)

RETURN

END

```

      SUBROUTINE RYFOR(BONX1,BONY1,BONZ1,BONX2,BONY2,BONZ2,
&   BONX3,BONY3,BONZ3,FORX1,FORY1,FORZ1,FORX2,FORY2,
&   FORZ2,FORX3,FORY3,FORZ3,FORX4,FORY4,FORZ4,ETOR,
&   CODI,GR)

```

C

```

      DATA A1,A2,A3,A4,A5/-1.462,-1.578,0.368,
&          3.156,3.788/

```

C

C CALCULATE NORMAL TO PLANE OF BONDS 1 AND 2

E=BONY1*BONZ2-BONZ1*BONY2

D=BONZ1*BONX2-BONX1*BONZ2

C=BONX1*BONY2-BONY1*BONX2

ANORM2=C*C+D*D+E*E

ANORM =SQRT(ANORM2)

ANORMR=1./ANORM

AX=E*ANORMR

AY=D*ANORMR

AZ=C*ANORMR

C

C CALCULATE NORMAL TO PLANE OF BONDS 2 AND 3

H=BONY2*BONZ3-BONZ2*BONY3

G=BONZ2*BONX3-BONX2*BONZ3

F=BONX2*BONY3-BONY2*BONX3

BNORM2=F*F+G*G+H*H

BNORM =SQRT(BNORM2)

BNORMR=1./BNORM

BX=H*BNORMR

BY=G*BNORMR

BZ=F*BNORMR

C

C DETERMINE COSINE OF THE DIHEDRAL ANGLE, PHI

CODI= AX*BX+AY*BY+AZ*BZ

C

C DETERMINE TORSIONAL ENERGY

CODISQ=CODI*CODI

CODI3 =CODI*CODISQ

ETOR = GR*(1.116+A1*CODI+A2*CODISQ+A3*CODI3

& +A4*CODISQ*CODISQ+A5*CODISQ*CODI3)

C

C CALCULATE DU/COS(PHI)

DUDCO=(A1+2.*A2*CODI+3.*A3*CODISQ+4.*A4*CODISQ*CODI

& +5.*A5*CODISQ*CODISQ)*GR

C

C START EVALUATION OF FORCE ON GROUP 1

C CALCULATE DANORM/DR1

FACT1=(C*BONY2-D*BONZ2)/ANORM2

DADX1X= -FACT1*AX

DADX1Y= -FACT1*AY-BONZ2*ANORMR

DADX1Z= -FACT1*AZ+BONY2*ANORMR

C

FACT2 =(E*BONZ2-C*BONX2)/ANORM2

DADY1X= -FACT2*AX+BONZ2*ANORMR

DADY1Y= -FACT2*AY

DADY1Z= -FACT2*AZ-BONX2*ANORMR

C

FACT3 =(D*BONX2-E*BONY2)/ANORM2

DADZ1X= -FACT3*AX-BONY2*ANORMR

DADZ1Y= -FACT3*AY+BONX2*ANORMR

DADZ1Z= -FACT3*AZ

C

C CALCULATE D(AB)/DR1

DABDX1=BX*DADX1X+BY*DADX1Y+BZ*DADX1Z

DABDY1=BX*DADY1X+BY*DADY1Y+BZ*DADY1Z

DABDZ1=BX*DADZ1X+BY*DADZ1Y+BZ*DADZ1Z

C

C CALCULATE FORCE ON GROUP 1

FORX1= -DUDCO*DABDX1

FORY1= -DUDCO*DABDY1

FORZ1= -DUDCO*DABDZ1

C

C START EVALUATION OF FORCE ON GROUP 2

C CALCULATE DANORM/DR2

$$\text{FACT4} = (\text{D} * \text{BONZ1} - \text{C} * \text{BONY1}) / \text{ANORM2}$$

$$\text{DADX2X} = -\text{FACT4} * \text{AX} - \text{DADX1X}$$

$$\text{DADX2Y} = -\text{FACT4} * \text{AY} + \text{BONZ1} * \text{ANORMR} - \text{DADX1Y}$$

$$\text{DADX2Z} = -\text{FACT4} * \text{AZ} - \text{BONY1} * \text{ANORMR} - \text{DADX1Z}$$

C

$$\text{FACT5} = (\text{C} * \text{BONX1} - \text{E} * \text{BONZ1}) / \text{ANORM2}$$

$$\text{DADY2X} = -\text{FACT5} * \text{AX} - \text{BONZ1} * \text{ANORMR} - \text{DADY1X}$$

$$\text{DADY2Y} = -\text{FACT5} * \text{AY} - \text{DADY1Y}$$

$$\text{DADY2Z} = -\text{FACT5} * \text{AZ} + \text{BONX1} * \text{ANORMR} - \text{DADY1Z}$$

C

$$\text{FACT6} = (\text{E} * \text{BONY1} - \text{D} * \text{BONX1}) / \text{ANORM2}$$

$$\text{DADZ2X} = -\text{FACT6} * \text{AX} + \text{BONY1} * \text{ANORMR} - \text{DADZ1X}$$

$$\text{DADZ2Y} = -\text{FACT6} * \text{AY} - \text{BONX1} * \text{ANORMR} - \text{DADZ1Y}$$

$$\text{DADZ2Z} = -\text{FACT6} * \text{AZ} - \text{DADZ1Z}$$

C

C EVALUATE D(BNORM)/DR2

$$\text{FACT7} = (\text{F} * \text{BONY3} - \text{G} * \text{BONZ3}) / \text{BNORM2}$$

$$\text{DBDX2X} = -\text{FACT7} * \text{BX}$$

$$\text{DBDX2Y} = -\text{FACT7} * \text{BY} - \text{BONZ3} * \text{BNORMR}$$

$$\text{DBDX2Z} = -\text{FACT7} * \text{BZ} + \text{BONY3} * \text{BNORMR}$$

C

$$\text{FACT8} = (\text{H} * \text{BONZ3} - \text{F} * \text{BONX3}) / \text{BNORM2}$$

$$\text{DBDY2X} = -\text{FACT8} * \text{BX} + \text{BONZ3} * \text{BNORMR}$$

$$\text{DBDY2Y} = -\text{FACT8} * \text{BY}$$

DBDY2Z= -FACT8*BZ-BONX3*BNORMR

C

FACT9 =(G*BONX3-H*BONY3)/BNORM2

DBDZ2X= -FACT9*BX-BONY3*BNORMR

DBDZ2Y= -FACT9*BY+BONX3*BNORMR

DBDZ2Z= -FACT9*BZ

C

C CALCULATE D COS(PHI)/DR2

DABDX2=BX*DADX2X+BY*DADX2Y+BZ*DADX2Z

& +AX*DBDX2X+AY*DBDX2Y+AZ*DBDX2Z

DABDY2=BX*DADY2X+BY*DADY2Y+BZ*DADY2Z

& +AX*DBDY2X+AY*DBDY2Y+AZ*DBDY2Z

DABDZ2=BX*DADZ2X+BY*DADZ2Y+BZ*DADZ2Z

& +AX*DBDZ2X+AY*DBDZ2Y+AZ*DBDZ2Z

C

C FORCE ON GROUP 2

FORX2 = -DUDCO*DABDX2

FORY2 = -DUDCO*DABDY2

FORZ2 = -DUDCO*DABDZ2

C

C START EVALUATION OF FORCE ON GROUP 4

C CALCULATE D(BNORM)/DR4

FACT1 =(F*BONY2-G*BONZ2)/BNORM2

DBDX4X= -FACT1*BX

DBDX4Y= -FACT1*BY-BONZ2*BNORMR

DBDX4Z= -FACT1*BZ+BONY2*BNORMR

C

FACT2 =(H*BONZ2-F*BONX2)/BNORM2

DBDY4X= -FACT2*BX+BONZ2*BNORMR

DBDY4Y= -FACT2*BY

DBDY4Z= -FACT2*BZ-BONX2*BNORMR

C

FACT3 =(G*BONX2-H*BONY2)/BNORM2

DBDZ4X= -FACT3*BX-BONY2*BNORMR

DBDZ4Y= -FACT3*BY+BONX2*BNORMR

DBDZ4Z= -FACT3*BZ

C

C EVALUATE D COS(PHI)/DR4

DABDX4=AX*DBDX4X+AY*DBDX4Y+AZ*DBDX4Z

DABDY4=AX*DBDY4X+AY*DBDY4Y+AZ*DBDY4Z

DABDZ4=AX*DBDZ4X+AY*DBDZ4Y+AZ*DBDZ4Z

C

C EVALUATE FORCE ON GROUP 4

FORX4= -DUDCO*DABDX4

FORY4= -DUDCO*DABDY4

FORZ4= -DUDCO*DABDZ4

C

C EVALUATE FORCE ON GROUP 3 BY NEWTON'S THIRD LAW

FORX3 = -FORX1-FORX2-FORX4

FORY3 = -FORY1-FORY2-FORY4

FORZ3 = -FORZ1-FORZ2-FORZ4

C

RETURN

END

BLOCK DATA

COMMON/DER/X2(216),Y2(216),Z2(216),X3(216),Y3(216),
 & Z3(216),X4(216),Y4(216),Z4(216),X5(216),Y5(216),
 & Z5(216)
 COMMON/FOR/FX(216),FY(216),FZ(216)
 COMMON/DISP/DAX(216),DAY(216),DAZ(216),X0L(216),
 & Y0L(216),Z0L(216)
 COMMON/PROP/SUME,XSUM
 COMMON/MASS/MASS(216)
 DATA X3,Y3,Z3,X4,Y4,Z4,X5,Y5,Z5/1944*0./
 DATA DAX,DAY,DAZ,FX,FY,FZ/1296*0./
 DATA MASS/216*1/
 END

APPENDIX E

ESTIMATION OF RUN 3 HEAD GROUP PARAMETERS

In Run 3 of the molecular dynamics simulations of micelles, the head group was given the mass and diameter of a sulfate ion. While it was desirable to model this ion as the polar head due to its common usage in surfactants, information on its intramolecular potentials is incomplete. Data pertaining to other molecular groups was used to estimate intramolecular potential parameters necessary to complete the model of the sulfate head group (O'Connell, 1987).

Muller and coworkers have measured the mean bond lengths, bond angles, and the vibrational and bending amplitudes for the HSO_4^- ion (Muller and Nagarajan, 1967; Muller et al., 1968). The values are assigned to the bonds and angles in Figure E-1a. Blukis et al. (1963) have measured the C-O bond length and C-C-O angle of dimethyl ether. These values are given in Figure E-1b. These are used in the estimation of bond lengths, angles and amplitudes for the C-O-S- O_3^- arrangement of the sulfate head group and the alpha carbon of the surfactant chain.

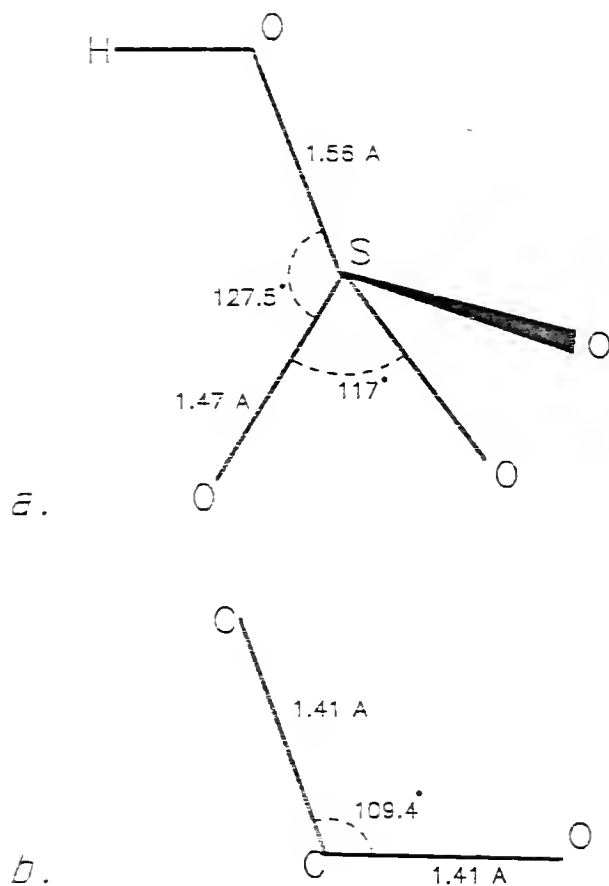


Figure E-1. a.) Schematic representation of the the HSO_4^- ion, showing mean bond lengths, bond angles, and vibrational and bending amplitudes (Muller and Nagarajan, 1967; Muller et al., 1968). b.) The C-C-O bonds of dimethyl ether, showing the mean angle and the mean length of the C-O bond (Blukis et al., 1963).

In the simulation model, the head group is represented as a homogeneous sphere connected to the surfactant chain through a single bond. The center of mass of the atoms of the sulfate group determines the length and angle of this bond. In Figure E-2, the sulfate group and alpha carbon are schematically represented. The appropriate bond lengths and angles have been used from Figure E-1. The center of mass of the sulfate group is shown in Figure E-2, and the dashed line connecting it to the alpha carbon is the bond for the model head group. Its length, 2.6 Angstrom, and angle, 146 degrees, are indicated in the figure.

The force constant for the harmonic bond vibration potential used in the simulation is determined from the mean amplitude of the vibration:

$$\gamma = 1.68 \times 10^{-4} \frac{\mu}{\alpha^4} \quad (\text{E.1})$$

where γ is the force constant in mdyne/Angstrom.

μ is the reduced mass of the two molecular groups.

α is the mean amplitude.

For the head group bond (dashed line in Figure E-2) a mean amplitude of vibration is calculated from its components to be .078 Angstrom. In equation E.1 this yields vibrational force constant for the head group bond to the alpha carbon of .37 mdyne/Angstrom.

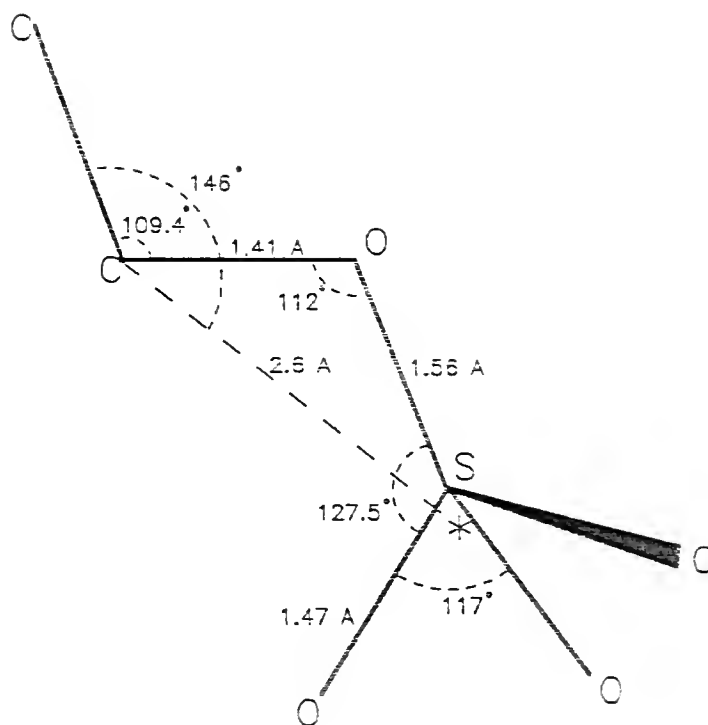


Figure E-2. The sulfate head group, shown with two segments of the surfactant chain. Its center of mass is designated by the "*" and the dashed line connecting it to the alpha carbon designates the bond length and angle of the head group of Run 3. In this simulation, the sulfate group is modeled by a single sphere, centered at the sulfate center of mass, with intramolecular potentials derived from the sulfate group.

The force constant for the bond angle bending potential is proportional to the mass of the head group. It is therefore seven times greater in Run 3 than in the other runs. Note that although Run 2 used the same head group mass, only the mass effect was investigated in that simulation; all intramolecular potentials were the same as in Run 1.

Rotational potential barriers were obtained for molecular groups of geometry similar to that of the sulfate group (Cahill et al., 1968). They are, in kcal/mole:

methyl formate	1.2
propionaldehyde	2.3
methyl vinyl ether	3.8
cis-1-butene	4.0

By comparison to these values the rotational barrier for the larger, more polar sulfate group is estimated to be 5.0 kcal/mole.

APPENDIX F
MOLECULAR DYNAMICS PROGRAM LISTING
FOR SIMULATION 3

C MOLECULAR DYNAMICS SOURCE PROGRAM FOR A SIMPLE
 C MODEL OF A MICELLE ENCLOSED IN A SHELL. A
 C FIFTH-ORDER PREDICTOR-CORRECTOR ALGORITHM IS
 C USED TO SOLVE THE EQUATIONS OF MOTION. A
 C SKELETAL MODEL DUE TO WEBER IS USED FOR EACH
 C ALKANE MOLECULE.
 C
 C HEAD GROUP MASS CAN BE SET. SHIFTED-FORCE
 C POTENTIALS AND NEIGHBOR LIST ARE USED.
 C

```

PARAMETER(MHEAD=1)

COMMON/POS/X0(216),Y0(216),Z0(216)

COMMON/VEL/X1(216),Y1(216),Z1(216)

COMMON/DER/X2(216),Y2(216),Z2(216),X3(216),Y3(216),
&  Z3(216),X4(216),Y4(216),Z4(216),X5(216),Y5(216),
&  Z5(216)

COMMON/FOR/FX(216),FY(216),FZ(216)

COMMON/DISP/DAX(216),DAY(216),DAZ(216),X0L(216),
&  Y0L(216),Z0L(216)

COMMON/NABLST/LIST(12000),NABORS(216)

COMMON/CONT/GAB,CT0,GTHA,GTHE,B0,B2I,A1,A0,EPS

COMMON/PARM/F02,F12,F32,F42,F52

COMMON/PROP/SUME,XSUM

COMMON/PROPA/RC,RLIST,FSHFT,ESHFT,ESHFTA,
&  CUBE,CUBE2,RDMAX,RCHH,HSHT,HSHTA,HFSHT,REQUIL,
  
```

```

COMMON/CONT/A1,A0,EPS

COMMON/PAARM/F02,F12,F32,F42,F52

COMMON/PROP/SUME,XSUM

COMMON/PROPA/REQUIL,FORCON,HDSIG,SIG12

COMMON/ENERGY/TOTE,TOTLJ,ETOR,EBON,EBEN,EINTR,TRFRAC,
&  EXTPRS,FTOTWL

COMMON/NUM/NM,NAM,NP,NP1,NP2,NP22,KSORT,KB

COMMON/SCAL/RSPHER,RWALL,DELRS,ISCALE

COMMON/MASS/MASS(216)

COMMON/INTRA/B0(216),GAB(216),CT0(216),GTHA(216),
&  GTHE(216)

C
C  FLAG, IF IFLAG.NE.1 USES INTPOS AND RANDOM VELOCITIES
C  IF IFLAG.EQ.1 X0,Y0,Z0,AND ALL DERIVATIVES ARE READ
C  FROM PREVIOUS RUN.
C
      IFLAG=1

C
C === SET NUMBER OF PARTICLES IN PRIMARY CELL
      NAM=9
      NM=24
      NP=NM*NAM
      PART=NP
      NP1=NP-1
      NP2=NP-2

```

NP22=.5*PART+.01

C

C === SET HEAD GROUP MASS, BOND, AND FORCE PARAMETERS

DO 20 I=1,NP,NAM

MASS(I)=MHEAD

B0(I)=BLHEAD

GAB(I)=GLHEAD

CT0(I)=BAHEAD

GTHA(I)=GAHEAD

GTHE(I)=GTHEAD

20 CONTINUE

C

C === SET RELATIVE SIGMA OF HEAD-ALKANE PAIR

HDSIG=HDSGMA

SIG12=(1.+HDSIG)/2

C

C === SET RADIUS OF SPHERE ON WHICH HEAD GROUPS ARE ATTACHED

RSPHER= 6.000

DELRS=0.0025

ISCALE=0

RWALL =RSPHER+1.0

REQUIL=1.

FORCON=30.

C

C === SET VALUES OF PHYSICAL CONSTANTS


```
XNAM=FLOAT(NAM)
WTMOL=XNAM*14.+2.
WTPART=WTMOL/XNAM
RSTAR=0.4
EPS=419.
AVO=6.0225E+23
BOLZ=1.38054D-23
EPSI=EPS/BOLZ/AVO
THIRD=1./3.
PI=3.1415926535
```

C

C === SET DESIRED FLUID STATE CONDITION

```
TR=5.913
T=TR*EPSI
VOL=1.333333*PI*RSPHER**3
DR=FLOAT(NM)/VOL
```

C

C === SET RUN FLAGS AND PARAMETERS

```
IFLG=-1
KB=0
KSAVE=10
KSORT=10
KWRITE=10
MAXKB=40000
XDIST=0.1
```

C

C === SET TIME-STEP AND ITS MULTIPLES

DELTA=0.00060

DELSQ=DELTA*DELTA

DELTSQ=.5*DELSQ

TSTEP=SQRT(WTPART*RSTAR**2/EPS/1.E21)*1.D+12

TT1=TSTEP*DELTA*1.D-12

C

C === SET PARAMETERS IN PREDICTOR-CORRECTOR METHOD

F02=3./16.

F12=251./360.

F32=11./18.

F42=1./6.

F52=1./60.

C

C === SCALE FACTOR FOR VELOCITIES DURING EQUILIBRATION

AHEAT=DELSQ*PART*3.*TR

C

C === WRITE TAPE HEADING

```
OPEN(20,FILE='C872DAT2',ACCESS='SEQUENTIAL',
& FORM='UNFORMATTED')
```

WRITE(20) NP,NAM,NM,DR,TR,EPS,RSTAR

WRITE(20) VOL,DELTA,TSTEP

C

C === INITIALIZE SUM ACCUMULATORS

XSUM=0.

SUME=0.

C

C === PRINT PARAMETERS

WRITE(*,900)

900 FORMAT(1H1///)

WRITE(*,902)

902 FORMAT(7X,49('*'))

WRITE(*,904)

904 FORMAT(7X,'*',T56,'*')

WRITE(*,906) NM

906 FORMAT(7X,'*',2X,'MOLECULAR DYNAMICS FOR',I3,

A ' N-ALKANE MOLECULES',T56,'*')

WRITE(*,904)

WRITE(*,917) NAM

917 FORMAT(7X,'*',5X,'WITH',I3,' PARTICLES PER MOLECULE'

& ,T56,'*')

WRITE(*,904)

WRITE(*,902)

WRITE(*,904)

WRITE(*,908) EPSI,RSTAR

908 FORMAT(7X,'*',2X,'EPSI/K = ',F7.3,T36,'RSTAR = ',

& F7.3,T56,'*')

WRITE(*,910) TR,T

910 FORMAT(7X,'*',2X,'TR = ',F7.3,T36,' T = ',

```

&    F7.3,T56,'*')
      WRITE(*,912) DR,VOL
912   FORMAT(7X,'*',2X,'DR      = ',F7.3,T36,'VOL    = ',
&    F8.3,T56,'*')
      WRITE(*,920) DELTA
920   FORMAT(7X,'*',2X,'DELTA  = ',F9.5,T56,'*')
      WRITE(*,904)
      WRITE(*,922) TSTEP
922   FORMAT(7X,'*',2X,'TIME UNIT = ',F6.3,'E-12 SEC',
&    T56,'*')
      WRITE(*,924) TT1
924   FORMAT(7X,'*',2X,'TIME STEP = ',1PE10.3,' SEC',
&    T56,'*')
      WRITE(*,904)
      WRITE(*,926) DE
926   FORMAT(7X,'*',2X,'ENERGY  CORRECTION = ',F7.3,
&    T56,'*')
      WRITE(*,904)
      WRITE(*,902)
      WRITE(*,932) RSPHER
932   FORMAT(////10X,'RADIUS OF SPHERE = ',F6.2)
      WRITE(*,934) GTHE(2)
934   FORMAT(/10X,'ROTATIONAL POTENTIAL PARAMETER = ',
&    F7.3/)

```

C

C -----

C

```

      OPEN(30,FILE='LASTDAT',ACCESS='SEQUENTIAL',
&    FORM='UNFORMATTED')
      IF(IFLAG.EQ.1) GOTO 199

```

C

C === LOAD INITIAL POSITIONS OF ATOMS

```

      CALL INTPOS(RSPHER)
      CALL POSPRI(KB,NM,NAM)

```

C

C === PRINT RUN-TABLE HEADING

```

      WRITE(*,930)
930   FORMAT(1H1////4X,'KB',5X,'RSPH',4X,'ENRG',5X,'E1',
A     4X,'DIST',6X,'TEMP',3X,'TRFRC',3X,'TOT ENR',
A     3X,'FTOTWL',3X,'PRESSURE'/)

```

C

C === LOAD INITIAL VELOCITIES OF ATOMS

```

      CALL INTVEL(AHEAT,PART)

```

C

C === ASSIGN INITIAL ACCELERATIONS BASED ON INITIAL

C POSITIONS

```

      CALL EVAL(RWALL)

```

C

C === SCALE ACCELERATIONS AND STORE STARTING POSITIONS

```

DO 530 I=1,NP

    X2(I)=FX(I)*DELTSQ/MASS(I)

    Y2(I)=FY(I)*DELTSQ/MASS(I)

    Z2(I)=FZ(I)*DELTSQ/MASS(I)

530  CONTINUE

    GOTO 188

C
C ----- READ POSITIONS AND DERIVATIVES INSTEAD OF USING
C ----- FCC, INVEL, ACCELERATION -----
C
199  WRITE(*,930)

    READ(30) KB,IFLG,NM,NAM,RSPHER,XSUM,SUME

    RWALL=RSPHER+1.0

    DO 200 K=1,NP

        READ(30) X0(K),Y0(K),Z0(K)

        READ(30) X1(K),Y1(K),Z1(K)

        READ(30) X2(K),Y2(K),Z2(K)

        READ(30) X3(K),Y3(K),Z3(K)

        READ(30) X4(K),Y4(K),Z4(K)

        READ(30) X5(K),Y5(K),Z5(K)

        READ(30) DAX(K),DAY(K),DAZ(K)

200  CONTINUE

    REWIND 30

188  DO 377 I=1,NP

        X0L(I)=X0(I)

```

```

        YOL(I)=YO(I)
        ZOL(I)=ZO(I)
377      CONTINUE
C
C -----
C
C === ENTER MAIN LOOP OF SIMULATION
        IF(IFLAG.NE.1) GOTO 777
        CALL PREDCT(NP)
        CALL EVAL(RWALL)
        CALL CORR(DELTSQ)
        IF(ISCALE.EQ.1) RSPHER=RSPHER+DELRS
        RWALL=RSPHER+1.0
777      NS=KB+1
        DO 599 NTIMES=NS,MAXKB
            KB=KB+1
            CALL PREDCT(NP)
            CALL EVAL(RWALL)
            CALL CORR(DELTSQ)
C
C === CALCULATE MEAN SQUARE DISPLACEMENT & KINETIC ENERGY
        SUMVEL=0.
        TDIST=0.
        DO 540 I=1,NP
            TDIST=TDIST+DAX(I)**2+DAY(I)**2+DAZ(I)**2

```

```

SUMVEL=SUMVEL+(X1(I)**2+Y1(I)**2+Z1(I)**2)*
&      MASS(I)
540    CONTINUE

      TDIST=TDIST/PART

      EK=SUMVEL/(2.*PART*DELSQ)

C
C === ACCUMMULATE SUMS FOR PROPERTY AVERAGES

      XSUM=XSUM+SUMVEL

      SUME=SUME+TOTE

C
C === PROPERTY CALCULATION & PRINT-OUT AT INTERVALS

      IF(MOD(KB,KWRITE).NE.0) GOTO 550

      FKB=FLOAT(KB)*PART

      TMP=XSUM/(3.*DELSQ*FKB)

      ENR=(SUME/FKB)

      E1=TOTE/PART

      ETOT=E1+EK

      RLTIM=DELTA*FLOAT(KB)*TSTEP

      WRITE(*,940) KB,RSPHER,ENR,E1,TDIST,TMP,TRFRAC,
&      ETOT,FTOTWL,EXTPRS

C

      IF(MOD(KB,1000).NE.0) GOTO 550

      CALL POSPRI(KB,NM,NAM)

      WRITE(*,930)

940    FORMAT(1H ,I6,F6.3,3F9.2,F10.3,1X,F6.3,1X,F9.3,

```



```

      &          2(2X,F9.3))

C
C === DURING FIRST OF RUN, SCALE VELOCITIES FOR TEMPERATURE
550      IF(IFLG.LT.1) CALL EQBRAT(SUMVEL,AHEAT,TDIST,
      &          XDIST,NP,IFLG,KB,NAM)

C
C ---- WRITE DATA ONTO TAPE FOR LATER USE ----
      IF(KB.EQ.0) GOTO 777

C      IF(IFLG.EQ.0) GOTO 588
      IF(MOD(KB,10).NE.0) GOTO 588
      WRITE(20) KB,TMP,ETOT,E1,EK,TOTE,EINTR,TOTLJ,ETOR,
      &      EBON,EBEN
      WRITE(20) X0,Y0,Z0
      WRITE(20) X1,Y1,Z1
      WRITE(20) X2,Y2,Z2

C      WRITE(20) X3,Y3,Z3
C      WRITE(20) X4,Y4,Z4
C      WRITE(20) X5,Y5,Z5

588      IF(MOD(NTIMES,100).NE.0) GOTO 599
      WRITE(30) KB,IFLG,NM,NAM,RSPHER,XSUM,SUME
      DO 598 K=1,NP
          WRITE(30) X0(K),Y0(K),Z0(K)
          WRITE(30) X1(K),Y1(K),Z1(K)
          WRITE(30) X2(K),Y2(K),Z2(K)
          WRITE(30) X3(K),Y3(K),Z3(K)

```

```

WRITE(30) X4(K),Y4(K),Z4(K)
WRITE(30) X5(K),Y5(K),Z5(K)
WRITE(30) DAX(K),DAY(K),DAZ(K)

```

```

598 CONTINUE
REWIND 30

```

```

599 CONTINUE
CLOSE(20)
CLOSE(30)

```

```
STOP
```

```
END
```

```
SUBROUTINE POSPRI(KB,NM,NAM)
```

```
COMMON/POS/X0(216),Y0(216),Z0(216)
```

C

```
II=0
```

```
WRITE(*,942) KB
```

```

942 FORMAT(1H1///7X,'POSITIONS OF GROUPS AT TIME-STEP:'
&      ,I6//)

```

```
DO 404 JJ=1,NM
```

```
WRITE(*,935)
```

```

935 FORMAT(/2X,'MOLECULE',7X,'X',11X,'Y',12X,'Z',
&      12X,'R',9X,'BOND LEN'/)

```

```
DO 404 KK=1,NAM
```

```
II=II+1
```

```
RR=SQRT(X0(II)**2+Y0(II)**2+Z0(II)**2)
```

```
XXX=X0(II)-X0(II-1)
```

```

      YYY=Y0(II)-Y0(II-1)
      ZZZ=Z0(II)-Z0(II-1)
      BB=SQRT(XXX*XXX+YYY*YYY+ZZZ*ZZZ)
      IF(KK.EQ.1) WRITE(*,909) JJ,X0(II),Y0(II),
&      Z0(II),RR
      IF(KK.GT.1) WRITE(*,911) X0(II),Y0(II),Z0(II),
&      RR,BB
404      CONTINUE
909      FORMAT(5X,I2,4(5X,F8.4))
911      FORMAT(7X,5(5X,F8.4))
      RETURN
      END

```

```

      SUBROUTINE INTPOS(RSPHER)
C
C  SET-UP INITIAL POSITIONS OF PARTICLES. HEAD GROUPS ARE
C  ASSIGNED TO FIXED POSITIONS ON THE SURFACE OF A SPHERE
C  OF RADIUS "RSPHER".
C
      COMMON/POS/X0(216),Y0(216),Z0(216)
      COMMON/NUM/NM,NAM,NP,NP1,NP2,NP22,KSORT,KB
      COMMON/CONT/A1,A0,EPS
      COMMON/INTRA/B0(216),GAB(216),CT0(216),GTHA(216),
&      GTHE(216)

```

```
DIMENSION THETA(50),PHI(50)
```

```
C
```

```
PI=3.1415926535
```

```
PI180=PI/180.
```

```
C
```

```
C TWENTY-FOUR MOLECULES
```

```
THETA(1)=0.
```

```
PHI(1)=0.
```

```
THETA(24)=PI
```

```
PHI(24)=0.
```

```
PH24=0.
```

```
DO 70 I=2,5
```

```
PHI(I)=PH24
```

```
PH24=PH24+PI/2.
```

```
70 THETA(I)=36.*PI180
```

```
DELPHI=2.*PI/7
```

```
PH24=DELPHI/2.
```

```
DO 71 I=6,12
```

```
PHI(I)=PH24
```

```
PH24=PH24+DELPHI
```

```
71 THETA(I)=72.*PI180
```

```
PH24=0.
```

```
DO 72 I=13,19
```

```
PHI(I)=PH24
```

```
PH24=PH24+DELPHI
```

```

72  THETA(I)=108.*PI/180
    PH24=PI/4.
    DO 73 I=20,23
        PHI(I)=PH24
        PH24=PH24+PI/2.
73  THETA(I)=144.*PI/180
C
60  WRITE(*,909)
909  FORMAT(1H1////7X,'INITIAL POSITIONS OF HEAD GROUPS'
&    //7X,'MOLECULE',5X,'THETA',8X,'PHI'//)
    DO 101 I=1,NM
        TTT=THETA(I)/PI/180
        PPP=PHI(I)/PI/180
        WRITE(*,900) I,TTT,PPP
900  FORMAT(10X,I3,2(6X,F7.3))
101  CONTINUE
C
C
C  STANDARD DISTANCES ALONG TRANS CHAIN
    XLEN=0.5*B0(2)*SQRT(2.*(1.-CT0(2)))
    ZLEN=SQRT(B0(2)*B0(2)-XLEN*XLEN)
    ZLENSQ=ZLEN*ZLEN
C
C  HEAD-TO-ALPHA DISTANCE
    XLEN1=0.5*B0(1)*SQRT(2.*(1.-CT0(1)))

```

```
ZLEN1=SQRT(B0(1)*B0(1)-XLEN1*XLEN1)
```

```
ZLN1SQ=ZLEN1*ZLEN1
```

```
C
```

```
C === ADD ATOMS TO FORM MOL IN TRANS POS =====
```

```
DO 120 I=1,NM
```

```
IADD=(I-1)*NAM
```

```
THR=THETA(I)
```

```
PHIR=PHI(I)
```

```
SR=SIN(THR)
```

```
CR=COS(THR)
```

```
SPR=SIN(PHIR)
```

```
CPR=COS(PHIR)
```

```
C
```

```
C HEAD GROUP ON A MOLECULE
```

```
J=1
```

```
K=IADD+J
```

```
RK=RSPHER
```

```
X0(K)=RK*SR*CPR
```

```
Y0(K)=RK*SR*SPR
```

```
Z0(K)=RK*CR
```

```
C
```

```
C ALPHA GROUP ON A MOLECULE
```

```
J=2
```

```
K=IADD+J
```

```
RDISA=RSPHER-XLEN1
```

RK=SQRT(RDISA*RDISA+ZLN1SQ)

BETA=ASIN(ZLEN1/RK)

THE=THR-BETA

ST=SIN(THE)

X0(K)=RK*ST*CPR

Y0(K)=RK*ST*SPR

Z0(K)=RK*COS(THE)

C

C ODD NUMBERED GROUPS ON A MOLECULE

DO 92 J=3,NAM,2

K=IADD+J

RK=RDISA-FLOAT(J-2)*XLEN

X0(K)=RK*SR*CPR

Y0(K)=RK*SR*SPR

Z0(K)=RK*CR

92 CONTINUE

C

C EVEN NUMBERED GROUPS ON A MOLECULE

DO 95 J=4,NAM,2

K=IADD+J

RDIS=RDISA-FLOAT(J-2)*XLEN

RK=SQRT(RDIS*RDIS+ZLENSQ)

BETA=ASIN(ZLEN/RK)

THE=THR-BETA

ST=SIN(THE)

```

      X0(K)=RK*ST*CPR
      Y0(K)=RK*ST*SPR
      Z0(K)=RK*COS(THETA)

95      CONTINUE

120     CONTINUE

      RETURN

      END

```

```

      SUBROUTINE INTVEL(AHEAT,PART)

```

```

C

```

```

C === ASSIGN INITIAL VELOCITIES TO ATOMS

```

```

C

```

```

      COMMON/NUM/NM,NAM,NP,NP1,NP2,NP22,KSORT,KB
      COMMON/VEL/X1(216),Y1(216),Z1(216)
      COMMON/MASS/MASS(216)

      SUMX=0.
      SUMY=0.
      SUMZ=0.

      DO 200 I=1,NM
          XX=RANF(DUM)
          YY=RANF(DUM)
          ZZ=RANF(DUM)
          NX=(I-1)*NAM
      DO 200 J=1,NAM

```



```

      X1(J+NX)=XX
      Y1(J+NX)=YY
      Z1(J+NX)=ZZ
      SUMX=SUMX+X1(J+NX)*MASS(J+NX)
      SUMY=SUMY+Y1(J+NX)*MASS(J+NX)
      SUMZ=SUMZ+Z1(J+NX)*MASS(J+NX)
200  CONTINUE
C
C === SCALE VELOCITIES SO THAT TOTAL MOMENTUM = ZERO
      X=0.
      DO 210 I=1,NP
          X1(I)=X1(I)-SUMX/PART/MASS(I)
          Y1(I)=Y1(I)-SUMY/PART/MASS(I)
          Z1(I)=Z1(I)-SUMZ/PART/MASS(I)
          X=X+(X1(I)**2+Y1(I)**2+Z1(I)**2)*MASS(I)
210  CONTINUE
C
C === SCALE VELOCITIES TO DESIRED TEMPERATURE
      HEAT=SQRT(AHEAT/X)
      DO 220 I=1,NP
          X1(I)=X1(I)*HEAT
          Y1(I)=Y1(I)*HEAT
          Z1(I)=Z1(I)*HEAT
220  CONTINUE
      RETURN

```

END

SUBROUTINE PREDCT(NP)

C

C === USE TAYLOR SERIES TO PREDICT POSITIONS & THEIR

C DERIVATIVES AT NEXT TIME-STEP

C

COMMON/POS/X0(216),Y0(216),Z0(216)

COMMON/VEL/X1(216),Y1(216),Z1(216)

COMMON/DER/X2(216),Y2(216),Z2(216),X3(216),Y3(216),
& Z3(216),X4(216),Y4(216),Z4(216),X5(216),Y5(216),
& Z5(216)

COMMON/FOR/FX(216),FY(216),FZ(216)

DO 300 I=1,NP

X0(I)=X0(I)+X1(I)+X2(I)+X3(I)+X4(I)+X5(I)

Y0(I)=Y0(I)+Y1(I)+Y2(I)+Y3(I)+Y4(I)+Y5(I)

Z0(I)=Z0(I)+Z1(I)+Z2(I)+Z3(I)+Z4(I)+Z5(I)

X1(I)=X1(I)+2.*X2(I)+3.*X3(I)+4.*X4(I)+5.*X5(I)

Y1(I)=Y1(I)+2.*Y2(I)+3.*Y3(I)+4.*Y4(I)+5.*Y5(I)

Z1(I)=Z1(I)+2.*Z2(I)+3.*Z3(I)+4.*Z4(I)+5.*Z5(I)

X2(I)=X2(I)+3.*X3(I)+6.*X4(I)+10.*X5(I)

Y2(I)=Y2(I)+3.*Y3(I)+6.*Y4(I)+10.*Y5(I)

Z2(I)=Z2(I)+3.*Z3(I)+6.*Z4(I)+10.*Z5(I)

X3(I)=X3(I)+4.*X4(I)+10.*X5(I)

$Y3(I) = Y3(I) + 4. * Y4(I) + 10. * Y5(I)$

$Z3(I) = Z3(I) + 4. * Z4(I) + 10. * Z5(I)$

$X4(I) = X4(I) + 5. * X5(I)$

$Y4(I) = Y4(I) + 5. * Y5(I)$

$Z4(I) = Z4(I) + 5. * Z5(I)$

$FX(I) = 0.$

$FY(I) = 0.$

$FZ(I) = 0.$

300 CONTINUE

RETURN

END

SUBROUTINE CORR(DELT SQ)

C

C === CORRECT PREDICTED POSITIONS AND THEIR DERIVATIVES

C

COMMON/POS/X0(216),Y0(216),Z0(216)

COMMON/VEL/X1(216),Y1(216),Z1(216)

COMMON/DER/X2(216),Y2(216),Z2(216),X3(216),Y3(216),
& Z3(216),X4(216),Y4(216),Z4(216),X5(216),Y5(216),
& Z5(216)

COMMON/FOR/FX(216),FY(216),FZ(216)

COMMON/DISP/DAX(216),DAY(216),DAZ(216),X0L(216),
& Y0L(216),Z0L(216)

COMMON/PARM/F02,F12,F32,F42,F52

COMMON/NUM/NM,NAM,NP,NP1,NP2,NP22,KSORT,KB

COMMON/PROP/SUME,XSUM

COMMON/SCAL/RSPHER,RWALL,DELRS,ISCALE

COMMON/MASS/MASS(216)

C

IF(MOD(KB,10).NE.0.OR.ISCALE.NE.1) GOTO 610

C

IF(RSPHER.LE.3.6) GO TO 610

RSPHER=RSPHER-DELRS

RWALL =RWALL -DELRS

C

610 DO 690 I=1,NP

XERR=X2(I)-DELTSQ*FX(I)/MASS(I)

YERR=Y2(I)-DELTSQ*FY(I)/MASS(I)

ZERR=Z2(I)-DELTSQ*FZ(I)/MASS(I)

X0(I)=X0(I)-XERR*F02

X1(I)=X1(I)-XERR*F12

X2(I)=X2(I)-XERR

X3(I)=X3(I)-XERR*F32

X4(I)=X4(I)-XERR*F42

X5(I)=X5(I)-XERR*F52

Y0(I)=Y0(I)-YERR*F02

Y1(I)=Y1(I)-YERR*F12

Y2(I)=Y2(I)-YERR

Y3(I)=Y3(I)-YERR*F32

$Y4(I) = Y4(I) - YERR * F42$

$Y5(I) = Y5(I) - YERR * F52$

$Z0(I) = Z0(I) - ZERR * F02$

$Z1(I) = Z1(I) - ZERR * F12$

$Z2(I) = Z2(I) - ZERR$

$Z3(I) = Z3(I) - ZERR * F32$

$Z4(I) = Z4(I) - ZERR * F42$

$Z5(I) = Z5(I) - ZERR * F52$

690 CONTINUE

IF(MOD(KB, KSORT) .NE. 0 .OR. ISCALE .NE. 1) GOTO 680

DO 691 I=1, NP

$RSQ = X0(I) * X0(I) + Y0(I) * Y0(I) + Z0(I) * Z0(I)$

$R = \text{SQRT}(RSQ)$

$RFACT = 1.0 - DELRS / R$

$X0(I) = X0(I) * RFACT$

$Y0(I) = Y0(I) * RFACT$

$Z0(I) = Z0(I) * RFACT$

691 CONTINUE

C

C === DISPLACEMENTS

680 DO 692 I=1, NP

$DAX(I) = DAX(I) - X0(I) + X0L(I)$

$DAY(I) = DAY(I) - Y0(I) + Y0L(I)$

$DAZ(I) = DAZ(I) - Z0(I) + Z0L(I)$

C

C === STORE NEW POSITIONS

X0L(I)=X0(I)

Y0L(I)=Y0(I)

Z0L(I)=Z0(I)

692 CONTINUE

RETURN

END

SUBROUTINE EQBRAT(SUMVEL,AHEAT,TDIST,XDIST,NP,IFLG,
& KB,NAM)

C

C === SCALE VELOCITIES DURING INITIAL TIME-STEPS

C

COMMON/VEL/X1(216),Y1(216),Z1(216)

COMMON/PROP/SUME,XSUM

COMMON/SCAL/RSPHER,RWALL,DELRS,ISCALE

C

IF(IFLG.EQ.-1) GOTO 720

IF(TDIST.GT.XDIST.OR.IFLG.EQ.-2) GOTO 750

720 HEAT=SQRT(AHEAT/SUMVEL)

DO 730 I=1,NP

X1(I)=X1(I)*HEAT

Y1(I)=Y1(I)*HEAT

Z1(I)=Z1(I)*HEAT

730 CONTINUE

RETURN

C

C === AT END OF EQUILIBRATION STAGE, SET PROPERTY SUMS

C TO ZERO

750 IFLG= 1

KB=0

SUME=0.

XSUM=0.

RETURN

END

SUBROUTINE EVAL(RWALL)

C

COMMON/POS/X0(216),Y0(216),Z0(216)

COMMON/FOR/FX(216),FY(216),FZ(216)

COMMON/CONT/A1,A0,EPS

COMMON/PROP/SUME,XSUM

COMMON/PROPA/REQUIL,FORCON,HDSIG,SIG12

COMMON/ENERGY/TOTE,TOTLJ,ETOR,EBON,EBEN,EINTR,

& TRFRAC,EXTPRS,FTOTWL

COMMON/NUM/NM,NAM,NP,NP1,NP2,NP22,KSORT,KB

COMMON/INTRA/B0(216),GAB(216),CT0(216),GTHA(216),

& GTHE(216)

```
DIMENSION B(216),BX(216),BY(216),BZ(216)

C
C  INITIALIZE ACCUMULATORS

      ICOUNT=0

      K=0

      ITRAN =0

      TOTE=0.0

      TOTLJ=0.0

      FTOTWL=0.0

      ETOR=0.0

      EBON=0.0

      EBEN=0.0

      EINTR=0.0

      DO 150 I=1,NP

          FX(I)=0.0

          FY(I)=0.0

          FZ(I)=0.0

150  CONTINUE

C
C  CALCULATE LJ FORCES

C
C  OUTER LOOP OVER PARTICLES

      DO 300 I=1,NP1

          ICHK=I-1+NAM

          XI=X0(I)
```



```

      YI=Y0(I)

      ZI=Z0(I)

      IF(I.GE.NP2) GOTO 788

C
C  DECIDE WHICH MOLECULE ATOM I IS ON
      IM=(I-1)/NAM+1.0001

C
C  INNER LOOP
      DO 290 J=I+1,NP

C
C  IF I & J ARE HEAD GROUPS, CALCULATE HEAD-HEAD REPULSIONS
      JCHK=J+NAM-1

      IF(MOD(ICHK,NAM).NE.0.OR.MOD(JCHK,NAM).NE.0)GOTO 614

      X=XI-X0(J)
      Y=YI-Y0(J)
      Z=ZI-Z0(J)

      RSQ=X*X+Y*Y+Z*Z

      RIJ=SQRT(RSQ)

      RI=HDSIG/RIJ

      R3=RI*RI*RI

      R4=R3*RI

      R8=R4*R4

      HS3=1.0/HDSIG**3

      HS4=HS3/HDSIG

C

```

```
ELJ=R3*(R8*RI+HS3)
FLJS=3.0*R4*(4.0*R8*RI+HS4)
FXD=FLJS*X*RI
FYD=FLJS*Y*RI
FZD=FLJS*Z*RI
FX(I)=FX(I)+FXD
FX(J)=FX(J)-FXD
FY(I)=FY(I)+FYD
FY(J)=FY(J)-FYD
FZ(I)=FZ(I)+FZD
FZ(J)=FZ(J)-FZD
GO TO 290
```

C

C DECIDE WHICH MOLECULE ATOM J IS ON

```
614 JM=(J-1)/NAM+1.0001
```

C

C CHECK WHETHER I AND J ARE ON SAME MOL

```
IF(IM.NE.JM) GOTO 289
```

C

C CHECK IF I AND J ARE FOURTH NEIGHBORS OR GREATER

```
KIJ=J-I
```

```
IF(KIJ.LE.3) GOTO 290
```

C

```
289 X=XI-X0(J)
```

```
Y=YI-Y0(J)
```

Z=ZI-ZO(J)

C

RSQ=X*X+Y*Y+Z*Z

RIJ=SQRT(RSQ)

C

C IF ONE IS A HEAD GROUP, CALCULATE HEAD-ALKANE INTERACTION

IF(MOD(ICHK,NAM).EQ.0.OR.MOD(JCHK,NAM).EQ.0) THEN

RI=SIG12/RIJ

R3=RI**3

R6=R3*R3

ELJ=2.0*R6*(R3-1.50)

FLJ=18.*RI*R6*(R3-1.0)

C

C IF NOT, CALCULATE ALKANE-ALKANE INTERACTION

ELSE

RI=1./RIJ

R3=RI**3

R6=R3*R3

ELJ=2.0*R6*(R3-1.50)

FLJS=18.*RI*R6*(R3-1.0)

ENDIF

TOTLJ=TOTLJ+ELJ

FXD=FLJS*X*RI

FYD=FLJS*Y*RI

FZD=FLJS*Z*RI

```
      FX(I)=FX(I)+FXD
      FX(J)=FX(J)-FXD
      FY(I)=FY(I)+FYD
      FY(J)=FY(J)-FYD
      FZ(I)=FZ(I)+FZD
      FZ(J)=FZ(J)-FZD
290  CONTINUE
C
C  CALCULATE BOND LENGTHS
C  CHECK IF LAST ATOM ON MOLECULE
788  IF(MOD(I,NAM).EQ.0) GOTO 300
      BX(I)=XI-X0(I+1)
      BY(I)=YI-Y0(I+1)
      BZ(I)=ZI-Z0(I+1)
      BSQ=BX(I)**2+BY(I)**2+BZ(I)**2
      B(I)=SQRT(BSQ)
300  CONTINUE
C
C
C  LOOP CALCULATES INTRAMOLECULAR FORCES
499  DO 600 I=1,NP1
C
C  CHECK IF LAST ATOM ON MOLECULE
      IF(MOD(I,NAM).EQ.0) GOTO 600
C
```

C CALCULATE BOND FORCES

$$BDIFF = B(I) - B0(I)$$

$$EBON = EBN + 0.5 * GAB(I) * BDIFF * BDIFF$$

$$FBON = GAB(I) * BDIFF$$

$$BI = 1. / B(I)$$

$$BXI = BX(I) * BI$$

$$BYI = BY(I) * BI$$

$$BZI = BZ(I) * BI$$

$$FXB = FBON * BXI$$

$$FYB = FBON * BYI$$

$$FZB = FBON * BZI$$

$$FX(I) = FX(I) - FXB$$

$$FX(I+1) = FX(I+1) + FXB$$

$$FY(I) = FY(I) - FYB$$

$$FY(I+1) = FY(I+1) + FYB$$

$$FZ(I) = FZ(I) - FZB$$

$$FZ(I+1) = FZ(I+1) + FZB$$

C

C CALCULATION BENDING FORCE

C CHECK IF NEXT-TO-LAST ATOM ON MOLECULE

$$IF(MOD(I+1, NAM) .EQ. 0) \text{ GOTO } 600$$

$$BII = 1. / B(I+1)$$

$$BXJ = BX(I+1) * BII$$

$$BYJ = BY(I+1) * BII$$

$$BZJ = BZ(I+1) * BII$$

```

CTI=- (BXJ*BXI+BYJ*BYI+BZJ*BZI)
CDIFF=CT0(I)-CTI
EBEN=EBEN+0.5*GTHA(I)*CDIFF*CDIFF
FT=GTHA(I)*CDIFF
FT1=FT*BI
FT2=FT*BII
FX1=FT1*(BXJ+CTI*BXI)
FY1=FT1*(BYJ+CTI*BYI)
FZ1=FT1*(BZJ+CTI*BZI)
FX2=FT2*(BXI+CTI*BXJ)
FY2=FT2*(BYI+CTI*BYJ)
FZ2=FT2*(BZI+CTI*BZJ)
FX(I)  =FX(I)  -FX1
FX(I+1)=FX(I+1)+FX1-FX2
FX(I+2)=FX(I+2)+FX2
FY(I)  =FY(I)  -FY1
FY(I+1)=FY(I+1)+FY1-FY2
FY(I+2)=FY(I+2)+FY2
FZ(I)  =FZ(I)  -FZ1
FZ(I+1)=FZ(I+1)+FZ1-FZ2
FZ(I+2)=FZ(I+2)+FZ2

```

C

C CALCULATION OF TORSION FORCES

C CHECK WHETHER FIRST ATOM OF MOLECULE

```

IF(MOD(I+NAM-1,NAM).EQ.0) GOTO 600

```

```

      CALL RYFOR(BX(I-1),BY(I-1),BZ(I-1),BX(I),BY(I),BZ(I),
&    BX(I+1),BY(I+1),BZ(I+1),FX1,FY1,FZ1,FX2,FY2,FZ2,
&    FX3,FY3,FZ3,FX4,FY4,FZ4,ETQ,CODI,GTHE(I-1))

```

C

```

      ICOUNT=ICOUNT+1
      IF(CODI.LT.-0.50) ITRAN=ITRAN+1
      FX(I-1)=FX(I-1)+FX1
      FY(I-1)=FY(I-1)+FY1
      FZ(I-1)=FZ(I-1)+FZ1
      FX(I)  =FX(I)  +FX2
      FY(I)  =FY(I)  +FY2
      FZ(I)  =FZ(I)  +FZ2
      FX(I+1)=FX(I+1)+FX3
      FY(I+1)=FY(I+1)+FY3
      FZ(I+1)=FZ(I+1)+FZ3
      FX(I+2)=FX(I+2)+FX4
      FY(I+2)=FY(I+2)+FY4
      FZ(I+2)=FZ(I+2)+FZ4
      ETOR=ETOR+ETQ

```

```

600    CONTINUE

```

C

```

C    CALCULATE GROUP-SHELL INTERACTION

```

```

      EWALL=0.0
      RCHKSQ=(RWALL-2.0)**2
      DO 650 I=1,NP

```

```
      ICHK=I-1+NAM
```

```
C
```

```
      XI=X0(I)
```

```
      YI=Y0(I)
```

```
      ZI=Z0(I)
```

```
C
```

```
C  DISTANCE FROM CENTER TO GROUP
```

```
      RSQ=XI*XI+YI*YI+ZI*ZI
```

```
C  IF HEAD GROUP, CALCULATE INTERACTIONS WITH WALL USING
```

```
C    A POTENTIAL OF THE FORM --  GAMMA*(R-R0)**2
```

```
      IF(MOD(ICHK,NAM).NE.0) GO TO 384
```

```
C  DURING SCALE-DOWN, DO NOT CALCULATE HEAD-WALL INTERACTION
```

```
C    GOTO 650
```

```
C
```

```
      RR=SQRT(RSQ)
```

```
      RI=1.0/RR
```

```
      RD=RWall-RR
```

```
C
```

```
      EWall=EWall+FORCON*(RD-REQUIL)*(RD-REQUIL)
```

```
      FWall=-2.0*FORCON*(RD-REQUIL)
```

```
      FTOTWL=FTOTWL+FWall
```

```
C
```

```
      FX(I)=FX(I)-FWall*XI*RI
```

```
      FY(I)=FY(I)-FWall*YI*RI
```

```
      FZ(I)=FZ(I)-FWall*ZI*RI
```



```
                GO TO 650
C IF NOT A HEAD GROUP, CALCULATE REPULSIVE INTERACTION
C   WITH THE WALL
384      IF(RSQ.LT.RCHKSQ) GOTO 650
C
C   DISTANCE FROM GROUP TO SHELL
      RR=SQRT(RSQ)
      RI=1.0/RR
      RD=RWALL-RR
      RDR=1.0/RD
      R3 =RDR*RDR*RDR
      R6 =R3*R3
      R12=R6*R6
C
C   FORCE AND ENERGY FOR R-12 WALL
      EWALL=EWALL+R12
      FWALL=12.0*R12*RDR
      FTOTWL=FTOTWL+FWALL
      FX(I)=FX(I)-FWALL*XI*RI
      FY(I)=FY(I)-FWALL*YI*RI
      FZ(I)=FZ(I)-FWALL*ZI*RI
650      CONTINUE
C
C   CALCULATE WALL PRESSURE IN ATMOSPHERES
      EXTPRS=0.0085382*FTOTWL/RWALL**2
```

C

C CALCULATE INTRAMOLECULAR AND TOTAL ENERGY

EINTR=ETOR + EBON + EBEN

TOTE = TOTLJ + EINTR + EWALL

TRFRAC=FLOAT(ITRAN)/FLOAT(ICOUNT)

RETURN

END

SUBROUTINE RYFOR(BONX1,BONY1,BONZ1,BONX2,BONY2,

& BONZ2,BONX3,BONY3,BONZ3,FORX1,FORY1,FORZ1,FORX2,

& FORY2,FORZ2,FORX3,FORY3,FORZ3,FORX4,FORY4,FORZ4,

& ETOR,CODI,GR)

C

DATA A1,A2,A3,A4,A5/-1.462,-1.578,0.368,

& 3.156,3.788/

C

C CALCULATE NORMAL TO PLANE OF BONDS 1 AND 2

E=BONY1*BONZ2-BONZ1*BONY2

D=BONZ1*BONX2-BONX1*BONZ2

C=BONX1*BONY2-BONY1*BONX2

ANORM2=C*C+D*D+E*E

ANORM =SQRT(ANORM2)

ANORMR=1./ANORM

AX=E*ANORMR

AY=D*ANORMR

AZ=C*ANORMR

C

C CALCULATE NORMAL TO PLANE OF BONDS 2 AND 3

H=BONY2*BONZ3-BONZ2*BONY3

G=BONZ2*BONX3-BONX2*BONZ3

F=BONX2*BONY3-BONY2*BONX3

BNORM2=F*F+G*G+H*H

BNORM =SQRT(BNORM2)

BNORMR=1./BNORM

BX=H*BNORMR

BY=G*BNORMR

BZ=F*BNORMR

C

C DETERMINE COSINE OF THE DIHEDRAL ANGLE, PHI

CODI= AX*BX+AY*BY+AZ*BZ

C

C DETERMINE TORSIONAL ENERGY

CODISQ=CODI*CODI

CODI3 =CODI*CODISQ

ETOR = GR*(1.116+A1*CODI+A2*CODISQ+A3*CODI3

& +A4*CODISQ*CODISQ+A5*CODISQ*CODI3)

C

C CALCULATE DU/COS(PHI)

DUDCO=(A1+2.*A2*CODI+3.*A3*CODISQ+4.*A4*CODISQ*

```

      &    CODI+5.*A5*CODISQ*CODISQ)*GR
C
C  START EVALUATION OF FORCE ON GROUP 1
C    CALCULATE DANORM/DR1
      FACT1=(C*BONY2-D*BONZ2)/ANORM2
      DADX1X= -FACT1*AX
      DADX1Y= -FACT1*AY-BONZ2*ANORMR
      DADX1Z= -FACT1*AZ+BONY2*ANORMR
C
      FACT2 =(E*BONZ2-C*BONX2)/ANORM2
      DADY1X= -FACT2*AX+BONZ2*ANORMR
      DADY1Y= -FACT2*AY
      DADY1Z= -FACT2*AZ-BONX2*ANORMR
C
      FACT3 =(D*BONX2-E*BONY2)/ANORM2
      DADZ1X= -FACT3*AX-BONY2*ANORMR
      DADZ1Y= -FACT3*AY+BONX2*ANORMR
      DADZ1Z= -FACT3*AZ
C
C  CALCULATE D(AB)/DR1
      DABDX1=BX*DADX1X+BY*DADX1Y+BZ*DADX1Z
      DABDY1=BX*DADY1X+BY*DADY1Y+BZ*DADY1Z
      DABDZ1=BX*DADZ1X+BY*DADZ1Y+BZ*DADZ1Z
C
C  CALCULATE FORCE ON GROUP 1

```

FORX1= -DUDCO*DABDX1

FORY1= -DUDCO*DABDY1

FORZ1= -DUDCO*DABDZ1

C

C START EVALUATION OF FORCE ON GROUP 2

C CALCULATE DANORM/DR2

FACT4 =(D*BONZ1-C*BONY1)/ANORM2

DADX2X= -FACT4*AX-DADX1X

DADX2Y= -FACT4*AY+BONZ1*ANORMR-DADX1Y

DADX2Z= -FACT4*AZ-BONY1*ANORMR-DADX1Z

C

FACT5 =(C*BONX1-E*BONZ1)/ANORM2

DADY2X= -FACT5*AX-BONZ1*ANORMR-DADY1X

DADY2Y= -FACT5*AY-DADY1Y

DADY2Z= -FACT5*AZ+BONX1*ANORMR-DADY1Z

C

FACT6 =(E*BONY1-D*BONX1)/ANORM2

DADZ2X= -FACT6*AX+BONY1*ANORMR-DADZ1X

DADZ2Y= -FACT6*AY-BONX1*ANORMR-DADZ1Y

DADZ2Z= -FACT6*AZ-DADZ1Z

C

C EVALUATE D(BNORM)/DR2

FACT7 =(F*BONY3-G*BONZ3)/BNORM2

DBDX2X= -FACT7*BX

DBDX2Y= -FACT7*BY-BONZ3*BNORMR

DBDX2Z= -FACT7*BZ+BONY3*BNORMR

C

FACT8 =(H*BONZ3-F*BONX3)/BNORM2

DBDY2X= -FACT8*BX+BONZ3*BNORMR

DBDY2Y= -FACT8*BY

DBDY2Z= -FACT8*BZ-BONX3*BNORMR

C

FACT9 =(G*BONX3-H*BONY3)/BNORM2

DBDZ2X= -FACT9*BX-BONY3*BNORMR

DBDZ2Y= -FACT9*BY+BONX3*BNORMR

DBDZ2Z= -FACT9*BZ

C

C CALCULATE D COS(PHI)/DR2

DABDX2=BX*DADX2X+BY*DADX2Y+BZ*DADX2Z

& +AX*DBDX2X+AY*DBDX2Y+AZ*DBDX2Z

DABDY2=BX*DADY2X+BY*DADY2Y+BZ*DADY2Z

& +AX*DBDY2X+AY*DBDY2Y+AZ*DBDY2Z

DABDZ2=BX*DADZ2X+BY*DADZ2Y+BZ*DADZ2Z

& +AX*DBDZ2X+AY*DBDZ2Y+AZ*DBDZ2Z

C

C FORCE ON GROUP 2

FORX2 = -DUDCO*DABDX2

FORY2 = -DUDCO*DABDY2

FORZ2 = -DUDCO*DABDZ2

C

C START EVALUATION OF FORCE ON GROUP 4

C CALCULATE $D(BNORM)/DR4$

$$FACT1 = (F*BONY2 - G*BONZ2) / BNORM2$$

$$DBDX4X = -FACT1 * BX$$

$$DBDX4Y = -FACT1 * BY - BONZ2 * BNORMR$$

$$DBDX4Z = -FACT1 * BZ + BONY2 * BNORMR$$

C

$$FACT2 = (H*BONZ2 - F*BONX2) / BNORM2$$

$$DBDY4X = -FACT2 * BX + BONZ2 * BNORMR$$

$$DBDY4Y = -FACT2 * BY$$

$$DBDY4Z = -FACT2 * BZ - BONX2 * BNORMR$$

C

$$FACT3 = (G*BONX2 - H*BONY2) / BNORM2$$

$$DBDZ4X = -FACT3 * BX - BONY2 * BNORMR$$

$$DBDZ4Y = -FACT3 * BY + BONX2 * BNORMR$$

$$DBDZ4Z = -FACT3 * BZ$$

C

C EVALUATE $D \cos(\Phi)/DR4$

$$DABDX4 = AX * DBDX4X + AY * DBDX4Y + AZ * DBDX4Z$$

$$DABDY4 = AX * DBDY4X + AY * DBDY4Y + AZ * DBDY4Z$$

$$DABDZ4 = AX * DBDZ4X + AY * DBDZ4Y + AZ * DBDZ4Z$$

C

C EVALUATE FORCE ON GROUP 4

$$FORX4 = -DUDCO * DABDX4$$

$$FORY4 = -DUDCO * DABDY4$$

FORZ4= -DUDCO*DABDZ4

C

C EVALUATE FORCE ON GROUP 3 BY NEWTON'S THIRD LAW

FORX3 = -FORX1-FORX2-FORX4

FORY3 = -FORY1-FORY2-FORY4

FORZ3 = -FORZ1-FORZ2-FORZ4

C

RETURN

END

BLOCK DATA

COMMON/DER/X2(216),Y2(216),Z2(216),X3(216),Y3(216),
& Z3(216),X4(216),Y4(216),Z4(216),X5(216),Y5(216),
& Z5(216)

COMMON/FOR/FX(216),FY(216),FZ(216)

COMMON/DISP/DAX(216),DAY(216),DAZ(216),X0L(216),
& Y0L(216),Z0L(216)

COMMON/PROP/SUME,XSUM

COMMON/MASS/MASS(216)

COMMON/INTRA/B0(216),GAB(216),CT0(216),GTHA(216),
& GTHE(216)

DATA X3,Y3,Z3,X4,Y4,Z4,X5,Y5,Z5/1944*0./

DATA DAX,DAY,DAZ,FX,FY,FZ/1296*0./

DATA MASS/216*1/

C FOR SCALE-DOWN, GTHE SET TO GTHE/10.

DATA B0,GAB,CT0,GTHA,GTHE/216*.38475,216*35322.1957,
& 216*-.377032668,216*310.26253,216*19.84248/

C NORMAL GTHE IS 19.84248

END

REFERENCES

- Aveyard, R.; B.J. Briscoe and J. Chapman 1972. Journal of the Chemical Society--Faraday I, 68, 10 "Adhesion at the Alkane/Water and Ester/Water Interfaces"
- Balmbra, R.R.; J.S. Clunie; J.M. Corkill and J.F. Goodman 1962. Transactions of the Faraday Society, 58, 1661 "Effect of Temperature on the Micelle Size of a Homogeneous Nonionic Detergent"
- Balmbra, R.R.; J.S. Clunie; J.M. Corkill and J.F. Goodman 1964. Transactions of the Faraday Society, 60, 979 "Variations in the Micelle Size of Nonionic Detergents"
- Bendedouch, D.; S.H. Chen and W.C. Koehler 1983a. Journal of Physical Chemistry, 87, 153 "Structure of Ionic Micelles from Small Angle Neutron Scattering"
- Bendedouch, D.; S.H. Chen and W.C. Koehler 1983b. Journal of Physical Chemistry, 87, 2621 "Determination of Interparticle Structure Factors in Ionic Micellar Solutions by Small Angle Neutron Scattering"
- Benedek, G.B. 1985. In Physics of Amphiphiles: Micelles, Vesicles, and Microemulsions; V. Degiorgio and M. Corti, eds.; North Holland, Amsterdam "On the Molecular Basis for Micellar Formation and Growth"
- Ben-Naim, A. and F.H. Stillinger 1980. Journal of Physical Chemistry, 84, 2872 "Critical Micelle Concentration and the Size Distribution of Surfactant Aggregates"
- Ben-Shaul, A.; I. Szleifer and W.M. Gelbart 1985. Journal of Chemical Physics, 83, 3597 "Chain Organization and Thermodynamics in Micelles and Bilayers. II. Model Calculations"
- Birdi, K.S. 1975. In Proceedings of the International Conference on Colloid and Surface Science, E. Wolfram, ed.; Elsevier Scientific, New York "A Study of Mixed Micelles of Cationic and Nonionic Surfactants by Membrane Osmometry"

- Blankschtein, D.; G.M. Thurston and G.B. Benedek 1985. Physical Review Letters, 54, 955 "Theory of Phase Separation in Micellar Solutions"
- Blukis, V.; P.H. Kasic and R.J. Myers 1963. Journal of Chemical Physics, 38, 2753 "Microwave Spectra and Structure of Dimethyl Ether"
- Buff, F.P. 1955. Journal of Chemical Physics, 23, 419 "Spherical Interface. II. Molecular Theory"
- Burchfield, T.E. and E.M. Woolley 1984. Journal of Physical Chemistry, 88, 2149 "Model for Thermodynamics of Ionic Surfactant Solutions. 1. Osmotic and Activity Coefficients"
- Cabane, B.; R. Duplessix and T. Zemb 1985. Journal de Physique, 46, 133 "High Resolution Neutron Scattering on Ionic Surfactant Micelles: SDS in Water"
- Cahill, P.; L.P. Gold and N. Owen 1968. Journal of Chemical Physics, 48, 1620 "Microwave Spectrum, Conformation, Dipole Moment, and barrier to Internal Rotation in Methyl Vinyl Ether"
- Chevalier, Y. and C. Chachaty 1985. Journal of Physical Chemistry, 89, 875 "Hydrocarbon Chain Conformations in Micelles. A Nuclear Magnetic Relaxation Study"
- Clint, J.H. 1975. Journal of the Chemical Society, 71, 1327 "Mixed Micellization"
- Corkill, J.M.; J.F. Goodman and R.H. Ottewill 1961. Transactions of the Faraday Society, 57, 1627 "Micellization of Homogeneous Nonionic Detergents"
- Corti, M. and V. Degiorgio 1981a. Journal of Physical Chemistry, 85, 711 "Quasi-Elastic Light Scattering Study of Intermicellar Interactions in Aqueous Sodium Dodecyl Sulfate Solutions"
- Corti, M. and V. Degiorgio 1981b. Journal of Physical Chemistry, 85, 1442 "Micellar Properties and Critical Fluctuations in Aqueous Solutions of Nonionic Amphiphiles"
- Eriksson, J.C. and S. Ljunggren 1985. Journal of the Chemical Society, Faraday II, 81, 1209 "The Mechanics and Thermodynamics of Rod-shaped Micelles"

- Gear, C.W. 1971. Numerical Initial Value Problems in Ordinary Differential Equations; Prentice-Hall, Englewood Cliffs, N.J.
- Gruen, D.W.R. 1981. Journal of Colloid and Interface Science, 84, 281 "The Packing of Amphiphile Chains in a Small Spherical Micelle"
- Haan, S.W. and L.R. Pratt 1981a. Chemical Physics Letters, 79, 436 "Monte Carlo Study of a Simple Model for Micelle Structure"
- Haan, S.W. and L.R. Pratt 1981b. Chemical Physics Letters, 81, 386 Errata of 79, 436
- Haile, J.M. 1980. A Primer on the Computer Simulation of Atomic Fluids by Molecular Dynamics, Unpublished
- Haile, J.M. and J.P. O'Connell 1984. Journal of Physical Chemistry, 88, 6363 "Internal Structure of a Model Micelle via Computer Simulation"
- Hall, D.G. and B.A. Pethica 1967. Nonionic Surfactants; M.J. Schick, ed.; Marcel Decker, New York
- Hayter, J.B. and T. Zemb 1982. Chemical Physics Letters, 93, 91 "Concentration-Dependent Structure of Sodium Octanoate Micelles"
- Henderson, J.R. and J.S. Rowlinson 1984. Journal of Physical Chemistry, 88, 6484 "Statistical Mechanics of Fluid Interfaces in Cylindrical Symmetry"
- Hoeve, C.A.J. and G.C. Benson 1957. Journal of Physical Chemistry, 61, 1149 "On the Statistical Mechanical Theory of Micelle Formation in Detergent Solutions"
- Hourani, M. J. 1984. Ph.D. Dissertation, University of Florida "A Molecular Thermodynamic Model for Surfactant Aggregate Formation"
- Ikeda, S. 1984. Journal of Physical Chemistry, 88, 2144 "Sphere-Rod Transition of Surfactant Micelles and Size Distribution of Rodlike Micelles"
- Israelachvili, J.N.; D.J. Mitchell and B.W. Ninham 1976. Journal of the Chemical Society--Faraday II, 72, 1525 "Theory of Self-Assembly of Hydrocarbon Amphiphiles into Micelles and Bilayers"

- Jasper, J.J. 1972. Journal of Chemical Reference Data, 1, 841 "Surface Tension of Pure Liquid Compounds"
- Jonsson, B.; O. Edholm and O. Teleman 1986. Journal of Chemical Physics, 85, 2259 "Molecular Dynamics Simulation of a Sodium Octanoate Micelle in Aqueous Solution"
- Kalyanasundaram, K. and J.K. Thomas 1976. Journal of Physical Chemistry, 80, 1462 "On the Conformational State of Surfactants in the Solid State and in Micellar Form"
- Kamrath, R.F. and E.I. Franses 1983. IEC Fundamentals, 22, 230 "Thermodynamics of Mixed Micellization. Psuedo-Phase Separation Models"
- Leinonen, P.J.; D. MacKay and C.R. Phillips 1971. Canadian Journal of Chemical Engineering, 49, 288 "A Correlation for the Solubility of Hydrocarbons in Water"
- Ljunggren, S. and J.C. Eriksson 1984. Journal of the Chemical Society, Faraday II, 80, 489 "Shape Fluctuations of Spherical Micelles"
- Ljunggren, S. and J.C. Eriksson 1986. Journal of the Chemical Society, Faraday II, 82, 913 "The Mechanics and Thermodynamics of Disc-shaped Micelles"
- Matijevic E. and B.A. Pethica 1958. Transactions of the Faraday Society, 54, 587 "Heats of Micelle Formation of Sodium Dodecyl Sulfate"
- McAulliffe, C. 1966. Journal of Physical Chemistry, 70, 1267 "Solubility in Water of Paraffin, Cycloparaffin, Olefin, Acetylene, Cycloolefin and Aromatic Compounds"
- McBain, J.W. and C.S. Salmon 1920. Journal of the American Chemical Society, 43, 426 "Colloidal Electrolytes. Soap Solutions and their Constitution"
- Menger, F.M. 1979. Accounts of Chemical Research, 12, 111 "On the Structure of Micelles"
- Missel, P.J.; N.A. Mazer; G.B. Benedek and M.C. Carey 1983. Journal of Physical Chemistry, 87, 1264 "Influence of Chain Length on the Sphere-to-Rod Transition in Alkyl Sulfate Micelles"
- Mitra, P.; K.N. Ganesh and D. Balasubramanian 1984. Journal of Physical Chemistry, 88, 318 "Amplification of the Surface Activity of Solubilizates in Amphiphile Aggregates: Relevance to Studies on Micelle Structure"

- Moroi, Y.; K. Motomura and R. Matuura 1974. Journal of Colloid and Interface Science, 46, 111 "The Critical Micelle Concentration of Sodium Dodecyl Sulfate--Bivalent Metal Dodecyl Sulfate Mixtures in Aqueous Solutions"
- Moroi, Y.; N. Nishikido and R. Matuura 1975. Journal of Colloid and Interface Science, 50, 344 "The Critical Micelle Concentration of Multicomponent Mixtures of Metal Alkyl Sulfates in Aqueous Solutions. II."
- Moroi, Y.; N. Nishikido; M. Saito and R. Matuura 1975. Journal of Colloid and Interface Science, 52, 356 "The Critical Micelle Concentration of Ionic--Nonionic Detergent Mixtures in Aqueous Solutions. III."
- Moroi, Y.; R. Sugii and R. Matuura 1984. Journal of Colloid and Interface Science, 98, 184 "Examination of Micelle Formation by the Phase Rule"
- Mukerjee, P. 1972. Journal of Physical Chemistry, 76, 565 "The Size Distribution of Small and Large Micelles: A Multiple Equilibrium Analysis"
- Muller, A.; B. Krebs; A. Fadini; O. Glemser; S.J. Cyvin; J. Brunvoll; B.N. Cyvin; I. Elvebredd; G. Hagen and B. Vizi 1968. Zeitschrift fur Naturforschung A, 23a, 1656 "Mean Amplitudes of Vibration, Force Constants and Coriolis Coupling Constants of $ZXY_2(C_{2v})$ and $ZXY_3(C_{3v})$ Type Molecules and Ions"
- Muller, A. and G. Nagarajan 1967. Zeitschrift fur Anorganische und Allgemeine Chemie, 349, 87 "Mittlere Schwingungsamplituden in verschiedenen Ionen und Molekeln vom Typ ZXY_3 mit C_{3v} -Symmetrie"
- Muller, N. 1973. In Reaction Kinetics in Micelles; E. Cordes, ed.; Plenum Press, New York "Recent Advances in the Chemistry of Micelles: Thermodynamics of Micellization"
- Murray R.C. and G.S. Hartley 1935. Transactions of the Faraday Society, 31, 183 "Equilibrium Between Micelles and Simple Ions, with Particular Reference to the Solubility of Long-Chain Salts"
- Murrell, J.N.; S.F.A. Kettle and J.M. Ledder 1978. The Chemical Bond; John Wiley & Sons, New York
- Nicolas, J.J.; K.E. Gubbins; W.B. Streett and D.J. Tildesley 1979. Molecular Physics, 37, 1429 "Equation of State for a Lennard-Jones Fluid"

- O'Connell, J.P. 1987. Unpublished notes.
- Owen, B.B.; R.C. Miller; C.E. Milner and H.L. Cogan 1961. Journal of Physical Chemistry, 65, 2065 "The Dielectric Constant of Water as a Function of Temperature and Pressure"
- Owenson, B. and L.R. Pratt 1984. Journal of Physical Chemistry, 88, 2905 "Molecular Statistical Thermodynamics of Model Micellar Aggregates"
- Polak, J. and C.B.Y. Lu 1973. Canadian Journal of Chemical Engineering, 51, 4018 "Mutual Solubilities of Hydrocarbons and Water at 0 and 25 C."
- Reed, T.M. and K.E. Gubbins 1973. Applied Statistical Mechanics; McGraw-Hill, New York
- Rosen, M.J. 1978. Surfactants and Interfacial Phenomena; Wiley-Interscience, New York
- Rubingh, D. N. 1979. In Solution Chemistry of Surfactants, vol. 1; K.L. Mittal, ed.; Plenum, New York "Mixed Micelle Solutions"
- Ruckenstein, E. and R. Nagarajan 1975. Journal of Physical Chemistry, 79, 2622 "Critical Micelle Concentration. A Transition Point for Micellar Size Distribution"
- Ryckaert, J.-P. and A. Bellemans 1975. Chemical Physics Letters, 30, 123 "Molecular Dynamics of Liquid n-Butane Near Its Boiling Point"
- Scamehorn, J.F.; R.S. Schechter; and W.H. Wade 1982. Journal of Dispersion Science and Technology, 3, 361 "Micelle Formation in Mixtures of Anionic and Nonionic Surfactants"
- Stillinger, F.H. 1973. Journal of Solution Chemistry, 2, 141 "Structure in Aqueous Solutions of Nonpolar Solutes from the Standpoint of Scaled-Particle Theory"
- Sutton, C. and J.A. Calder 1974. Environmental Science and Technology, 8, 654 "Solubility of Higher-Molecular-Weight n-Paraffins in Distilled Water and Sea Water"
- Szleifer, I.; A. Ben-Shaul and W.M. Gelbart 1985. Journal of Chemical Physics, 83, 3612 "Chain Organization and Thermodynamics in Micelles and Bilayers. I. Theory"

- Tabony, J. 1984. Molecular Physics, 51, 975 "Structure of the Polar Head Layer and Water Penetration in a Cationic Micelle. Contrast Variation Neutron Small Angle Scattering Experiments"
- Tanford, C. 1972. Journal of Physical Chemistry, 76, 3020 "Micelle Shape and Size"
- Tanford, C. 1974. Journal of Physical Chemistry, 78, 2469 "Theory of Micelle Formation in Aqueous Solutions"
- Van De Sande, W. and A. Persoons 1985. Journal of Physical Chemistry, 89, 404 "The Size and Shape of Macromolecular Structures: Determination of the Radius, the Length, and the Persistence Length of Rodlike Micelles of Dodecyl-dimethylammonium Chloride and Bromide"
- Verlet, L. 1967. Physical Review, 159, 98 "Computer 'Experiments' on Classical Fluids. I. Thermodynamical Properties of Lennard-Jones Molecules"
- Vold, M.J. 1985. Langmuir, 1, 501 "Role of Shape in Models of Micellar Equilibria"
- Vold, R.D. 1950. Journal of Physical and Colloid Chemistry, 51, 797 "Phase Boundaries in Concentrated Systems of Sodium Oleate and Water"
- Watanabe, K.; M. Ferrario and M.L. Klein 1988. Journal of Physical Chemistry, 92, 819 "Molecular Dynamics Study of a Sodium Oleate Micelle in Aqueous Solution"
- Warr, G.G.; F. Grieser; and T.W. Healy 1983. Journal of Physical Chemistry, 87, 1220 "Composition of Mixed Micelles of Polydisperse Nonionic Surfactants"
- Weber, T.A. 1978. Journal of Chemical Physics, 69, 2347 "Simulation of n-Butane Using a Skeletal Alkane Model"
- Weston, R.E., Jr. and H.A. Schwarz 1972. Chemical Kinetics; Prentice-Hall, Englewood Cliffs, N.J.
- Woods, M.C. 1985. MS Thesis, Clemson University "Internal Structure of a Model Micelle via Computer Simulation"
- Woods, M.C.; J.M. Haile and J.P. O'Connell 1986. Journal of Physical Chemistry, 90, 1875 "Internal Structure of a Model Micelle via Computer Simulation. 2. Spherically Confined Aggregates with Mobile Head Groups"

Woolley, E.M. and T.E. Burchfield 1984. Journal of Physical Chemistry, 88, 2155 "Model for Thermodynamics of Ionic Surfactant Solutions. 2. Enthalpies, Heat Capacities, and Volumes"

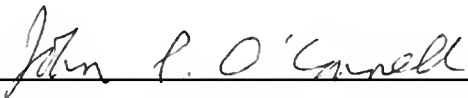
Woolley, E.M. and T.E. Burchfield 1985. Journal of Physical Chemistry, 89, 714 "Model for Thermodynamics of Ionic Surfactant Solutions. 3. Enthalpies, Heat Capacities, and Volumes of Other Surfactants"

BIOGRAPHICAL SKETCH


The author was born in 1956 in Orlando, Florida, the son of Richard T. Farrell and the former Teresa Corcoran. He was graduated from Winter Park High School in 1974 and entered the Georgia Institute of Technology in the fall of that year. During his undergraduate years, he joined the staff of the campus newspaper as a music writer and progressed to the position of managing editor. This period also included intern positions in engineering with the Union Carbide Nuclear Division in Oak Ridge, Tennessee, and the Procter and Gamble Paper Products Division in Albany, Georgia. Taking the degree of Bachelor of Chemical Engineering in 1979, he was subsequently employed by Procter and Gamble in various production engineering capacities.

He entered graduate study in the Department of Chemical Engineering at the University of Florida in the fall of 1982, receiving a Master of Science the following year. Upon completion of the doctoral program, he will hold a position with Westvaco Research in Laurel, Maryland.

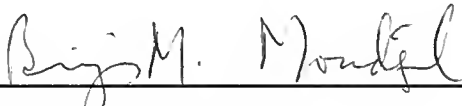
I certify that I have read this study and that in my opinion it conforms to acceptable standards of scholarly presentation and is fully adequate, in scope and quality, as a dissertation for the degree of Doctor of Philosophy.


John P. O'Connell, Chairman
Professor of Chemical
Engineering

I certify that I have read this study and that in my opinion it conforms to acceptable standards of scholarly presentation and is fully adequate, in scope and quality, as a dissertation for the degree of Doctor of Philosophy.

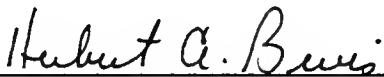

Dinesh O. Shah
Professor of Chemical
Engineering

I certify that I have read this study and that in my opinion it conforms to acceptable standards of scholarly presentation and is fully adequate, in scope and quality, as a dissertation for the degree of Doctor of Philosophy.


Brij M. Moudgil
Professor of Materials
Science and Engineering

This dissertation was submitted to the Graduate Faculty of the College of Engineering and to the Graduate School and was accepted as partial fulfillment of the requirements for the degree of Doctor of Philosophy.

April, 1988


Dean, College of Engineering

Dean, Graduate School

UNIVERSITY OF FLORIDA



3 1262 08556 7708